Durham E-Theses

Predicting weld distortion in the design of automotive components

O'Brien, Roger William

How to cite:

O'Brien, Roger William (2007) *Predicting weld distortion in the design of automotive components*, Durham theses, Durham University. Available at Durham E-Theses Online: http://etheses.dur.ac.uk/2462/

Use policy

Durham University

Predicting Weld Distortion in the Design of Automotive Components

by

Roger William O'Brien

Thesis submitted to
The School of Engineering,
Durham University

In fulfillment of the requirements
for the degree of:

Master of Science
(by Research)

Supervisor: Dr Hui Long

March 2007

Predicting Weld Distortion in the Design of Automotive Components

Roger William O'Brien

Abstract

This project was set up in order to investigate whether it may be valid to use a simplified approach to weld distortion prediction in order to make an assessment of the distortions occurring in a welded structure. Distortion may manifest as problems associated with production, which increase costs and reduce profit. In order to validate the proposed prediction approach an experiment was developed to gain detailed information about distortions occurring in a series of simple welded joints. The joints and the parameters used for the experiment were based on the processes and applications of the case study company. The experiment was set up with the aim of evaluating the general magnitude and directions of distortion in bead on plate and butt weld joints to develop a database of distortion. The method for inspection of the experimental samples was to scan the parts using a 3D laser scanner to collect a detailed resolution point cloud that could be analysed. From the experimental results a number of key factors relating to the welded joints were found relating to material thickness, weld speed and penetration for the four different modes of distortion occurring. The experimental results were compared with the published data and equations presented by other authors, and some general agreements found, however, some differences were evident. In order for a designer to adjust the shape and form of a components design to counteract the distortions to achieve a nominal tolerance, based on these results, it was necessary to develop some new models specific to the materials and process variables of the case study company. Using an approach based on DoE software techniques, response surfaces for the experimental results were generated. This allowed equations to be developed for each distortion mode, which a designer could use to make predictions in the design phase to reduce risk from distortion.

Acknowledgements

Firstly, I would like to acknowledge and thank my Father, William O'Brien, and late Mother, Doreen O'Brien, for their constant support, encouragement, sacrifice and faith in me, they have provided, and continue to provide, throughout my life to date. Without this I would no doubt have not achieve what I have and be where I am today.

I would also like to express my deepest thanks, and love, to my partner, Caroline Hughes, for her support, understanding and love, which not only have helped me through this, but also through what has been a very difficult period in my life which has been blighted by illness and self doubt. Thanks for standing by me and helping me on my way back from the clouds of mental depression and stress, the most debilitating of illnesses, to start to find my way back to my true self again. Each day I get better knowing I have your support and faith in me. Your support has been unswerving even when perhaps I have not deserved it. I know I don't always show my appreciation to you, but this is one way to clearly acknowledge it.

To my children Matthew and Emma, thanks for your love and being there to provide me a meaning and strength to go on. Without you I would be nothing, and this may never have been completed.

I would like to extend my thanks to Dr Hui Long for her support, input and guidance in the undertaking of this research at Durham University.

Special thanks to Mr. David Kilpatrick, Prof. John MacIntyre, my fellow NEPA Engineering Fellows, and all the staff of AMAP at University of Sunderland involved in Engineering Fellows project, for your support, discussions, encouragement and involvement. Thanks also to Mr. Eddie Leng, formerly TKA Training Manager, who with John, had the original idea and concept for Engineering Fellows as part of the NEPA and regional framework.

Executive Overview

The project was set up in order to investigate whether it may be valid to use a simplified approach to weld distortion modelling and prediction in order to make a qualitative, and possibly quantitative, assessment of the distortions occurring in a welded structure during assembly. Based on such an approach the aim would be to introduce a tool that would allow the distortions occurring to be assessed and appropriate adjustments made into designs early in the product realisation process. This would reduce the risk of late changes to the product due to distortion effects and the associated costs these can bring. The project set out to bring consideration of weld distortion effects further upstream and into the design process to allow for earlier introduction of changes. As many authors have demonstrated early design change is far more cost effective, and indeed the cost of design change increases exponentially during the duration of product development.

The background to the project and an introduction to the case study company was presented in Chapter 1. Here it was also discussed that distortion may manifest as problems associated with creating excessive movements, reduced or out of tolerance effects, excessive fit up gaps, or form changes, which in turn increases costs and reduces profit. It was shown by a real example that the direct costs associated with problems arising from distortion late in the realisation of components can have a sizeable cost implication.

Chapter 2 took a detailed look at the welding processes and particularly those of the case study company. The theory, along with the residual stresses and distortions occurring were discussed. The various primary distortion modes were discussed and it was seen that the key factors which influence the distortion are:

- The material properties.
- The stresses inherent in components from manufacturing processes.
- The restraint applied during welding.
- The process variables of welding and the weld procedure itself.

- The actual design of the product to be manufactured including the position of the weld, its fit up, accuracy and tolerance of the weld joint.

It was discussed that it is possible to control this distortion; however there are both commercial and practical implications for doing so. The work relating to distortion prediction of many researchers was discussed, which would form the basis for subsequent comparison of the experimental results of this investigation.

The direction chosen to validate the proposed prediction approach was to develop an experiment in order to learn detailed information about distortions occurring in a series of simple welded joints. The joints and the parameters used for the experiment would be based on the processes and applications of the case study company. The experiment was set up with the aim of evaluating the general magnitude and directions of distortion in a selection of representative joints to develop a database of distortion values and factors. This information could then be used and applied to real designs to predict distortion by a designer so that right at the start of a product's development they can understand the distortion effects and make value added decisions about whether a design needs to be changed to account for these. In addition the process engineers can plan accordingly and decide if it is better for a designer to alter the design to attempt to overcome the distortion effects or plan the processes knowing where distortions will occur with a view to minimising it or accounting for the distortion by additional processes and operations. For the experiment a special fixture was designed to enable the experiment to be conducted in a repeatable and controlled manner. The experimental procedure was developed and documented and consideration given to each of the key stages of the process. In setting up the experiment it was necessary to pay careful attention to the methods of measuring the distortion results, and it was seen that the initial methodology had to be changed in order to find a more robust and accurate method of capturing all of the distortion data requiring to be analysed. The final method settled upon for inspection of the post weld experimental samples was to scan the parts using a 3D laser scanner to collect a detailed and high resolution point cloud that could be analysed without needing further additional manipulation.

v

The welded joints used for the experiment in this work were chosen based on the experience of the case study company. Prior to any measurement study being undertaken a visual assessment of the weld quality was undertaken. From the experimental results presented in Chapter 4 a number of key factors relating to the welded joints were found. It was found that generally there was a high degree of repeatability in the processes of the case study company which resulted in consistent and repeatable experimental results. It was demonstrated that both increasing the material thickness and increasing the speed of welding act, in general, to reduce the overall magnitude of the distortions. The experiment showed that the longitudinal distortion in the welds occurred with a peak distortion at the weld centreline and decreased to lower distortion values as the distance from the weld increased towards the edges of the plates. Generally this produced a double V shaped pattern of longitudinal distortion. The transverse distortions occurring in the plates were seen to be relatively constant in the main body of the weld, away from the start and stop effects. Angular distortions were seen to be influenced by not only the material thickness and weld speed but also the level of penetration occurring in the weld itself. The angular distortions themselves occurred consistently along the length of the plates with little variation. Bowing distortions were very repeatable and consistent. Based upon the results seen from the experiments then it would be possible for a designer to adjust the shape and form of the components design in order to counteract the effects of these distortions to achieve the idealised nominal design that was intended in the initial concept. However in order to be able to do this they would need a tool to predict the values and allowances to be made in components to overcome the distortion effects.

The experimental results did not appear to readily agree with the published data and equations presented by other authors. However further investigation into many of these differences showed that it was the effect of the combination of the various distortions occurring together that were acting to give measured results higher than would be predicted. The longitudinal distortions were seen to be influenced by the value of bowing occurring which in some cases had a significant effect on the individual result. Likewise for transverse distortion the influence of the angular

vi

distortion on the measured results was demonstrated. It was also found that due to the set up of the case study company an additional influence on the transverse distortion was the weld gap size. The angular distortions were found to be influenced by material thickness, welding speed and penetration, however generally poor agreement was found to the published equations. In the case of bowing distortion there was good agreement on the butt weld samples to the published models from Okerblom's equation for bowing distortion, however the agreement for bead on plate samples was not as specific to one particular model.

Using an approach based on DoE software techniques response surfaces for the experimental results were obtained. Following this specific equations relating to the design space of the case study company were developed for each distortion type and for each joint. These were presented as equations and in a graphical form that a designer could quickly used to evaluate the effect. The equations for each joint type, specific to the case study company, and considered to be valid over a range of material thicknesses (t) based on XF350 material from 1.5mm to 5.0mm thick and weld speeds (v) from 500mm/min to 1500mm/min, are defined and presented.

Based on these findings then the combined effects of the distortions can be characterised and evaluated by using the four equations for each weld type. If this is carried out then a designer can adjust the design of a component to allow for the effects of these distortions by incorporating an allowance for these into the design. Therefore in doing this a post welded component produces a product to nominal dimensions. An example of how this could be done for a simple component was demonstrated to provide an illustration of the method, calculation and application to a simple design.

Table of Contents

List of Figures

List of Tables

Predicting Weld Distortion in the Design of Automotive Components
Roger O'Brien, MSc Thesis, March 2007

Nomenclature

α Coefficient of thermal expansion $\left(\dfrac{1}{K}\right)$ (12 x 10^{-6} for steel)

$\alpha_{pl}\Delta T$ Linear thermal expansion of the plate between Tr and $\dfrac{T_y - T_r}{2}$ (0.0044

           for steel)

$\alpha_w\Delta T$ Linear thermal expansion of the weld between Tr and $\dfrac{T_y - T_r}{2}$

           (0.0093 for steel)

a   Weld throat thickness (*mm*)

A   Cross section of the structure to be welded (*mm^2*)

A_w Cross sectional area of the weld (*mm^2*)

A'_w Cross sectional area of the weld with reinforcement (*mm^2*)

β Restrained angular distortion (°)

β_f Free angular distortion (°)

b   Average width of the plate material (*mm*)

b_w Average width of the welded area (*mm*)

c   Specific thermal heat capacity $\left(\dfrac{J}{kg.K}\right)$ (460 for steel)

δ_L Longitudinal shrinkage (mm)

δ_T Transverse shrinkage (mm)

E   Young's Modulus $\left(\dfrac{N}{mm^2}\right)$ (210000 for steel)

ε_Y Yield strain

ε_L Longitudinal strain (= δ_L/L)

ε_T Transverse strain (= δ_T/b)

g   Gap or root opening (*mm*)

I   (Welding) Current (*A*)

I   Second moment of area (*mm^4*)

J   Moment of inertia (*mm^4*)

κ Thermal Diffusivity $\left(=\dfrac{\lambda}{\rho.c}\right)$

λ Coefficient of thermal conductivity $\left(\dfrac{W}{m.K}\right)$ (46…58 for steel)

l_w Leg length of weld (*mm*)

L   Length of weld (*mm*)

η Process efficiency for welding

μ Deposition efficiency of a welding rod

v Poisson's ratio

p   Weld penetration (*mm*)

q   Heating energy (*W*) (=U.I)

$\dfrac{q}{v}$ Heat input $\left(\dfrac{J}{mm}\right)$

q_{lin} Linear heat input $\left(=\eta \cdot \dfrac{q}{v}\right)$

ρ Density $\left(\dfrac{kg}{m^3}\right)$ (7800 for steel)

ρc Volumetric specific heat capacity $\left(\dfrac{J}{m^3.K}\right)$

$\dfrac{1}{R}$ Curvature of a section (bowing) $\left(\dfrac{1}{mm}\right)$

R   Radius of curvature (mm)

σ_Y Yield stress $\left(\dfrac{N}{mm^2}\right)$

t   Average plate thickness (*mm*)

t_c Thickness of fused plate material (*mm*)

t_w Average thickness of welded area (*mm*)

T_r Room/ambient temperature (°)

T_Y Temperature above which the deformation is plastic (°)

U   (Welding) Voltage (*V*)

v Welding speed $\left(\dfrac{mm}{s}\right)$

y   Distance of weld to neutral axis (*mm*)

Chapter 1: Introduction

1.1 Introduction

The aim of this chapter is to introduce the problem facing industry with regards to weld distortion and the problems facing industry in predicting these in the design phase of the product life cycle.

In the first section the problem to be investigated will be defined and set out, giving an example of the sort of impact the problems of weld distortion can present to industry. There is a brief discussion of the limitation of existing methods and the benefits to be gained from a cost and time effective approach to predicting weld distortion.

Section two sets out the proposed project and describes briefly the work undertaken and how it relates to the problem. Along with a brief statement of aims and objectives that will be discussed further in subsequent chapters.

The third and forth section shall introduce the company that will be used for the case studies and examples relating to cost impact that this research may help address. The problems facing this company are typical of those facing high volume fabrication manufacturers, particularly in the automotive industry but also in similar industries.

Finally, this chapter will summarise the problems and thoughts on these important issues in a brief discussion and summary section.

1.2 Identification of the Problem

This section sets out to define the problem and its specific relation to high volume automotive manufacturing. It sets out to give an overview of the pressures facing automotive suppliers in relation to process development of their products. It discusses methods to identify and solve some of these process areas, and highlights briefly the shortcomings of the current techniques relating to weld processes, which are discussed in detail in the literature review sections in Chapter 2.

2

In the competitive automotive market there is a strong drive by the OEMs (Original Equipment Manufacturers) to accelerate product development and bring ever more models to market in shorter development lead-times. This is often referred to as reducing time to market. The mass advent and encompassment of CAE (computer aided engineering) technologies, along with their significant advancement, has enabled significant reductions to be made in this time to market. It is now common to bring new vehicles to the market based on a vehicle development program lasting in the region of less than 36 months. In most cases with the principal structural and mechanical components, then it is usual for the design iteration activity to occupy around the first 18 months of such a program to allow for a 12 month tooling, fixture and facility lead-time, with the final six months being used for installation, commissioning and quality proving/debugging of the line so volume production can commence smoothly at the required date. Underpinning all of this is significant testing throughout the development phase.

During the program there are often a number of prototype stages to both verify the structural and vehicle performance, of products, systems and overall vehicle. However especially in the early stages these prototype vehicles are extremely expensive due to parts being produced off prototype tooling and also not off production processes and facilities. In order to reduce the numbers of high cost prototype vehicles, there has been and continues to be an increasing trend of applying analysis and simulation technologies to replace these prototypes with a 'virtual' vehicle concept and 'virtual testing'. There is significant work undertaken now in the 'virtual' CAE world before the commencement of any 'true' prototype production. Most OEMs have already cut the number of 'true' prototype builds to around about two, and many have just used basic simulator vehicles to capture and collect appropriate data for analysis followed by one true prototype phase. The downside of this is that, especially for Tier 1 suppliers, much of the learning about the problems faced in manufacturing and assembly processes which is accumulated though the prototype stages is reduced. Therefore, the opportunity to develop solutions feeding into the planning of the production process is reduced, whilst the cost of late modifications increases exponentially with time.

3

One of the major problems arising in the assembly process, and also a significant area of weakness to CAE investigations is the effect of the welding process on dimensional stability of the structure. During the manufacturing of automotive chassis components it is usual to use Metal Inert Gas, MIG, (or Active Gas, MAG) welding technology as a means to assembling complex pressed parts. Inherent to this welding process some degree of weld-induced distortion is expected in the final component. The net effect of this distortion (direction and magnitude) is difficult to predict on newly designed parts, however it has been proven on numerous occasions to be repeatable (within limits) on established products. The severity of these distortions is not always evident or repeatable during prototype manufacture, partly because the pedigree of the parts is not always consistent. This is because the process does not necessarily follow that proposed for volume production, and welding parameters/speeds can vary along with differences in clamping, location and also cooling time. As a consequence of this it is common in industrial practice to protect critical dimensional and package constraints by the application of other technology (i.e. setting /machine operations) downstream to where the distortion occurs. These additional operations prove to be costly, have there own inherent problems and usually add little or no value to the finished part, other than guaranteeing its dimensional conformance at specific locations or features.

The development of CAE technologies and computational methods based on Finite Element Analysis, FEA, has provided powerful and effective tools for manufacturing and assembly process simulation and assessment. For example, tools such as ROBCAD exist for manufacturing process simulation, primarily to look at component movement coupled with fixture and robot movements to guarantee access and avoid clashes. However, tools for genuine process simulation are only now starting to emerge in some of the core process such as welding. Finite Element simulation based on coupled thermo-elastic/plastic methods has enabled process simulation of pressed parts produced by sheet metal forming or hydroforming. For individual pressings it is possible to analyse their processing using such software that can predict items of interest in the forming process such as thinning, splitting, thickening, wrinkling, spring back and residual stress state. This can be done using

4

packages such as Pam-Stamp. These residual stresses and material thicknesses can in some instances now be mapped onto a dissimilar Finite Element mesh that may be required for any particular structural analysis and used to assist in the life or performance assessment of the product. The application of multi-step forming simulation requires detailed material information and in depth process knowledge to actually ensure the accuracy of the simulation. This type of analysis is time consuming and complex, and at present can be viewed as the form of analysis that would be carried out as a final verification of a process before committing to the hard production tools.

During the design phase the design team needs to be able to make quick design iterations with broad-brush tools that allow rapid design changes to be assessed. This enables quick decision making that will be generally and directionally correct, without support from specialist areas and functions, such as tooling engineers. Therefore a method of pressing simulation emerged onto the market several years ago that allows such speedy iterations to be considered, and whilst the results are not always totally accurate they provide a means of quick and good feasibility assessment for drawn pressings. The process used for this is single step forming analysis, which in simple terms is geometric and topology based, mapping formed parts onto a flat sheet to predict thinning. This has been found to give very acceptable initial results when used with developed criteria for assessment, and allows a pressed panel to be assessed by a none specialist for initial feasibility in a matter of minutes. Once the designs have been developed and input sought from the specialist functions, then prior to final sign off the detailed multi-stage analysis can be carried out to confirm the parts process with the majority of the potential errors or problems designed out by the one step studies.

Apart from the effects of forming processes on the material of the pressings, the weld itself is a non-homogeneous structure making accurate prediction very difficult, and this must be combined with the effects the welding process has on the individual components that assemble to make the finished product.

5

The welding process may change the material properties of sub-components, especially in the heat affected zone (HAZ). This also changes the pre-stress state both by an annealing action to stress relieve the pre-stress state of the pressings and also by introducing residual stresses from the weld solidification (material phase change) process during the welding and subsequent cooling of the component. The introduction of these phase changes results in the residual stresses that in turn can produce some significant distortion effects on the finished product.

The challenges facing the implementation of simulating the welding process are many and can be briefly summarised here in the introduction to the project as follows. The welding process consists of heating, melting, addition, solidification, and cooling, Masubuchi [1980]. During these processes material phase changes take place in complex material structures. The welding processes cause highly non-uniform temperature distributions which cause thermal expansion and contraction, with phase change, which result in plastic deformations. It is these plastic deformations that lead to both distortions and residual stresses being left in the fabricated assembly. The weld process itself is driven by a number of process parameters which relate to it, such as gas mix, arc current, weld speed and materials, each of these in turn is difficult to control and simulate. Being able to understand and account for these process and material factors from welding is paramount to planning a robust manufacturing process, while still being able to eliminate prototype builds without losing knowledge about distortion.

FEA simulation is limited in its application to the simulation of the welding processes of complex structures for a number of reasons. The need for coupled thermal mechanical analysis leads to long computing time for real structures. Individual sub models, each with their own limitations and approximations of the actual physics occurring are needed for many of the phase change and process parameters, even before things like the final sequencing of welding is taken into consideration. It can therefore be seen that the exact problem of simply welding a component is very complex and therefore not easy to simulate accurately or in a timely manner. This is further discussed in Chapter 2, which is set out to discuss in

detail the state of the art challenges in welding simulation and issues, methodologies and approaches aimed at addressing these.

The desire from the product developer and manufacturer is to find a methodology to allow rapid assessment of a products design for its performance under welding. The aim of any such method is to provide a greatly simplified weld assessment tool that can predict the general magnitude and direction of weld distortion on a fabrication, to perhaps allow optimization to take place on weld sequencing, and the protection in the assembly fixture and processes for areas where high degrees of distortion may result from the weld process. Repeatedly, on the development of products, late changes are faced to either assembly fixtures or to pressed panels and tooling to accommodate the effects of the production weld processes and their induced distortions on the product to achieve dimensionally capable and stable products. In order to achieve this then the challenges and obstacles set out in the previous paragraph need to be overcome or worked around, for any simulation method to be successful and appropriate.

The assessment of distortions early in the design stage would provide a significant benefit to the overall development of the product and process. For example a structure prone to excessive distortions could be redesigned to provide a more feasible welded solution even before the manufacture of prototype parts had commenced. Alternatively if such changes were not possible this could clearly be identified and the provision planned into the process, rather than being a late and costly addition that may not have been budgeted for. The existing software tools that predict weld properties and distortion are in their early days of acceptance and not widely used, at the same time being expensive, and very time consuming more aimed at final sign off. Therefore an early indicative solution for weld distortion prediction would greatly aid designers in the development process of products, especially if such a tool is quick and simple to use.

1.3 Project Proposal

The aim of this project is to assess the validity of a simplified approach to weld distortion, to be used in quantifying the degree and direction of movement that a welded structure undergoes during the assembly process. Additionally from this assessment it should be possible to develop a method / technique for the analysis most suitably employed to achieve either a quick indication of the net effect (for example in order to predict concept feasibility), or also a result that may allow distortions to be countered and engineered out (necessary to reverse engineer 'out' distortions by making component parts 'wrong' to achieve final dimensions after welding).

Initially it will be necessary to gather information and characterise the key weld types commonly found in manufacturing processes. For the sake of this project the scope will focus primarily on the joint types, materials, thicknesses and process parameters of the case study company as a generalised example. From this work it should then be possible to determine what needs to be undertaken to transfer this to other products, companies, industries or processes.

The initial direction will be to assess the degree and direction of distortion that a welded structure undergoes during the assembly process. From this assessment, it should be possible to develop a quick method/technique for the analysis of weld distortions. This portion of the project will be different from many other projects carried out into the investigation of weld distortion as it is primarily a means of providing a company knowledge base and method of analysing potential distortion in the design stage of a products development as opposed to calculating actual distortion values. In order to achieve this then it will be necessary to build and analyse a variety of welded joint parts to evaluate and understand the general magnitude and direction of distortion under different variables to help at the design stage of a products development. From this it is possible to build up a database of distortion results from the tests carried out which can then be used to develop a simple weld distortion predictor tool based on experimental data.

In undertaking this project the author would develop a sound knowledge into what causes distortion in sheet metal welded parts. Combined with this is an understanding of practically and theoretically what can be done to eliminate/reduce distortion in parts in the manufacturing process.

In doing these studies it is possible to attempt to identify the key variables which contribute most to distortion trends. From this it is possible to investigate the development of analytical methods to predict distortion based upon these key factors and compare these against the experimental data, in order to determine the success of the method.

1.4 Introduction to the Case Study Company

ThyssenKrupp Automotive Tallent Chassis (subsequently referred to as TKA Tallent) is a high volume manufacturer of complex pressed and welded structural chassis components for the global automotive market. By this it means that they produce automotive subframes, axles, suspension control arms/links, cross-members and perimeter frames. The company tends to focus on the high volume proportion of the automotive market place. Their definition of high volume is products produced in excess of approximately 60000 units per annum. Volumes can range up to 1.8 million units per annum in the example of control arms where 2 per car are produced for a global platform. The company are responsible as a design development source for many of the products they produce.

The majority of TKA Tallent products are pressed sheet, or formed tubular, steel components that are welded together into finished fabrications, which then may be machined, if appropriate, before painting and finishing operations. Additional components such as rubber bushings or ball joints are often assembled to the components before being shipped to the vehicle or modular assembly plant. The components are designed to a nominal condition and processes are planned to provide robust manufacture to achieve dimensionally stable and capable products. The eventual manufacturing processes and their limitations or special needs have to

9

be considered and planned for at the design stage. However, at this stage clearly much is still unknown about the detail of the final process or how the component will behave under that assembly process.

Conventional analysis is done on the final design component and at present practically this is limited to carrying out the calculations based on a nominal zero pre-stress condition at the end of the process. The range of analysis carried out by the company at present includes both linear and non-linear static and dynamic analysis, modal performance, fatigue prediction, crash studies, and forming simulation, both single and multi-step methods.

1.5 Cost Impact of Distortion on Product Development

The arrangement of a typical MIG weld joint on one of TKA Tallents components can be seen in Figure 1.1. This is a joint on an example of a two piece assembly made from two pressings welded together. Distortions in such assemblies are hard to predict at the design stage due to the long runs of weld required and variations in material thickness, along with other properties and parameters.

Figure 1.1: Typical welds on one of TKA Tallents components

10

To highlight the importance of being able to predict weld distortion at the design stage, so that costly modifications do not have to be made either to press tooling or to assembly fixtures, a previous subframe project carried out at TKA Tallent has been used as an example. The subframe for which the figures in this example are based is shown in Figure 1.2, which shows why modifications had to be made to press tooling at great expense to the company to compensate for distortion occurring in the welded pressed parts.
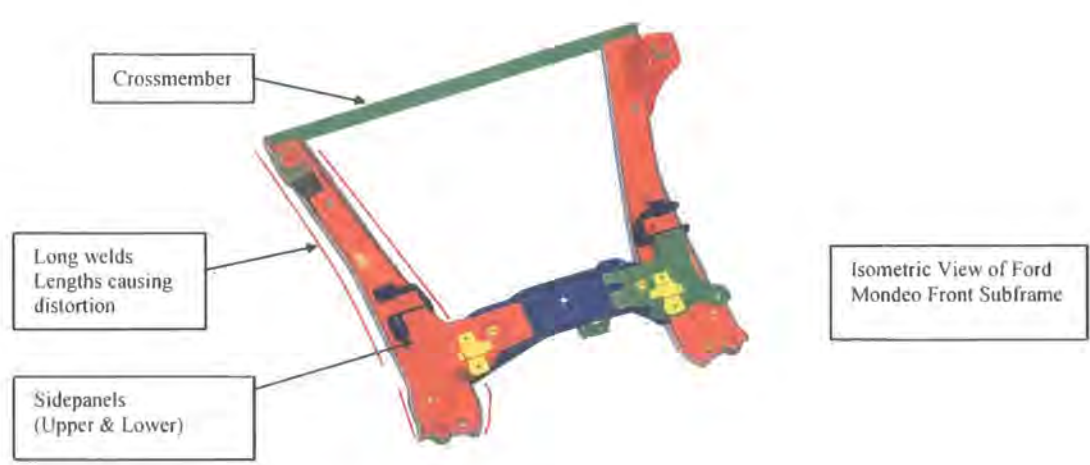
Figure 1.2: Subframe as designed and manufactured by TKA Tallent

In assembly, the Crossmember bracket would not fit to the side panels on the Mondeo Subframe due to distortion caused by long runs of weld that were required to fit both the Upper and Lower Side panels together. Expensive rework had to be carried out to the press tools so that side panels could be modified to compensate for distortion in assembly.

Tables 1.1 and 1.2 show a breakdown of the costs to TKA Tallent, for the initial tooling and then due to these modifications. The cost are conservative as they are incurred cost only and so exclude additional costs of labour for rework, reprogramming and redeveloping processes.

Table 1.1: Initial costs of tooling

Press Tool	Cost Of Original Tool (£)
Upper Panel Tool	261,000
Lower Panel Tool	172,000
Total	**433,000**

Table 1.2: Additional costs for modification due to unexpected/unpredicted distortion

Tooling Modifications	Cost To Tallent (£)
Siderail Upper - Extend around Rear Bush	24,950
Siderail Lower - Extend around Rear Bush	44,500
Laser Cut Panels	30,294
Temp Tool	3,800
Total Cost For Modifications	**103,544**

From the figures presented in Table 1.1 and 1.2, it can be seen that an extra 24% had to be spent on top of the original £433,000 spent on press tools in order to solve the assembly issues caused through weld distortion problems.

It is these types of financial costs that companies could save on if distortion problems were predicted at the design stage and the appropriate redesign or less costly countermeasure put in place in a pro-active rather than reactive manner.

1.6 Summary of Introduction

In this chapter the problems facing the fabrication industry with regards to distortion control and prediction have been set out. From the information and financial examples presented it should therefore be clear that gaining a greater and earlier knowledge of distortion in the development and design process has significant benefits to successful project delivery of such products into mass production.

The project has been set out and formulated in order to bring the consideration of weld distortion further upstream in the design process to allow changes to be introduced earlier if required. Earlier changes in design is more cost effective, as it is

12

generally acknowledged that the cost of change increases exponentially though the duration of a product development, and increases significantly once the manufacturing phases start. Additional controls and processes can be put in place when budgets are available if the problem can not be designed away, if this is identified early in the process. The benefits from such an approach are significant and worthwhile. Currently distortion problems typically are discovered when it is too late to redesign, and therefore modifications have to be made to tooling, fixtures or processes that already exist and have been facilitised for the product. Tooling modifications or addition operations add costs, either of which can be catastrophically expensive or even eliminate profitability from a project.

Early knowledge is the key to avoiding late changes and this project sets out to develop some fundamental steps to facilitate prediction of weld distortion in the design stages. In order to do this it is necessary to review the current state of the art and practices for distortion control and simulation. These are set out in the literature review that follows in Chapter 2.

Chapter 2: Review of Welding Distortion

2.1 Background and Introduction to Welding Distortion Review

Having investigated the work carried out previously, it is evident there is a large variety of work that can be carried out to help a company with weld distortion problems in manufacturing projects. The work here sets out to help to achieve and investigate the company building up a knowledge base about weld distortion and methods of minimising it.

No matter what welding procedures are used in practise for different applications, there are certain essential variables which need to be addressed while performing a welding procedure. Such essential variables involved in the procedure can be found listed in Table 2.1, below.

Table 2.1: Welding process variables

The welding process and its variation	The method of applying the process
Material: • type, specification, or composition • the need for pre- or post-heat • geometry and thickness	Process Design: • the joint type of the weld • the travel progression (uphill or downhill) • features of the weld joint design
The polarity of the welding current	Welding position & filler material
Operational parameters involved	The size of the electrode or filler wire

It is needless to mention that a considerable amount of information can be provided on welding technology; however this report focuses on a specific experimental study on welding distortions of sheet metal components. A brief overview of distortion behaviour due to welding is therefore included in this chapter, as this document also serves to document the process for the case study company.

15

2.2 The Welding Process

The simplest and most understandable definition for welding can be given as a process used to join metals by the application of heat. However, and more completely, The American Welding Society (AWS) definition for a welding process is "a materials joining process which produces coalescence of materials by heating them to suitable temperatures with or without the application of pressure or by the application of pressure alone and with or without the use of filler material".

Today, in our ever vibrant and constantly changing industrial environment, more than fifty processes, used in different applications, are available commercially to join metals. The chart from AWS website, in Figure 2.1 shows a summary of many of the weld and weld related processes that exist.

There are numerous main advantages of welding, and the relative merits can be discussed extensively however the key benefits can be summarised as follows:

Welding gives a high joint efficiency with comparison to riveted or bolted joints, due to the nature of the weld joint itself and the strength it provides. In many applications it is vital to have water and air tightness, especially when submarine and storage tanks are concerned, welding can provide this with appropriate process controls. It is possible to deliver weight saving, again with comparison to other joint types, up to 20%, this may be achievable due to the lack of adding additional fasteners and the compact nature of welds. The welding process itself has virtually no limit in thickness to be welded, with applications being found on thin and micro plate structures, through the range of sheet materials to heavy plate applications and beyond. In most cases the design for a weld to be included in a product is a simple structural design. Finally and most importantly, reduction in fabrication time and consequently overall cost is achieved by welding to create complex assemblies.

MASTER CHART OF WELDING AND ALLIED PROCESSES

ARC WELDING (AW)

atomic hydrogen welding	AHW	electrogas welding	EGW
bare metal arc welding	BMAW	flux cored arc welding	FCAW
carbon arc welding	CAW	gas metal arc welding	GMAW
– gas	CAW-G	–pulsed arc	GMAW-P
– shielded	CAW-S	–short circuiting arc	GMAW-S
– twin	CAW-T	gas tungsten arc welding	GTAW

– pulsed arc	GTAW-P
plasma arc welding	PAW
shielded metal arc welding	SMAW
stud arc welding	SW
submerged arc welding	SAW
– series	SAW-S

SOLID-STATE WELDING (SSW)

coextrusion welding	CEW
cold welding	CW
diffusion welding	DFW
explosion welding	EXW
forge welding	FOW
friction welding	FRW
hot pressure welding	HPW
roll welding	ROW
ultrasonic welding	USW

RESISTANCE WELDING (RW)

dip soldering	DS
furnace soldering	FS
induction soldering	IS
infrared soldering	IRS
iron soldering	INS
resistance soldering	RS
torch soldering	TS
wave soldering	WS

SOLDERING (S)

flash welding	FW
high frequency resistance welding	HFRW
percussion welding	PEW
projection welding	RPW
resistance seam welding	RSEW
resistance spot welding	RSW
upset welding	UW

THERMAL SPRAYING * (THSP)

electric arc spraying	EASP
flame spraying	FLSP
plasma spraying	PSP

* Sometimes a welding process

OXYGEN CUTTING (OC)

chemical flux cutting	FOC
metal powder cutting	POC
oxyfuel gas cutting	OFC
– oxyacetylene cutting	OFC-A
– oxyhydrogen cutting	OFC-H
– oxynatural gas cutting	OFC-N
– oxypropane cutting	OFC-P
oxygen arc cutting	AOC
oxygen lance cutting	LOC

WELDING PROCESSES

ALLIED PROCESSES

THERMAL CUTTING (TC)

BRAZING (B)

arc brazing	AB
block brazing	BB
diffusion brazing	DFB
dip brazing	DB
flow brazing	FLB
furnace brazing	FB
induction brazing	IB
infrared brazing	IRB
resistance brazing	RB
torch brazing	TB
twin carbon arc brazing	TCAB

OTHER WELDING

electron beam welding	EBW
– high vacuum	EBW-HV
– medium vacuum	EBW-MV
– nonvacuum	EBW-NV
electroslag welding	ESW
flow welding	FLOW
induction welding	IW
laser beam welding	LBW
thermit welding	TW

OXYFUEL GAS WELDING (OFW)

air acetylene welding	AAW
oxyacetylene welding	OAW
oxyhydrogen welding	OHW
pressure gas welding	PGW

ADHESIVE BONDING (ABD)

ARC CUTTING (AC)

air carbon arc cutting	AAC
carbon arc cutting	CAC
gas metal arc cutting	GMAC
gas tungsten arc cutting	GTAC
metal arc cutting	MAC
plasma arc cutting	PAC
shielded metal arc cutting	PAC

OTHER CUTTING

electron beam cutting	EBC
laser beam cutting	LBC

Figure 2.1: Master chart for welding and allied processes (AWS).

In understanding the welding process, and specifically the processes used in the case study company and for this project then it is necessary to review and summarise the important technologies of the process itself.

Fusion welding, which includes gas, arc, and resistance welding, requires the parent metals to be melted. This distinguishes fusion welding from brazing. The case study

17

company for this project, TKA Tallent, uses fusion welding processes throughout its facilities. Although numerous types of welding procedures have been identified in American or British standards (as shown in Figure 2.1) the scope of this report shall however, be limited to the detailed discussion of Metal Inert Gas (MIG) welding.

The use of noble gases in welding started during the Second World War in the production of airplanes from aluminium and magnesium parts. The use of active gases started after 1950s. A typical schematic for modern gas welding processes is shown in Figure 2.2 to illustrate the general welding arrangement.
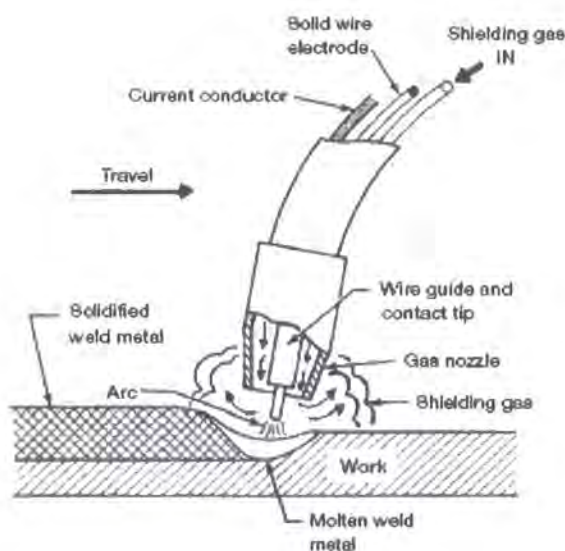
Figure 2.2: A schematic of a typical MIG/MAG weld process and welding gun (Masubuchi)

The basic principle of MIG (and also MAG) welding is that a metallic wire is fed through the welding gun and melted in an arc. This can be seen in the schematic in Figure 2.2 and also in the illustration of the actual process in Figure 2.3. The wire serves the dual purpose of acting as the current-carrying electrode and the weld metal filler material. Usually a bare wire is used but flux covered wires are used also. Electrical energy is supplied by a welding power source.

18
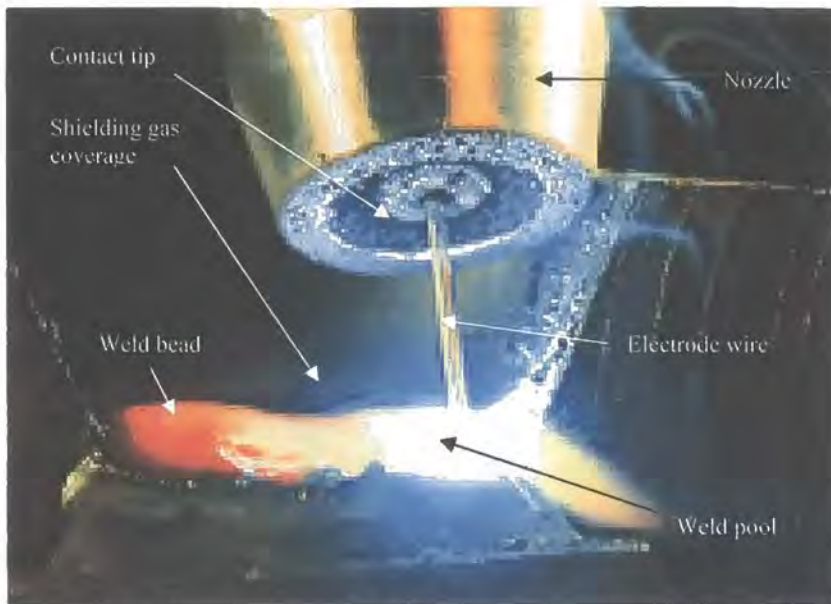
Figure 2.3: View of the weld pool and process in MAG welding

At TKA Tallent, the case study company for this project, the filler wire used is to specification code AWS A 5.18-01 ER70S-6 type, 1 or 1.2mm thick solid MIG/MAG welding wire held in 300kg endless drum. This is used in conjunction with the company's robotic welding processes. A typical robotic welding arrangement for the company is shown in Figure 2.4.

Figure 2.4: Motomann robotic welding system at TKA Tallent

To describe the process in more detail it can be stated that in the MIG / MAG welding process, the arc burns under the atmosphere of inert Argon or active Carbon

19

Dioxide gas. The process where a gas like Carbon Dioxide acts as a shielding gas is called "Metal Active Gas" and abbreviated as MAG. On the other hand, where Argon is used, the process is referred as "Metal Inert Gas" and abbreviated as MIG respectively. In this context, an inert gas is one that does not react with the molten material. Examples of gases in this category are Argon and Helium. Active gases, on the other hand, participate in the process between the arc and the molten material. Argon containing a small proportion of Carbon Dioxide or Oxygen is an example of an active gas.

Even just from the definitions, it can easily be seen how these 2 processes interact and interchange with each other. Its suitability for automation makes MIG/MAG Welding possibly the most desirable and practical process choice.

Figure 2.5 represents a schematic arrangement of the MIG welding procedure and equipment. It can be observed that a basic MIG welding system essentially consists of a power source, a wire feeding mechanism, a shielding gas cylinder, a regulator/flow meter and a MIG gun.
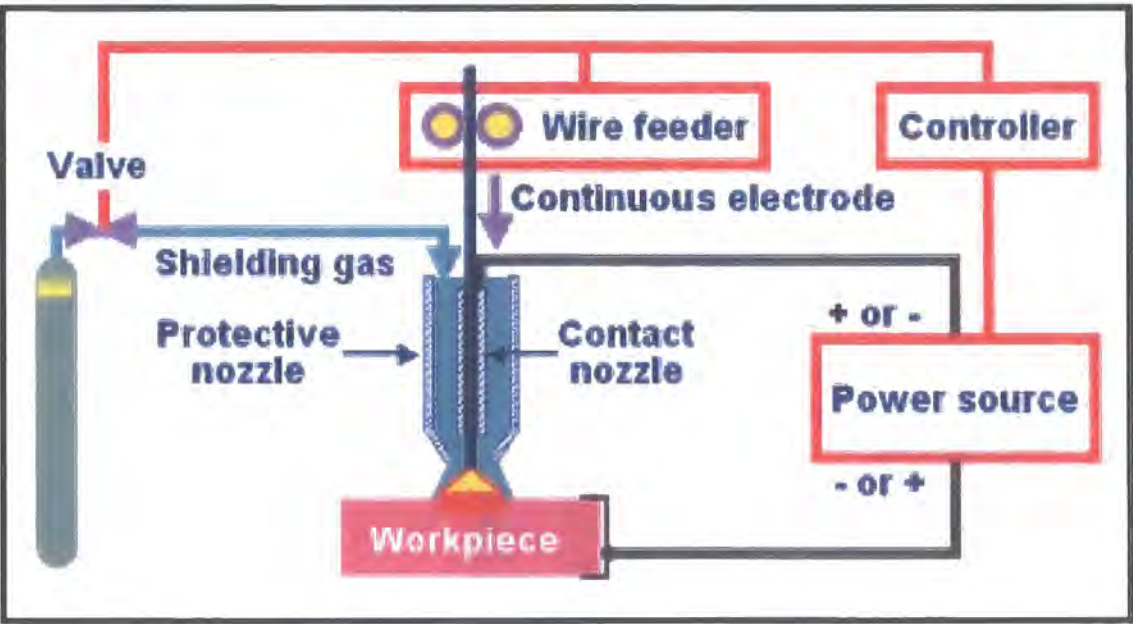
Figure 2.5: MIG welding system schematic

Shielding gases for arc welding and cutting are specified according to EN 439 'Welding consumables - shielding gases for arc welding and cutting' in Europe

20

(BS EN 439 in the UK), examples of which are shown in Table 2.2. The classification of gases according to EN 439 is given in Table 2.3. Selection of shielding gases for MIG/MAG welding is primarily dependent on the parent material for achieving better arc operation. At the same time it should be cost effective. The choice of gas is often a compromise between achieving stable metal transfer, minimising the risk of defects and obtaining the desired bead profile, penetration and considering any metallurgical effects of oxidation, as discussed by Gourd [1995].

Table 2.2: Shielding gases used for different metals and alloys

Metal	Shielding gas
Aluminium and alloys	Pure Argon
Nickel and alloys	Argon + Helium / pure Argon
Copper	Argon + Helium
Stainless steel	Argon + 3% Oxygen
Low carbon steel and carbon-manganese steel	Argon + Helium + CO_2 / Carbon Dioxide / Argon + 5-20% CO_2/ Argon + 5% CO_2
Steels with 1-2% chromium	Argon + 5-20% CO_2 / Argon +5% O_2
Steels with more than 2% chromium	Argon +5% O2

Table 2.3: Classification of shielding gases

Group code	Characteristic
R	Reducing gas mixtures
I	Inert gas mixtures
M	Oxidising mixtures containing either O_2, CO_2 or both
C	Highly oxidising mixtures
F	Unreactive gasses for specific applications

Table 2.2 represents the application of different shielding gases for welding of different parent metals. For welding carbon and low alloy steels it is essential to use active or oxidising gases to stabilise the arc and wetting of the weld pool. In case of stainless steel, Agon-CO_2/O_2 mixtures for spray transfer, or Argon-Helium-CO_2

21

mixtures for all modes of transfer are used for austenitic stainless steel. This is because austenitic steels have a high thermal conductivity, the addition of Helium helps to avoid lack of fusion defects and overcome the high heat dissipation into the material. Inert gases or their mixtures are used for light alloys and alloys that are sensitive to oxidation. Typical of such metals are Aluminium and Magnesium, Copper and Nickel and their alloys.

The flow rate of the shielding gas is also an important parameter in the welding procedure. This is because, if the flow rate is too low, the shielding atmosphere is merely a diluted air and will be ineffective. Similarly if it set too high, it shall cause turbulence in the gas stream and shall lead to air entrainment. It is therefore, essential to correctly select the welding gun nozzle. Figure 2.6 represents typical flow rates for different diameter nozzles and welding currents.
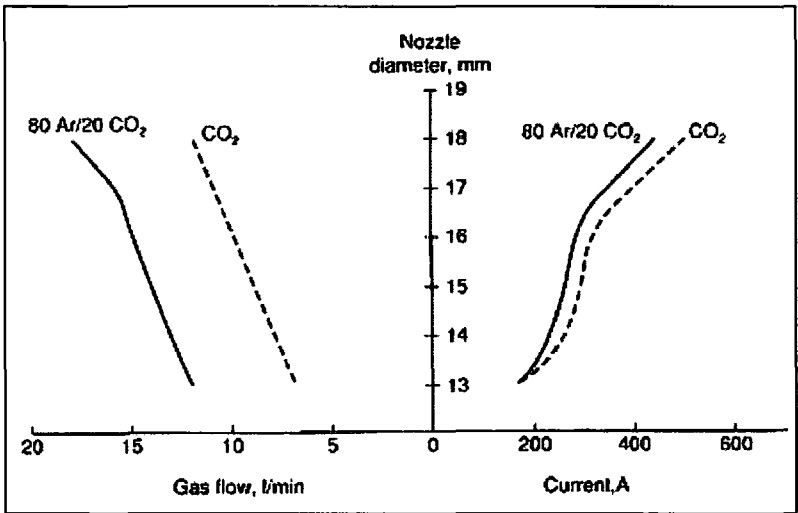
Figure 2.6: Flow rate for shielding gases at different nozzle diameters and for different welding gases (Gourd)

MIG/MAG wires are available in a wide range of compositions to suit different metallic materials, e.g. ferritic steels, austenitic stainless steels, aluminium alloys, nickel alloys, titanium alloys. These wires are normally specified by composition. Wires are typically supplied with diameters in the range 0.8mm to 2.4mm, normally available on 15kg reels, but large packs, as used at Tallent (up to 300kg) are available for robotic welding to minimise downtime in wire change operations. The

wire is often layer wound to ensure smooth feeding. Solid wires are commonly used but tubular cored wires may offer added benefits for some applications.

For most commercial applications, MIG is operated exclusively with a DC power source. Welding current is determined by wire feed speed, and arc length is determined by power source voltage level (open circuit voltage). Wire burn-off rate is automatically adjusted for any slight variation in the gun to workpiece distance, wire feed speed, or current pick-up in the contact tip.

In most cases, two current ranges are normally used for MIG welding. The higher range covers from 300A onwards which results in greater penetration. The lower current range 50-80A produces a small weld pool and naturally has less penetration. For both higher and lower current range, a wide range of power sources are available, with mode of metal transfer being either spray, dip or pulsed.

In the spray type transfer mode, metal is transferred as a spray of fine droplets without the wire touching the weld pool. The pool is retained in the position by an oxide skin which forms over the surface. The droplets are detached regularly from the end of the electrode and are transferred to the pool by electromagnetic force acting in the arc along the line of axis of the electrode. Both the welding current level and the arc voltage should be kept high and certainly above the minimum threshold level. Gourd [1995] states that the typical welding parameters for a 1.2mm diameter wire are within 250A \ 28V to 400A \ 35V. The common practice of the case study company is to operate its weldsets in spray transfer mode.

For the dip transfer mode for welding sheet metal, the heat input has to be significantly reduced. In case of dip transfer, a short arc is established at a low voltage and at current below 200 A, the end of electrode starts melting slowly. The output from the power supply is short circuited which enables the flow of a very high current. Ultimately the molten metal is transferred to the workpiece by the wire dipping into the weld pool. Circuit inductance is used to control the surge in current when the wire dips into the weld pool (which causes a spatter). Modern electronic

power sources automatically set the inductance to give a smooth arc and metal transfer.

In the pulse transfer technique, the arc is operated at normal arc length with a low background current of 50-100A. Pulses of high current are superimposed on to the low background current which results in the transfer of a single droplet before the current is returned to a low level, thereby giving a spray type transfer at a low heat input. As control of the arc and metal transfer requires careful setting of pulse and background parameters, a more sophisticated power source is required. According to Gourd [1995], Synergic pulsed MIG power sources, which are advanced transistor-controlled power sources, are pre-programmed so that the correct pulse parameters are delivered automatically as the welder varies wire feed speed.

Additional and comprehensive information on the welding process itself can be found in Lancaster [1992] which provides a review of welding and associated processes.

2.3 Weld Distortion

2.3.1 Weld Distortion and Residual Stresses

To be able to develop a tool to predict weld distortion, it is important to understand how different types of distortion are caused in welded fabrications and what effect they will have on the finished part.

Distortion is always a perennial problem resulting from most industrial metal working processes, which employs a concentrated nature of heat source. However, our focus in this report shall be concentrated primarily on welding distortions, and not of those from other heating processes.

Distortion in a welding procedure is actually, a result of non-uniform expansion and contraction of weld and the parent metal caused by the heating and cooling of the

weld process. Such a phenomenon can be explained by considering a weld bead depositing along the longitudinal axis of a plate with infinite width. The heated zone tries to expand but is restrained by the surrounding colder material, causing this zone to yield in compression. During the cooling cycle, the colder material prevents the contraction of this region, causing tensile stresses to be developed. This tensile stress around the weld with simultaneous generation of compressive stresses shall result in distortion if they exceed certain levels.

The welding process causes a highly non-uniform heating of the parts being joined. Areas close to the weld arc are heated up to several thousands degrees Celsius, and then cooled down, the heat being conducted to the bulk of the body. The local heating and subsequent cooling induces volumetric changes producing temporary and residual stresses and deformation. If, during heating, the elements of the weld were stressed elastically, then, after cooling, the body will return to its initial stress-free condition. However if, during heating, an element was deformed plastically, then, after cooling, it tends to change dimensions proportionally to the amount of the plastic deformation. All the elements now have different size and cannot be reassembled into a solid body without some changes in their stress and deformation state. As a result, residual stresses and deformation form in the body.

In general, the non-uniformity of the temperature distribution during welding of a real structure causes a complex three-axial stress. In other words, all elements in the structure expand differently in all three directions. But, in most cases some components of the stress are negligible, and it is possible to consider 2D or even 1D stressed states.

A simple model, first presented by Gunnert [1955], that can help to understand the process of 1D-stress formation, is presented in Figure 2.7, which assists in understanding how weld stresses develop. The model consists of one central rod and two limiting rods, joined with each other by the rigid plates, and each of the rods have the same initial length. The central rod is exposed to a high temperature simulating the zone close to the weld. The limiting rods are kept at a constant temperature, representing the rest of the joining plates.

Heating the central rod up will cause it to try to expand. The limiting rods do not allow a free expansion of the central one, causing rising compression stresses in the central rod. If the central rod has been compressed elastically, then, after cooling, the system comes to its initial stress, and deformation, free state. But, if during heating the central rod was compressed plastically, then a plastic compressive strain is introduced into the rod. During the cooling stage the central rod tends to contract while the limiting rods are trying to keep their initial length. Hence, in the central rod tensile stresses occur, and the limiting rods are being subjected to compressive stresses.

It should however be remembered that during welding the process of stress-strain field development is characterised by the elastic-plastic behaviour of the metal, non-stationary temperature conditions with a high temperature limit, and very high temperature gradients. The transient and residual stress development is based on volumetric change of the structure elements. With the heat propagating through the body and the temperature equalisation, the metal redistribution continues. The transient stress field during welding is a process of stress development lasting the whole period of welding and subsequent cooling. The transient stress investigation is therefore a complicated task because of the huge amount of variables affecting the process.

initial condition   *heating*   *cooled down*   *butt-welded plates*
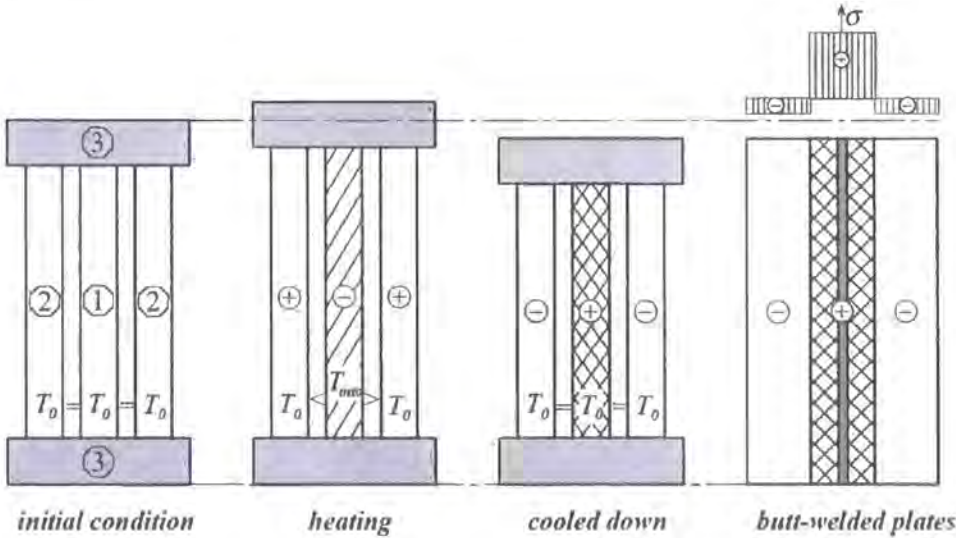
Figure 2.7: 3 rod system to represent a butt weld (Gunnert)

Residual stresses can be defined as stresses that are locked into a component or assembly of parts. Such internal stresses can be developed by mechanical processing of the parts such as bending, rolling and forging. Such stresses can also be induced due to other factors like surface removal operations (e.g. machining), surface treatment operations (e.g. shot peening) or by heat treatment. In addition to that, residual stresses can be generated due to thermal stresses generated during welding which have a major influence on welding distortions. Although residual stresses have a major influence on welding distortions, from manufacturing point of view, residual stresses do not always have detrimental effects. Though tensile stresses reduce the mechanical performance of materials, compressive residual stresses can actually increase the fatigue life of a component and stress corrosion by delaying crack initiation and propagation.

All fusion welds which are not subjected to post weld treatment, contains residual stresses. The residual stress distributions found across a typical small sample butt weld are show in Figure 2.8, and it should be noted that the peak stress value can be up to just below the yield value. Welding procedures that are developed to minimise distortion cannot actually eliminate residual stresses or reduce their peak value, they aim to alter the distribution of the residual stresses. If residual stresses are not desired in some service requirements, designers take them into account while selecting material and determining the safe working stress. A typical example of it is in the design of ships where a combination of low temperature and residual stresses could lead to a type of failure called a brittle fracture. To counter this effect, appropriate material is generally selected which is not susceptible to this mode of failure even at low temperatures. However, in certain other applications e.g. in case of pressure vessels, it is essential to reduce the existence of residual stresses in the welded joint. To reduce the level of residual stresses in such cases, special operations are carried out e.g. stress relieving.
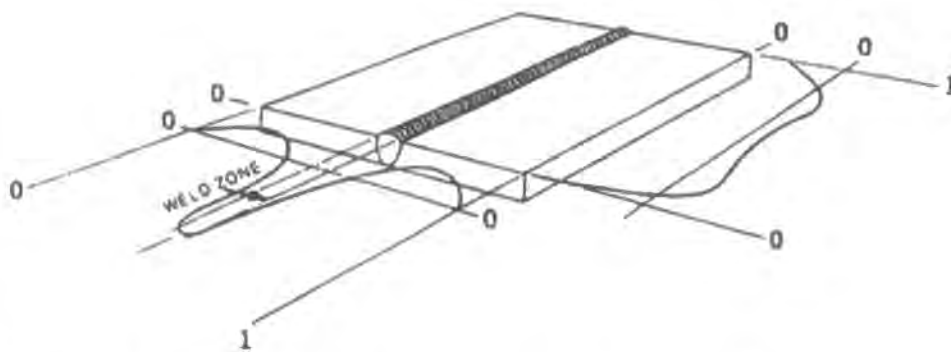
Figure 2.8: Residual stress distribution in a butt weld sample.

Recent years have witnessed a considerable research work on prediction of residual stresses by numerical modelling of welding. Further investigations have been carried out in different experiments to validate the results predicted by numerical modelling. Residual stresses in as-welded structures may be minimised by appropriate selection of materials, welding process and parameters, structural geometry and fabrication sequence. Residual stresses may be reduced by various special welding techniques including low stress non-distortion welding (LSND), last pass heat sink welding (LPHSW) or inter-run peening.

Residual stresses, as discussed here, and resultant distortion can have negative influence on the production in terms of performance, aesthetics and finished quality. Tensile residual stresses reduce the fatigue strength and on the other hand compressive stresses reduce the stability. In addition, distortion can have negative impact on permissible tolerances resulting in bad alignments, and unacceptable gaps in joints.

2.3.2 Types of Weld Distortion

Distortion in welded fabrications is caused by three fundamental dimensional changes, which are:

1. Transverse shrinkage perpendicular to the weld line.
2. Longitudinal shrinkage parallel to the weld line.
3. Angular distortion (and bowing, buckling and twisting) – rotation around the weld line.

These distortions can be seen represented diagrammatically in Figure 2.9. The distortion types will each be discussed in greater detail, subsequently but in summary the following can be stated:

Both the transverse and longitudinal shrinkage occurs due to contraction of weld area on cooling. In transverse shrinkage the contracting weld metal tries to pull the plates towards the centre line of the joint and as a result the whole joint is in transverse tension. Since the hot weld metal has a lower yield stress than the cold plates, deformation first takes place at the weld but gradually when the relative yield stress becomes more equal, some yielding of the parent material occurs and overall width of the welded plates is reduced. Non-uniform contraction (through thickness) produces angular distortion in addition to longitudinal and transverse shrinkage. Longitudinal bowing in welded plates can occur when the weld centre is not coincident with the neutral axis of the section so that longitudinal shrinkage in the welds bends the section into a curved shape. Dishing is generally produced in stiffened plating, where plates tend to dish inwards between the stiffeners, because of angular distortion at the stiffener attachment welds, Furthermore in plating, long range compressive stresses can cause elastic buckling in thin plates, resulting in dishing, bowing or rippling. Twisting can be observed in a box section due to shear deformation at the corner joints which is caused by unequal longitudinal thermal expansion of the abutting edges.

29
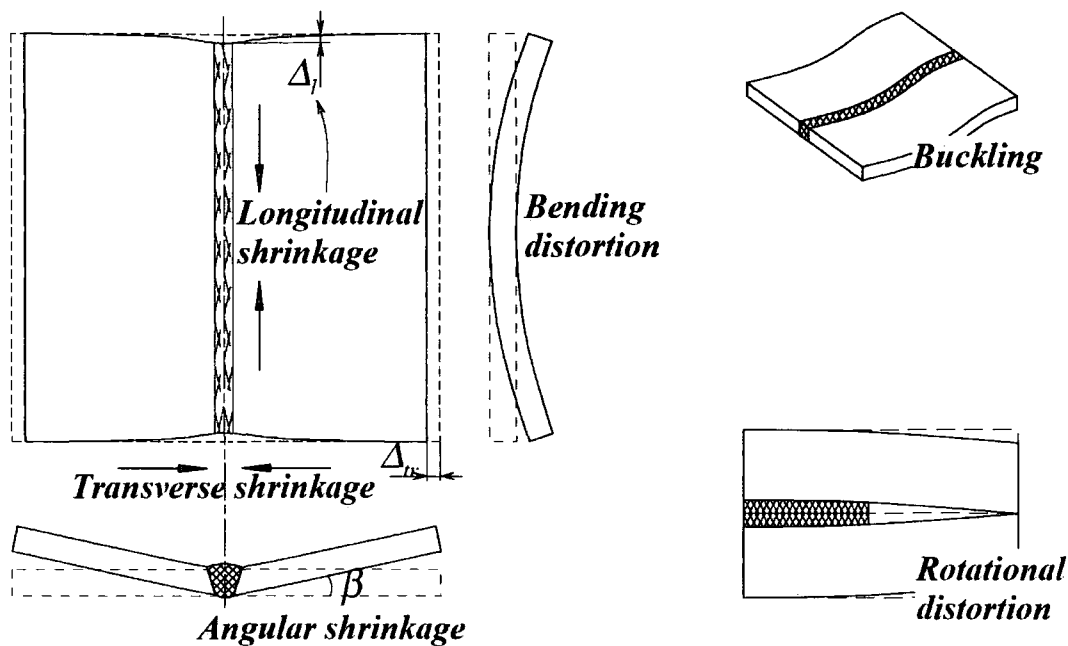
Figure 2.9: Primary types of weld distortion shapes

There now follows a further brief discussion on each of these distortion modes, however it should be noted that it is rare for each of the specifically mentioned distortion types to occur in absolute isolation, with the final resultant distortion usually being a combination of a number of these modes.

Firstly let us consider longitudinal and transverse shrinkage in butt welds as a basic joint to understand the mechanism further. After the welding high heat cycle and during cooling the elements of the plate gradually return to their initial geometrical state, except the elements close to the weld centreline (not only the elements of the HAZ). Some elements of the HAZ during the heating period could also achieve plastic deformation. As a result in the cooled down state, the outer edges of the plate come closer to the weld centreline.

Gatovskii [1973] in his works, based on several simplifications, introduces a physical model for residual transverse and longitudinal shrinkage. Also, according to Gatovskii and Karkin [1980], the residual longitudinal and transverse shrinkage can be expressed in similar terms.

30

$$\Delta_{tr} = \mu_{tr} \cdot \frac{\alpha}{c\rho} \cdot \frac{q_w}{h} = -1.25 \cdot \frac{\alpha}{c\rho} \cdot \frac{q_w}{h}$$

$$\Delta_l = \mu_l \cdot \frac{\alpha}{c\rho} \cdot \frac{q_w}{h} = -0.335 \cdot \frac{\alpha}{c\rho} \cdot \frac{q_w}{A} \cdot L_w$$

where:

μ_{tr} and μ_l are coefficients of transverse and longitudinal shrinkage;

q_w is net heat input per unit length of weld [$J.s^{-1}.m^{-1}$];

A – cross-section area [m^2];

L_w – weld length [m].

Vinokurov [1977] in his works assign the value of the μ_{tr} to be in the interval between 1.0 and 1.4 (μ_{tr}=1.0 |1.4). He also postulates that the transverse shrinkage equation works for low-carbon, low-alloy and austenitic steels for the thickness up to 16mm.

The equations introduced above are approximate, but for the most cases they work quite well according to the research, with some exceptions such as significant effects of the heat loss from the surfaces. In these exceptional cases then longitudinal and transverse shrinkage can be noticeably reduced. Also exceptions would occur for the welding of pre-stressed parts and welding with incomplete penetration, as the cold metal beneath the weld gives additional stiffness to the structure, hence reducing the longitudinal and transverse deformations.

These equations give only estimates because according to them, the plates are shrunk proportionally. But, the real shape of the deformed plates is more complicated than a simple rectangle. In Figure 2.10 an example of the real shape of deformation is shown, in comparison to the uniform distortion calculated by the equations.

31
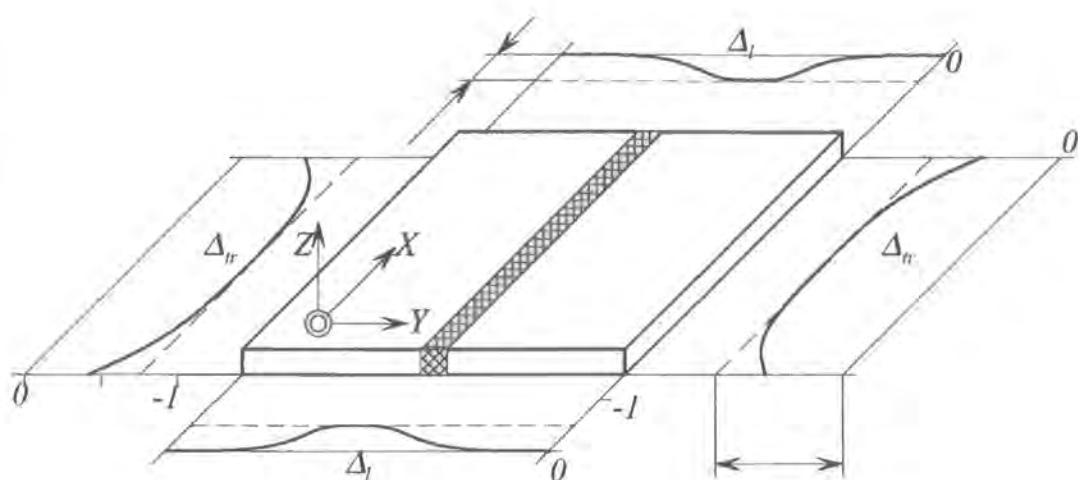
Figure 2.10: In plane distortions and magnitudes (Gatovskii)

It is evident that the longitudinal shrinkage is concentrated mostly close to the weld. Over the rest of the plate width it is close to zero if the plates are wide and, hence, stiff enough to withstand the longitudinal load applied along the weld centreline. The transverse shrinkage is larger in the middle section of the plate compared to that at both ends. This gives the U-shaped distribution along the length of the plate. The uneven character of the distribution smoothes out with increasing plate width. The U-shaped transverse shrinkage distribution can be explained by the reduced stiffness of the plates close to the edges. The section situated close to the beginning or end of the weld, is less restricted during the initial weld heat stages. It leads to reduced transverse shrinkage close to the plate ends. At the same time, such a U-shape is not uniquely defined. In some instances (for example, small specimens) a barrel-like distortion can be achieved.

Transverse shrinkage is shrinkage perpendicular to the weld line, in other words across the joint. Shrinkage occurs over the total weld length. The mechanisms of transverse shrinkage have been studied by several investigators including Naka [1950] and Fujita, Nomoto and Matsui [1978]. Findings from these mathematical studies show that the major part of transverse shrinkage is due to contraction of the base plate. The base plate expands during welding. As the weld metal solidifies, the weld metal must shrink which accounts for the transverse

32

shrinkage mechanism as described earlier. According to Iwamura [1974], in his study on aluminium joints, in a butt weld, this is mainly caused by the expansion and contraction of the base material. Also according to the same author, only 10 % of the overall transverse shrinkage occurs because of the contraction of weld metal. After welding, the heat is transmitted to the parent or base material, which causes it to expand. At this point, the weld has no strength and yields under the forces causing it to contract. At a certain temperature, the weld metal starts resisting the additional expansion of the plate. It is at this moment that the thermal deformation of the plate and the contraction of the weld metal during cooling cause the shrinkage.

Angular change is caused by a non uniform thermal distribution in the thickness direction close to the weld line. When a joint is free from external restraint, the structure bends at the joint during the welding process. The solidification from the weld bead causes contraction while the bottom side of the plate expands causing the plates to lift. In a tee joint, it is expected that the bottom plate will form a wavy pattern due to the top plate acting as a stiffener. If the top plate remains unrestrained, this is expected to pull over to the weld bead side.

This type of distortion is also called warpage. The distortion measurement is actually the angle between the materials joined by welding. When two plates are welded together especially in butt configuration, the amount of weld metal deposited on the top surface is the cause for this type of distortion. The base material under the solidifying weld metal expands again due to the heating cycle. This time there are two forces, i.e. double forces acting together. The contraction of the weld and the expansion of the unfused material underneath the weld pool are the causes. Okerblom [1955], who has looked at this type of distortion in butt welds, however noted that during experiments it was observed that this movement did not happen simultaneously over the whole length of the weld. It was rather like a twisting and buckling movement on the plates.

Longitudinal shrinkage is shrinkage in the direction of the weld line. It is caused when material yields in the heat affected area behind the weld torch. This area restrained by the stiff, cold surrounding parent metal. Tensile stresses acting on the

33

rest of the plate counter balance this. When the area cools down, the reaction reverses itself as tension then acts on the weld and the rest of the plate is in compression. Guyot [1947] carried out extensive studies into this, whilst Okerblom [1955] has also extensively studied this type of distortion and carried out many experiments, and is frequently cited.

Rotational distortion is angular distortion in the plane of the plate due to thermal expansion. Studies have been carried out by Kihara and Masubuchi [1956] who found that rotational distortion is affected by both heat input and welding speed. It is caused by the separating forces during MIG welding that cause the joints to open up. To overcome this, it is necessary to tack the plates together before welding.

Buckling is caused by thermal compressive stresses that result in instability in thin plates. Watanabe and Satoh [1961] have both investigated the buckling that occurs in long steel strips. It has been found that buckling distortion occurs when the specimen length exceeds the critical length for a given thickness. It differs from bending distortion as there is more than one stable deformed shape and the amount of deformation is much greater.

Longitudinal bending is distortion in a plane through the weld line and perpendicular to the plate. It is caused when the weld line does not line up with the neutral axis of the welded fabrication. The longitudinal shrinkage of the weld metal induces bending moments resulting in the longitudinal distortion. Various studies have been carried out into this theory. Sasayama, Masubuchi and Moriguchi [1955] found that when welding Tee joints and I beams in low carbon steel, the deformation gradually increases as the weld line progresses. Again Okerblom [1955] has a model describing this kind of distortion. Nevertheless, authors like Blodgett [1966] have similar studies and models.

It must however be emphasized that although it might seem straight forward in terms of classification and understanding of the distortion phenomena, when there are several factors involved, the residual stresses may act in a complex way, more so

34

than each of the distortion type separately. The discussions here are kept brief as specific models are discussed later in this chapter and further in Chapter 5.

2.3.3 Factors Affecting Distortion

In welding process, there are numerous differing and interacting factors. When this combines with the several parameters involved in the process itself, it is not hard to realise the enormous possible combinations and outcomes. The factors affecting distortion can be summarised and described as per the follow sections:

The inherent stresses in the material to be welded are important in the final distortion outcome. Stresses in a material usually originate from a mechanical cause, usually the manufacturing process, for example from cold forming, rolling, shearing/guillotining, and others. These give the material its required shape but create internal residual stresses. The general view that can be gathered from research states that the greater the shape change, the greater the residual stresses become. During the welding process, extra stresses are created, as previously described which either result in increase or reversely decrease of these inherent stresses that already existed.

It is usual to apply restraint, such as clamping, to material to be welded. Applying any form of restraint prevents or opposes shrinkage which in return reduces the overall distortion. The final shape of the member being welded is dependent on the type and amount of intensity of the restraint that has been applied. However, this restraining causes the stresses to build up in the fabrication. The general acceptance and common practice are the use of heavy restraint in order to stop distortion happening. In the example of the case study company this is the usual current industrial practice in the majority of their welding operations.

If a component is welded without any external restraint, it distorts to relieve the welding stresses. Therefore, methods of restraint, such as 'strong-backs' in butt welds, can prevent movement and reduce distortion. As restraint produces higher

35

levels of residual stress in the material, there is a greater risk of cracking in weld metal and heat affected zone, HAZ, especially in crack-sensitive materials.

Mechanical, thermal and physical properties of metals also influence the degree of distortion taking place. Some of these properties are modulus of elasticity, yield strength, thermal conductivity, coefficient of thermal expansion and specific heat capacity. As distortion is determined by expansion and contraction of the material, the coefficient of thermal expansion of the material plays a significant role in determining the stresses generated during welding and, hence, the degree of distortion. For example, as stainless steel has a higher coefficient of expansion than plain carbon steel, it is therefore more likely to suffer from greater distortion.

The joint design, tolerance and the accuracy of manufacture also influence distortion. Both butt and fillet joints can be subject or vulnerable to distortion. It can be minimised in butt joints by adopting a joint type which balances the thermal stresses through the plate thickness, for example, a double-sided application instead of a single-sided weld. Double-sided fillet welds should eliminate angular distortion of the upstanding member, especially if the two welds are deposited at the same time. However, this is not always practical or achievable, possibly due to access restriction or even design consideration. The usual practice to reduce the amount of distortion is to use the minimum number of weld runs of weld and also minimise weld volume. The design and preparation of the joint was found to be utmost important in order to accomplish this. Presetting and welding uniformly around the neutral axis are common practices to assist in the goal of minimising distortion.

In order to have the best possible weld result, including the lowest possible distortion, fit-up should be uniform to produce predictable and consistent shrinkage. Excessive joint gap can also increase the degree of distortion by increasing the amount of weld metal needed to fill the joint. The joints are usually adequately tacked to prevent relative movement between the parts during welding, if clamping and fixturing is not possible or appropriate.

The welding procedure itself influences the degree of distortion, mainly through its effect on the heat input. As welding procedure is usually selected for reasons of quality, consistency, repeatability and productivity, the welder has limited scope for reducing distortion. As a general rule, weld volume should be kept to a minimum. Also, the welding sequence and technique should aim to balance the thermally induced stresses around the neutral axis of the component.
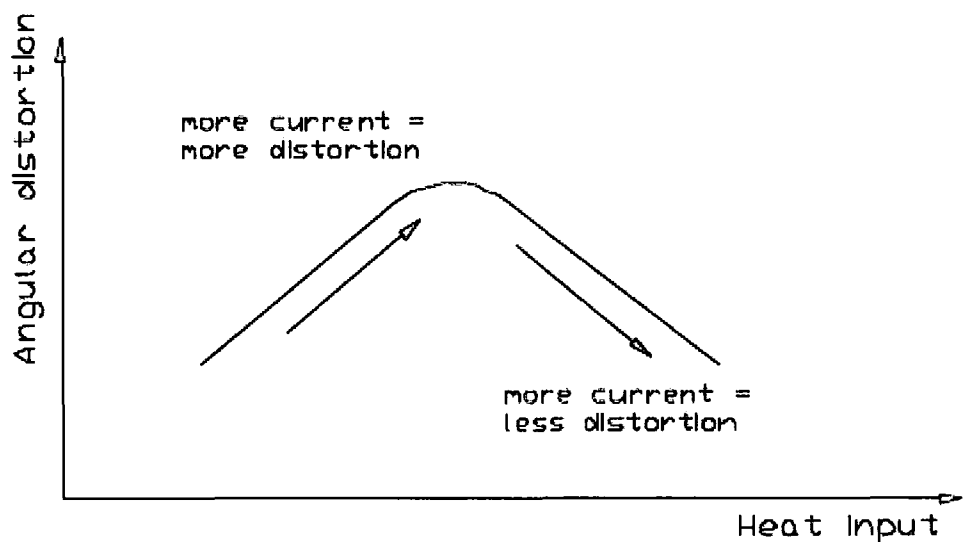
Figure 2.11: Influence of welding current on angular distortion (Mishler)

The influence of welding current on angular distortion is shown in Figure 2.11, by Mishler [1989], where it is evident that with increasing welding current, it results in deeper penetration of weld, effectively giving better quality and more fully fused weld. Another factor is the travel speed of the heat source or arc. Mishler also states that if the travel speed is relatively fast, the effect of the heat of the arc will cause expansion of the edges of the plates, and they will bow outward and open up the joint.

37

2.4 Prevention of Welding Distortion

Distortion can often be prevented, or at least restricted, by considering a number of factors in the product, process and fixturing. These can be classified into reduction of distortion by:

- Product design considerations
- Process design considerations
- Assembly and fixture design
- Weld process selection

It is important that each of these is given appropriate consideration during the development phase to attempt to plan for the lowest possible distortion outcomes.

2.4.1 Prevention of Welding Distortion by Product Design

Welding can often be eliminated at the design stage by forming the plate or using a standard rolled section. If such a design is not possible then it may be possible to reduce the amount of weld to be laid down. In such cases intermittent welds should be employed rather than a continuous run, to reduce the amount of welding. For example, in attaching stiffening plates, a substantial reduction in the amount of welding can often be achieved whilst maintaining adequate strength. Placing and balancing of welds are important. For example, the closer a weld is positioned to the neutral axis of a fabrication, the lower the leverage effect of the shrinkage forces and the final distortion. As most welds are deposited away from the neutral axis, distortion can be minimised by designing the fabrication so that the shrinkage forces of an individual weld are balanced by placing another weld on the opposite side of the neutral axis. Whenever possible, welding should be carried out alternately on opposite sides, instead of completing one side first. The volume of weld metal should be limited to the design requirements. For a single-sided joint, the cross-section of the weld should be kept as small as possible to reduce the level of angular distortion. Joint preparation angle and root gap should be minimised - provided that the weld can be made satisfactorily. To facilitate access, it may be possible to

38

specify a larger root gap and smaller preparation angle. By cutting down the difference in the amount of weld metal at the root and at the face of the weld, the degree of angular distortion will be correspondingly reduced.

2.4.2 Prevention of Distortion by Choice of Welding Process and Technique

The amount of distortion will be influenced by:
- Choice of welding process
- Reduction in the amount of weld metal
- Reduction in the number of runs
- Use of balanced welding techniques

Choice of welding process: Butt joints made in a single pass using deep penetration have little angular distortion, especially if a closed butt joint can be welded. For example, thin section material can be welded using plasma and laser welding processes and thick section can be welded, in the vertical position, using electrogas and electroslag processes. Although angular distortion can be eliminated, there will still be longitudinal and transverse shrinkage.

Reduction in the amount of weld metal: In thick section material, as the cross-sectional area of a double-V joint preparation is often only half that of a single-V preparation, the volume of weld metal to be deposited can be substantially reduced. The double-V joint preparation also permits balanced welding about the middle of the joint to eliminate angular distortion. As weld shrinkage is proportional to the amount of weld metal, both poor joint fit-up and over-welding will increase the amount of distortion. Angular distortion in fillet welds is particularly affected by over-welding. As design strength is based on throat thickness, over-welding to produce a convex weld bead does not increase the allowable design strength but it will increase shrinkage and distortion.

Reduction in the number of runs: There are conflicting opinions on whether it is better to deposit a given volume of weld metal using a small number of large weld

passes or a large number of small passes. Experience shows that for a single-sided butt joint, or a single-side fillet weld, a large single weld deposit gives less angular distortion than if the weld is made with a number of small runs. Generally, in an unrestrained joint, the degree of angular distortion is approximately proportional to the number of passes. Completing the joint with a small number of large weld deposits results in more longitudinal and transverse shrinkage than a weld completed in a large number of small passes. In a multi-pass weld, previously deposited weld metal provides restraint, so the angular distortion per pass decreases as the weld is built up. Large deposits also increase the risk of elastic buckling particularly in thin section plate.

Use of balanced welding techniques: Balanced welding is an effective means of controlling angular distortion in a multi-pass butt weld by arranging the welding sequence to ensure that angular distortion is continually being corrected. The balanced welding technique can also be applied to fillet joints. If welding alternately on either side of the joint is not possible, an asymmetrical joint preparation may be used with more weld metal being deposited on the second side. The greater contraction resulting from depositing the weld metal on the second side will help counteract the distortion on the first side.

2.4.3 Prevention of Distortion by Assembly Techniques

Distortion can often be prevented by employing suitable assembly techniques including:
- Pre-setting of parts
- Pre-bending of parts
- Tack welding
- Back-to-back assembly
- Stiffening
- Restraint

Pre-setting of parts: The parts are pre-set and left free to move during welding. In practice, the parts are pre-set by a pre-determined amount so that distortion occurring during welding is used to achieve overall alignment and dimensional control. The main advantages compared with the use of restraint are that expensive equipment is not needed and there will be lower residual stress in the structure. Unfortunately, as it is difficult to predict the amount of pre-setting needed to accommodate shrinkage, a number of trial welds will be required. For example, when MMA or MIG welding butt joints, the joint gap will normally close ahead of welding, but when submerged arc welding, the joint may open up during welding. When carrying out trial welds, it is also essential that the test structure is reasonably representative of the full-size structure in order to produce the level of distortion likely to occur in practice. For these reasons, pre-setting is a technique more suitable for simple components or assemblies.

Pre-bending of parts: Pre-bending, or pre-springing the parts before welding is a technique used to pre-stress the assembly to counteract shrinkage during welding. Pre-bending by means of strong-backs and wedges can be used to pre-set a seam before welding to compensate for angular distortion. Releasing the wedges after welding will allow the parts to move back into alignment.

Tack welding: Tack welds are ideal for setting and maintaining the joint gap but they can also be used to resist transverse shrinkage. To be effective, the number of tack welds, their length and the distance between them should be considered. With too few, there is the risk of the joint progressively closing up as welding proceeds. In a long seam, using MMA or MIG, the joint edges may even overlap. It should be noted that when using the submerged arc process, the joint might open up if not adequately tacked. In the tack welding sequence it is important to maintain a uniform root gap along the length of the joint. Directional tacking is a useful technique for controlling the joint gap, for example closing a joint gap which is (or has become) too wide. When tack welding, it is important that tacks which are to be fused into the main weld are produced to an approved procedure using appropriately qualified welders. The procedure may require preheat and an approved consumable

41

as specified for the main weld. Removal of the tacks also needs careful control to avoid causing defects in the component surface.

Back-to-back assembly: By tack welding or clamping two identical components back-to-back, welding of both components can be balanced around the neutral axis of the combined assembly. It is recommended that the assembly is stress relieved before separating the components. If stress relieving is not done, it may be necessary to insert wedges between the components, so when the wedges are removed, the parts will move back to the correct shape or alignment.

Stiffening: Longitudinal shrinkage in butt welded seams often results in bowing, especially when fabricating thin plate structures. Longitudinal stiffeners, in the form of flats or angles, welded along each side of the seam are effective in preventing longitudinal bowing stiffener location is important: they must be placed at a sufficient distance from the joint so they do not interfere with welding, unless located on the reverse side of a joint welded from one side.

Restraint: Owing to the difficulty in applying pre-setting and pre-bending, restraint is the more widely practised technique. The basic principle is that the parts are placed in position and held under restraint to minimise any movement during welding. When removing the component from the restraining equipment, a relatively small amount of movement will occur due to locked-in stresses. This can be cured by either applying a small amount of pre-set or stress relieving before removing the restraint. When welding assemblies all the component parts should be held in the correct position until completion of the welding cycle. This is along with use of a suitably balanced fabrication sequence to minimise distortion. Restraint is relatively simple to apply using clamps, jigs and fixtures to hold the parts.

42

2.4.4 Prevention of Distortion by Welding Procedure

A welding procedure is usually determined by productivity and quality requirements, rather than the need to control distortion. Nevertheless, the welding process, technique and welding sequence do influence the level of distortion.

Special welding techniques have also been developed which minimises, infact, almost eliminates distortions, e.g. LSND welding (Low Stress No Distortion). Figure 2.12, as shown by Guan, Leggatt and Brown [1988] represents a comparative distortion behaviour between conventional welding and low stress non distortion welding.
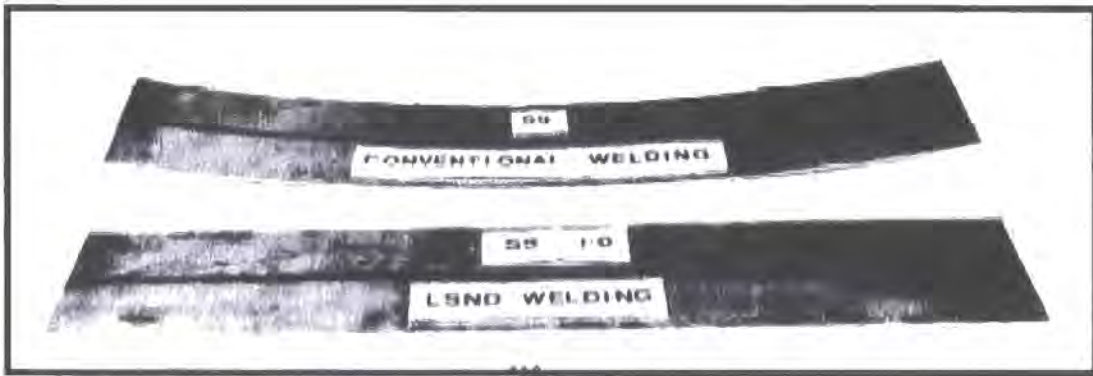
Figure 2.12: Distortion behaviour in LSND welding

2.5 Techniques to Correct Distortion

The following sections briefly explain the commonly used industrial methods for overcoming actual distortions that occur in the fabrication of products through the welding process. Each process has it relative strengths and also, however, some shortcomings and drawbacks that must be considered and taken into account before any course of rework is decided upon. The techniques can be broadly split into two categories, which are the application of mechanical rework techniques, or those that require the application of heat via a thermal process.

43

2.5.1 Mechanical Techniques

The principal mechanical techniques to correct distortion are hammering and pressing. Hammering may cause surface damage and work-hardening, which in turn can lead to other problems such as reduced durability due to stress defects, or changed structural performance. In cases of bowing or angular distortion, the complete component can often be straightened on a press without the disadvantages of hammering. Packing-pieces are inserted between the component and the platens of the press. It is important to impose sufficient deformation to give over-correction so that the normal elastic spring-back will allow the component to assume its correct shape after the correction process.

2.5.2 Thermal Techniques

The basic principle behind thermal techniques is to create sufficiently high local stresses so that, on cooling, the component is pulled back into shape. This is achieved by locally heating the material to a temperature where plastic deformation will occur as the hot material with reduced yield strength tries to expand against the surrounding cold metal with higher yield strength. On cooling to room temperature, the heated area will attempt to shrink to a smaller size than before heating. Local heating is, therefore, a relatively simply but effective means of correcting welding distortion. Shrinkage level is determined by the size, number, location and temperature of the heated zones. The number and placement of heating zones are largely determined from previous experience. Therefore, for new designs, tests will often be needed to quantify the level of shrinkage. Spot, line or wedge-shaped heating techniques can all be used in thermal correction of distortion. However, the potential shortcoming of using thermal straightening methods is the risk of over-shrinking too large an area or causing metallurgical changes by heating to an excessively high temperature.

44

2.6 Distortion Prediction Methods

Many methods and approaches exist and have been postulated to classify and predict the various types of weld distortion occurring in components. These methods can be split into two broad areas which will be discussed in this section. Firstly, we will look at some of the analytical, theoretical and experimental methods and models, before we later look at the more complicated and advanced computational based methods, which try to take into consideration various aspect of the physics of welding in order to improve both the application and generality of the prediction method.

2.6.1 Prediction of Weld Distortions – Analytical, Theoretical and Experimental Methods

With increasing stringent accuracy requirements in specialised fabrication processes, quantification of the level of distortion due to welding has become essential. However, it is needless to mention that a simple numerical model cannot be established to predict distortion, since it depends on a number of factors and different welding procedures.

There have been numerous research works undertaken to predict weld distortion behaviour models in order to reduce practical works involved to predict actual distortion in a process. However, in most industrial applications such models may not be enough to predict the actual distortions encountered in the process. Most companies therefore tend to carry out prototype welding procedures to figure out the actual distortions that can be encountered during the production process.

A brief account of a few of the weld distortion key theoretical prediction models have been outlined below, from the comprehensive review of the subject undertaken by Verhaeghe [1998], indicating where the models have been validated and their limitations. Tables 2.4 to 2.7 look at each of the key distortion types, and list some

45

of the important existing analytical models for predicting the distortion, highlighting some of the key points or limitations specific to each approach.

Table 2.4: Summary of sample longitudinal shrinkage models

MODEL	COMMENTS
Okerblom $\varepsilon_L = \dfrac{\delta_L}{L} = 0.335 \cdot \dfrac{1}{A} \cdot \dfrac{q}{v} \cdot \dfrac{\alpha}{\rho c}$	Assumed that the weld is deposited simultaneously over the whole length. Model is therefore valid for fast moving heat sources or short welds.
Horst Plufg $\dfrac{\delta_L}{L} = 42 \cdot \dfrac{\sigma_r}{E} \cdot \dfrac{A_w}{A - A_w}$	Model is based on and similar to OkerBlom's reasoning. Therefore this model has similar limitations.
Guyot $\dfrac{\delta_L}{L} = \dfrac{A_w}{A} \cdot 0.025$	Model is valid only if the resisting (cross sectional area of the colder parent metal) cross sectional area is less than 20 times the cross sectional area of the weld.

Table 2.5: Summary of sample angular distortion models

MODEL	COMMENTS
Okerblom $\beta_f = C \cdot \eta_m \cdot \dfrac{q}{vt^2}$	Valid for a parabolic shaped butt weld where p/t < 0.6 (partially penetrated bead on weld) and b/t < 1.5
Leggatt $\beta_f = 0.22 \cdot \dfrac{q}{v} \cdot \dfrac{1}{t_c^2}$	Model is applicable for weld penetration less than half the plate thickness; maximum penetration is observed when the penetration is approximately half the plate thickness.
Blodgett $\beta_f = 0.053 \cdot \dfrac{b_f \cdot a^{1.3}}{t_f^2}$	Thickness of the weld plate and the weld throat thickness have been considered to be the most important factors. (For Fillet welds).

Table 2.6: Summary of sample transverse shrinkage models

MODEL	COMMENTS
Okerblom $$\delta_T = 0.293 \cdot \frac{\alpha}{\rho c} \cdot \frac{q}{v} \cdot \frac{1}{t}$$	Model is valid for fast moving heat sources or short welds. Formula is only valid for butt welds where the penetration(p) is more than 0.4 times the plate thickness(t).
Watanabe and Satoh $$\delta_T = \left(\frac{\eta \cdot V}{\varnothing^{0.25}} \right)^2 \cdot \left(\frac{I}{t\sqrt{v}} \right)^2$$	Model is valid for one pass welding such as bead on plate weld (derived based on MMA).
Leggatt $$\delta_T = (1 + v) \cdot \eta \cdot \frac{\alpha}{\rho c} \cdot \frac{q}{v \cdot t}$$	Model indicates the maximum value of a single pass weld, assuming all thermal expansion being prevented, shrinkage taken place freely.
Capel $$\delta_T = C \cdot \frac{q}{v} \cdot \frac{1}{t_w}$$	Constant C depends on the material being used, e.g. 3.78x 10^{-3} and 2.90x 10^{-3} for structural steels.
Hansen $$\delta_T = 1 + 0.044 \cdot t$$	Model is based on an unrestrained double V butt weld, with included angle 60° and material thickness in between 16- 64 mm.
Gilde $$\delta_T = \eta \cdot \frac{q}{v \cdot t} \cdot \alpha \cdot \frac{\kappa}{\lambda} = \eta \cdot \frac{\alpha}{\rho c} \cdot \frac{q}{v} \cdot \frac{1}{t}$$	Model is applicable for both structural steels and stainless steels.

47

Table 2.7: Summary of sample bowing distortion models

MODEL		COMMENTS
Okerblom	$\dfrac{1}{R} = 0.335 \cdot \dfrac{q}{v} \cdot \dfrac{\alpha}{\rho c} \cdot \dfrac{y}{J}$	Formula has been derived from distortion model of longitudinal shrinkage.
Blodgett	$\dfrac{1}{R} = 0.04 \cdot \dfrac{A_w \cdot y}{J}$	Formula has been derived from the basic formula defined by the author for actual flex, applicable for various structures.
Horst Pflug	$\dfrac{1}{R} = 42 \cdot \dfrac{\sigma_Y}{E} \cdot \dfrac{A_w \cdot y}{J}$	Model is based on Okerblom's line of reasoning.

An investigation into distortion analysis and prediction of welded 'T-type' stiffeners, related to the shipbuilding industry, at Pennsylvania State University by Deo and Michaleris [2002], provides an informative study into weld distortion. Although this is not an investigation into sheet steel welded components, it is still useful information as both 2D and 3D predictive techniques have been used and compared to experimental results.

If the only concern is with the magnitude and direction of distortion after welding is completed, analytical simulation is unnecessary. The distortion is treated as an elastic stress field containing incompatible strains. The mathematics involved in this is relatively simple, making this approach useful in analysing actual practical joints. Kihara and Masubuchi [1960] developed a concept to analytically determine distortion in under these types of conditions. They looked at the effect of the degree of restraint and the ratio between the shrinkage of free welds and restrained welds. Watanabe and Satoh [1961] later looked at results obtained by different investigators using different types of specimens. The distortion formulas pioneered in the 1950's by these Japanese investigators are still used today as references in many weld distortion investigations as a base to compare FE methods with.

Many of the models discussed here will form a basis for comparison to the experimental results of this project and therefore will be discussed in further specific details in Chapter 5.

2.6.2 Prediction of Weld Distortions – Computational Based Methods

There are several ways to analyse residual stresses and distortion as discussed in the book 'The Analysis of Welded Structures', Masubuchi [1980]. Many of these are recognised as being too complex meaning computer programs are needed. For many years, researchers have studied the predictive methods for welding distortions using Finite Element Analysis (FEA). Complex models have contributed to the knowledge of distortion but are often impractical for industrial use due to the required computational intensity.

Finite element methods have been used in the prediction of welding residual stress and distortion for an established period of time dating back over 20 years. However, due to the inherent nature of the welding process, the FEA of welding involves additional complexity compared to that of traditional structural mechanics. These additional complexities include temperature and history dependent material properties, high temperature gradients, high gradients of both stress and strain fields, both in time and spatial co-ordinates, large deformations in thin structures and phase transformation phenomena.

Most of the early studies into welding simulation accounted for the non-linearities due to temperature dependent material properties and plastic deformations, such as the work of Goldak, Chakravarti and Bibby [1984], Goldak, Bibby, Moore, House and Patel [1986], and also Hibbit and Marcal [1973]. In most cases these analyses were restricted to 2D on the plane perpendicular to the welding direction. It has been noted by a number of authors however that, especially for residual stress prediction, the 2D models provide accurate estimations comparable to 3D analyses, since the stress field exhibits a fairly uniform distribution through the length of the work-piece.

2D models have been useful due in part to their high efficiency and also accuracy in determining the solution in the plane of the analysis, with reduced computational requirements. However, for practical situations, where the reality is fixturing or tack welding allow out of plane movement then 2-D analysis may not, particularly with

49

respect to distortions, be accurate. In addition the other effects such as weld start/stop effects, longitudinal heat transfer and instability cannot be obtained or considered from 2D models.

Many of the welding simulations performed in the literature, both 2D and 3D, appear based on small deformation theory, and tend to be limited to simple structures and basic weld geometries, or they limit their study to the immediate heat effected zone ignoring the remaining structure

The American Weld Society (AWS) has carried out many studies into areas surrounding weld distortion. Recently work by Tsai, Park and Cheng [1999] from the AWS have worked on a study investigating 'welding distortion of a thin plate panel structure'. With the knowledge gained from previous studies in welding distortion control, they addressed the basics of the warping mechanisms by studying the thermal and mechanical behaviours of thin aluminium panelled structures using the FE method. As well as this, they investigated the optimum welding sequence for minimum distortion. Weld sequencing optimisation is not of so much interest to this investigation as it is more of a manufacturing problem than a design issue; the work carried out into warping mechanisms is particularly useful and informative for this project. The study goes into great depth about the effect of global bending, the effect of residual stresses and the angular distortion created in a thin panel structure.

The Edison Welding Institute in Columbus, Ohio has investigated methods of predicting weld distortion. A study carried out by Michaleris and DeBiccari [1997] investigates a numerical analysis which combines two dimensional welding simulations with three dimensional structural analysis, 2D/3D Integration method. The numerical predictions can be utilized as either a design evaluation or manufacturing analysis tool. The methodology presented appears to be both efficient and effective. The predictive approach used can be implemented at various stages in the design and production cycle. In the design stage, welding procedures can be set and optimised and then various designs investigated.

Weldsim is a 3D FEA software package, developed at the University of South Carolina used in weld distortion analysis. A report Zhu and Chao [2002] investigates the accuracy of this package. The efficiency of the software has been verified through comparisons of computed results with experimental data. Although experiments carried out were for aluminium samples, a similar approach can be extended for a welding simulation of steels.

Taylor, Hughes, Strusevich and Pericleous [2002] explain that the numerical simulation of the process of welding can take place in two alternative ways, using Finite Volume methods. Firstly, the complex fluid and thermo-dynamics local to the weld pool are modelled by looking at the weld pool and the HAZ. The conservation of mass, momentum and heat together with the latent heat and surface tension boundary conditions are equated to represent the physical phenomena of the molten weld pool and thermal behaviour of the HAZ. Secondly, the solid mechanics approach is adopted by modelling the global thermo-mechanical behaviour of the weld structure, paying special attention to the heat source. A variety of simplified heat source models can be used in the simulation of welding, the accuracy of which relying on the theoretical and empirical parameters describing the weld pool size and shape. The research is aimed at drawing agreement between the two simulation methods, ultimately verifying the modelling parameters of the most appropriate heat source. PHYSICA is the software package used for either the thermo-fluid dynamics or thermo-mechanical approach, and it is applied to a girth welding of a thin pipe, to obtain distortion and residual stresses, without any metallurgical phase transition effects. The convective heat transfer in the weld pool is accounted for by modifying the conductivity of the molten metal. In their introduction, Taylor et al refer to a set of publications forming the basis of the two investigated general methods of weld simulations.

Bachorski, Painter, Smailes and Wahab [1999] are concerned with distortion during gas metal arc welding in their shrinkage volume approach. They define the Shrinkage Volume Method as a linear elastic FE modelling technique for predicting post weld distortion. By assuming that the linear thermal contraction of a nominal shrinkage volume, as it cools from elevated to ambient temperature, is the main

51

cause for distortion, there is no longer a need to determine the transient temperature field and microstructural changes, thus substantially reducing the time for FE distortion analysis. The thermal contraction of the shrinkage volume is resisted by the surrounding parent metal, resulting in the formation of internal forces, leading to distortion by the parent metal to accommodate the shrinkage forces until equilibrium is achieved. The method is applied to the distortion of plain carbon steel plates having butt welded joints with different vee-angles. Bachorski et al explain that although significant progress has been in FE weld modelling, in actual structures many FE techniques are short of being successful at the control of residual stress and distortion. For simplicity, they describe the use of linear spring elements to model the thermal contraction of the weld metal in a welded joint. This crude method can predict distortion reasonably in a fraction of the time needed for the more sophisticated fully transient thermal elastic-plastic modelling regimes. It is therefore that this approach presents a possible direction for moving the techniques of predictive weld distortion forward to earlier in the design cycle, as per the aims of the research being undertaken here. However the drawback is that whilst this is an analytical approach its success is dependent upon a library of empirical and experimental data for a library of welds, configurations and thicknesses of joints. The Shrinkage Volume Method assumes that a constant linear thermal strain is responsible for post weld distortion. Linear thermal strains are imposed as the weld metal elements cool from the assigned temperature, elastically distorting the weldment. Thermal strains produced in the temperature range 800-1500°C are hence ignored. The heating-up thermal cycle of the welding process is also ignored, neglecting the stress history and rendering the produced stress field invalid. For the FE distortion analysis, eight-noded brick elements allow for a parabolic distribution along the element edge and are used for all the models.

Goldak, Chakravarti, and Bibby [1984] developed a heat source designed to compensate for the absence of flow in conduction models by distributing the heat source within an ellipsoidal volume below the welding arc and enhancing the conductivity for any molten material. Bachorski et al proposes the more recent heat source representation by Smailes, Wahab and Painter [1995] who have shown that a more effective heat definition for vee-joint butt welds for a plate is the 'split' heat

52

source comprised of the heat content of the welding arc, applied to the weld surface with a Gaussian distribution, and a cylindrical volume heat source for the molten material. Any discrepancy between the shrinkage volume distortion results and experimental data is attributed to the difference between the assumed shrinkage (fusion) volume and the actual fusion zone determined from macro-graphs.

Brickstad and Josefson [1998] simulate the residual stresses due to welding using ABAQUS to perform the finite element analysis. Their analysis consists of two main parts, the thermal and the structural. They assume rotational symmetry of the modelled multi-pass butt welded stainless steel pipes. Hence the analysis is two-dimensional and axi-symmetric. The thermal analysis models the heat input from the welding torch into the weld elements causing the weld to melt. Heat losses allow the weld region to solidify. The temperature contours obtained from this part of the analysis are used in the sequential, structural analysis to derive the stresses generated as the material heats up and cools down again. The behaviour of the material involves nonlinearity and therefore residual stresses remain in the welded pipe after cooling.

Tsirkas, Papanikos, Kermanidis [2003] have carried out a three-dimensional FE analysis of laserwelded butt-joint thick AH36 shipbuilding steel plates using SYSWELD. Their work takes into account metallurgical transformations using the temperature dependent material properties and the continuous cooling transformation (CCT) diagram. The heat input to the welded plates is represented by a keyhole formation model, generated by a Gaussian distribution of heat flux with the aid of a moving heat source with a conical shape. The welded panel distortions obtained from the FE analysis agree with experimental measurements.

There are many papers and much research on the detailed and complex modelling of weld physics, weld heat source models, also weld pool effects and even fluid flow in the weld pool. However, whilst these exist they are at this stage outside the core direction of this research at this stage of the investigation, and are mentioned here for completeness and to give the reader a true feeling for the vast variety and complexity of the research being undertaken into simulation of the welding

53

processes. These approaches cross most of the common and also emerging weld technologies, from the well established fusion welding, to more recent developments such as laser, hybrid and even friction stir welding.

2.7 Measurement of Welding Distortion by Application of Scanning Technology

The last few years have seen a considerable amount of applications in the field of range scanning technology. Automatic 3D acquisition devices (often referred to as 3D scanners) allow us to build highly accurate models of real 3D objects in a cost and time-effective manner, resulting in increasing number of its applications. These models are ideal for measurement, inspection and analysis.

2.7.1 3D Scanning and Reverse Engineering

Reverse engineering is the process of capturing the geometry of existing physical objects and then using the data obtained as a foundation for designing something new. The new design can be a duplicate of the original or an entirely new adaptation. The design applications are used for wide range of industries including art and sculpture, architecture, industrial design, manufacturing, medical applications, automotive and aerospace etc. Nowadays three-dimensional scanning is playing an increasingly large role in reverse engineering of automotive and aerospace parts. It is for this reason that in many cases, aircraft and automotive parts are out of stock, since the original parts were made years ago using two-dimensional drawings, or, in some cases no drawings exist. Since most modern manufacturing companies will only, or prefer to, accept true 3-dimensional file formats, such as iges(128) or native CAD formats, it is therefore essential to build a solid model of the component. Figure 2.13, presented in the work by Vergeest and Horváth [2000], represents how a physical object with the aid of 3D scan is actually able to produce a solid model, ready for further downstream processes. They discuss both the conventional reverse engineering approach and scanning for conceptual purposes. In the figure the arrows

54

represent transfer of objects or data and the dashed arrows represent the exchange of data between the two methods or routes.
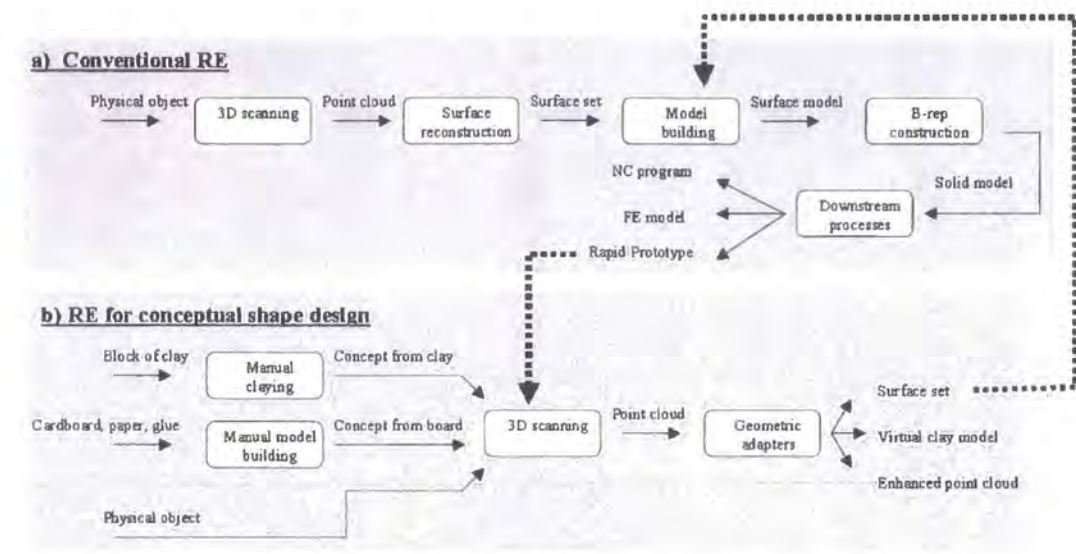
Figure 2.13: Process map for 3D scanning (Vergeest and Horváth)

It is therefore evident that such a 3D model can further be used creating a finite element model for analysis and data for inspection, generating a NC program for machining purposes or a creating a rapid prototype model. It is worthwhile to mention that the rapid prototype model can be created by variety of processes like FDM (fused deposition modelling), LOM (laminated object moulding), MLM (multi jet modelling), SLA (StereoLithography), SLS (selective laser sintering) etc. The details of such rapid prototype processes are not included in the scope of this report.

2.7.2 Component and Process of 3D Scanning

3D scanning devices can broadly be classified into contact and non-contact types. Since our main application involves only a non-contact device, we can further classify such devices based on the adoption of optical technology. Rocchini, Cignoni, Montani, Pingi and Scopigno [2001] describe the classification of such non-contact scanning devices, and classify optical systems as shown in Figure 2.14.

Active optical devices typically consists of an emitter, which produces structured illumination on the object to be scanned, and a sensor, typically a CCD camera which acquires images of the distorted pattern reflected by the object surface. In most applications, the information is reconstructed by triangulation techniques, calculations of which are usually performed in the hardware integrated with the scanner. It is to be noted that different technologies can be employed to produce the structured light pattern e.g. laser emitters, custom white light projectors, photographic slide projectors, and even digital video projectors.
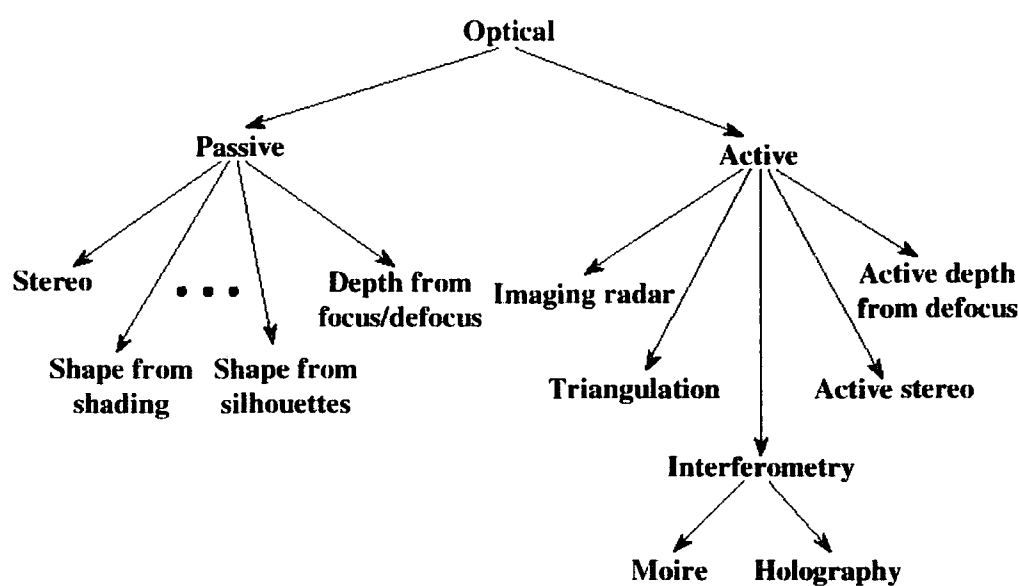
Figure 2.14: Classification of 3D non-contact scanning devices (Rocchini et al)

The scanner operates by sending out a thin strip of low power laser beam from the head unit. The laser reflects from the surface of the item, and is returned to the head unit, where it is captured by CCD camera. Rocchini et al illustrated the scheme of a typical optical scanner, which can be seen in Figure 2.15, and stated where the 3D positions of the sampled points are computed on the sensor plane by triangulation given the sampled point projection P(a) on the sensor plane and the known relative position/orientation of the sensor and the emitter. This allows the distance to be calculated for the hundreds of small points projected back to the unit. This allows the surface of an object to be mapped as a series of 3D data points, called a point cloud. In this way, information relating to the surface of the item being scanned is

recorded in the computer attached to the scanner unit. Figure 2.16, courtesy of Faro UK Ltd, shows a typical example of a laser scanner (as used for the project application), with its head unit, and portable CMM inspection arm, which can then be mounted either on a tripod or by clamping to the work piece or appropriate fixture. The provision of 6 joints in the CMM arm allows a number of degrees of freedom making it highly flexible.
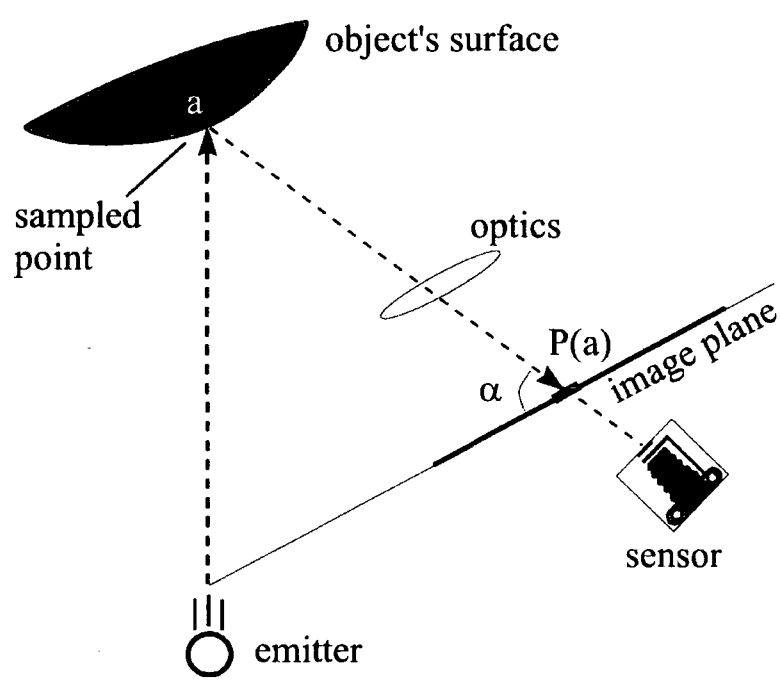
Figure 2.15: Schematic of an optical measuring device (Rocchini et al)

It is evident, that the scanned data is capable of providing an outstanding combination of sub-millimetre accuracy and flexibility. The combination of the entire system enables it to record an extremely wide range of objects of different sizes. Objects from a few cubic millimetres up to several cubic metres can be scanned. The scanners are portable and recording can be done in almost any location, either on-site or at the laboratory. The scanner is even equipped with multiple scanning options (by relocating the scanner unit) in order to facilitate scanning of large objects.

Figure 2.16: Typical 3D laser scanning device mounted on portable CMM arm(Faro)

2.8 Summary

In this chapter we have set out the principles of the welding process, paying specific attention to the weld processes of the case study company, and the application of their key process of MAG welding to the primary joint types in thin plate, those being butt weld, and also tee joints. A detailed description is included in the document for the reference of the case study company.

We have seen that residual stresses and distortions occur in the welding of metal plates, and discussed in detail the theory and understanding being this. Notably that, the heated weld zone tries to expand but is restrained by the surrounding colder material, causing this zone to yield in compression. During the cooling cycle, the colder material prevents the contraction of this region, causing tensile stresses to be developed. This tensile stress around the weld with simultaneous generation of compressive stresses shall result in distortion. The residual stress and the distortion generated have been discussed in detail particularly for butt welds.

The three main distortion modes can be identified as longitudinal shrinkage, transverse shrinkage, and angular distortion (which can result in bowing, dishing, twisting, buckling and warpage). However in most cases it is unusual is any of these distortion modes occur in isolation and the final distortion pattern is usually made up of a complex combination of these especially in real components with complex geometry and multiple welds. It has been explained and discussed that the key factors which influence distortion are the material properties themselves, the inherent stresses in the components and material from manufacture, the restraint applied during welding, the process variables from the welding process and the weld procedure itself, and also the actual design, fit up, accuracy and tolerance of the weld joint and component.

In creating distortion through the welding process it has been discussed that this can indeed be controlled, however, often with many practical or commercial implications. It is possible through the design of the weld joint and component, the design of the process and weld sequence, assembly and fixture design, and actual choice of the weld process and parameters to limit, or occasionally almost eliminate, and control distortion.

It has been shown that extensive research exists into the prediction of weld distortion. This has been summarised and we have looked at some of the basic empirical methods and formulae that exist to calculate distortion predictions. Furthermore there is a wealth of research being undertaken to utilise computer aided methods such as finite element prediction to simulate the weld process. However we have seen that these models require complex physics which push the boundaries of CAE applications and it is difficult to accommodate all of the influencing factors into a comprehensive yet efficient model to predict weld distortion. Approaches exist that will provide relatively efficient and quick predictions of distortion but these are at the reduction of quantitative accuracy especially when applied to real world problems. However it is such quantitative approaches that may be best leveraged to see maximum early benefit in the design phase of components as possible.

Finally, whilst not strictly related to weld distortion, the process of scanning measurement has been introduced as this is the methodology employed in this study to capture as much knowledge of the distortions on the sample components.

With all these in place we can move on to discuss the investigations undertaken, to capture knowledge about the case company's welding processes. This data will be presented and analysed in subsequent chapters. This provides the basis for a weld prediction tool that could be used on simple joints, and which will be later discussed as to how the data can and will be used in future for further work. This further work will aim to develop parameters that will lead toward a quantitative tool for design engineers to apply to quickly assess real components early in the design stages of projects.

Chapter 3: Experimental Investigations

3.1 Introduction to the Experimental Design

In order to undertake a successful experiment to investigate the parameters and variables associated with weld distortion, it is necessary to design an appropriate experiment to enable this to be carried out in a controlled and repeatable manner. To facilitate this, investigations were carried out to identify the predominant factors that have an affect on the distortion of a welded component, so as to find suitable limiting factors that can be applied. Having developed the suitable factors an experimental matrix must be designed to cover the range of properties required. Furthermore work had to be undertaken to design both the test fixtures and specimens to be representative to the needs of the case study company. This chapter presents the background and work of the experimental investigation.

3.2 Experimental Objectives and Proposal

In order to carry out the experimental investigation, the following techniques/methods were utilized:

- Design of suitable test plates to be used for comparing welding variables.
- Design for fixture and component design work.
- Design of experiments (DOE) using Full Factorial Design.
- MIG welding process to simulate welding technique used in high production component manufacture.
- Measurement processes to accurately measure test pieces before and after the welding processes.

Due to 'Just in Time' manufacturing methods being used in the case study company, production can not be interrupted for long periods of time due to tight production schedules. It was therefore necessary to setup a separate welding cell for the weld tests, that would replicate the processes used in the production environment but facilitating greater access and flexibility.

The main objectives are to build and analyse simple representative welded joint parts to evaluate and understand the general magnitude and direction of distortion under different variables to give greater understanding of these effects on real parts. This in turn can then be applied, and help assist at the design stage of a new product development, to plan for more robust production of products by taking greater consideration of distortion effects into account at these early stages. Using the data from these experiments this can be applied to build up a knowledge base and to build up a database of distortion results. In turn this can be used in further work to develop a simple weld distortion predictor tool based on experimental data. In a longer term view, this data can be utilised to correlate finite element models of welding simulation to develop a 'quick' prediction tool. Although this work lies outside and beyond the scope of this dissertation it is mentioned for completeness to give a full background to the full and initial plans set out for the work and is discussed further in the closing chapters relating to further work.

In undertaking this work then a number of minor objectives are completed in achieving and supporting the main objectives. These can be described as follows:

- Developing a sound knowledge into what causes distortion in sheet metal welded parts which can be disseminated within the case study company.
- Gaining an insight into what can be done to eliminate/reduce distortion in parts in the manufacturing process.
- Establishing and documenting, for the case study company's processes, which variables contribute most to distortion trends.
- Finally, to investigate analytical methods used to predict distortion and compare these against the experimental data.

To be able to assess the distortion a welded structure undergoes in the assembly process, weld tests will be carried out on a variety of joint types that will resemble typical joints used in automotive chassis structures. Joint types commonly used include Butt Joints, Lap Joints, Overlap Joints and Flanged Joints. The tests will involve welding plates of different thicknesses under variable process conditions and measuring the results to build up a company knowledge base of distortion values.

3.3 Selection of Joints for Investigations

To be able to assess the distortion that a welded structure undergoes in the assembly process, weld tests will be carried out on a variety of joint types that will resemble typical joints used in automotive chassis structures. Joint types commonly used include Butt Joints, Lap Joints, Tee Joints and Flanged Joints.

It was crucial and utmost important to decide on the joint types of the weld samples to be welded in this experiment. Initially it was proposed and stated all possible joint types to be included, i.e. bead-on-plate, butt, tee, lap, flange, etc. But it was soon discovered due to the diversity of grades, gauges and materials as well as joint types used by the case study company this was not practical so sampling would be necessary. The fixture for welding joints however has been designed to accommodate all joint types in a range of gauges suitable to the case study company. For the purposes of this study it was decided to focus on a simple joint type to validate the approach and for that reason a simple butt joint sample was chosen as the baseline for the experiment.

3.4 Factors Affecting Distortion in Experimentation

As has already been discussed in Chapter 2, in order to carry out any experimental study into the distortion in welded fabrications it is necessary to gain a full understanding of the factors that affect the distortion. Therefore experiments must be designed with suitable and varying parameters. From the literature studied in Chapter 2 numerous factors affecting weld distortion have already been discussed and described in detail. In relation to the industrial welding process of the case study company many of these factors cannot be altered significantly, as this would not be practical in a high volume production environment due to the risk of increased variability and loss of process control. In order that the basic distortion properties of the individual basic weld types are understood, the initial study will be limited to basic weld geometries. By examination of many of the components manufactured from the case study company, the application of these basic geometries to more

64

complex geometries can be deemed to be valid, as many of the joints in real components comprise of a variation on the basic joints presented in this work.

It has been seen that the position of the weld in relation to the neutral axis had an influence on distortion, however in this exercise only simple joint geometries of a defined dimension will be used and sections eliminated. Therefore this variable can be removed from the experimental matrix to be developed. Other factors such as the size of the fillet weld, the weld preparation, the quantity of weld metal and gap sizes between the plates have also been selected in reference to the design and technology in use by the case study company. In this instance the company does not use any weld preparation on either butt or fillet welds and therefore this to can be excluded from the experimental matrix. Weld gap size has an influence on the final distortion, however well designed fixturing in order to control the gap size between the plates to be welded, and the actual gap sizes used, will be in common with those used by the case study company and its industrial applications. Therefore at this stage it is not planned to investigate the affects for varying gap size. For most joints in the production environment, the target gap size used is set between zero and one millimetre, with a nominal target gap size of 0.5 mm. The length of weld it will be chosen to facilitate measurable distortions and based on standards that exist. Clamping and restraint clearly indicate different distortion parameters and therefore investigation will incorporate the ability to carry out some experiments to find the influence of restraint and clamping on the variability of the experiment. The case study company generally welds single weld runs from one side of the material because of the thin gauge material involved, typically in the range of 2 to 4mm thick. The target for this experiment was to weld in the horizontal position so removing the influence of a weld orientation to the weld head and weld flow from the distortion results. Again material type, thickness and diameter of weld wire, along with weld settings and speeds will be chosen to be representative of the industry and case study company.

65

3.5 Experimental Set-up and Procedure

3.5.1 Sample Selection, Design and Preparation

It was necessary to come up with some relevant and standardised 'Weld Samples' design in order to carry out the distortion test. For this reason, the corresponding British Standard was searched. The BS EN 2883 gave the necessary information about the requirements and specifications for welding experiments. From the standards, the dimensions were figured out in order to cut out the sheet metal plates. The minimum required dimensions as stated by the BS EN 288-3 for any type of plates to be welded together are given as 150mm by 350mm. In addition the test plates were designed to meet the following requirements:

1. To be of sufficient size to ensure a reasonable heat distribution.
2. All plates to be cut in the same direction of roll from the steel coil to keep any stresses in the test material uniform.
3. Test pieces must fit fixture to be used when welding.
4. To be free from sharp burrs for health and safety reasons and so that edge profile of plates can be scanned accurately.
5. Profile of plates to be guillotined to size as this is a similar trimming operation as production parts manufactured from press tools.

The case study company uses predominantly a range of steels with yield stresses from the mid-200MPa yield range up to around 500MPa yield. This is driven by the pressures on the case study company for structural performance in terms of strength and durability, combined with the commercial pressures for weight reduction and competitiveness. As most of the company's components involved forming via stamping and drawing then the elongation is key to the manufacturability of these components. However, as elongation decreases with increasing yield strength then a balance has to be struck between formability and strength for the component. Most commonly materials in the 300 to 400MPa yield strength range tend to be used for striking an optimum balance between formability and strength. The optimum balance for the company's needs is to manufacture the majority this structural components out of a mid-range material that is specified as BS1449:1982 HR43F35

66

which is a 350MPa minimum yield material. Therefore this is the material grade selected for the investigations. It was the most common steel grade used at the case study company and it is a High Strength Low Alloy steel manufactured by Corus and having the trade name Tenform XF350. This is manufactured to a BS EN 288 and the typical properties are show in Table 3.1. The material was chosen in the thickness range consistent with that used by the case study company in the majority of its applications, which gave a typical common range of gauge thicknesses as 2.0, 2.5 and 3.0 mm thick. This thickness range was found to cover approximately 70% of the press product manufactured at the case study company and therefore appropriate to this study.

Table 3.1: Material specification taken from BS EN 288-3

Rolled condition and grade	Yield strength R_e, min.[1]	Tensile strength R_m, min.	Elongation A, min.			Bend mandrel diameter (180° bend)[2]
			Original gauge length L_0			
			50 mm	80 mm[3]	200 mm	
	N/mm^2	N/mm^2	%	%	%	
HR40/30	300	400	26	(24)	18	2a
HR43/35	350	430	23	(21)	16	2a
HR46/40	400	460	20	(18)	12	3a
HR50/45	450	500	20	(18)	12	3a

Although, the 'Tensile Strength Test' information and data for the given material XF350 is already presented by Corus, it was decided that tensile tests of the selected material would be relevant and beneficial to the analysis of overall experimental parameters in terms of the whole inputs going into the process. The relevant standard for the manufacturing of testing specimens was found in BS EN 10002-1:2001. From each plate thickness, 2 strips were machined according to the shape that is defined in the standard and then they were subjected to tensile testing.

The plates had to be prepared from rolls of production steel taken from the end of press runs at the case study company. The plates were guillotined to size as this is the closest process to the mass production practice of blanking. Samples were acquired from production coil ends so actual production steel was used to give a

67

similar edge condition to the plate and avoid inducing any other pre-distortions to the plate through processes such as laser cutting. Two datum edges were marked up on the cropped plates for reference. Plates were checked for dimensional accuracy after every ten were guillotined to check that the stop had not moved out of position and to provide a consistent plate size, even though each plate would also be measured prior to welding. The plates were subsequently set up from the datum faces on a milling table and location holes were drilled in the plates using a vertical milling machine, to allow accurate location onto the weld fixture, and again to be representative of the type of fixturing process used in production. All plates were deburred, cleaned and uniquely numbered for future identification and tracking ready for measurement and use in the experiment.
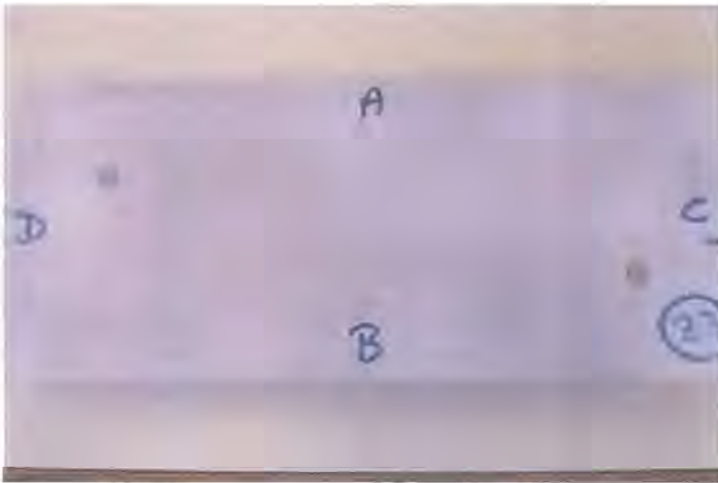
Figure 3.1: Birdseye view of sheet metal plate sample

As it can be seen from Figure 3.1, the two location holes have been drilled in the plates, which are 50 mm away from each edge thus providing a clear and safe distance from the HAZ (Heat Affected Zone). The idea of having location holes in the plates which will mate with location pins of the fixture was to replicate the standard production fixturing practices of the company. This also serves purpose to be able to hold the plates in position without any movements in any longitudinal and transversal directions before and during welding. In addition it also would allow angular distortion to occur without any need for clamping if desired, i.e. the effect of restraint factor was mentioned in the literature review. This would allow comparison of clamp and unclamp plates in certain joint configurations in the future.

68

3.5.2 Fixture Design

To be able to carry out the welding experiment, an appropriate fixture was needed. Several options were considered such as an existing base plate at the company's shop floor or a rotating table with some clamps, sited at the company's robot welding training facility. However, due to the fact that there were some critical factors to be considered during welding especially if weld distortion was the intended outcome, then a special fixture was required.

Fixture Design Considerations:
The physical structure of the fixture had to be rigid, stiff, portable for welding operation and practical in a way that it was suitable for the required combinations of envisaged weld joints for the current and future studies. Because the main aim of the project was to determine the actual weld distortion, the fixture had to be designed in a way that it did not act as a heat sink and allow distortion to occur.

Fixture Design Concept:
Having considered the above factors and also after consulting process engineers and weld programmers a fixture proposal was developed. The fixture concept shown in Figure 3.2 was designed on CAD software. Initially, the idea was to manufacture the boundary frames for the fixture from angle section as seen in Figure 3.2. The reason for the use of angle section was to utilise the existing stock at the case study company's test facility.

Diameter 12mm
location pins
6 off

Machined location
pads
15 off

Gap condition for
welding - to avoid heat sink
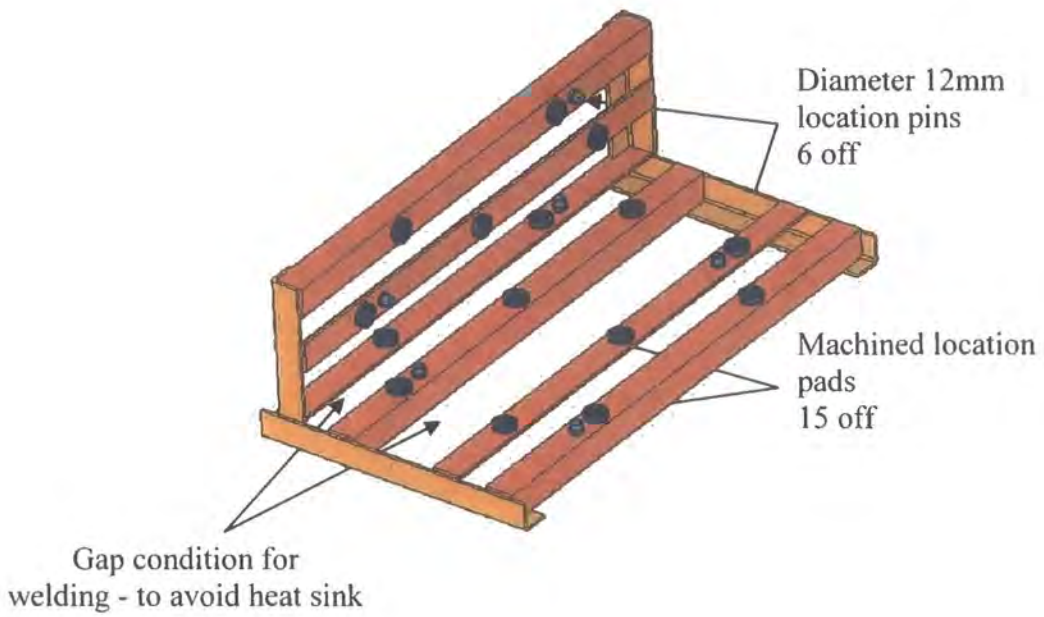
Figure 3.2: Initial fixture design

As seen in Figure 3.2 the fixture has location pads which were to be machined after the fixture has been welded together so that a straight and flat reference or datum plane can be created for the plates to rest on during welding operation for butt joint arrangement as seen on Figure 3.3.
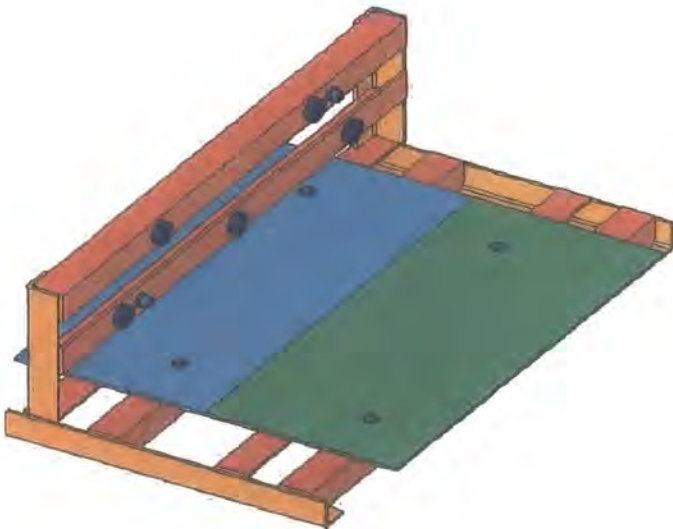
Figure 3.3: Butt joint weld arrangement

70

As shown in Figure 3.2, the fixture has location pins on the horizontal and side face of the fixture, which mate with the fixturing and locations holes on the plates, described previously in section 3.5.1. Figure 3.3 shows the experimental butt weld arrangement with no gap condition during welding i.e. plates are supposedly to touch each other provided the plates are guillotined to theoretical dimensions.
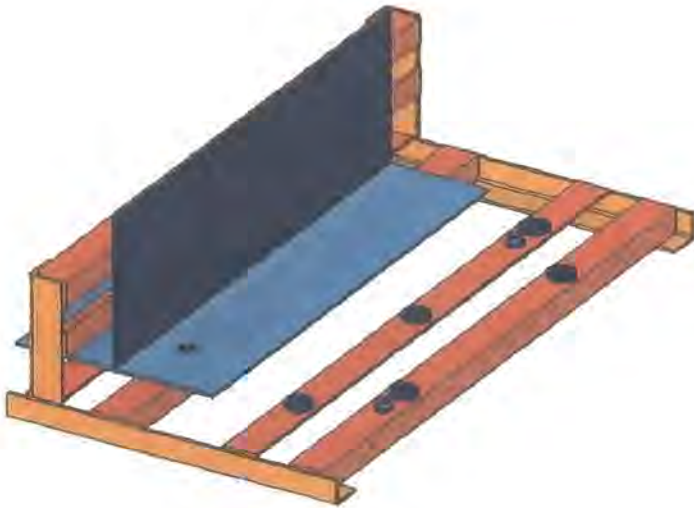
Figure 3.4: Tee joint weld arrangement

Figure 3.4 shows the tee joint weld arrangement, which was one of the other primary type of weld joint considered in the fixture design, for future investigations. Variations on these basic geometries by inclusion of flanges or joggles to the sample plates would then cover the vast majority of the weld situations seen in the company's product range.

To ease removal for welding in the tee joint set up it was decided to make the location pins removable and this would also allow for variations and distortions. The angled section was vulnerable to distortion itself during manufacturing, so it was changed to box section. Therefore the pins on the perpendicular face were removed and also the design was modified to be of box section as shown in Figure 3.5, which offered a stiffer, and more durable structure to resist distortion affects.

71

Figure 3.5: Modified final fixture design

The fixture was manufactured by the case study company's prototype fixture and assembly supplier in the south of the UK according to the detailed drawings generated and supplied to them. The manufactured fixture can be seen in Figure 3.6.
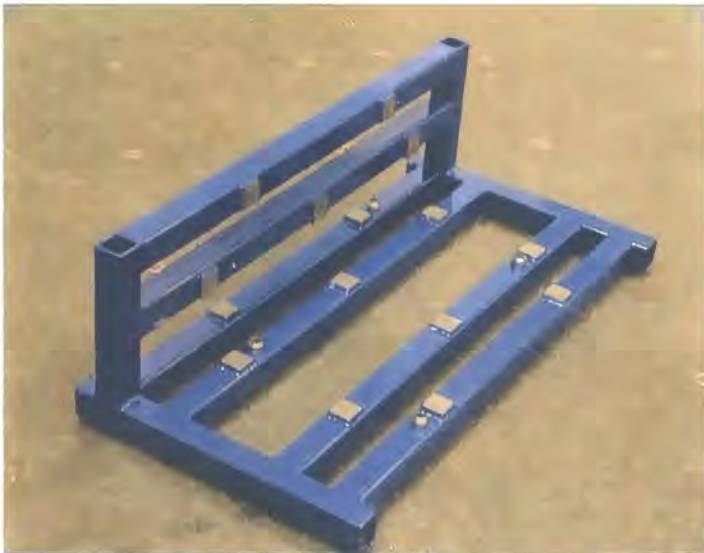
Figure 3.6: Fixture as manufactured

A final refinement process was carried out on the location pins upon arrival at site. The 4 screw pins were to serve a unique and critical purpose. As it was mentioned previously, they had to hold the plates in position for each pair, each time and every time. This was important again for the repeatability of the experiment itself. Although the diameters of the pins and the holes on the plates to mate with the pins had supposedly and theoretically the same diameter of 12 mm, it was clearly seen from the measurements that the actual figures could be have slight variation on the plates datum holes. In order to overcome this problem, the pins were machined to a have tolerances to accommodate each pair of plates. The outer ones were machined to be 11.40 mm in diameter whilst the inner ones were 11.60 mm. The reason for the outer ones to have smaller diameter was to avoid jamming and to allow angular rotation i.e. to allow distortion to happen easily.

3.5.3 Limiting Factors, Welding Parameters and Recording

Welding tests were carried out, using a robotic weld-set, on a number of different plate thicknesses (2.0mm, 2.5mm & 3.0mm) to determine an optimum weld speed. Although weld quality was not of importance for the experiments, the speed still had to be within a limit so that the welder did not cut out by burning through the plates by creating too much heat at low weld speeds. An example of the problem and burn through is shown in Figure 3.7.

The optimum speed that could be used across all three plate thicknesses was determined to be 1.0m/min with the variables varying +/- 30% of this value. Using these parameters then significant burn through was avoided and a consistent production representative quality weld was produced from the resultant process.

73

Burn through due to
excessive heat

Figure 3.7: Example of burn through due to incorrect weld speed

In common with the practice of the case study company, due to its high volume environment, all other factors on the weld-set were fixed and held at contact value.

In addition it was decide to use a Portable Arc Monitor System (PAMS) device connected to the weld set to record and monitor the weld process. The PAMS unit is a multi channel data logger, originally developed by OIS, capable of accurate, fast, efficient and real time data acquisition of the main parameters in the arc welding process. The unit also then provides a hard copy print out of the data and all measured properties together with a summary of the key parameter settings and calculates items such as heat input. An example of this unit and a typical output log is shown in Figure 3.8.

74

Figure 3.8: PAMS monitoring device and typical sample printout it generates

3.5.4 Experimental Procedure

After considering the main factors that affect distortion, it was decided to investigate how the change in material thickness and weld speeds caused a variation in magnitude and direction of distortion based on the case to the company's experience. Weld parameters are generally set to constant during the production weld programs and weld speeds are modified according to geometries to give the appropriate level of weld penetration. In order to understand the relationship of these variables it is necessary to pick at least three levels from the experimental curve to indicate whether variables have either a linear or non-linear effect.

The two factors chosen for the experiment were material thickness, and weld speed. The three variable levels used to determine if there is a linear relationship between the results were given in Table 3.2.

Table 3.2: Experimental variable ranges

	Factor X Material thickness (mm)	Factor Y Weld Speed (m/min)
Level 1	2.0	0.7
Level 2	2.5	1.0
Level 3	3.0	1.3

75

Due to the low number of variables being used for the two factors, a Full Factorial Design Matrix was used. Table 3.3 shows the Full Factorial Experimental Design Matrix used. 3 replicates for each test will be used in order to check repeatability, ideally this would have been 6 to provide a higher level of basic statistical significance but it was found that even with such a simple set up as this the volume of data generated would prove prohibitive to analyse in the time available if 6 samples were used. However some basic work was carried out to demonstrate that the general magnitude and directions of the distortions shown in the experiment were very repeatable and stable.

Table 3.3: Full factorial experimental design matrix

Experiment Number	Level		Result/Repetition		
	X	Y	1	2	3
1	1	1			
2	1	2			
3	1	3			
4	2	1			
5	2	2			
6	2	3			
7	3	1			
8	3	2			
9	3	3			

3 Variable Levels, 2 Factors, ∴ 3^2 Design = 9 conditions

The number of test pieces required to carry out the tests was calculated using the experimental design, based on using three replicates.

Number of experiments = 9, Number of replicates = 3

9 x 3 = 27 tests per joint type

2 plates required per test,

∴   27 x 2 = 54 plates needed per joint type

54/3 = 18 plates per material thickness required for each joint

More plates were prepared for spares and for testing before carrying out the experiments.

Parts were welded in the fixture using the robot weld set up. Clamping was applied during the welding process in order to ensure repeatability of the process and avoid any movement of the plates from distortion during welding which may affect the results. It is common practice in production for the company to clamp its products during welding. The clamping is released as soon as the weld cycle finishes making maximum use of the cycle time available for manufacture and welding. In this experiment clamping was therefore appropriate. However it was then removed immediately upon completion of the weld cycle and the samples removed from the fixture and allowed to air cool on a wooden rack. This is to avoid any heat sink effects removing heat from the sample quicker than may otherwise occur if the parts were placed onto a surface that could rapidly transfer heat out of the parts. Once the part had fully cooled and any distortions developed to their final state and mode then the parts could be measured.

3.6 Distortion Measurement and Procedure

3.6.1 Initial Measurment Methods

To be able to ensure exact information about the plates going into the experiment then it would be necessary to measure all thicknesses, and dimensions for each plate, both before being welded and also after welding. This would allow for the most accurate understanding of the real distortions occurring from the welding process. A number of approaches were considered before finalising on the initial measurement scheme. It would be possible to measure all plates by hand however this would be a time consuming and labour intensive process. In addition measurement by hand using tools such as vernier callipers and surface gauges is prone to both measurement and reading errors occurring. Therefore, with the number of samples involved this approach was decided to be unsuitable for the nature of the investigation being undertaken. The case study company has numerous co-ordinate

77

measuring machines, CMMs, which utilise conventional touch probe/ contact measurement. It would have been possible to utilise the company's CMMs but these are heavily utilised in the production and prototype environments and therefore access as required to these resources could not be guaranteed. In addition many points would need to be taken to collect data relating to the edge profiles and surface curvatures and these would be quite time consuming to gather and the data itself relatively sparse in comparison to other methods that utilise contact or non-contact measurement. However, within Durham University, there are facilities for contact measurement using laser systems. The particular system employed uses a tracking laser scanner to track a special trackball. As access to this facility could be guaranteed and the data output generated from this approach more sophisticated and detailed then either the hand measurement or CMM approach, it was decided to utilise trackball laser scanning as the initial measurement method.

The laser scanning system used in this phase of the experiment was manufactured by Leica. In this system a fixed base transmits a laser from a rotating head, which is the emitter. The beam from the laser is used to measure parts by using special tracking devices. In this case, a track ball was utilised, which contains a small reflective prism to return the laser to the main scanning unit where the receiving sensor is mounted. The unit then computes from the returned signal a position in space for the trackball at that time. The benefit of this type of system is that is can scan a full 360° area around the base unit, and depending upon the power of the laser source it is capable of scanning large areas and also smaller samples such as the plates employed here. Figure 3.9 shows the set-up used to scan the samples from the experiment, with the Laser scanner a distance away from the objects to be measured, which are mounted in a fixed orientation on a measurement table. The trackball is then moved around the surface and the edges of the component in order to generate the 3D point cloud of scan data. The unit outputs the cloud data in the format of a list of points each with an individual x, y and z co-ordinate in space relative to the position of the scanner.

78

Figure 3.9: Arrangement and set-up for track ball laser scanning process

3.6.2 Limitations and Shortcomings of Initial Measurements

The plates were all scanned both prior to welding and after welding using the arrangement shown in Figure 3.9. Whilst the procedure itself was relatively straight forward some problems were observed once post-processing of the data commenced. When the object is scanned in this method the actual position the system records is the point at the centre of the trackball, rather than the point on the surface of the plate. Therefore all of the data has to be translated to allow for the known dimension from the trackball to the measured objects surface, due to this offset. In addition as the trackball is round then to measure edges and surfaces whilst maintaining orientation to the scanning unit the trackball must be mounted in holders. The trackball sits into this holder on a ball bearing racer to allow free movement, but as the holder itself has a relatively large dimension in comparison to the dimension of the feature to be measured then it is possible for some loss of accuracy to occur. This can be seen in Figure 3.10 which shows the trackball mounted in holder for surface scanning. The base of the holder is flat and the surface it is being used to scan is curved therefore there is an access limitation and it is not able to truly get a full definition of the surface to be measured. Also the size of this holder limits access into certain features, and clearly access to measure close to the weld is

79

restricted by this. For edge scanning the stepped holder can be seen, shown upside down, in Figure 3.10 also. Using this edge holder then not only do the dimensions need adjusting for the height to the trackball centre but also for the offset caused by the stepped spigot that is used to track along the edge.

Figure 3.10: Track ball and holders used in scanning process

In Figure 3.10 it is clear to see the flat bottom surface and how this will approximate the curved surface due to its relative dimension in relation to the small curvature of the surface.

The addition of all of these offsets greatly adds to the complexity of post processing the cloud data after collection. Each cloud needs to be read into the appropriate software package and then the edges offset in order to compensate for the presence of the spigot, before the surface and edges are offset to allow for relative dimensions between each of the holders. As the plates to be scanned do not exactly lie in a plane, then each plate must be processed and offset individually in 3 dimensions using CAD. Whilst this is a relatively straightforward exercise for the regularly

shaped pre-weld plates, albeit a time consuming one, it is a much more complex problem for the distorted welded samples. In addition, as will be discussed later then the relatively sparse surface data meant using the post processing software to generate representations of the curved surfaces was not producing smooth surfaces but rippled surfaces due to the spacing of the data. Therefore it was decided a better and more efficient method was needed for measuring the post weld samples.

3.6.3 Revised Measurement Methods and Procedures

Having found the problems associated with processing the data output from contact scanning processes then it was decided an alternative approach was needed. In order to accurately capture the full surface geometry of the distorted welded plates then it was necessary to use a method of data capture utilising a far higher number of points. The decision was made that non-contact laser scanning was the most time effective and cost efficient way to capture this data to the quality needed to the provide distortion results.

The system utilised is one that the case study company employ for surface scanning parts on an occasional basis in its production situations. Therefore the approach again fitted with the experience of the case study company's methods. The scanning was undertaken using a non contact laser scanning system developed by Faro. This was mounted onto a portable CMM arm to manipulate the scanning head around the part to be inspected. The system works in a very similar way to the track ball method however in this case there is no prism in a trackball to reflect the beam back from the source to the emitter. Instead the beam reflects back off the part, which means that the range of the scanner is greatly reduced, in this case the scanning head needs to be within around 100mm of the part surface. The point cloud is built up by making multiple passes of the laser head over the part until all areas of the inspected part have been fully covered.

The resultant point cloud is then an actual representation of the surface of the scanned part and requires no further offsetting or manipulation in order to be worked

with or for measurement to be taken. A sample point cloud from a scan of one of the welded components can be seen in Figure 3.11.
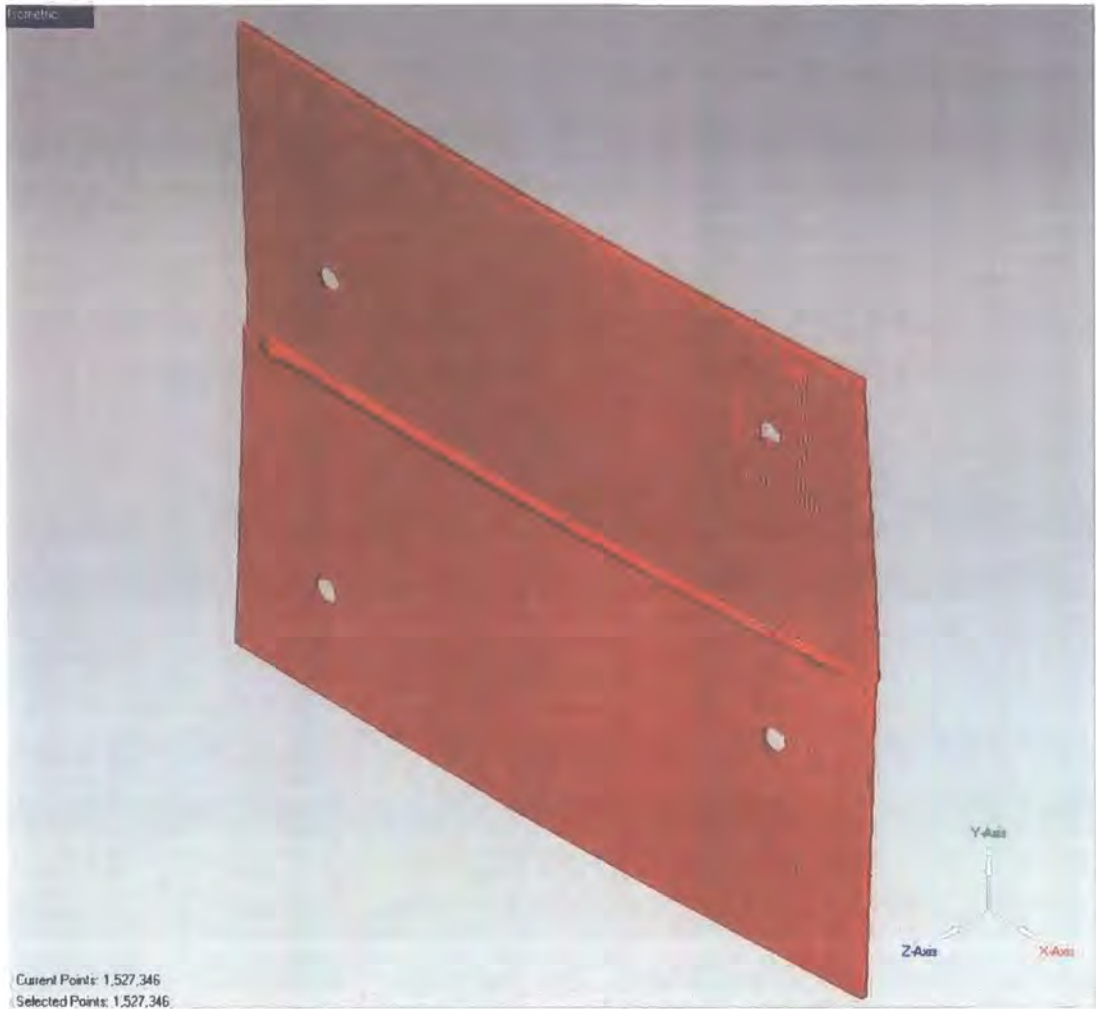
Figure 3.11: Typical point cloud from non contact laser scanning process (butt weld sample)

3.7 Summary

This chapter has discussed how the experiment to investigate the parameters and variables associated with weld distortion was designed to enable this to be carried out in a controlled and repeatable manner. The main objective of the experiment being to build and analyse simple representative welded joint parts to evaluate and understand the general magnitude and direction of distortion under different variables to give greater understanding of these effects on real parts. The work

82

undertaken to design both the test fixtures and specimens to be representative to the needs of the case study company has been documented. It has been shown how the fixture developed for this investigation has been designed with consideration for expanding the study in future to consider other joints of different geometry or dimensions. The experimental procedure used for this investigation has been documented and discussed in detail, along with an explanation of the methods used to measure and analyse the samples resulting from this series of investigations. The differing measurement methods used throughout the analysis of the results of the investigation have been discussed so that they can be understood prior to their application to the experimental results. Chapter 4 discusses how these measurement methods are subsequently used to investigate the results before presenting the results themselves.

Chapter 4: Results and Investigations

4.1 Introduction to the Results and Investigations

This chapter presents the results from the experimental investigations undertaken on both the bead on plate weld samples and the butt weld samples. A brief description of the measurements schema and how this was used to process the results is presented. This is then followed with detailed information about the welding distortion results. Firstly a general assessment of the welds is undertaken by both visual examination and destructive sectioning to allow macro investigations and micro hardness assessments to be undertaken. The subsequent sections then present the experimental results from each of the two sample types. These are set out to examine the detailed profiles and distortions occurring in a general plate from the sample range. Then the effects of varying speed on a constant thickness are examined, before then studying the effects of varying thickness on constant speed. Finally for each sample a summary of the full effects and trends from varying both of the experimental factors of speed and thickness is presented. Finally the chapter is summarised and the main conclusions presented.

4.2 Measurement Procedure and Method

In Chapter 3, the measurement method was discussed in detail. In this section the processing of the relevant measured results is discussed to aid understanding of the results presented and where these have been generated from.

The pre weld data collected via the track ball laser scanner had to be read into a 3D CAD package for each pre-weld plate. This was due to the limitations of the output from this scanner only being able to output raw point clouds in x,y,z data. This first had to be converted to IGES then read into the CAD package in order to be manipulated. The pre weld scan picked up the edges of the plate but due to using a track ball this data had to be manipulated to account for the dimensions of the track ball before it could be used. The edges of each plate had to be offset by the appropriate dimension to account for the trackball measurement method. Then the points along each edge could be processed to best fit a straight line to represent the

85

plate edge through these points. Again because of the limitations of track ball measurement the scan was not possible to capture the full edges of the plates and intersect at the corners. Therefore the constructed edges had to be extended in the CAD package so they could intersect, then they were trimmed to find the true corner positions of the pre weld plates. Once this was done then the dimensions could be accurately measured on the CAD package. The processed point cloud for a typical example plate can be seen in Figure 4.1(a), the offset edges can be clearly seen, relative to the final trimmed CAD generated surface.

Within the CAD package it was also possible to determine the maximum scatter on the surface points collected on the top face of the pre weld sample plate. These generally lay in a plate with a scatter about the average of the surface height. However in order to decide if the pre weld flatness would significantly contribute to the post weld dimensions a calculation of curvature had to be undertaken. In order to ensure this accounted for the worst case deviation then the extreme point dimensions were taken and assumed to be occurring at the edge and centre of the plate therefore providing a worst case possible for a radius of curvature along the plate. A sample calculation for this radius of curvature is presented below to illustrate how this was calculated for the pre weld plate:

From the measured data the maximum point deviation was found to be 0.08 mm. The plate length is nominally 350mm and plate width is 150mm. If it is assumed that the maximum deviation occurs at plate edges and middle of plate to give maximum curvature then the radius of curvature can be calculated using the following method. For segment of a circle the radius, $r = (h/2 + s2/8h)$, from geometry based on Pythagoras, where h represents the height of the curved portion of the segment, and s is the width of the segment. So in our case, along the length of the plate h = 0.08 and s = 350. Applying this in the equation it is possible to calculate the radius as follows:

$r = (0.08/2) + (3502/8x0.08)$.

From this the radius of curvature along the length of the plate is found to be:

$r = 191\ 406.29mm$ along length of plate;

If the same calculation is also conducted across the plate then for that case h = 0.08 and s =150, and therefore r= 35 156.29mm across width of plate.

All of the pre weld plates were found typically to have maximum deviation of the surface points of up to 0.1mm. Therefore when compared to the post weld dimensions as will be seen later then there is a significant difference in the scale of the dimensions in the range of 2-3 orders of magnitude therefore on this assumption the individual effects of the pre weld curvature have been neglected from the post weld analysis as it can be seen that in this case the pre weld flatness is consistent and small enough not to effect greatly the post weld results.

Due to the complex processing, by using a contact ball scanner in the pre weld plates, a relatively sparse point cloud was generated. Figure 4.1(a) shows an illustration of this point cloud. Along with the access restrictions (cannot scan exactly at the weld) then as discussed previously a decision was taken to process the post weld scans using a non contact measurement method using a 3D laser scanner. The benefit being that this data could be read directly into a post-processing package or CAD system and worked on directly with the need for further manipulation, and would also provide a much better resolution. The resolution on a post weld scan can clearly be seen in Figure 4.1(b) which shows a close up on the point cloud data collected on a butt weld sample near to the weld. Comparison between the two clouds in Figures 4.1(a) and 4.1(b) shows the far greater resolution available from the laser scanner over the trackball method and avoids inducing further errors in post processing by any errors that may occur in best fitting splines and surfaces through the trackball point cloud. Indeed on attempting to manipulate the trackball point cloud it was found that small inconsistencies occurred in the NURBS splines and surfaces fitted through the data making accuracy of the results from this method not suitable for measuring the degree of distortions produced in the welded samples. The fitted curves and surfaces to the trackball data showed minor irregularities which gave the surfaces a rippled effect due to the low cloud density.

The data from the laser scan is collected in a series of individual stripes which are of narrow width. Therefore multiple passes of the laser need to be made over the plates

87

to capture data across the whole plates as described in Chapter 3. The multiple overlapping stripes can be seen quite clearly Figure 4.1(b). In this exercise it was important to ensure that the edge of the plate as well as the top surface was scanned and captured to allow the necessary processing and measurement to take place as accurately as possible.
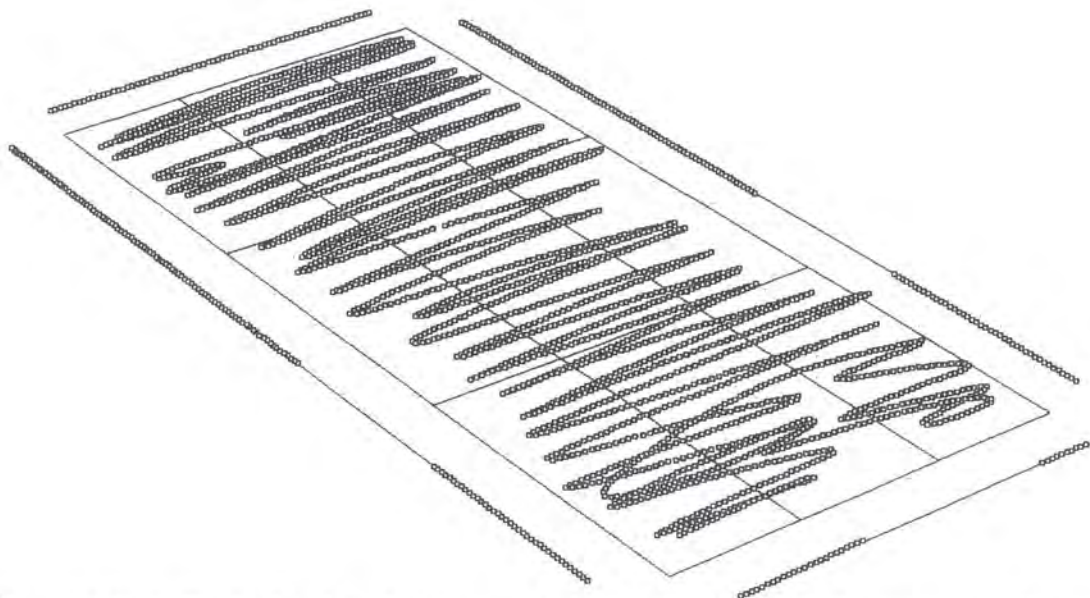
Figure 4.1(a): Typical point cloud generated using a track ball laser scanner (pre-weld plate)
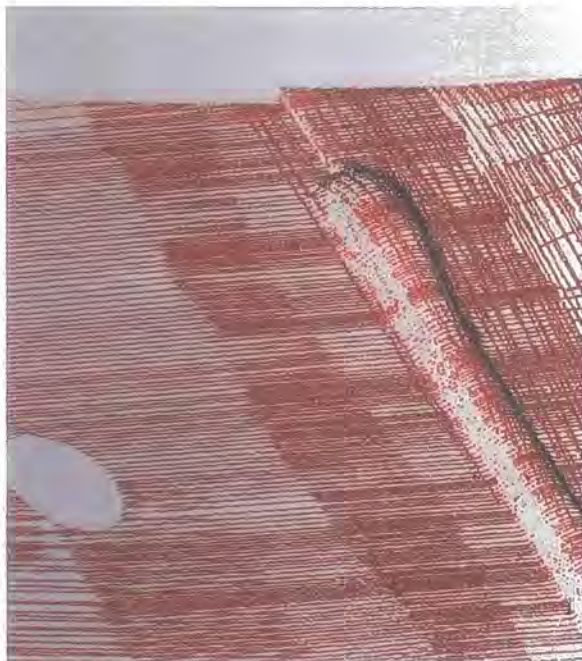
Figure 4.1(b): Close up of point cloud generated using a laser scanner (butt weld sample)

To process the point cloud the post weld samples were each cut at pre determined sections across the length and the width, i.e. parallel and transverse to the weld direction. In the length direction the measurements were taken every 50mm, and in the transverse direction the measurements were taken 9mm either side of the weld centreline and then twice more either side, at +/- 25 and 50mm for the bead on plate samples and 50 and 100mm for the butt weld samples. This provided a manageable amount of data that could be processed and interpreted in a timely manner. Measurements were not taken exactly on the weld centreline and immediately adjacent to the weld to ensure the accuracy of the measured results, especially for calculating the curvature results.

The dimensions from each section were then fed into a spread sheet and individual plate reports containing data, tables, results and diagrams generated. These could then also be compared for plates at the same speed and thickness, and also averaged across the weld samples for each factor position. This allowed a comprehensive understanding of the different distortions to be developed which is presented in the following sections of this chapter. The transverse and longitudinal dimensions could be gathered by direct measurement for the point cloud in the post processing software. The angles were measured by averaging a best fit line through the points on either side of the weld in a transverse section and then measuring between these two best fit lines. The radius of curvature was measured by developing a best fit curve through the points on the top surface of a longitudinal, or transverse, section and then using this to determine the radius by direct measurement in the post processing CAD software. Examples of these typical measured dimensions on a single scan section are shown in Figure 4.2. Appendix II contains some examples of the reports generated for each of the individual plate samples.

Dimension 2D: 50MM FROM PLANE 2

(D1) R 2172.398

(D2) 300.050

Y Axis

Z Axis   X Axis

Units: mm

Name	Measured	Nominal	Deviation	Tolerance –	Tolerance -
D1	2172.398	2172.398	0.000		
D2	300.050	300.000	0.050		
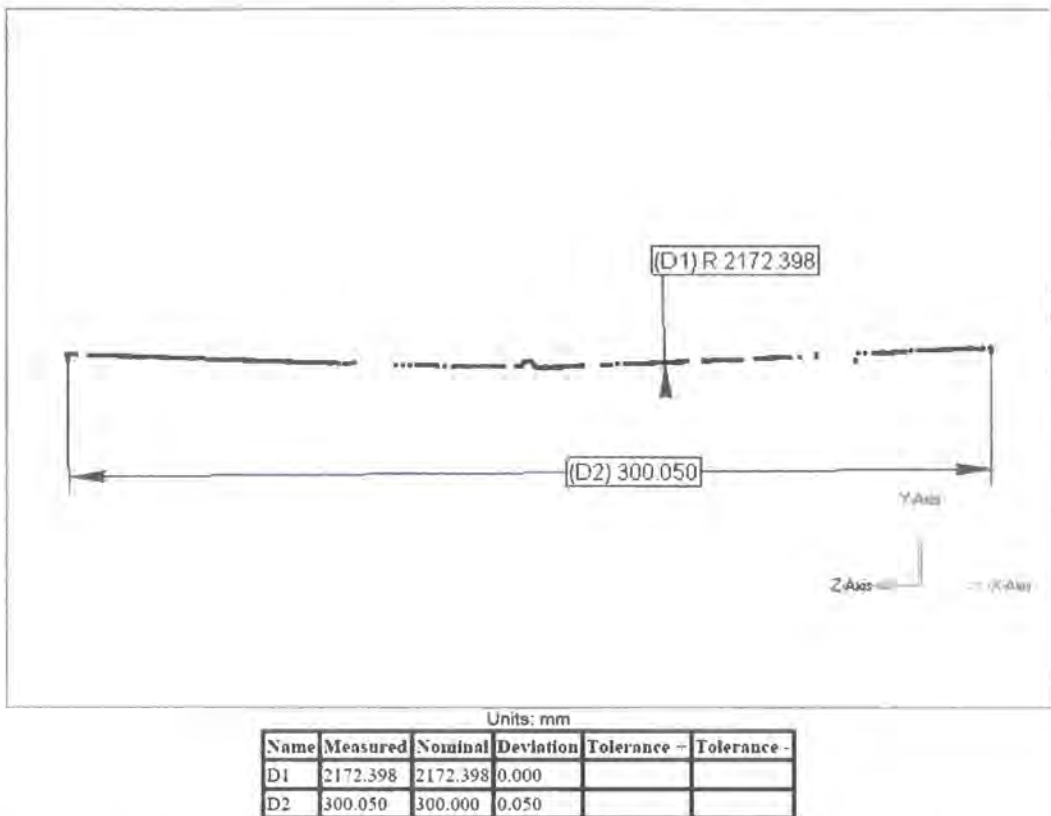
Figure 4.2: Typical section analysis on data point cloud (transverse section shown)

4.3 Weld Macro Study

In order to fully investigate the weld types identified, as part of the investigation it is necessary to carry out a detailed weld macrograph study and hardness investigation.

This investigation will provide detailed information about the welds. It will also ensure that the welds, rather than just visually looking like a production quality weld on the surface, conform to the requirements and standards of the case study company in terms of properties such as penetration, fusion, undercut, and weld dimensions. It is also possible from these destructive cut ups to assess the properties of the weld material in the various zones of the weld to observe the metallurgical changes that have taken place as a result of the welding operation.

90

It may be possible in future to use the results of this investigation to ensure correlation of future modelling efforts to simulate the weld production process, whereby not only can the distortions be calibrated but also the dimensions of the fusion zone and HAZ are compared and correlated.

For each of the sample speeds, weld types and material thicknesses a typical post weld sample was selected to undergo the destructive investigation. The samples were cut in the transverse direction at the position that corresponds to the measured positions used in the measurement exercise reported in the subsequent sections of Chapter 4. Six transverse cuts were therefore made at positions 50,100, 150, 200, 250, and 300mm along the weld direction.

Each section was then examined to determine the dimensions of the weld and this was tabulated and recorded for use in future calculations to assist correlation to the current published predictive formulas that exist.

4.3.1 Bead on Plate Sample Macros
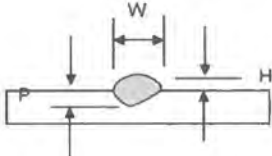
The bead on plate welds were subjected to visual examination prior to cut up. The weld appeared to be of a consistent high quality, and showed no significant undercut. However it could be observed that on the 2mm samples and also the 2.5mm at the slower weld speeds, when the parameters of the weld were at their limit, the weld was beginning to burn through the plate toward the last 20-30mm of the weld run.

For the discussion here a typical set of weld cut ups is chosen to look at in detail. The full results and photos from an example of each type of cut up are shown in Appendix I.

The results presented here are from plate sample 41 which was a 2mm thick bead on plate sample. This was welded at 700mm/min, which was the slowest weld speed used in the experiment and therefore the greatest heat input.

The dimensions measured at each section from the weld run are shown in Table 4.1.

Table 4.1: Illustrative bead on plate weld dimensions from macro study

Position along weld (in mm)	50	100	150	200	250	300	Note: XSA refers to weld cross section area
Bead on plate (ref plate samples 2.0mm plates 41 @ 700mm/min)							
W	6.4	5.9	5.9	6.2	5.9	5.5	
H	1.7	1.5	1.5	2	1.7	2.1	
P	0.9	1	0.7	0.7	1.1	2.1	
XSA	5.4	4.8	4.5	5.6	6.2	7.2	

From Table 4.1 it can be seen that the weld dimensions are relatively stable, penetration of the weld into the parent plate is typically around 35 to 50% of the material thickness. However as can be seen from the section at 300mm the residual heat build up occurring from the welding process is beginning to affect the stability of the plate and at this point full depth penetration is beginning to occur. As was observed in the full sample shortly after this section then burn through occurred in the plate and the process broke down. The burn through can be seen in Figure 4.3, which was taken prior to the cut up.

Figure 4.3: Picture of 2.0mm plate showing burn through at end of weld run

An additional investigation was undertaken to determine the hardening effects of the weld on the material and to assist in the determination of the range of each region across the weld. The section for the macro study was fine polished prior to the hardness study. The photograph of section used for the study, shown in Figure 4.4, taken at magnification clearly shows the different metallurgical regions created by the weld process.
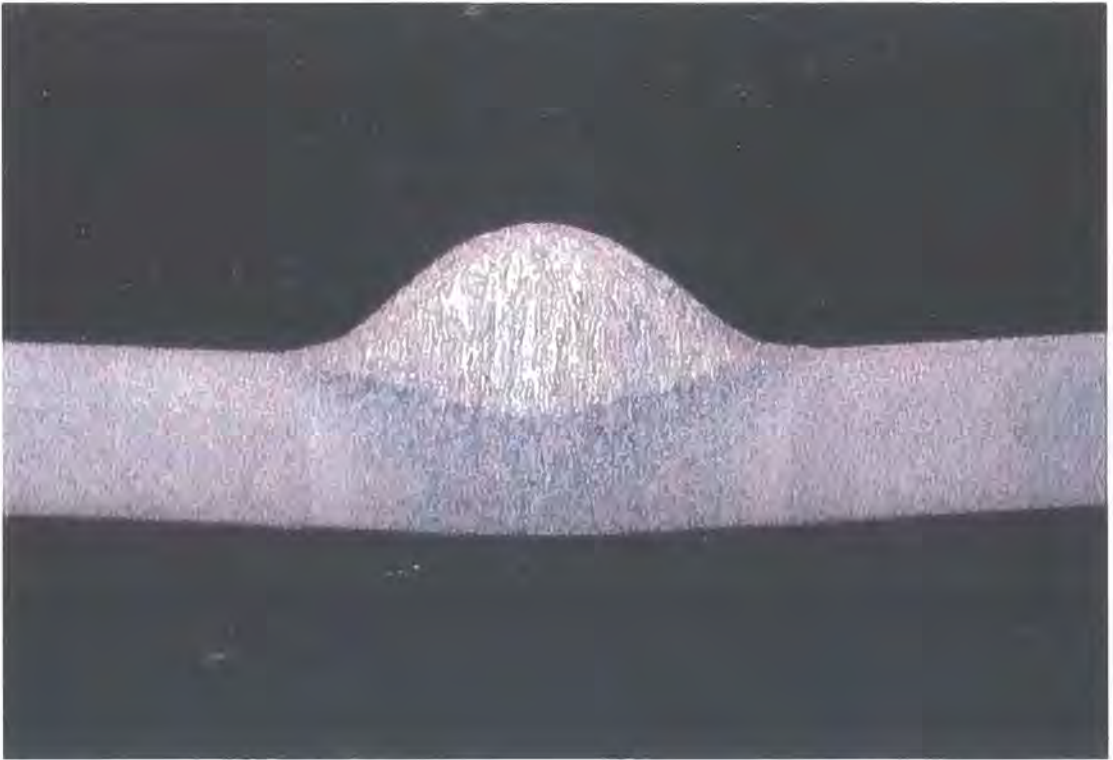
Figure 4.4: Fine polished section showing metallurgical regions (bead on plate)

The results of this hardness investigation are shown in Table 4.2. The hardness study was undertaken using the Vickers micro hardness method; this was done using a 300g load on the indenter. Readings were taken at 0.5mm intervals from the centre of the weld out over towards the edge of the plate. It can be seen from the change in mechanical properties that metallurgical changes have taken place in the various regions of the weld. From the value of hardness reference to the parent plate it is possible to say into which region the readings fall. The hardness study was undertaken at a section close to the middle of the weld run in order to ensure any start and end effects did not influence the results. Therefore the hardness study was taken at the section cut at 150mm along the plate.

93

Table 4.2: Hardness study results for bead on plate

Bead on plate			
2.0mm plates 41 @ 700mm/min			Micrograph for hardness indent positions
Positon	Description	Micro Hardnesss	
1	Weld	235	
2	Weld	219	
3	Weld	216	
4	Weld	212	
5	Haz	176	
6	Parent	162	
7	Parent	171	
8	Parent	157	
9	Parent	162	
10	Parent	158	
11	Parent	161	
12	Parent	156	

In addition to carrying out the dimensional and hardness study, additional high magnification images were taken to look at the grain structure and composition of the various regions within the weld. These images are shown in Figure 4.5.

(a) Weld Metal Zone

(b) Inner HAZ showing fusion line

(c) HAZ

(d) Parent Metal

All images taken using 200x magnification
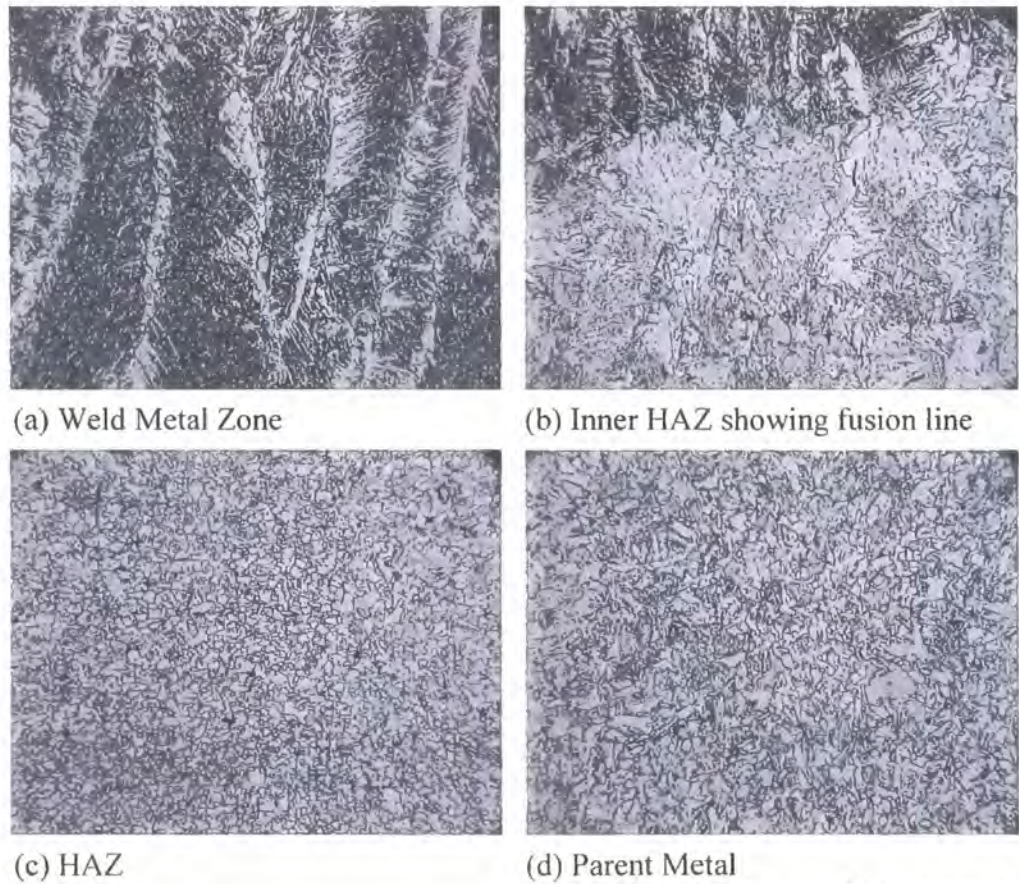
Figure 4.5: Weld microstructure images for bead on plate sample

The first image shows the grain structure in the weld itself. This is clearly very different in its structure and grain form from that of the base parent metal or even the HAZ, the weld material has much more of an Austentic grain form. The second image clearly shows the transition from the weld material into the fusion zone and the inner heat affected zone. The heat affected zone exhibits a larger and coarser grain structure than that of the base parent metal matrix. This is due to the formation of Martensite, and the longer and slightly narrower grain shape associated with Matrensite is in the image. The parent metal can be seen in this figure to exhibit the typical fine grain ferrite structure associated with High Strength Low Alloy Carbon steels. The structure is almost pure ferrite, and it can be seen clearly to show the fine dispersion of the alloy carbides as Pearlite, which is present in the image as the dark dots in the ferrite matrix. It is the fine grain structure of the ferrite, combined with the presence of some Pearlite that gives these steels their strength.

4.3.2 Butt Weld Sample Macros
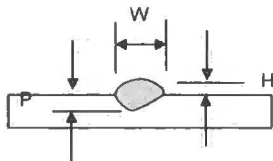
The butt weld samples were also subjected to visual examination prior to cut up. The weld again appeared to be of a consistent high quality, and showed no significant undercut. However again it could be observed that on the 2mm samples at the slower weld speeds, when the parameters of the weld were at their limit, the weld was beginning to burn through the plate toward the very end of the weld run. The burn through was much less evident than on the bead on plate samples and did not occur at 2.5mm. This may well be due to the fact that there is now twice the volume of plate present so a far greater heat sink and the residual heat effects that lead to the previous heat build up do not happen as quickly due to the increase in volume of the metal present in this joint configuration.

For the discussion here a typical set of weld cut ups is chosen to look at in detail. The full results and photos from an example of each type of cut up are shown in Appendix I.

95

The results presented here are from plate samples 1 and 1A which are a 2.5mm thick butt weld sample. This was welded at 700mm/min, which was the slowest weld speed used in the experiment and therefore the greatest heat input.

The dimensions measured at each section from the weld run are shown in Table 4.3.

Table 4.3: Illustrative butt weld dimensions from macro study

Position along weld (in mm)	50	100	150	200	250	300	
							Note: XSA refers to weld cross section area
Butt weld (ref plate samples 2.5mm plates 1/1A @ 700mm/min)							
W	7.2	7.1	6.8	7	7.2	6.3	
H	2.3	2.4	2.2	2.3	2.3	2.9	
P	2.6	2.6	2.6	2.6	2.6	2.6	
Gap	0	0	0	0	0	0	
XSA	10.6	10.7	10	9.8	11.8	15.3	

From Table 4.3 it can be seen that the weld dimensions are relatively stable, penetration of the weld is around 100% of the material thickness of the base material, in fact showing a very slight amount of over penetration. This is due to the speed for welding being the slowest speed in this trial and therefore maximum heat input, however in all cases the butt welds provide high levels of penetration. This is perhaps not surprising as the parameters were selected based on the case study company's production settings, and their internal specification is to achieve greater than 85% penetration on butt welds.

An additional investigation was undertaken to determine the hardening effects of the weld on the material and to assist in the determination of the range of each region across the weld. The section for the macro study was fine polished prior to the hardness study. The photograph of section used for the study, shown in Figure 4.6, taken at magnification clearly shows the different metallurgical regions created by the weld process.
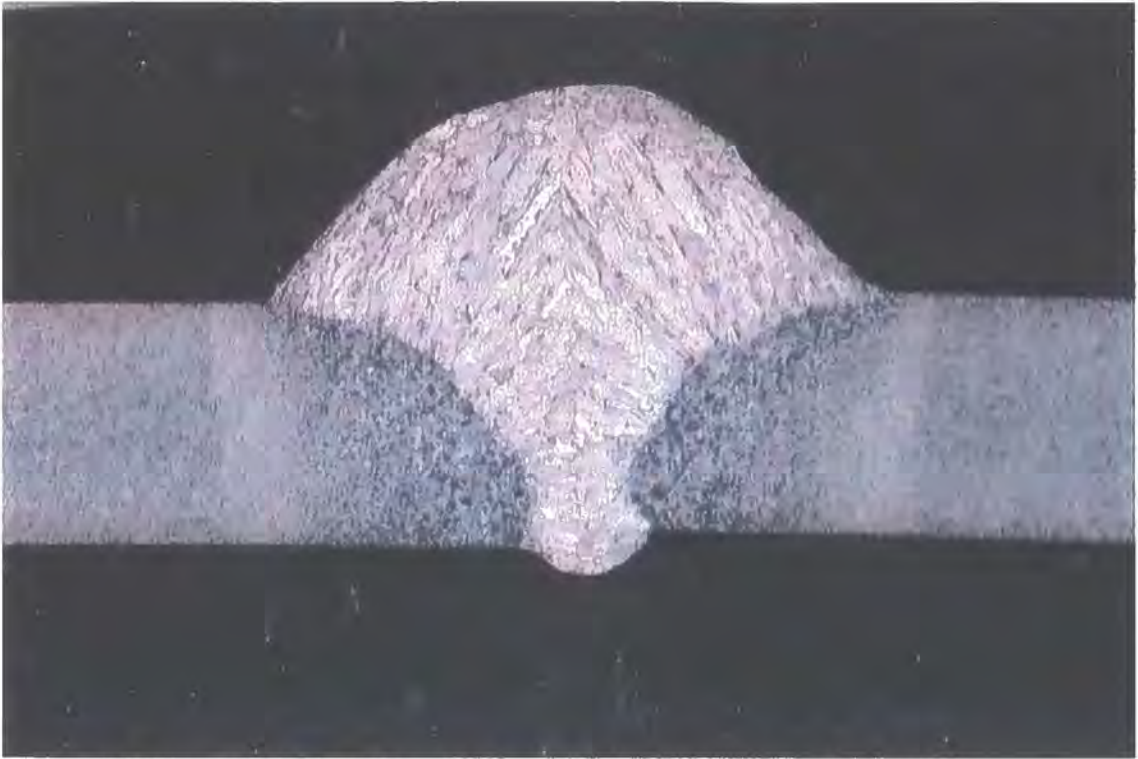
Figure 4.6: Fine polished section showing metallurgical regions (butt weld)

The results of this hardness investigation are shown in Table 4.4. The hardness study was undertaken using the Vickers micro hardness method, this was done using a 300g load on the indenter. Readings were taken at 0.5mm intervals from the centre of the weld out over towards the edge of the plate. It can be seen from the change in mechanical properties that metallurgical changes have taken place in the various regions of the weld. From the value of hardness reference to the parent plate it is possible to say into which region the readings fall. The hardness study was undertaken at a section close to the middle of the weld run in order to ensure any start and end effects did not influence the results. Therefore the hardness study was taken at the section cut at 150mm along the plate.

Table 4.4: Hardness study results for butt weld

Butt			
2.5mm plates 1/1A @ 700mm/min			Micrograph for hardness indent positions
Positon	Description	Micro Hardnesss	
1	Weld	222	
2	Weld	224	
3	FL	121	
4	Haz	189	
5	Haz	181	
6	Haz	173	
7	Haz	170	
8	Parent	164	
9	Parent	161	
10	Parent	169	
11	Parent	173	
12	Parent	174	
13	Parent	168	
14	Parent	169	

Finally after carrying out the dimensional and hardness study, additional high magnification images were taken to look at the gain structure and composition of the various regions within the weld. These images are shown in Figure 4.7.

(a) Weld Metal Zone

(b) Inner HAZ showing fusion line

(c) HAZ

(d) Parent Metal

All images taken using 200x magnification
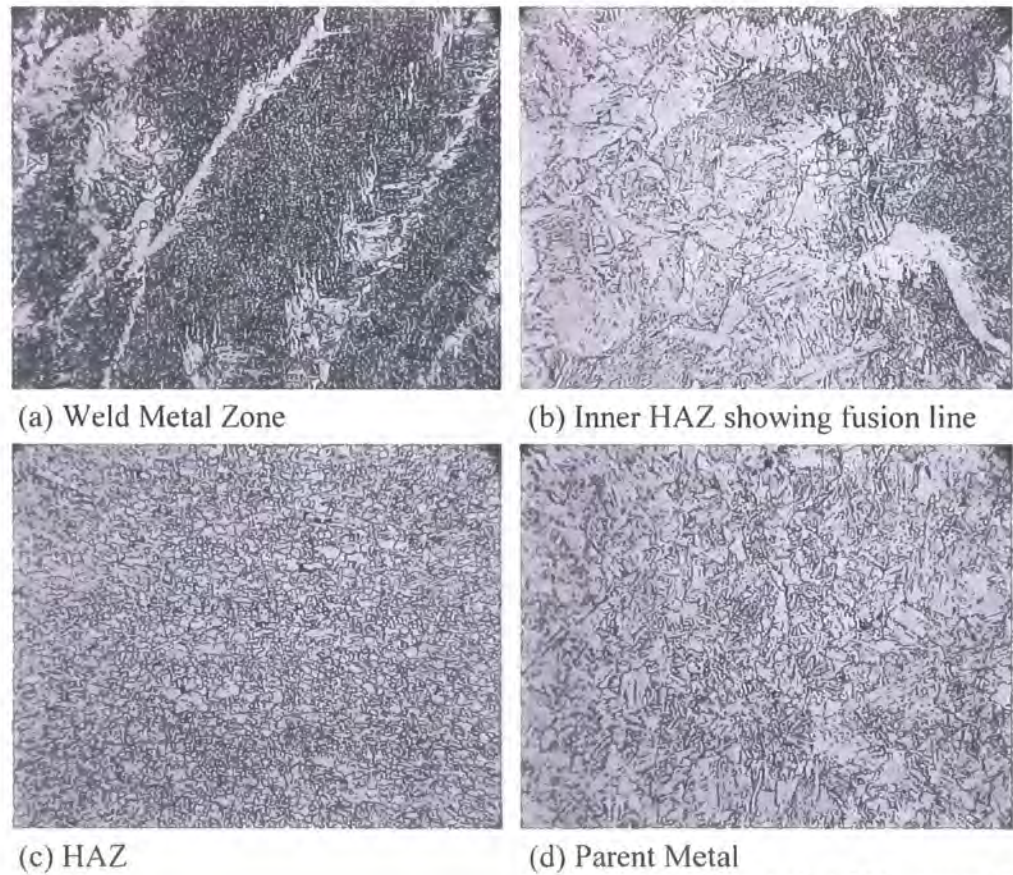
Figure 4.7: Weld microstructure images for butt weld sample

98

The first image shows the grain structure in the weld itself. Again it is clearly very different in its structure and grain form from that of the base parent metal or even the HAZ, the weld material has much more of an Austentic grain form. The second image shows the transition from the weld material into the fusion zone and the inner heat affected zone. The heat affected zone exhibits a larger and coarser grain structure than that of the base parent metal matrix. This is due to the formation of Martensite, and the longer and slightly narrower grain shape associated with Matrensite is in the image. The parent metal can be seen in this figure to exhibit the typical fine grain ferrite structure associated with High Strength Low Alloy Carbon steels.

Note: - Additionally it should be noted that a similar exercise was undertaken on the joint designed to investigate the fillet/tee weld configuration, and whilst this joint type does not form part of this report, due to the volume of data generated from the two basic joint types, then the investigation is mentioned and included in Appendix I, for completeness. This joint will be subject of a separate future report and investigation.

4.4 Bead on Plate Distortion Study

4.4.1 Individual Bead on Plate Samples and Results

In this section the basic profiles from a single bead on plate weld test sample will be discussed. An example of the typical post welded condition of a bead on plate sample is shown in Figure 4.8 to assist with the discussion and understanding of the results presented here and in subsequent sections.
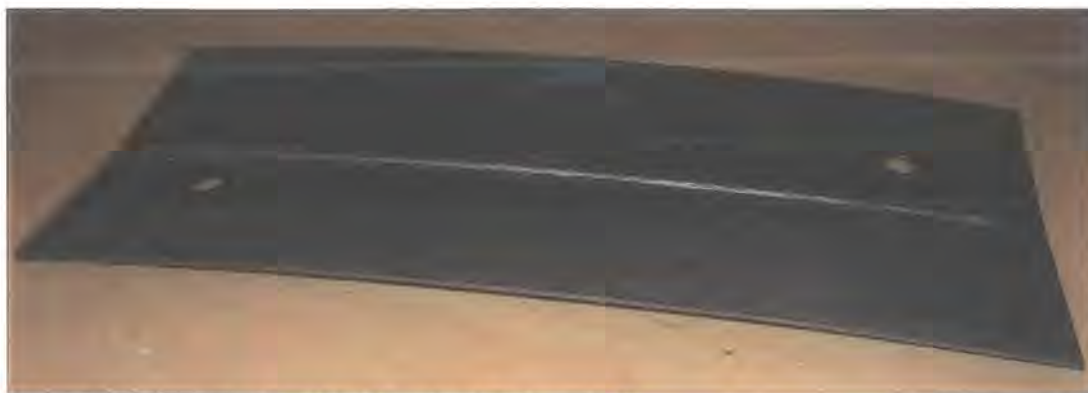
Figure 4.8: Image of welded bead on plate sample

For the purposes of this part of the report the sample chosen is a mid-range sample from the variables under investigation. Therefore the profiles reported here can be deemed to be typical and indicative of those arising from the bead on plate specimens. The sample that has been used for this section of the report is 2.5mm thick plate which has been welded at 1000mm/min weld speed. The typical measured results were recorded and inserted into the Excel spreadsheet using the method previously described in Section 4.2. These results for the plate discussed in this section are shown in Table 4.5 for illustrative purposes.

Due to the volume of data available for each specimen then it is not possible to discuss each individual plate in exact detail but sample summary data of the experimental results and outcomes for these plates are included for completeness in Appendix II.

Specimen and plate numbers	Plate thickness (mm)	Weld joint type	Weld speed (mm/min)	weld type	gas flow (l/min)	target weld length (mm)	actual weld length (mm)	wire stick out (mm)		
45	2.5	Bead on Pl	1000	mig	26	330		20		

section results	x = 50			x = 100			x = 150			x = 200			x = 250			x = 300			section results
	Welded	Pre welded	Delta	Welded	Pre welded	Delta	Welded	Pre welded	Delta	Welded	Pre welded	Delta	Welded	Pre welded	Delta	Welded	Pre welded	Delta	
width W (mm)	149.65	150.15	0.50	149.35	150.15	0.80	149.38	150.15	0.77	149.37	150.15	0.78	149.46	150.15	0.69	149.48	150.15	0.67	width W (mm)
angle (weld side) (deg)	172.4	180.0	7.6	171.7	180.0	8.3	171.8	180.0	8.2	172.0	180.0	8.0	172.7	180.0	7.3	174.1	180.0	5.9	angle 1 (weld side) (deg)
approx. Radius of curvature (mm)	560	flat within .6		566	flat within .6		470	flat within .6		539	flat within .6		471	flat within .6		542	flat within .6		approx. Radius of curvature (mm)

section results	y = -50			y = -25			y = -9			y = 9			y = 25			y = 50			section results
	Welded	Pre welded	Delta	Welded	Pre welded	Delta	Welded	Pre welded	Delta	Welded	Pre welded	Delta	Welded	Pre welded	Delta	Welded	Pre welded	Delta	
length L (mm)	349.84	349.97	0.13	349.56	349.98	0.42	349.42	349.99	0.57	349.28	349.99	0.71	349.41	350.00	0.59	349.84	350.01	0.17	length L (mm)
approx. Radius of curvature (mm)	1743	flat within .6		1780	flat within .6		1817	flat within .6		1801	flat within .6		1765	flat within .6		1731	flat within .6		approx. Radius of curvature (mm)

Firstly, was considered the longitudinal shrinkage occurring in this bead on plate sample. The graph showing the results for this sample can be seen in Figure 4.9. It can be seen that peak shrinkage in the longitudinal direction occurs close to or at the centreline of the weld, with the lowest shrinkage occurring at the edges of the plate which are the furthest from the weld itself. Considering the profile and distribution, it appears quite uniform and regular. From the measured results it can be seen that there is a maximum value occurring which is in the region of 0.7 to 0.8mm. Because the shrinkage was not measured and calculated exactly at centre line of the weld then this precise point on the peak of the distortion cannot be positioned, based on the curve fitting through these results. The variation in results from the centre line of the weld to the extremes of the plate does appear to be regular and fairly uniform either side of the weld and it could also be possible to define a parabolic distribution that could be fitted through these points. In order to determine the precise form of the distortion distribution then far more points and measurements would need to be taken.
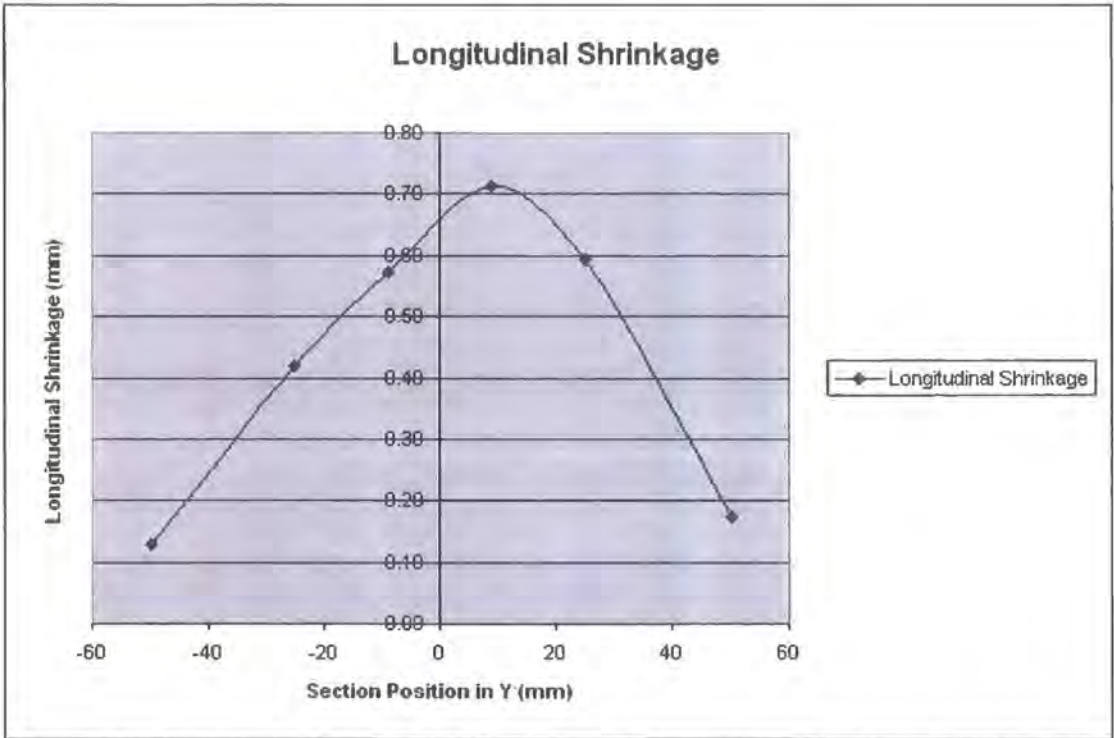
Figure 4.9: Variation of longitudinal distortion for typical bead on plate sample

The overall results for longitudinal shrinkage would appear to make sense in that the peak shrinkage is occurring at the weld line where the most physical changes are

102

occurring to the parent material. This reduces as the measurements move away from the effects of the heat and material changes. However some shrinkage will still occur as an effect of the weld due to the residual forces established in the plate as a result of the temperature changes that occur.
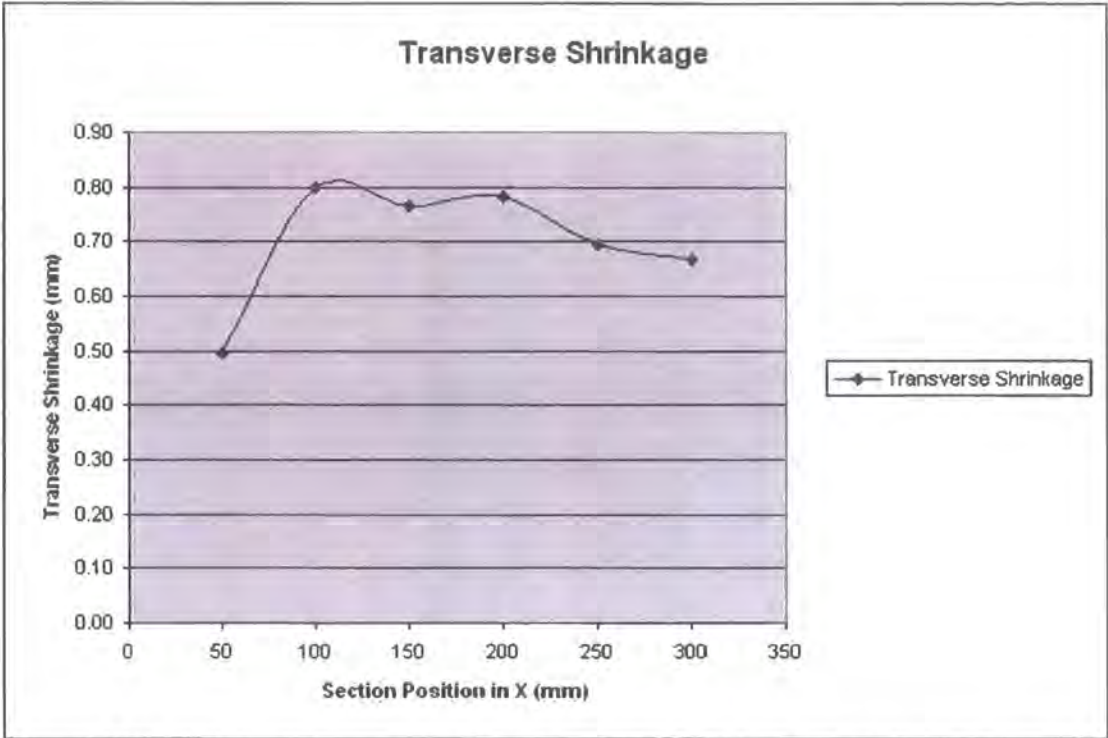
Figure 4.10: Variation of transverse distortion for typical bead on plate sample

Next to be considered is the transverse shrinkage, the results for this can be seen in Figure 4.10 showing the variation of the width of the plate for this typical bead on plate sample. From the distribution of these results it is possible to see that the lowest transverse shrinkage occurs at the start of the weld. This would appear to make sense as it is the area where there will have been least heat input and build up. As the weld progresses along its full length there will be a build up of heat in the material in the plate. This would appear to be in line with the increase in transverse shrinkage that occurs as the welding torch moves along the plate in welding it. Once the weld is established and moving at speed then a moving temperature field will develop during the weld phase. This develops a transient temperature field in the plate, but will tend to a steady state during the cooling process. The other points away from the weld start would appear to lie within this steady state field region. Therefore if the start effects can be considered to be removed the other points taken

103

along the length of the sample give a measure of transverse shrinkage. In the case examined here it can be seen that these all lie within less than +/-10 percent of each other. Therefore it could be stated that under steady-state conditions of welding an almost uniform transverse shrinkage is occurring in the plate. This transverse shrinkage can be seen to be being in the region of 0.75mm and with a scatter on this being less than 10 percent. It would therefore be possible to describe this profile is having a straight line average shrinkage in the transverse direction to the weld line.
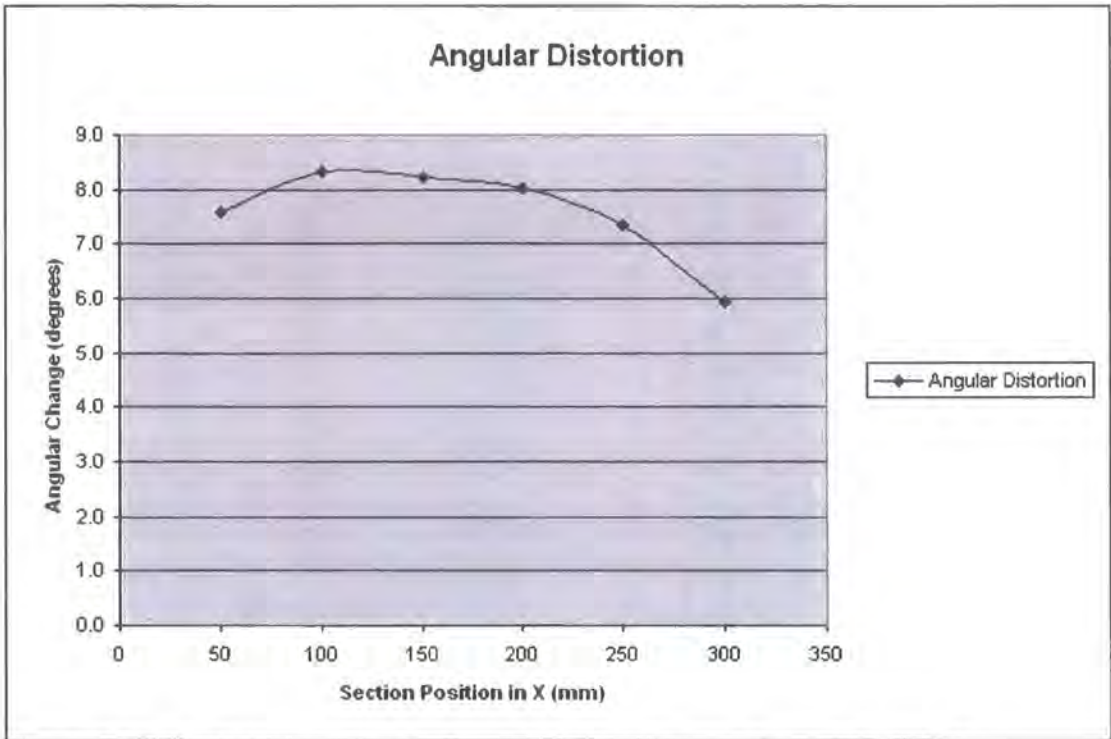
Figure 4.11: Variation of angular distortion for typical bead on plate sample

The next factor that will be considered is the change in angular distortion along the length of the weld. The angular distortion is measured either side of the weld line as previously described in this chapter. A graph showing the change in angular distortion over the length of the plate is shown in Figure 4.11. Here it can be seen that towards the start of the weld there is a slightly lower angular distortion. It is possible to surmise that this could be due to the build up of the heat input at the start of the weld when considered over the whole plate. Again, as in the transverse shrinkage case, as the heat in the plate builds up and so the angular distortion increases. However differently to transverse shrinkage it would appear that the

104

angular distortion actually reduces again as the weld length increases. This could in part be due to increased stiffness of the overall system due to the build-up of the weld and addition of material which would therefore reduce very slightly the angular distortion. However in the bead on plate samples it is unlikely that the addition of the weld significantly increases the stiffness of the resultant base plate when compared to weld joints such as butt weld or overlap, where the joining of the two plates will dramatically increase stiffness. Therefore it might be expected that in other sample results bigger changes in angular distortion may be observed due to the increased stiffness upon welding of the system if this belief is correct. However, it is of particular note that most of the measured values are relatively small and from the results accurate measurement is quite difficult. This is due to having to best fit straight lines through the point cloud either side of the weld and so the results could be sensitive to minor curve fitting errors.

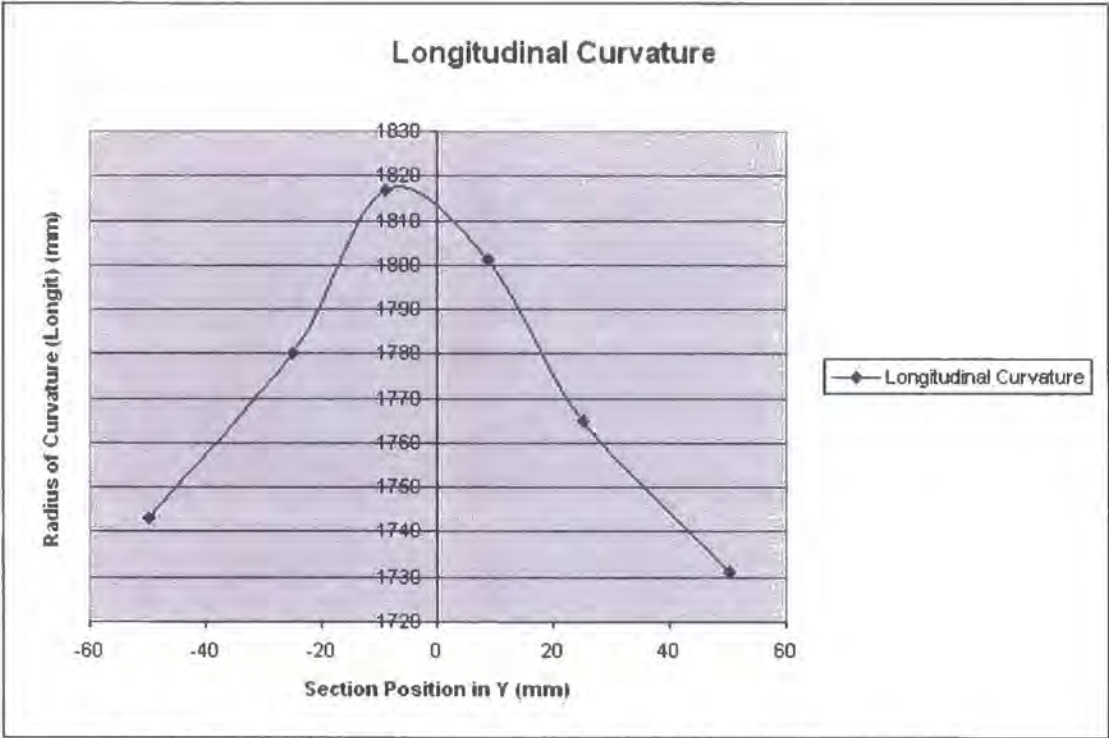Figure 4.12: Variation of bowing distortion for typical bead on plate sample

The final factor that will be considered and discussed is longitudinal curvature, or bowing of the plate, for the bead on plate weld sample. The graph showing the change to longitudinal curvature over the width of the sample can be seen in Figure 4.12. From these results it can be seen that highest value of curvature occurs

105

close to the weld and decreases as it moves towards the edges of the plate. This is possibly due to a stiffness effect as the flexibility of the plate will be greater at edges than it is in the centre. It needs to be noted that a smaller radius of curvature indicates greater degree of bowing, and that the larger the radius of curvature the closer the part is to been flat. Comparison to the pre welded bowing calculations for curvature of the plate show that there is a significant difference in the longitudinal bowing figures, ~1800 for welded plate versus ~19200 for pre-weld plate. Therefore as the bowing in the welded samples is in the order of 100 times greater than the pre weld plates it is safe to discount the influence of the pre weld curvature in the experimental results without significantly compromising the experimental analysis results. If the range of results across the whole plate is looked at these values are all very close to each other. In this particular sample the radius of curvature ranges only from approximately 1730mm to 1820mm and therefore for the sample considered here all these results actually lie within 5% of one another. It could therefore be stated that longitudinal bowing distortion is uniform across the plate with some scatter due to the slight geometry variations in relation to the weld at each different position. Therefore for future distortion prediction it may be possible to calculate and state one single bowing factor that can be applied across a whole plate for a bead on plate sample.

4.4.2 The Effect of Varying Speed on Bead on Plate Samples and Results

Having looked at the effects of the welding on the distortion profiles for an individual plate it is now possible to move on to look at the effect of other parameters. Firstly, it is possible to look at the effect of varying the weld speed whilst holding that the material thickness constant. This investigation will look at averaged results for each speed and compare distortions to make generalised assessments for the effects of varying speed. Having previously looked at an individual 2.5mm thick plates distortions these will now be used as a baseline to investigate the effect of increasing and decreasing the weld speed on the distortion results from this thickness of plate.

The first output to be considered is longitudinal shrinkage. This having been seen previously on the individual plates that to have occurred at a maximum near to the weld line and decreased towards the edges of the plate. Now considering the effects of increased and decreased weld speed above and below the previous sample, it can be seen from the graph in Figure 4.13 which compares the average results for the longitudinal shrinkage for the three different weld speeds used in this experiment on the 2.5mm thick bead on plate samples, that increasing weld speed decreases the overall longitudinal shrinkage that is occurring whilst reducing the weld speed increases the overall distortion values.
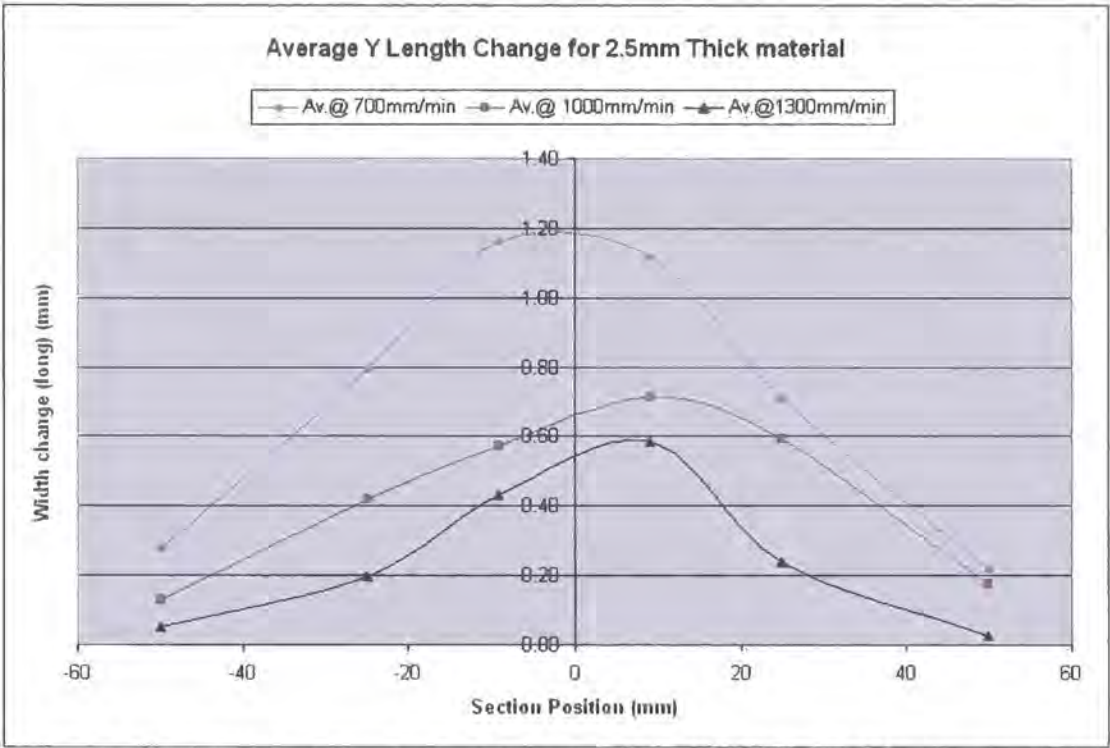
Figure 4.13: Variation of longitudinal distortion for varying speed (bead on plate)

On the full range of samples at different speeds it can be seen from the results that the peak distortion for longitudinal shrinkage always occurs at the weld line and is considerably less at the free edges of the plate. Based on results presented here then generally the distortions on either side of the weld line are equal and seemed to follow a broadly linear relationship, based on the number of measured points. The slowest weld speed at 700mm/min will generate the most heat input into the plate that has been welded whilst the higher weld speeds will proportionally put in less

107

heat input. From the graph in Figure 4.13 it is therefore clearly evident that increasing speed decreases longitudinal shrinkage which must mainly be attributed to the reduction in heat input per unit length as weld speed increases. At the fastest weld speeds very little distortion is occurring at the edges of the plate.
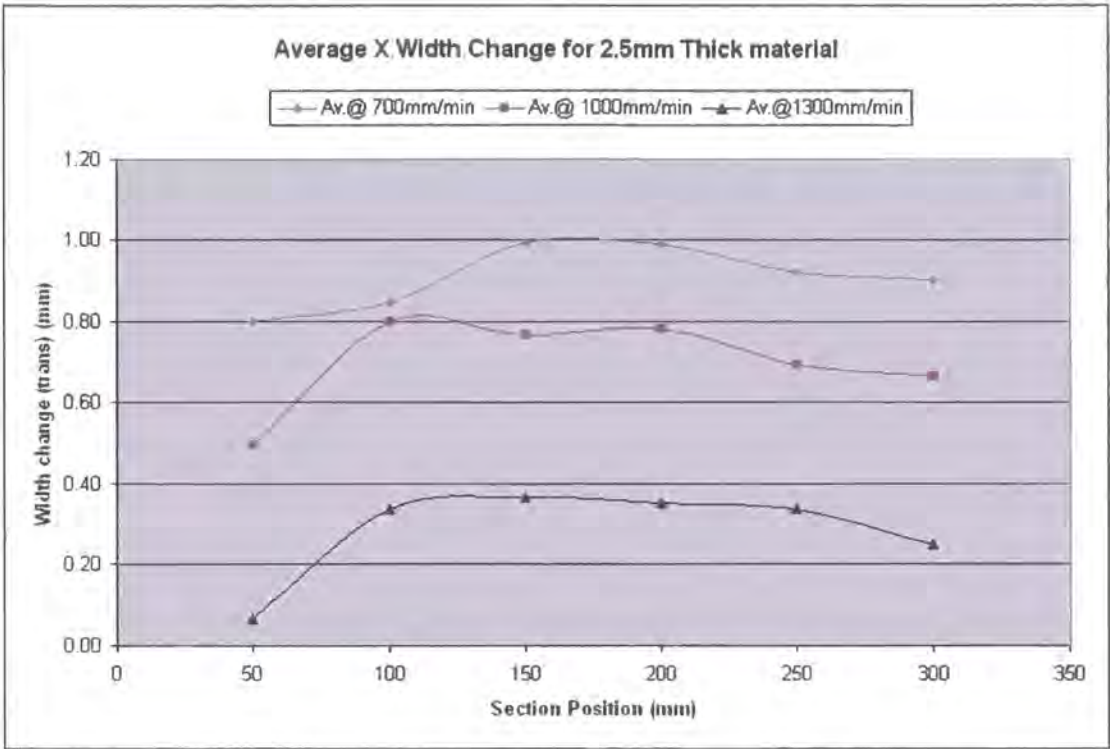
Figure 4.14: Variation of transverse distortion for varying speed (bead on plate)

The next to be considered is the effects of weld speed on the transverse shrinkage, as shown in the graph in Figure 4.14. Again as was the case in the individual plate in all instances the lowest transverse shrinkage occurs at start of the weld as the heat is building up in the plate. Once the heat has built up in the plate then consistent transverse shrinkage appears to occur over the remainder of the plate length. Although also it could be argued that this transverse shrinkage also reduces towards the end of the plate as the heat input stops, creating an end effect at the end of the weld. However all three average curves follow the similar general profile of uniformly consistent transverse shrinkage with the results being very closely packed and showing little variation in magnitude once the steady-state conditions away from the start effects have been established. As is the case with the longitudinal shrinkage, then for transverse shrinkage also, the maximum distortion is occurring at

the slowest weld speed; the slowest weld speed corresponding to the maximum heat input. Likewise also the lowest distortion is occurring for the highest weld speed. In this particular case for 2.5mm thick material then the curves appear at relatively evenly spaced proportional to the change in weld speed. Again these cases would substantiate the fact that transverse distortion could be approximated and calculated by a single uniform value over the width of a component which would allow for a designer to make an estimation and allowance to improve the accuracy and production readiness of a design.
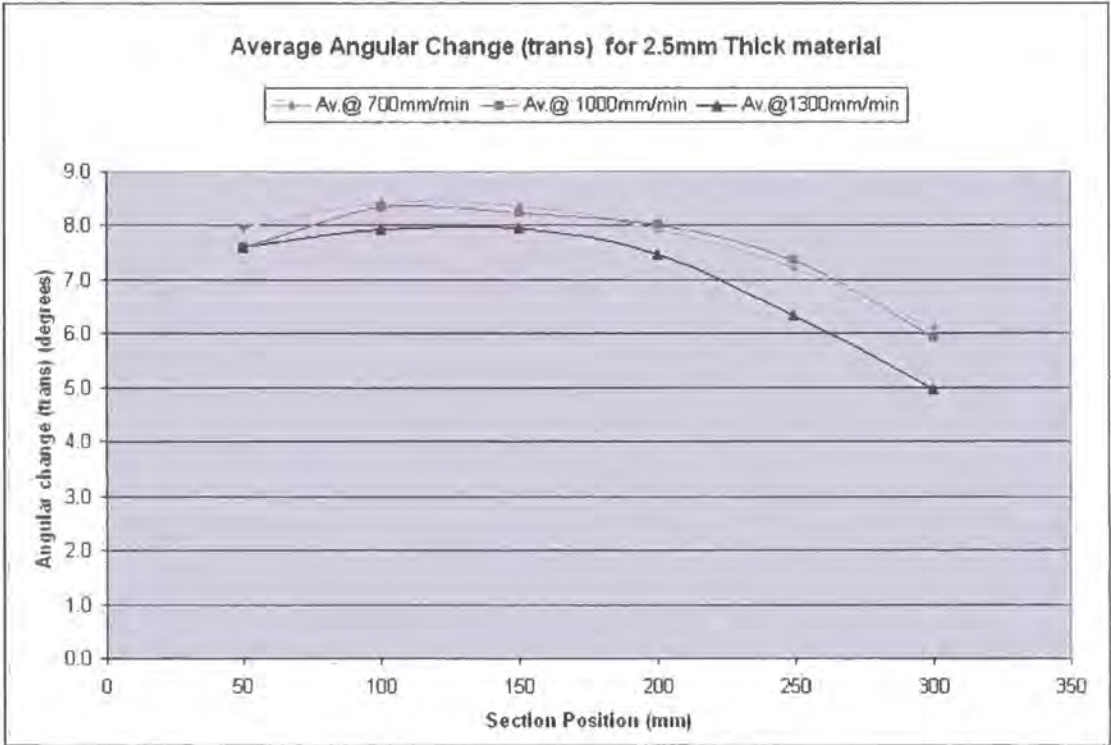
Figure 4.15: Variation of angular distortion for varying speed (bead on plate)

The next distortion that is considered is the effect of changing speed for a constant thickness plate on the angular distortion. The results for this investigation are presented as a summary in Figure 4.15. Looking at these results it is clear that for the slower weld speeds of 700 and 1000mm/min there is very little difference in the angular distortion results. The 1300mm/min weld speed results gave a very similar profile to the two previous results, however in that case all the angular distortions do appear to be slightly reduced which would be in keeping with the reduced heat input occurring from a higher weld speed. It is known that the case study company targets

109

high penetration values in their welding processes. Previous work by other researchers, including Mischler (1989), as discussed in section 2.3.3, have indeed shown that the effects of heat input in relation to angular change can be quite different from what would be expected from the previous results for the other distortion types. The welding current and speed are closely related factors, and it has been shown that up to a certain point increasing current is directly proportional to increase in distortion. However when this increasing the current results in a deeper penetration weld, then in the case of angular distortion, the increased current may result in reduced distortion. It is therefore from considering the above results then such effects as this could be part of the explanation for the findings are shown that in Figure 4.15. This is due to the case study company targeting a high penetration weld and therefore the penetration depth having greater influence over the angular distortion. Indeed it may be that the 1300mm/min weld speed is perhaps above the threshold and therefore reduced heat input also resulting in the lower distortion values. The values found for thinner material in this study would appear to bear this finding out in that for the 2.0mm material, which is towards the limit of the process values chosen, (as seen by the previously discussed burn through), there is very little difference in angular distortion for the three different weld speeds. This is consistent with the reasoning that it is due to the relatively high heat input creating deep and consistent penetration which is the overriding control on the distortion value.

Finally in the investigation comparing the change of speed for uniform thickness of material, these effects on the radius of curvature in longitudinal direction, or the bowing distortion, are considered. The results for the bowing distortion are presented in Figure 4.16. Again it is to be noted that in this case the greater the value of the radius of curvature than the lesser the distortion is occurring, i.e. a perfectly flat plate would have a very large indeed infinite radius of curvature, whereas a plate exhibiting a high amount of curvature would have a low radius. Again the series of curves appear to demonstrate a general relationship in this series proportional to the weld speed.
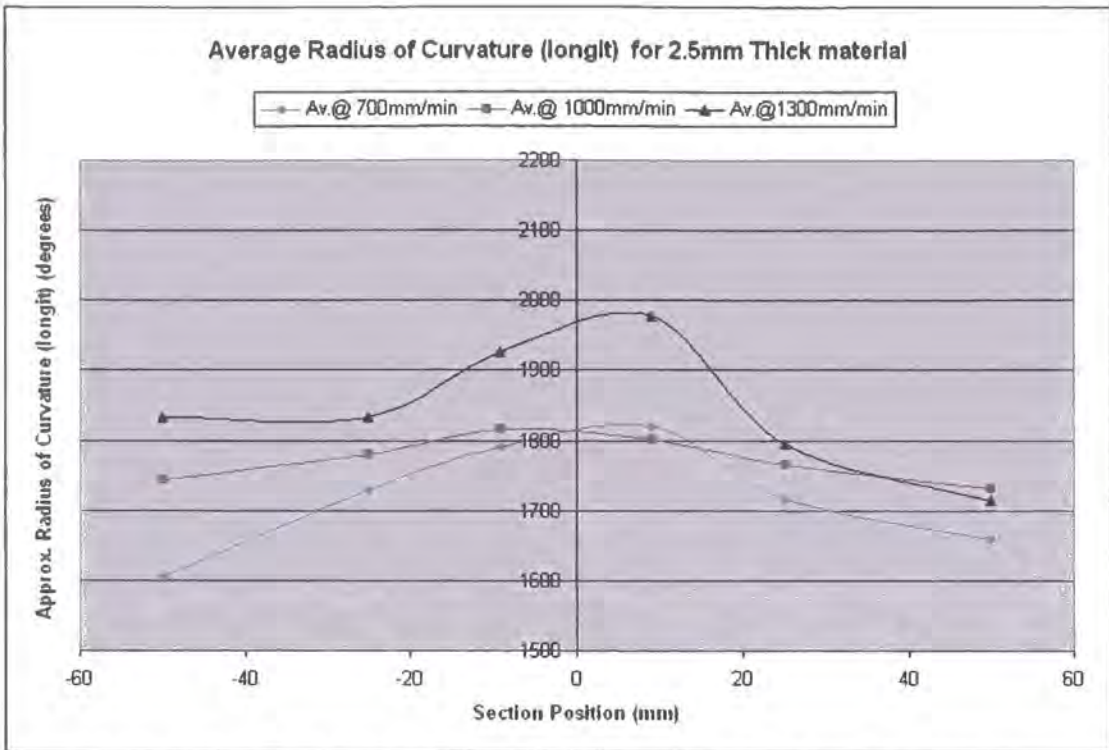
Figure 4.16: Variation of bowing distortion for varying speed (bead on plate)

There are some limitations in the method used to approximate the radius of curvature and these could contribute to the scatter on the results. However, as discussed in the single plate case if these results are all looked at in detail then overall there is very little scatter on the results when compared to the base plate flatness. Therefore it should be possible to characterise the radius of curvature as a single value occurring across the width of the plate which appears to be proportional to the weld speed. Therefore, again for simple components perhaps a designer could compensate for this and design a pre-bend in order to overcome this effect.

4.4.3 The Effect of Varying Thickness on Bead on Plate Samples and Results

In this section of the investigation the effect of varying plate thickness on distortions will be discussed whilst holding the welding speed constant. This investigation will look at averaged results for each material thickness and compare the distortion results to make generalised comparisons for the effects of varying thickness. Having previously looked at an individual 2.5mm thick sample, and the effects of speed, this

111

original plate will be used as a baseline to investigate the effect of increasing and decreasing the plate thickness on the distortion results from this original thickness, whilst holding the welding speed constant at 1000mm/min.

As with the other investigations the first factor to be considered is the effect on the longitudinal shrinkage of the plate. The results for this part of the investigation can be seen in the graph in Figure 4.17, which compares the longitudinal shrinkage based on varying material thickness. Again that it can be observed that the peak longitudinal distortion occurs at the weld centre line and reduces towards the free edges of the plate. It can be seen that increasing the thickness of the base material results in decreasing the longitudinal distortion, which is typical at all points throughout the data set.
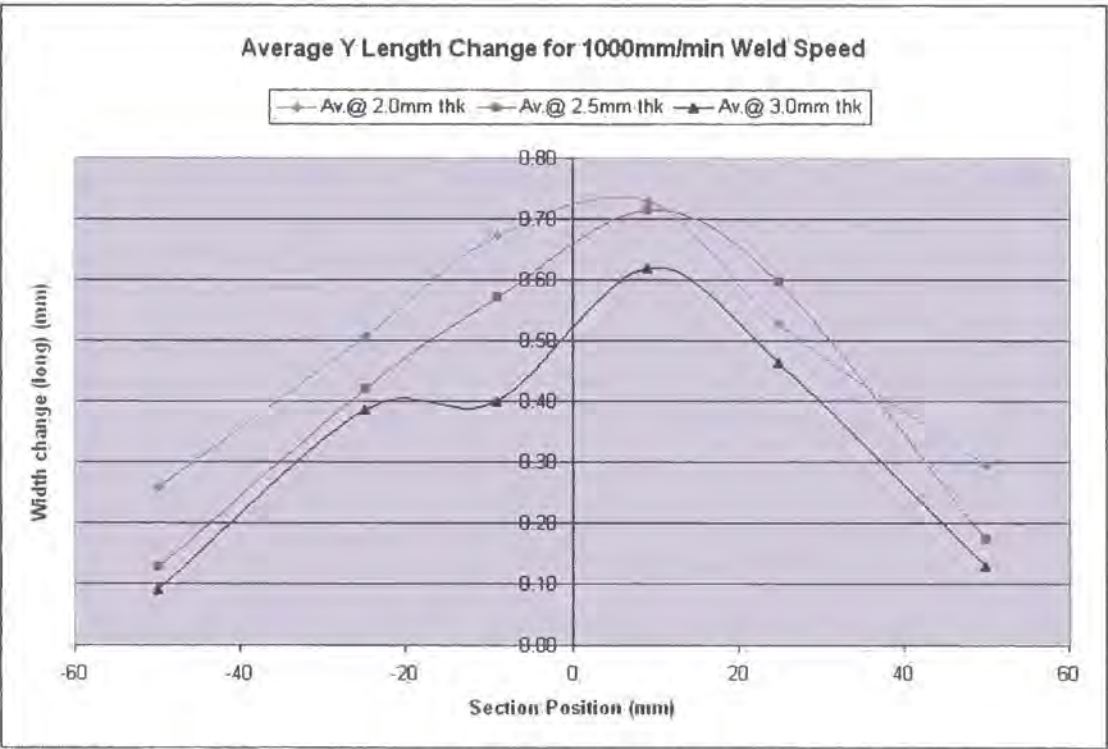
Figure 4.17: Variation of longitudinal distortion for varying thickness (bead on plate)

The decrease in distortion with increasing thickness will occur at for several reasons: Firstly increasing the thickness immediately increases the cross-sectional area of the plate and hence its I-section, which will directly result in an increase in the plates

ability to withstand the forces induced by the welding process and therefore increase its ability to inhibit distortion occurring. Also increasing at the thickness of the material will increase the volume of metal that is available to act as a heat sink and therefore for a constant welding speed the effect of the heat input is less.

As the profile for longitudinal shrinkage appears more complex than some of the other distortion profiles then it will be more difficult for a designer to accurately predict or build into their designs. An allowance for longitudinal shrinkage however may be able to be made based on the generalised pattern of distortion where the maxima occur at the weld centre line and the minima at the free edges. It may be possible to calculate a peak distortion and apply this at the weld centre line with the uniform distribution of distortions to the free edges where it may be assumed limited or no distortion occurs. Alternatively, it maybe suitable to apply an average overall longitudinal shrinkage compensation factor to the length of the plate to account for the distortion. However, based on the data presented here this may be too much of a simplification to allow accurate compensation for the welding in the design process.
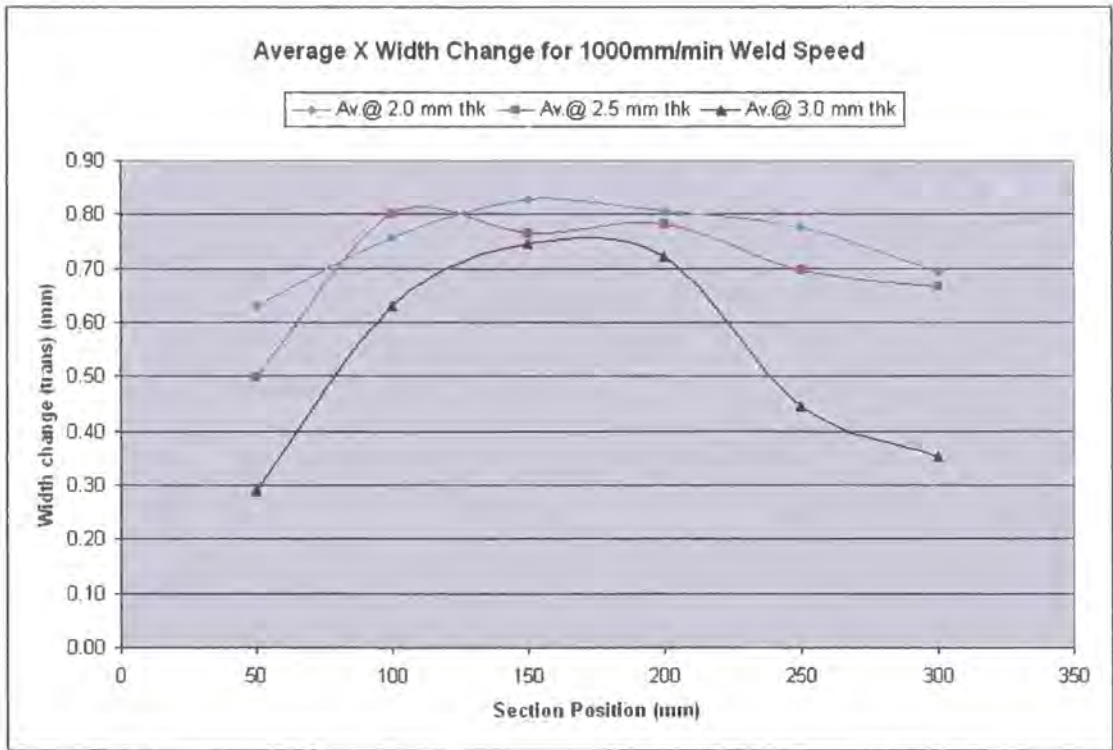
Figure 4.18: Variation of transverse distortion for varying thickness (bead on plate)

The same general comments and rules about longitudinal distortion can be made with respect to the transverse distortion in that increasing the thickness results in decrease in transverse distortion. The patterns for transverse distortion lend themselves more to apply into a common shrinkage factor in the design phase based on the very repeatable values of transverse shrinkage that appear to occur away from the ends of the plate where start and stop effects seem to predominate. Figure 4.18 shows the series of results in graphical form for the transverse shrinkage change based on constant weld speed and variant material thickness.
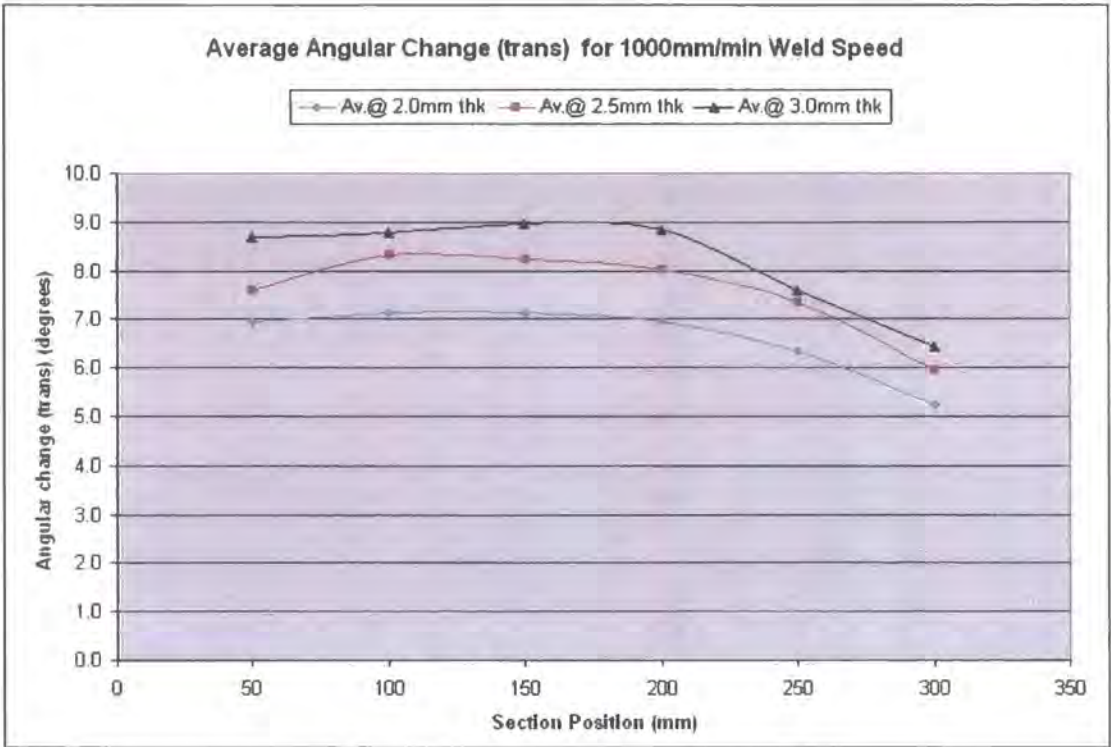
Figure 4.19: Variation of angular distortion for varying thickness (bead on plate)

The angular distortion results for varying material thickness at constant weld speed are shown in Figure 4.19. At first sight these results seem contrary to the effects already discussed for the effect of material thickness on transverse and longitudinal distortions. It would logically be expected that increasing the material thickness would result in a section that was more resistant to distortion effects, for the factors previously discussed. However as we have previously discussed angular distortion is not just dependent on material thickness but the degree of weld penetration has a direct bearing on the angular distortion. It would appear that in the lower thickness

114

materials the greater degree of penetration that has been achieved has more of an influence over the resulting angular distortion and effects of thick material thickness change at constant weld speed, for this particular set of data.
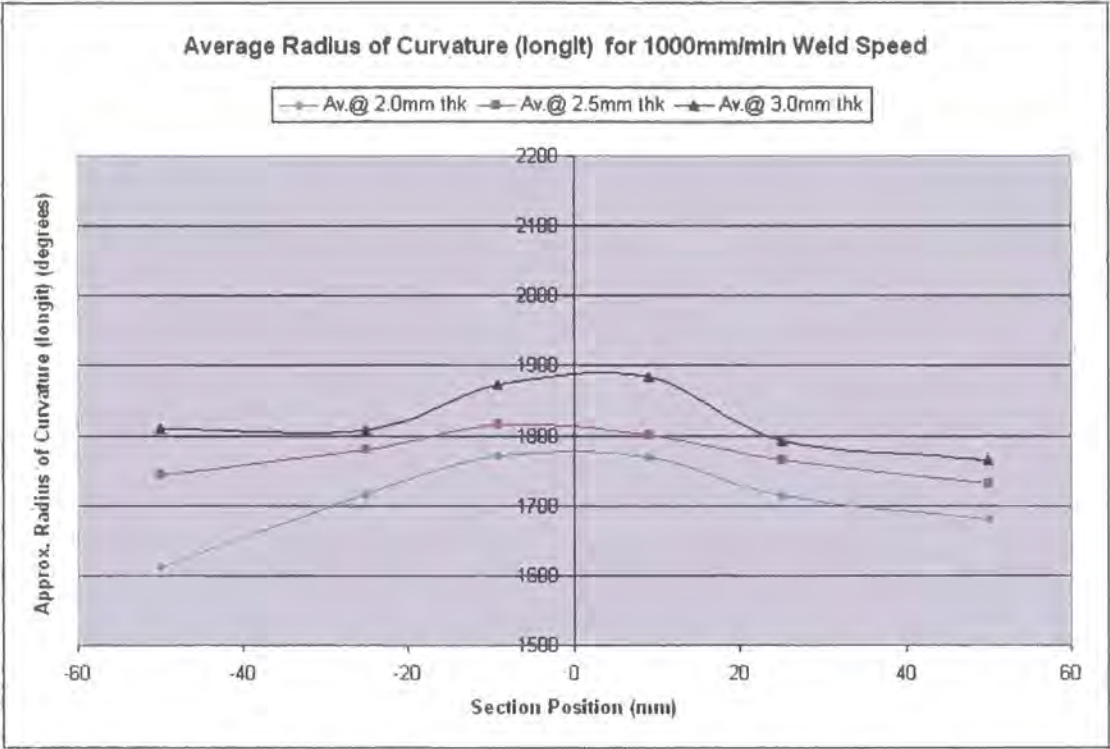
Figure 4.20: Variation of bowing distortion for varying thickness (bead on plate)

Finally in this section the effects of material thickness on the radius of curvature in the longitudinal direction, or the bowing distortion, are discussed. The graph in Figure 4.20 shows the data in this series. Remembering that that the bigger radius represents a smaller distortion, then again it can be seen at that increasing that material thickness at constant weld speed results in reduced bowing distortion. Again, this can be attributed to the increased strength of the section which will act to resist the distortion effects from the forces and deformations induced in the welding process.

4.4.4 Bead on Plate – Full Factor Trends

Having looked at the individual distortion profiles, and having also looked separately at the effects of varying weld speed on constant material thickness, and varying material thickness whilst holding the weld speed constant, then this section will present and discuss the overall effects of varying the both weld speed and material thickness on the distortions in order to try and draw out some generalised variation trends.

In order to investigate this further then an average summary for the individual material thicknesses and speeds had to be drawn on for each experiment. These results are presented in Tables 4.6, 4.7 and 4.8 as averaged results for the bead on plate samples for each material thickness at 2.0mm, 2.5mm and 3.0mm thickness. These averaged results will then be used to plot trend graphs that can be interpreted to identify the significant parameters and the effects they have on the individual distortion types.

Firstly the overall average results for the longitudinal distortion and shrinkage are presented in Figure 4.21. Here it can be seen that in order to minimise distortion then either increasing the weld speed or increasing the thickness will both have the desired effect. Increasing the speed of welding reduces the overall heat input into the sample and the overall resulting distortions reduce accordingly. Likewise, increasing the material thickness results in an increased cross sectional area and volume thereby providing greater resistance to the distortion induced by the forces occurring in the welding process. At the same time this is also acting as a bigger heat sink to take heat away from the immediate weld area. The results presented in Figure 4.21 appear to indicate that for this sample increasing that the speed of welding and thereby decreasing the heat input as a more significant effect in reducing distortion than simply increasing material thickness. However as could clearly be seen increasing of both factors act to reduce distortion in the longitudinal direction.

116

Table 4.6: Summary of average results for 2.0mm bead on plate samples

	W.Speed 700 mm/min	Average section results	OVERALL (700) Average	W.Speed 1000 mm/min	Average section results	OVERALL (1000) Average	W.Speed 1300 mm/min	Average section results	OVERALL (1300) Average
2.0mm		width change x (mm)	1.18		width change x (mm)	0.75		width change x (mm)	0.40
		angle (weld side)	6.45		angle (weld side)	6.63		angle (weld side)	6.59
		approx. Radius of curvature (mm)	601		approx. Radius of curvature (mm)	609		approx. Radius of curvature (mm)	680
		width change y (mm)	0.83		width change y (mm)	0.50		width change y (mm)	0.28
		approx. Radius of curvature (mm)	1686		approx. Radius of curvature (mm)	1711		approx. Radius of curvature (mm)	1722

Table 4.7: Summary of average results for 2.5mm bead on plate samples

	W.Speed 700 mm/min	Average section results	OVERALL (700) Average	W.Speed 700 mm/min	Average section results	OVERALL (1000) Average	W.Speed 700 mm/min	Average section results	OVERALL (1300) Average
2.5mm		width change x (mm)	0.91		width change x (mm)	0.70		width change x (mm)	0.28
		angle (weld side)	7.67		angle (weld side)	7.58		angle (weld side)	7.04
		approx. Radius of curvature (mm)	510		approx. Radius of curvature (mm)	525		approx. Radius of curvature (mm)	701
		width change y (mm)	0.71		width change y (mm)	0.43		width change y (mm)	0.25
		approx. Radius of curvature (mm)	1720		approx. Radius of curvature (mm)	1773		approx. Radius of curvature (mm)	1847

Table 4.8: Summary of average results for 3.0mm bead on plate samples

	W.Speed 700 mm/min	Average section results	OVERALL (700) Average	W.Speed 1000 mm/min	Average section results	OVERALL (1000) Average	W.Speed 1300 mm/min	Average section results	OVERALL (1300) Average
3.0mm		width change x (mm)	0.77		width change x (mm)	0.53		width change x (mm)	0.24
		angle (weld side)	8.65		angle (weld side)	8.21		angle (weld side)	6.19
		approx. Radius of curvature (mm)	492		approx. Radius of curvature (mm)	542		approx. Radius of curvature (mm)	758
		width change y (mm)	0.66		width change y (mm)	0.35		width change y (mm)	0.23
		approx. Radius of curvature (mm)	1762		approx. Radius of curvature (mm)	1822		approx. Radius of curvature (mm)	1899

117

From the results presented for the range of speeds used in this investigation the longitudinal distortion is reduced by 20%, 30% and 18% for the 700, 1000 and 1300 mm/min weld speeds respectively, across the material thicknesses in increasing from 2.0mm to 3.0mm thick. In holding the thickness constant then the longitudinal distortions decrease by 66%, 65% and 65% for the respective thicknesses of 2.0mm, 2.5mm and 3.0mm when increasing the welding speed from 700 to 1300mm/min.
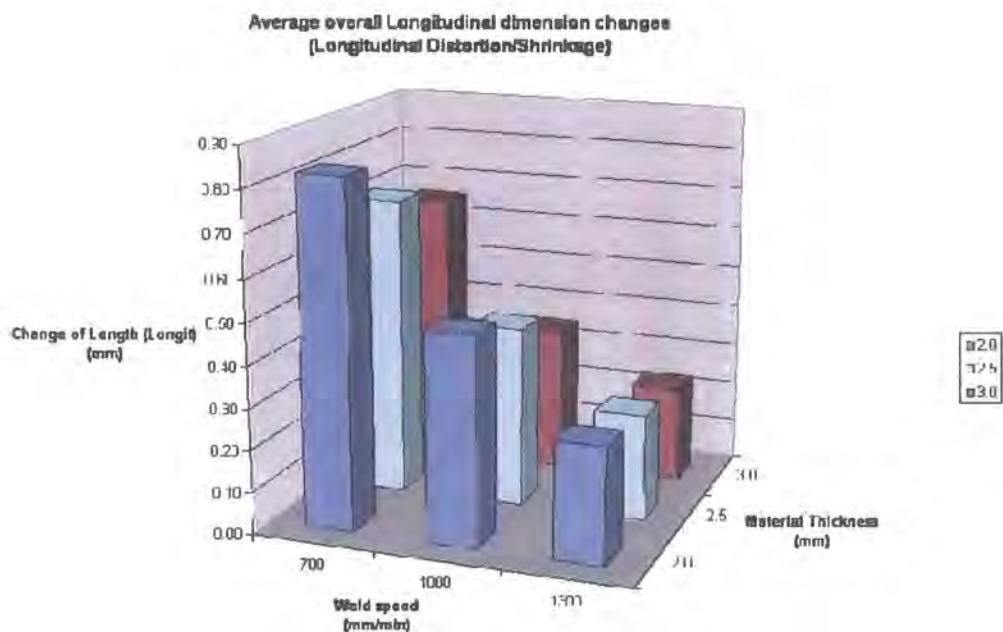
Figure 4.21: Trends for longitudinal distortion (bead on plate)

Increasing thickness also adds weight to any structure. Therefore if strength and stiffness requirements can be met at a particular material thickness in a structure increasing speed is a more effective way to reduce distortion. This is of course on the assumption that weld quality requirements continue to be met by the increased weld speed.

On consideration of the transverse shrinkage results as shown in Figure 4.22, then very similar trends can be observed as for the longitudinal shrinkage. Again, for this particular specimen, then the effect of increasing the weld speed appears more significant than increasing material thickness in reducing the overall distortion. However once again both weld speed and material thickness act to reduce distortion

118

when they are increased. The numerical values presented in these trend graphs can be seen in detail in the previous tables mentioned, Tables 4.6 to 4.8 inclusive.
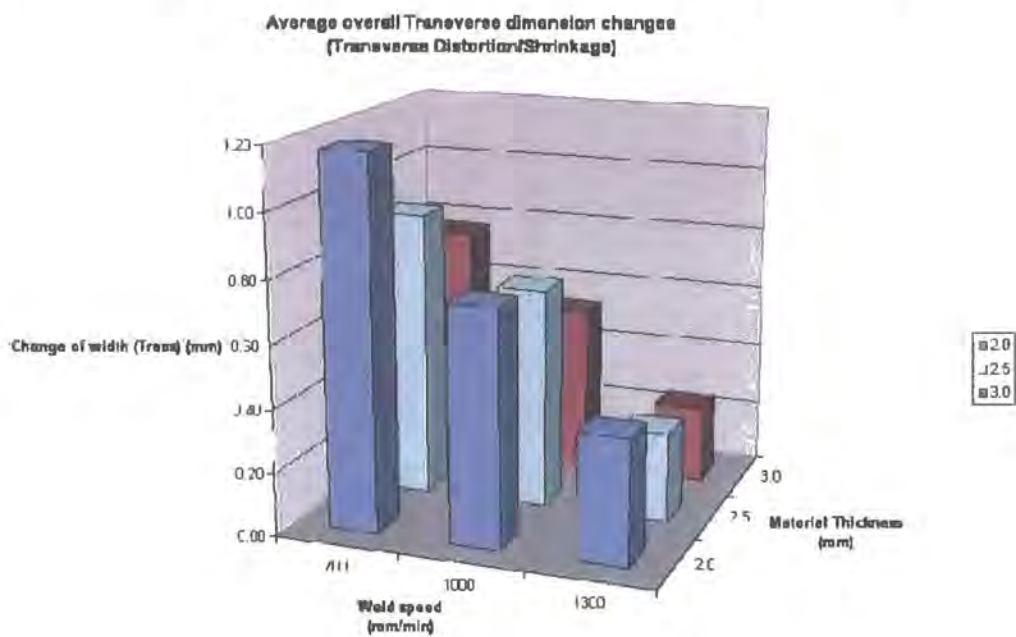
Figure 4.22: Trends for transverse distortion (bead on plate)

From the results presented for the range of speeds used in this investigation the transverse distortion is reduced by 35%, 29% and 40% for the 700, 1000 and 1300 mm/min weld speeds respectively, across the material thicknesses in increasing from 2.0mm to 3.0mm thick. In holding the thickness constant then the transverse distortions decrease by 66%, 69% and 69% for the respective thicknesses of 2.0mm, 2.5mm and 3.0mm when increasing the welding speed from 700 to 1300mm/min. These reductions are very consistent with the reduction seen from the longitudinal results.

From these two sets of results it appears that when the thickness is increased for a constant weld speed this gives rise to an average reduction in longitudinal and transverse distortion of around a third (or 33%) over the range used for the experiment. The increase in welding speed for a constant thickness gives rise to an average reduction of both longitudinal and transverse distortion of around two thirds (or 66%) over the range of speeds considered.

119

The next factor for consideration in the trend analysis is the effect of the parameters on angular distortion. The results for the studies are presented in Figure 4.23 showing the average angular distortion against weld speed and material thickness. From this graph it is possible to see that on the thinnest material thickness the angular distortion is relatively constant. This is in fact due to the higher levels of penetration occurring in these weld samples and as discussed previously in this chapter higher penetration reduces the overall angular distortion.
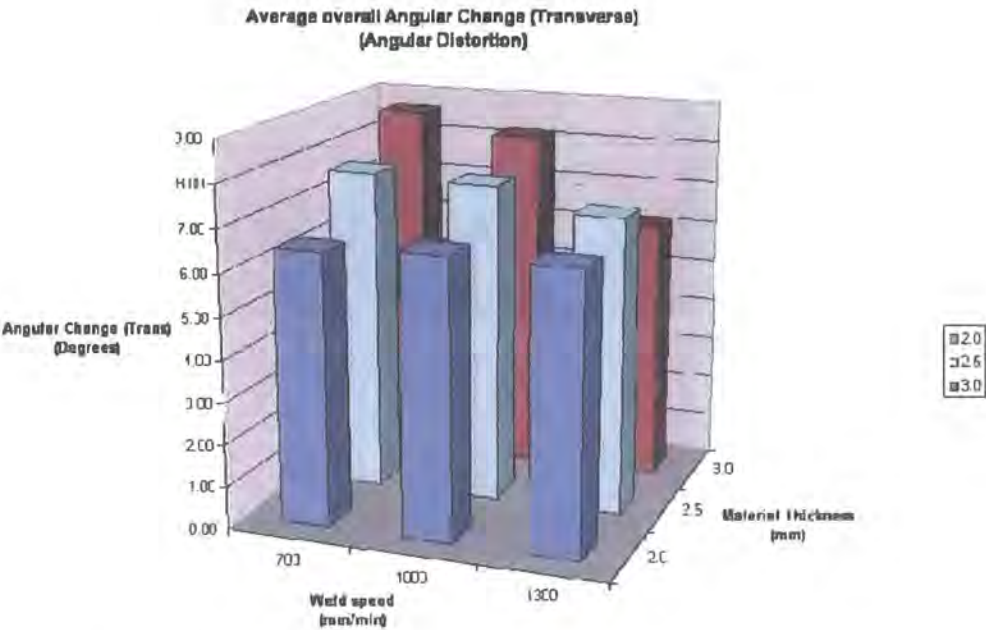
Figure 4.23: Trends for angular distortion (bead on plate)

In the case of the thinner material then all three samples at the differing weld speeds exhibit very similar levels of weld penetration and hence similar angular distortions. The middle material thickness does show some downward trend for reducing angular distortion based on increasing weld speed. However it should be noted that the actual angular distortions measured in the 2.5mm material thickness are greater than those occurring in the 2.0mm material thickness due to the reduced level of penetration that is occurring in the samples for the same heat input at each speed. The thickest sample shows a reduction in angular distortion as the weld speed increases but also has the effect of penetration of weld in the thicker sample producing higher levels of distortion for reduced penetration in comparison to the other thicknesses at the slower speeds. Increasing weld speed appears to have a

120

markedly greater effect in the thicker sample in reducing its weld distortion in the angular direction. Therefore for thin section material angular distortion can almost be defined as a constant factor if the penetration of the weld into the material is large. However once the material thickness increases to the point where the penetration is no longer the predominant factor then increasing weld speed will reduce angular distortion.

Finally, in this section, the effects of material thickness and weld speed on the bowing distortion are considered. These results can be seen in Figure 4.24. Again it is to be remembered that a bigger radius of curvature equates to less distortion. For the bowing distortions then increasing the weld speed or increasing the material thickness also result in reduced distortion. However it would appear that increasing material thickness has a marginally greater influence over increasing weld speed on reduction of distortion in the bowing direction for this joint configuration.
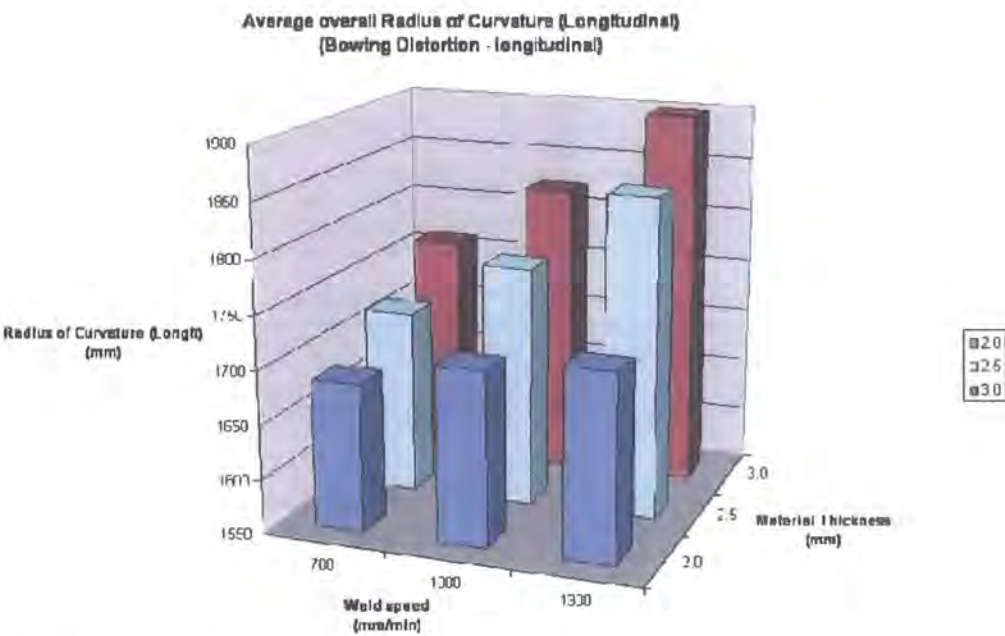

Figure 4.24: Trends for bowing distortion (bead on plate)

From the results presented for the range of speeds used in this investigation the bowing distortion is reduced by 4.5%, 6.5% and 10% for the 700, 1000 and 1300 mm/min weld speeds respectively, across the material thicknesses in increasing from 2.0mm to 3.0mm thick. In holding the thickness constant then the bowing distortions

121

decrease by 2%, 7% and 8% for the respective thicknesses of 2.0mm, 2.5mm and 3.0mm when increasing the welding speed from 700 to 1300mm/min.

Based on all of the results presented here for the bead on plate samples then it is clear that both increasing material thickness and increasing the speed of welding will give a reduction in the general overall distortion levels observed. It is worth stating however at this point that the weld speed and material thickness need to be chosen in consideration with cost, strength, and performance requirements of any particular product. Distortion is really an unwanted by product of the welding process and whilst it should be tried to be minimised, this is not usually a designers primary consideration in the design of a product.

4.5 Butt Weld Study

4.5.1 Individual Butt Weld Samples and Results

In this section the basic profiles arising from a single individual butt weld test sample will be discussed. An example of the typical post welded condition of a butt weld sample is shown in Figure 4.25 to assist with the discussion and understanding of the results presented here and in subsequent sections.

For the purposes of this part of the report then the sample chosen is again a mid-range sample from the variables under investigation. Therefore the profiles reported here can be deemed to be typical and indicative of those arising from the butt weld specimens. The sample that has been used for this section of the report is a pair of 2.5mm thick plates which has been welded together by a butt weld at 1000 mm/min weld speed (2.5mm thick plates ref 5-5A). The typical measured results were recorded and inserted into the Excel spreadsheet using the method previously described in Section 4.2 and processed as previously described.

Figure 4.25: Image of a typical welded butt weld sample

Again, due to the volume of data available for each specimen pair of plates then it is not possible to discuss each individual plate in exact detail but sample summary data of the experimental results and outcomes for these plates are included for completeness in Appendix II.

To begin the investigation into the butt weld distortions, the longitudinal shrinkage occurring in the butt weld will be considered. The graph showing the results for this sample can be seen in Figure 4.26. It can be seen that the longitudinal shrinkage peak value occurs close to or at the centre line of the weld, as was the case with the bead on plate results. Similarly the lowest shrinkage is occurring at the edges of the plate which are the furthest from the weld itself. Considering the profile and distribution, it appears quite uniform and regular. This is again similar to the pattern and profile found from the bead on plate experiments. From the measured results it can be seen that there is a maximum value occurring in the region of 0.8 to 1.0mm near to the weld. Because the shrinkage was not measured exactly at centre line of the weld then the precise point on the peak of the distortion, based on the curve fitting through these results, cannot be positioned with certainty. The variation in results from the centre line of the weld to the extremes of the plate does appear to be

regular and fairly uniform either side of the weld as was the case with the bead on plate samples, although perhaps in this case the shape of the distribution is tending more to a distinct peak at the weld-line. This is more evident if the left hand plate results are looked at on the graph. However the right hand also exhibits such a curve, if to a lesser extent. Also worth noting is that it may be the weld is slightly biased towards the right hand plate. This would result in a slight difference in heat input to the two plates of the joint, and could partially account for the greater distortion occurring in the right hand plate as a result of this.
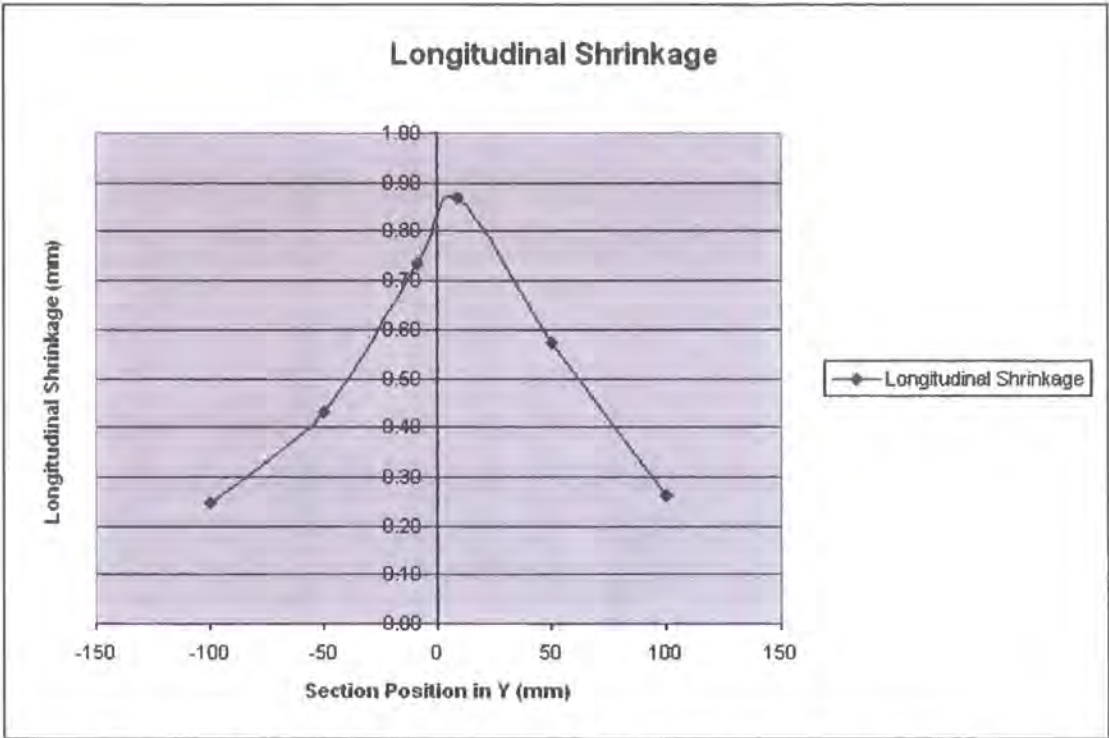
Figure 4.26: Variation of longitudinal distortion for a typical butt weld sample

The overall results for longitudinal shrinkage bear up to examination in that the peak shrinkage is occurring at the weld line where the most physical changes are occurring to the parent material. This reduces as we move away from the effects of the heat and material changes. However some shrinkage will still occur as an effect of the weld due to the residual forces and deformations established in the plate as a result of the temperature and phase changes that occur.

Next to be considered is the transverse shrinkage, the results for this can be seen in Figure 4.27 showing the variation of the width of the plate for this typical butt weld

sample. From the distribution of these results then it is possible to see that the lowest transverse shrinkage occurs at the start of the weld and also at the end of the weld. This would appear to make sense as these are the areas where there will have been least heat input and build up. The explanation for this is as per that stated in the corresponding section for the bead on plate sample. If the start and end effects of welding can be considered to be removed then the other points taken along the length of the sample to give us a measure of the consistent transverse shrinkage. These points all appear to lie very close together with little deviation. Therefore it could be stated that under steady-state conditions an almost uniform transverse shrinkage is occurring in the plate. In this case the transverse shrinkage is approximately 1.0mm. It would therefore be possible to describe this profile as having a straight line average shrinkage transverse to the weld line in the main body of the weld with reduced shrinkage towards the beginning and end of the weld run.

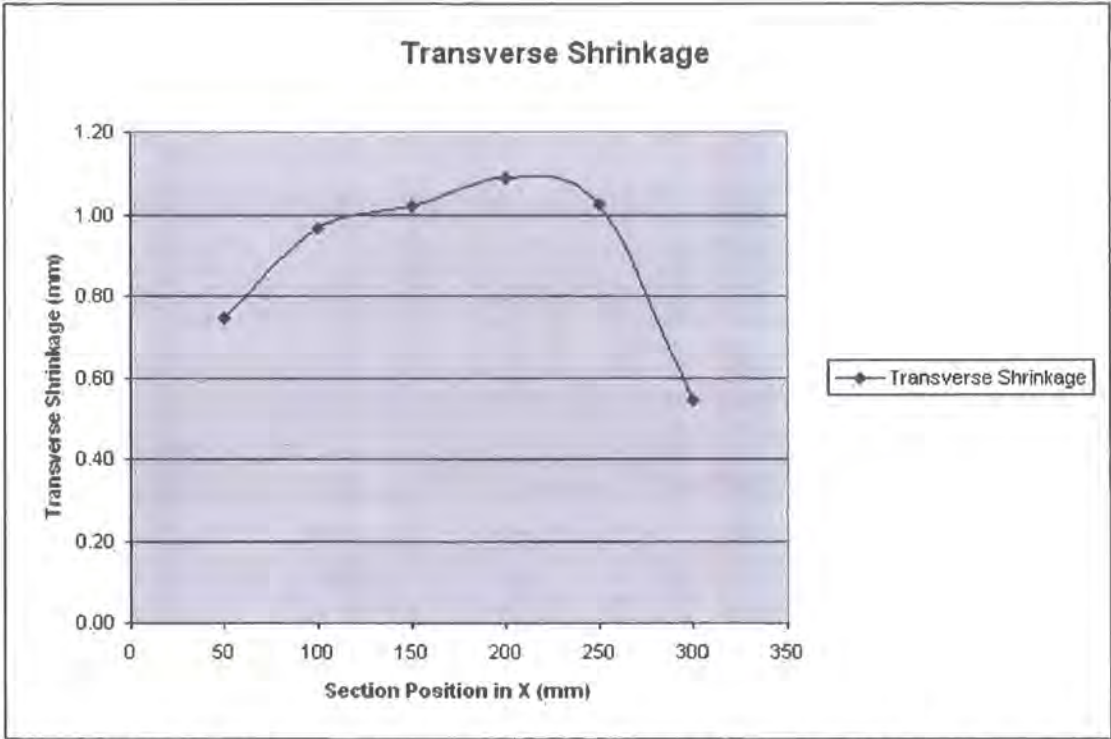Figure 4.27: Variation of transverse distortion for a typical butt weld sample

The next factor to be considered is the change in angular distortion along the length of the weld. A graph showing the change in angular distortion over the length of the plate is shown in Figure 4.28. Here it can be seen that towards the start of the weld then the highest angular distortion occurs. As the weld progresses then the angular

125

distortion very slowly decreases along the length of the curve. It is possible to surmise that this could be due to the effect of the joining of the two plates increasing the overall stiffness of the system as the weld progresses. Towards the start of the weld there is only a small amount of connection between the two plates and therefore the plate is able to distort more due to the relatively high flexibility in the angular direction in the system. However as the weld progresses then so the stiffness of the system will gradually increase and it is likely that this is what is contributing to the reducing angular distortion exhibited in the butt welded plates along the length of the weld.
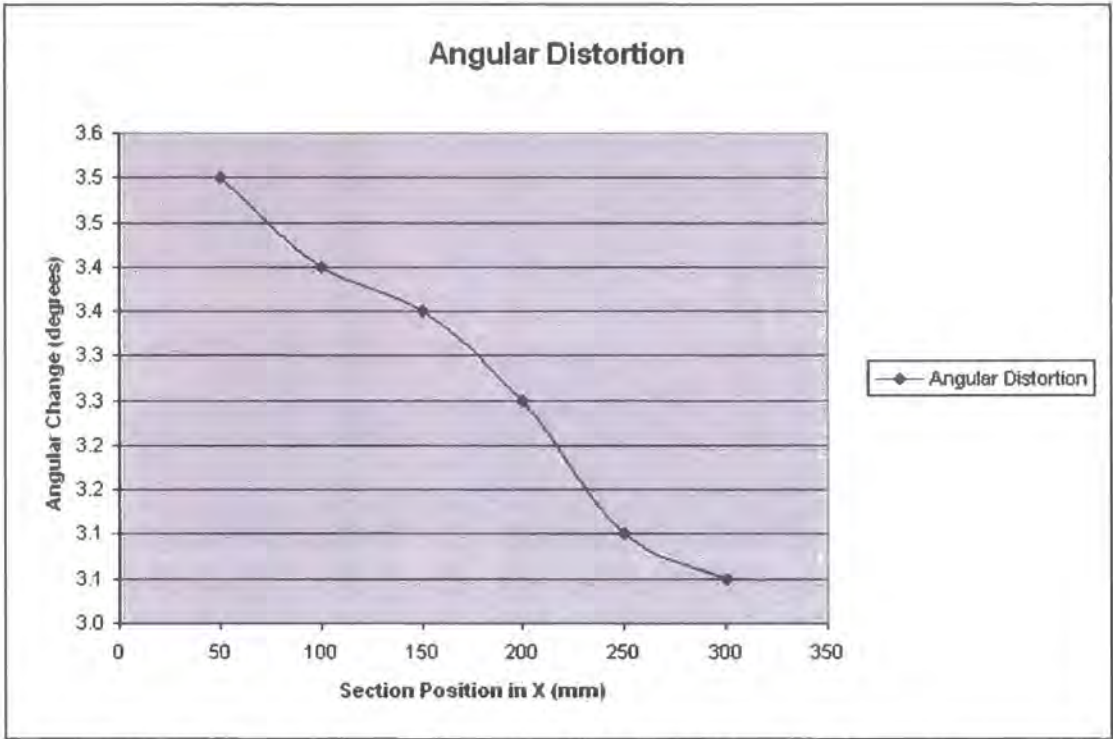
Figure 4.28: Variation of angular distortion for a typical butt weld sample

This is quite different to the mechanism occurring in the bead on plate samples but in this instance then the addition of the weld causes a gradual change in the stiffness of the plates, as the two plates are joined. This is clearly not occurring in the bead on plate system and hence it is purely more a penetration influence there as previously discussed. Therefore it might be expected that in other sample results then bigger changes in angular distortion may be observed due to the increased change in stiffness upon welding of the system if this belief is correct. It would be possible to determine if this was the case by repeating the experiment by varying the plate width

126

and hence the ability of the plates to withstand angular change. Again it is worth noting that most of the measured values are relatively small and from the results accurate measurement is quite difficult due to having to best fit straight lines through the point cloud at either side of the weld so could be sensitive to minor curve fitting errors.

The final factor that will be considered and discussed is longitudinal curvature, or bowing distortion, for the butt weld sample. The graph showing the change to longitudinal curvature over the width of the sample can be seen in Figure 4.29. From these results it can be seen that highest value of curvature occurs close to the weld and decreases as it moves towards the edges of the plate. This is possibly due to a stiffness effect as the flexibility of the plate will be greater at edges than it is in the centre. Again the bowing in the welded samples is in the order of 100 times greater than the pre weld plates it is safe to discount the influence of the pre weld curvature in the experimental results without significantly compromising the accuracy of the distortion results. If the range of results across the whole plate is looked at then these values are all very close to each other; in this particular sample the radius of curvature ranges only from approximately 3300mm to 4500mm. Therefore for the sample being considered here all these results actually lie relatively close to each other. Therefore it is reasonable to state that longitudinal bowing distortion is uniform across the plate with some slight scatter due to the slight geometry variations in relation to the weld at each different position.

The bowing distortion occurring in the butt weld sample is significantly less than that seen in the bead on plate section, and this must be attributable to the greatly increased section of the joined plates being more able to resist the distortion. It may also be that it is this gradual increase in stiffness as the plates are welded that is contributing to the gradual change in this bowing trend. However in this example it would appear that the bowing difference is not due to this as there appears it could be considered to be two separate profiles either side of the weld line. It may well be that what is being seen here is a uniform distribution of bowing but that the weld in this instance may be slightly biased to the right hand plate, and hence more heat input into that side of the joint. This may result in the greater bowing as seen by the

smaller radius on the right hand plate. Therefore for calculation it may be possible to calculate and state one single bowing factor that can be applied across a whole plate for a butt weld sample as well as bead on plate.
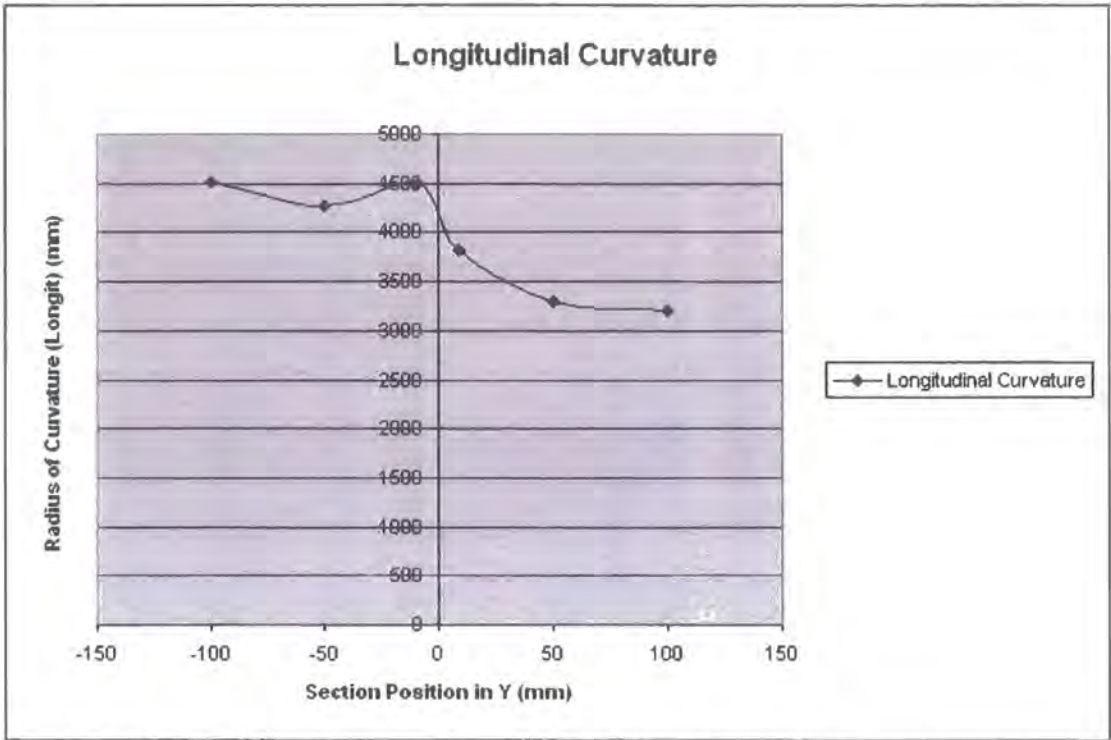
Figure 4.29: Variation of bowing distortion for a typical butt weld sample

4.5.2 The Effect of Varying Speed on Butt Weld Samples and Results

Having looked at the effects of the welding on the distortion profiles for an individual butt weld sample it is now possible to move on to look at the effect of other parameters. Firstly, it is possible to look at effect of varying the weld speed whilst holding that the material thickness constant. This investigation will look at averaged results for each speed and compare distortions to make generalised assessments for the effects of varying speed. Having previously looked at the distortions arising from an individual a 2.5mm thick sample then we will use this as our baseline and investigate the effect of increasing and of decreasing the weld speed on the distortion results from this thickness of plate in comparison to the original speed. Averaged results from a number of samples will be considered in order to avoid any minor inconsistencies that may have been associated with single

128

individual results and to attempt to guarantee a greater significance and generalised assessment from the results.

The first output to be considered is the longitudinal shrinkage. As seen previously on the individual samples the longitudinal shrinkage occurred at a maximum near to the weld line and decreased towards the edges of the plate. Here the effects of increased and decreased weld speed above and below our previous sample are considered. The results can be seen in Figure 4.30, which compares the average results for the longitudinal shrinkage for the three different weld speeds used in this experiment on the 2.5mm thick butt weld samples. This demonstrates that increasing weld speed decreases the overall longitudinal shrinkage that is occurring whilst reducing the weld speed increases the overall distortion values.

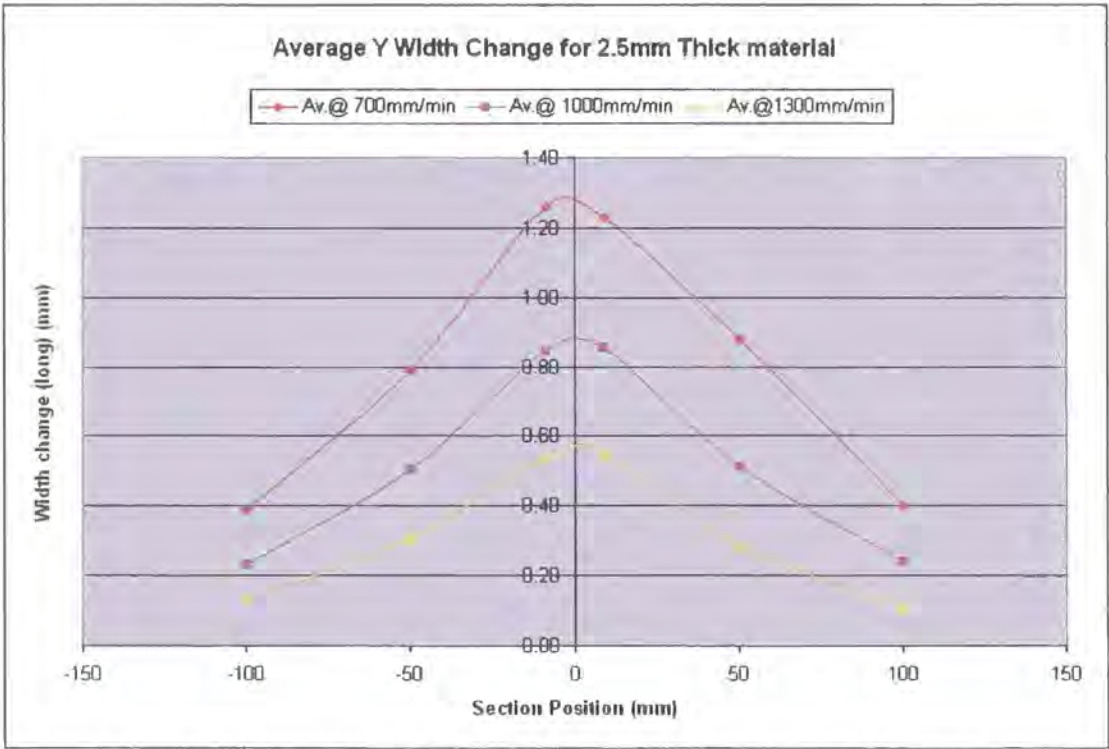Figure 4.30: Variation of longitudinal distortion for varying speed (butt weld)

On the full range of samples at different speeds it can be seen from the results that the peak distortion for longitudinal shrinkage always occurs at the weld line and is considerably less at the edges of the plate. Based on results presented here then generally the averaged distortions on either side of the weld line are equal and

129

seemed to follow a linear relationship. The slowest weld speed at 700mm/min will generate the most heat input into the plates. Those welded with higher weld speeds will proportionally put in less heat input. From the graph in Figure 4.30 it is therefore clearly evident that increasing speed decreases longitudinal shrinkage which must mainly be attributed to the reduction in heat input per unit length as weld speed increases. At the fastest weld speeds very little distortion is occurring at the edges of the plate.

Figure 4.31: Variation of transverse distortion for varying speed (butt weld)

The next distortion to be considered is the effects of the changing weld speed on transverse shrinkage. The results for this investigation are presented in Figure 4.31. Again as was the case in the individual plate in all instances the lowest transverse shrinkage occurs at start of the weld as the heat is building up in the plate. Once the heat has built up in the plate then a relatively consistent transverse shrinkage appears to occur over the remainder of the plate length. This transverse shrinkage also reduces towards the end of the plate as the heat input stops, creating an end effect at the end of the weld. However all three average curves follow the similar general profile of uniformly consistent transverse shrinkage with the results showing little

130

variation in magnitude once the steady-state conditions away from the start and end effects have been established. As is the case with the longitudinal shrinkage, then for transverse shrinkage also, the maximum distortion is occurring at the slowest weld speed; the slowest weld speed corresponding to the maximum heat input. Likewise also the lowest distortion is occurring for the highest weld speed. In this particular case for 2.5mm thick material then the curves appear relatively evenly spaced, especially in the mid section of the weld, and proportional to the change in weld speed. Again these cases would substantiate the fact that transverse distortion could be approximated and calculated by a single uniform value over the width of a component which would allow a designer to make an estimation and allowance to improve the accuracy and production readiness of a design.
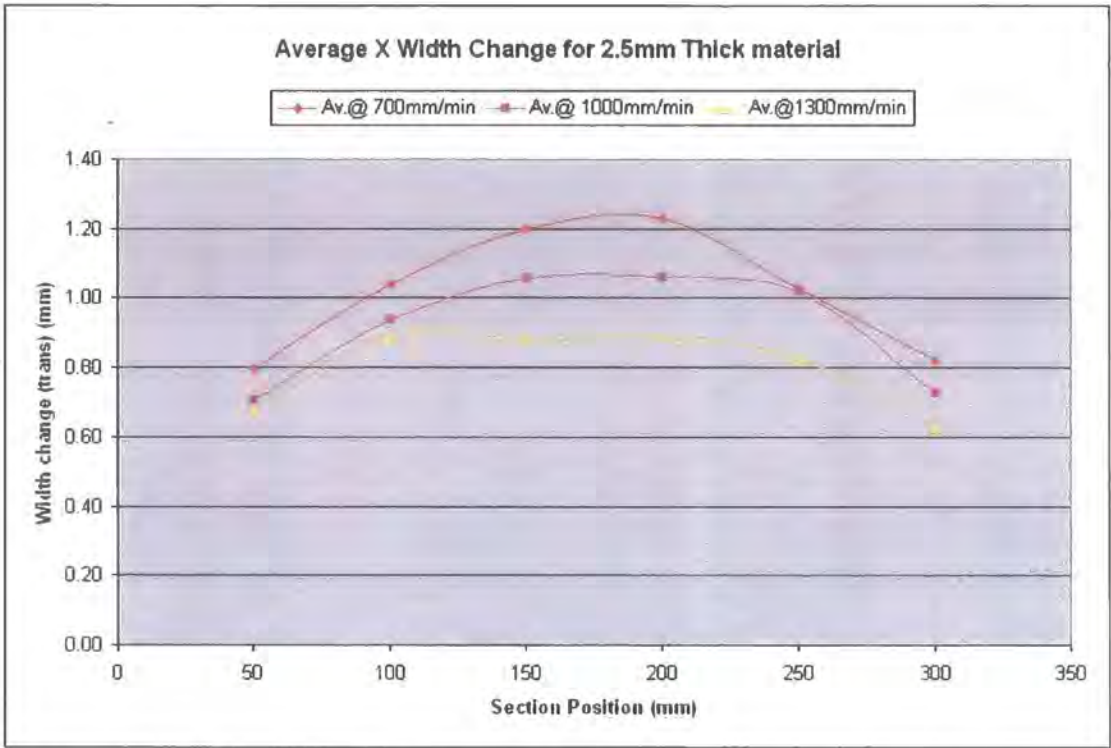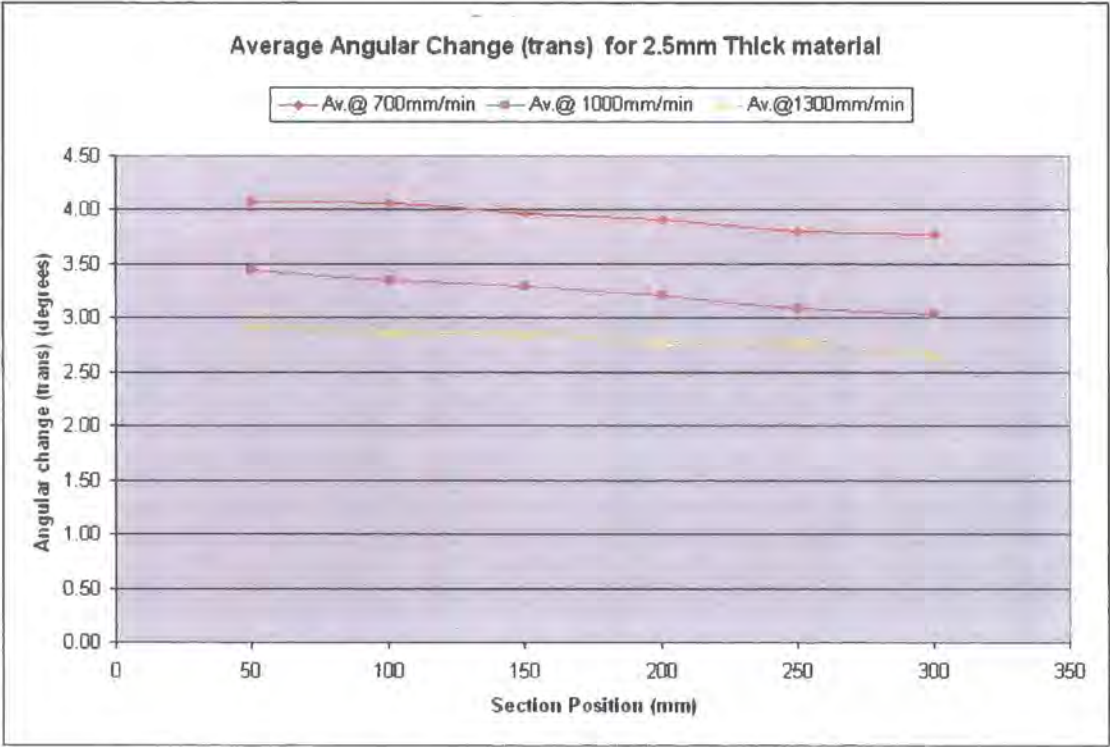

Figure 4.32: Variation of angular distortion for varying speed (butt weld)

The next to be considered is the effect of changing speed for a constant thickness plate on the angular distortion. The results for this investigation are presented as a summary in Figure 4.32. Looking at these results it can be seen that for increasing weld speed there is a reduction in the overall angular distortion. The angular distortion would appear decrease in all cases along the length of the weld. This

131

effect has previously been discussed and it is thought this may be due to the gradual increase in stiffness of the plates acting to restrain the angular distortion as the weld progresses and the plates are joined.
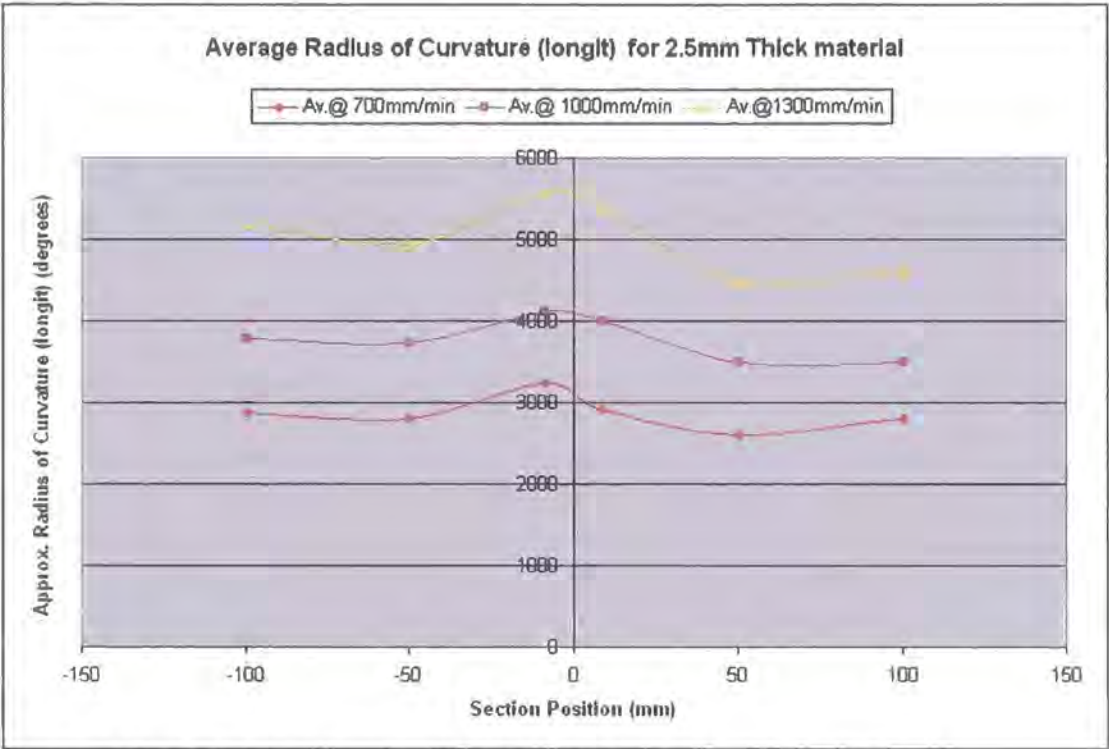
Figure 4.33: Variation of bowing distortion for varying speed (butt weld)

Finally in the investigation comparing the change of speed for uniform thickness of material, these effects on the radius of curvature in the longitudinal direction, or the bowing distortion are considered. The results for the bowing distortion are presented in Figure 4.33. Again it is to be remembered that in this case the greater the value of the radius of curvature than the lesser the distortion is occurring. Again the series of curves appear to demonstrate a general relationship in this series proportional to the weld speed. There are some limitations in the method used to approximate the radius of curvature and these could contribute to the scatter on the results. However, as discussed in the single plate case if these results are all looked at in detail then overall there is very little scatter on the results when compared to the base plate flatness. Therefore it should be possible to characterise the radius of curvature as a single value occurring across the width of the plate which appears to be proportional to the weld speed. Therefore, again for simple components perhaps a designer could compensate for this and design a pre-bend in order to overcome this effect.

132

4.5.3 The Effect of Varying Thickness on Butt Weld Samples and Results

In this section of the investigation the effect of varying plate thickness on distortions will be discussed whilst holding the welding speed constant. This investigation will look at averaged results for each material thickness and compare the distortion results to make generalised comparisons for the effects of varying thickness. Having previously looked at an individual 2.5mm thick plate, and the effects of speed, this original thickness will be used as a baseline to investigate the effect of increasing and decreasing the plate thickness on the distortion results from this original thickness, whilst holding the welding speed constant at 1000 mm/min.

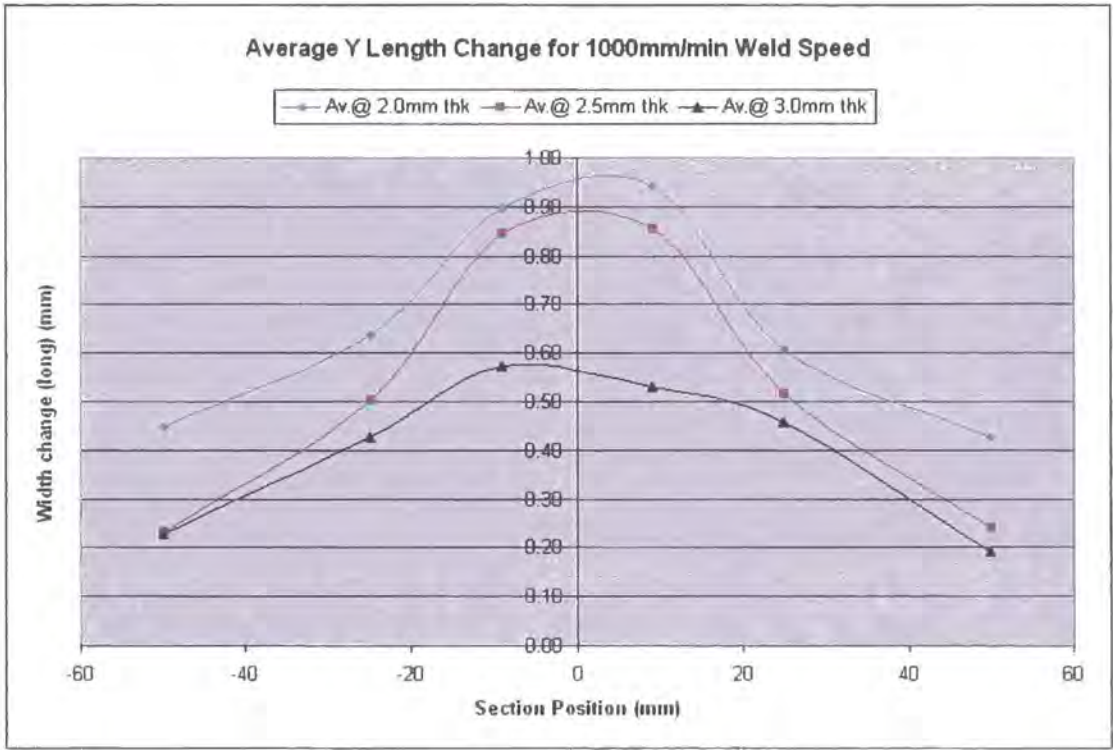Figure 4.34: Variation of longitudinal distortion for varying thickness (butt weld)

As with the other investigations the first factor to be considered is the effect on the longitudinal shrinkage of the plate. The results for this part of the investigation can be seen in Figure 4.34, which compares the averaged longitudinal distortions based on varying material thickness. It can be observed that the peak longitudinal

133

distortion occurs at the weld centre line and reduces towards the free edges of the plate. It can also be seen that increasing the thickness of the base material results in decreasing the longitudinal distortion, which is typical at all points throughout the data set. The decrease in distortion with increasing thickness will occur for several reasons as per the bead on plate discussions. Firstly increasing the thickness immediately increases the cross-sectional area of the plate and hence its I-section, which will directly result in an increase in the plates ability to withstand the forces induced by the welding process and therefore increase its ability to inhibit distortion occurring. Also increasing at the thickness of the material will increase the volume of metal that is available to act as a heat sink and therefore for a constant welding speed the effect of the heat input is less.

An allowance for longitudinal shrinkage may be able to be made based on the generalised pattern of distortion where the maxima occur at the weld centre line and the minima at the free edges. It may be possible to calculate a peak distortion and apply this at the weld centre line with the uniform distribution of distortions to the free edges where it may be assumed limited or no distortion occurs. Alternatively, it maybe suitable to apply an average overall longitudinal shrinkage compensation factor to the length of the plate as a simplistic assumption.

The same general comments and rules that we have made about longitudinal distortion can be made with respect to the transverse distortion in that increasing the thickness results in decrease in transverse distortion. The patterns for transverse distortion lend themselves more to apply into a common a shrinkage factor in the design phase based on the very repeatable values of transverse shrinkage that appear to occur away from the ends of the plate where start and stop effects seem to predominate. Figure 4.35 shows the series of results in graphical form for the transverse shrinkage change based on constant weld speed and variant material thickness. The profiles are relatively evenly spaced implying quite a linear relationship to the change in material thickness.

Figure 4.35: Variation of transverse distortion for thickness variation (butt weld)
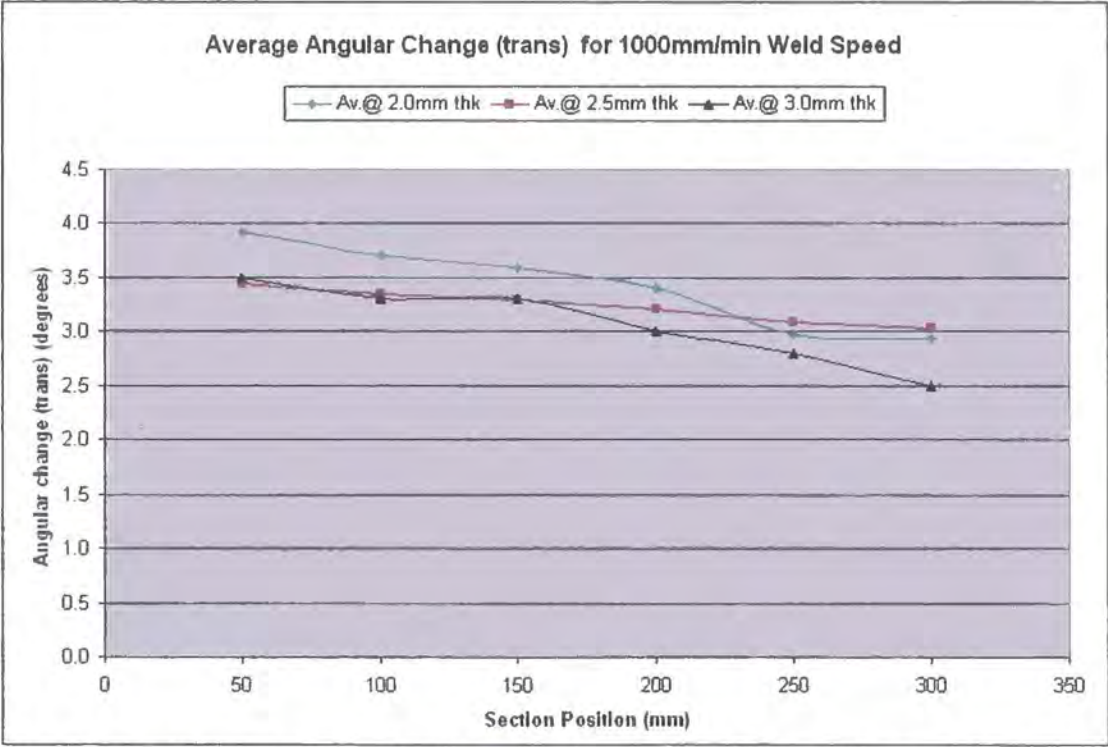
Figure 4.36: Variation of angular distortion for varying thickness (butt weld)

The angular distortion results with varying material thickness at constant weld speed are shown in Figure 4.36. These results are similar to the effects that have been already discussed for the effect of varying speed on angular distortions for butt welds. The general trend is that increasing material thickness reduces the angular distortion. However there appears to be some degree of scatter and overlap on these results which may in part be due to the very small angles that are being measured and any errors therefore being more significant. As seen previously the angular distortion decreases as the weld progresses, which is considered to be due to the increasing stiffness of the system as the plates are progressively joined.
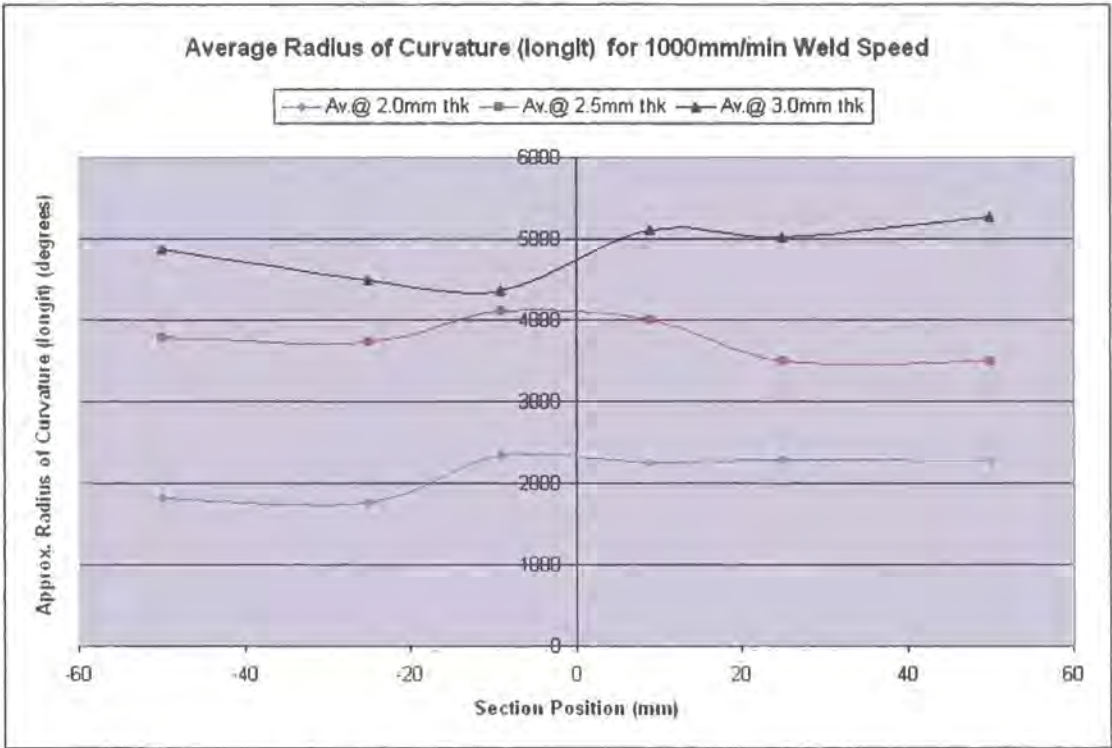
Figure 4.37: Variation of bowing distortion for varying thickness (butt weld)

Finally in this section the effects of material thickness on the radius of curvature in the longitudinal direction, or bowing distortion, are discussed. The graph in Figure 4.37 shows the data in this series. Remembering that that the bigger radius equals smaller distortion, then again it can be seen at that increasing that material thickness at constant weld speed results in reduced bowing distortion. Again, this can be attributed to the increased strength of the section which will act to resist the distortion effects from the forces and deformations induced in the welding process.

136

The values of the bowing distortions for each of the thicknesses can be seen to be relatively constant and exhibit little variation across the plates.

4.5.4 Butt Weld – Full Factor Trends

This section will present and discuss the overall effects of varying both the weld speed and material thickness on distortions in order to try and draw out some generalised variations and trends.

In order to do this then an average summary for the individual material thicknesses and speeds had to be drawn on for each experiment. These results are presented in Tables 4.9, 4.10 and 4.11 as averaged results for the butt weld samples for each material thickness at 2.0mm, 2.5mm and 3.0mm thickness. These averaged results will be used to plot trend graphs that can be interpreted to identify the significant parameters and the effects they have on the individual distortion types.

Firstly the overall average results for the longitudinal distortion and shrinkage are presented in Figure 4.38. Here it can be seen that in order to minimise distortion then either increasing the weld speed or increasing the thickness will both have the desired effect. Increasing the speed of welding reduces the overall heat input into the sample and the overall resulting distortions reduce accordingly. Increasing the material thickness results in an increased cross sectional area and volume thereby providing greater resistance to the distortion induced by the forces occurring in the welding process. At the same time it is acting as a bigger heat sink to take heat away from the immediate weld area. The results presented in Figure 4.38 appear to indicate that for this sample increasing the speed of welding and thereby decreasing the heat input has a more significant effect in reducing distortion than simply increasing material thickness. However as can clearly be seen the increasing of both factors act to reduce distortion in the longitudinal direction.
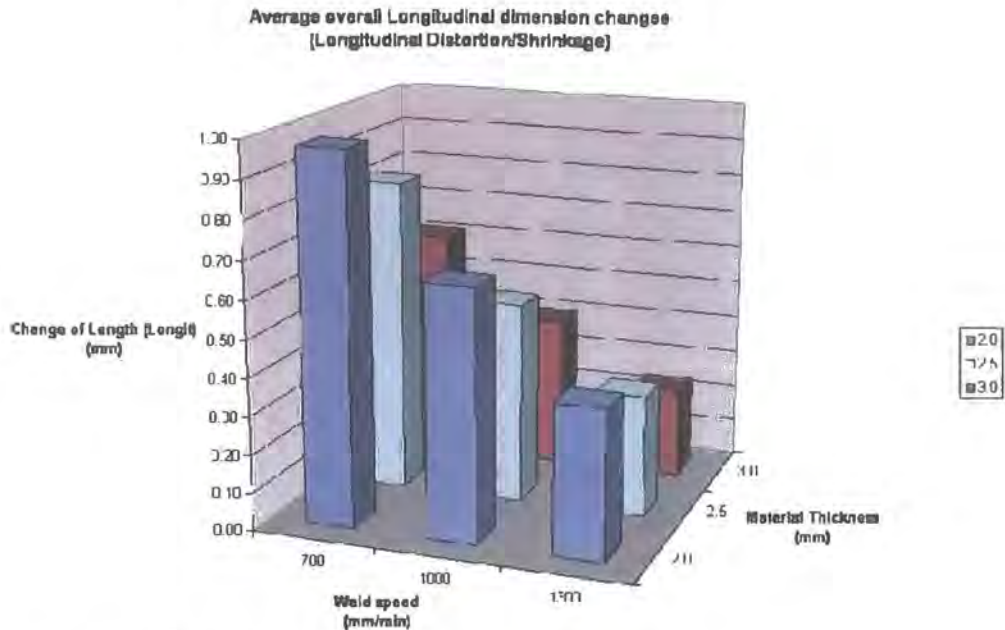
Figure 4.38: Trends for longitudinal distortion (butt weld)

From the results presented for the range of speeds used in this investigation the longitudinal distortion is reduced by 37%, 39% and 38.5% for the 700, 1000 and 1300 mm/min weld speeds respectively, across the material thicknesses in increasing from 2.0mm to 3.0mm thick. In holding the thickness constant then the longitudinal distortions decrease by 60%, 61% and 60.5% for the respective thicknesses of 2.0mm, 2.5mm and 3.0mm when increasing the welding speed from 700 to 1300mm/min. These reductions are very consistent with the reduction seen from the bead on plate results previously presented.

On consideration of the transverse shrinkage results as shown in Figure 4.39, then very similar trends can be observed as for the longitudinal shrinkage. Once again both weld speed and material thickness act to reduce distortion when they are increased. The numerical values presented in these trend graphs can be seen in detail in the previous tables mentioned, Tables 4.9 to 4.11 inclusive.

Table 4.9: Summary of average results for 2.0mm butt weld samples

	W.Speed 700 mm/min	Average section results	OVERALL (700) Average	W.Speed 1000 mm/min	Average section results	OVERALL (1000) Average	W.Speed 1300 mm/min	Average section results	OVERALL (1300) Average
2.0mm		width change x (mm)	1.19		width change x (mm)	1.01		width change x (mm)	0.91
		angle (weld side) (deg)	4.46		angle (weld side) (deg)	3.42		angle (weld side) (deg)	2.94
		approx. Radius of curvature (mm)	2021		approx. Radius of curvature (mm)	2127		approx. Radius of curvature (mm)	2583
		width change y (mm)	0.97		width change y (mm)	0.66		width change y (mm)	0.39
		approx. Radius of curvature (mm)	1966		approx. Radius of curvature (mm)	2318		approx. Radius of curvature (mm)	3659

Table 4.10: Summary of average results for 2.5mm butt weld samples

	W.Speed 700 mm/min	Average section results	OVERALL (700) Average	W.Speed 700 mm/min	Average section results	OVERALL (1000) Average	W.Speed 700 mm/min	Average section results	OVERALL (1300) Average
2.5mm		width change x (mm)	1.02		width change x (mm)	0.92		width change x (mm)	0.80
		angle (weld side) (deg)	3.93		angle (weld side) (deg)	3.24		angle (weld side) (deg)	2.81
		approx. Radius of curvature (mm)	2173		approx. Radius of curvature (mm)	2280		approx. Radius of curvature (mm)	2629
		width change y (mm)	0.82		width change y (mm)	0.53		width change y (mm)	0.32
		approx. Radius of curvature (mm)	2868		approx. Radius of curvature (mm)	3769		approx. Radius of curvature (mm)	5038

Table 4.11: Summary of average results for 3.0mm butt weld samples

|	W.Speed 700 mm/min	Average section results	OVERALL (700) Average	W.Speed 1000 mm/min	Average section results	OVERALL (1000) Average	W.Speed 1300 mm/min	Average section results	OVERALL (1300) Average
3.0mm		width change x (mm)	0.88		width change x (mm)	0.77		width change x (mm)	0.67
		angle (weld side) (deg)	3.62		angle (weld side) (deg)	3.07		angle (weld side) (deg)	2.45
		approx. Radius of curvature (mm)	2474		approx. Radius of curvature (mm)	3224		approx. Radius of curvature (mm)	3549
		width change y (mm)	0.61		width change y (mm)	0.40		width change y (mm)	0.24
		approx. Radius of curvature (mm)	4071		approx. Radius of curvature (mm)	4854		approx. Radius of curvature (mm)	6853

Figure 4.39: Trends for transverse distortion (butt weld)

From the results presented for the range of speeds used in this investigation the transverse distortion is reduced by 26%, 24% and 26% for the 700, 1000 and 1300 mm/min weld speeds respectively, across the material thicknesses in increasing from 2.0mm to 3.0mm thick. In holding the thickness constant then the transverse distortions decrease by 23.5%, 21.5% and 24% for the respective thicknesses of 2.0mm, 2.5mm and 3.0mm when increasing the welding speed from 700 to 1300mm/min. Therefore for this joint under these conditions then increasing the material thickness or increasing the weld speeds appear to have similar effects.

The next factor for consideration in the trend analysis is the effect of the parameters on angular distortion. The results for the studies are presented in Figure 4.40 showing the average angular distortion against weld speed and material thickness. From this graph it is possible to see that both increasing material thickness and increasing welding speed act to reduce the angular distortions.
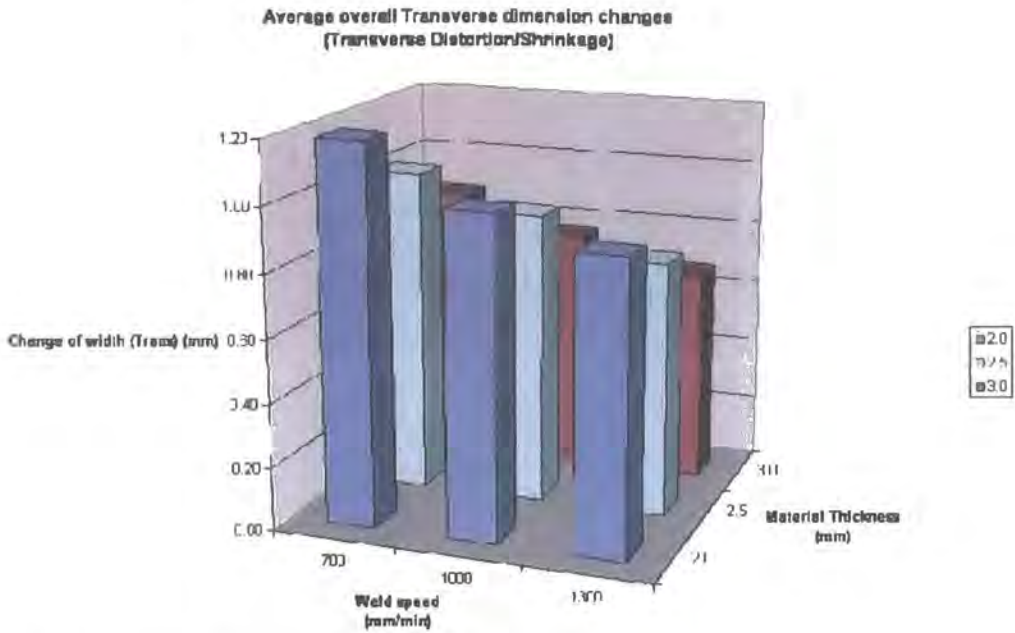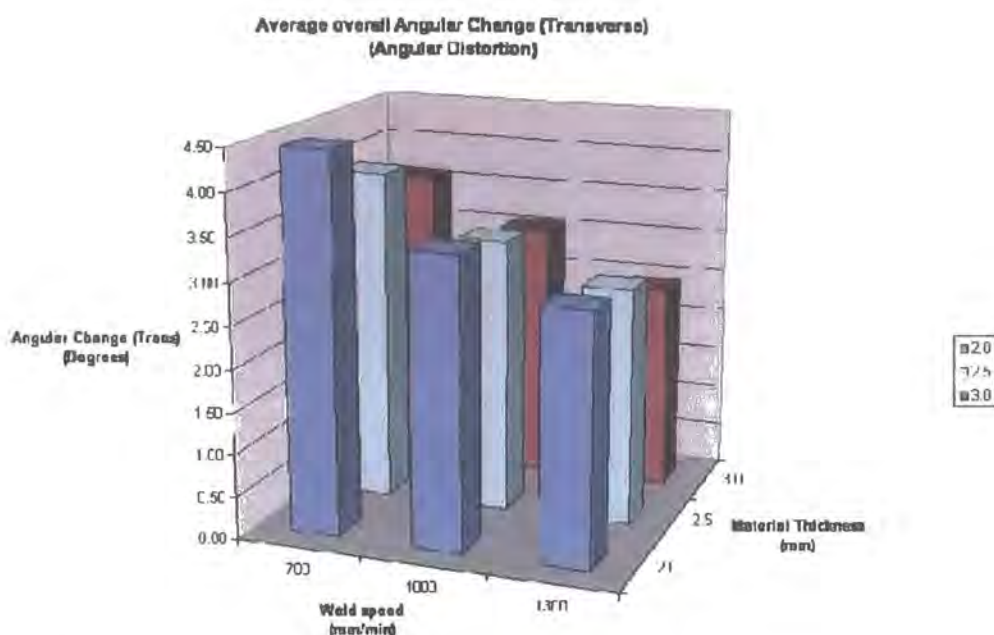
Figure 4.40: Trends for angular distortion (butt weld)

From the results presented for the range of speeds used in this investigation the angular distortion is reduced by 19%, 10% and 17% for the 700, 1000 and 1300 mm/min weld speeds respectively, across the material thicknesses in increasing from 2.0mm to 3.0mm thick. In holding the thickness constant then the angular distortions decrease by 34%, 28.5% and 32% for the respective thicknesses of 2.0mm, 2.5mm and 3.0mm when increasing the welding speed from 700 to 1300mm/min. Therefore it would appear that angular distortion is slightly more responsive to being reduced by increasing weld speed compared to increasing material thickness.

Finally, in this section, considering the effects of material thickness on weld speed on the bowing distortion then these results can be seen in Figure 4.41. Again it is to be remembered that a bigger radius of curvature equates to less distortion. For the bowing distortions then increasing the weld speed or increasing the material thickness also result in reduced distortion. However it would appear that increasing material thickness has a marginally greater influence over increasing weld speed on reduction of distortion in the bowing distortion for this joint configuration.
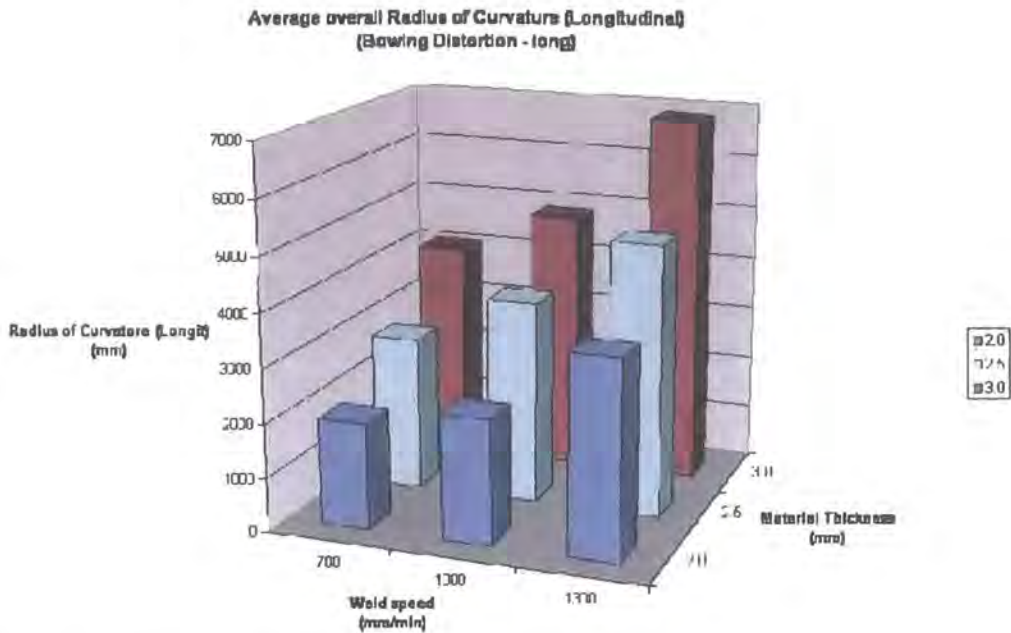
Figure 4.41: Trends for bowing distortion (butt weld)

From the results presented for the range of speeds used in this investigation the bowing distortion is reduced by 107%, 109% and 87% for the 700, 1000 and 1300 mm/min weld speeds respectively, across the material thicknesses in increasing from 2.0mm to 3.0mm thick. In holding the thickness constant then the bowing distortions decrease by 86%, 76% and 68% for the respective thicknesses of 2.0mm, 2.5mm and 3.0mm when increasing the welding speed from 700 to 1300mm/min.

Based on all of the results presented here for the butt weld samples then it is clear that both increasing material thickness and increasing the speed of welding will give a reduction in the general overall distortion levels observed.

4.6 Conclusions and Summary

This chapter has presented the results from the experimental investigations undertaken on both the bead on plate weld samples and the butt weld samples. The welds used for this experiment where seen to be representative of the case study company's welds, both in terms of their visual appearance, as well as the quality

142

factors associated with the weld such as penetration values. It has been demonstrated that both increasing the material thickness and increasing the speed of welding act to decrease the distortions generally. This has been quantified and the various magnitudes of these distortions reviewed and compared. In the case of the bead on plate welds it has also been observed that the penetration levels have a influence on the angular distortion values. In this case it was noted that very similar levels of distortion were observed due to the similar penetration values which exhibited more influence over the angular distortion, especially at the thinner of the material ranges, than the material thickness or weld speed effects. A great deal of detailed distortion information is presented which will enable subsequent predictions to be developed. The effects of varying speed on a constant thickness showed that increasing thickness resulted in decreased distortions, as did the study showing the effects of varying thickness on constant speed also decreased distortion.

From the results then it can be seen that for longitudinal distortion in both weld types, the peak distortion occurs at the weld centreline and decreases to lower levels at the edges of the plates. This produces a V shaped distribution, which may be considered as either a simple v varying from peak distortion to zero at the edges, or as a simple average length shrinkage to compensate for this in the design stages. The transverse distortions are seen to be relatively constant in the main body of the weld away from any start stop effects so could possible be accounted for in design by a constant width reduction allowance. Angular distortion has been seen to be a fairly consistent level but decreasing slightly along the length of the butt weld, due to increasing system stiffness as the joint is welded. This could be very simply accounted for by introducing a constant angular oversetting value at the design stages. Likewise bowing distortion was seen to be very consistent and repeatable and could be allowed for in design by calculating a bowing factor and introducing this as an allowance into the pre welded plates.

Chapter 5: Discussions and Distortion Prediction

5.1 Introduction

This chapter presents the discussions based on the experimental investigations undertaken on both the bead on plate weld samples and the butt weld samples. An initial comparison is made of the experimental results to the published literature, along with a discussion of the models chosen for this comparison. This is undertaken for each of the distortion types and the correlation or differences to the published data discussed, and possible explanations offered for any differences. There then follows a detailed section which derives appropriate equations that can model the distortion effects specific to the case study company's typical design space and discussions of various ways in which these could then be used by a designer. Finally there is a discussion of the possible sources of error and variation that may have occurred in the experiment.

5.2 Detailed Comparison to Existing Formulae

In order to understand fully the experimental results then it is necessary to make comparison to the previously published results and formulae established by other researchers. Therefore the subsequent sections present a brief comparison for the experimental results for each type of distortion to published work.

5.2.1 Longitudinal Distortion

The established formulae for predicting various distortions were previously briefly discussed in Chapter 2. Table 2.4 illustrated some sample formula for longitudinal distortion and brief discussions were given. Here the most applicable formulae for predicting longitudinal distortion have been used to calculate a prediction of the distortion effect. Five models are chosen for longitudinal distortion for this comparison, and these are summarised as follows:

145

Rule of thumb: $\delta_L = 0.001 \cdot L$ *(Equation 5.1)*

This is a commonly used approximation established based on 0.1% plastic strain, and therefore provides the simplest and easiest method to make a prediction of longitudinal distortion, however as it is a rule of thumb it really does not account at all for process or material parameters.

Okerblom: $\delta_L = 0.335 \cdot L \cdot \dfrac{1}{A} \cdot \dfrac{q}{v} \cdot \dfrac{\alpha}{\rho.c}$ *(Equation 5.2)*

Okerblom [1955] established his models based on experimentation using varying widths of steel bar. This concluded that the longitudinal shrinkage was related to the heat input and the cross sectional area of the plate. From these experiments a model was derived which assumed that the weld was deposited simultaneously over the whole length of the weld, and therefore his model is only valid for fast moving heat sources.

Okerblom Wells: $\delta_L = 0.35 \cdot L \cdot \dfrac{1}{A} \cdot \dfrac{q}{v} \cdot \dfrac{\alpha}{\rho.c} - 0.8 \cdot \dfrac{\kappa}{v} \cdot \dfrac{t}{A} \cdot \varepsilon_y$ *(Equation 5.3)*

Wells [1952] based his model on the work of Okerblom but chose to improve the equation for longitudinal shrinkage by including the effect of the temperature distribution transverse to the weld which will act to reduce the distortion effect.

Horst Pflug: $\delta_L = 42 \cdot L \cdot \dfrac{\sigma_y}{E} \cdot \dfrac{A_w}{A - A_w}$ *(Equation 5.4)*

Horst Pflug [1956] followed similar reasoning to Okerblom but the area that undergoes plastic deformation defined by Okerblom is replaced by an expression relating this to the weld area. However the exact reasoning behind this assumption is not clearly presented.

White et al: $\delta_L = L \cdot \dfrac{160}{E} \cdot \dfrac{q}{v} \cdot \dfrac{1}{A}$ *(Equation 5.5)*

White, Dwight, Legatt and Kamtekar [1980] developed their equation for longitudinal shrinkage based on the tendon force concept introduced in the 70's. In addition this work included the effects of process efficiency which had not been included in previous work by authors such as Okerblom.

Table 5.1: Calculated longitudinal distortions

Thickness	2.0mm					
Joint	Bead on Plate			Butt weld		
Speed	700	1000	1300	700	1000	1300
Rule of Thumb	0.350	0.350	0.350	0.350	0.350	0.350
Okerblom	0.450	0.315	0.242	0.225	0.158	0.121
Okerblom Wells	0.243	0.131	0.070	0.122	0.065	0.035
Horst Pflug	0.491	0.466	0.441	0.331	0.319	0.306
White et al	0.306	0.215	0.165	0.153	0.107	0.083

Thickness	2.5mm					
Joint	Bead on Plate			Butt weld		
Speed	700	1000	1300	700	1000	1300
Rule of Thumb	0.350	0.350	0.350	0.350	0.350	0.350
Okerblom	0.360	0.252	0.194	0.180	0.126	0.097
Okerblom Wells	0.168	0.078	0.029	0.084	0.039	0.015
Horst Pflug	0.475	0.449	0.424	0.289	0.277	0.264
White et al	0.245	0.172	0.132	0.123	0.086	0.066

Thickness	3.0mm					
Joint	Bead on Plate			Butt weld		
Speed	700	1000	1300	700	1000	1300
Rule of Thumb	0.350	0.350	0.350	0.350	0.350	0.350
Okerblom	0.300	0.210	0.162	0.150	0.105	0.081
Okerblom Wells	0.118	0.043	0.002	0.059	0.021	0.001
Horst Pflug	0.458	0.432	0.407	0.268	0.260	0.252
White et al	0.204	0.143	0.110	0.102	0.072	0.055

Whilst many other models exist, such as Guyot [1947] and Mamlin[1976] these are not considered here as they are limited in their application by being applicable to specific geometry, dimensional limits or being process specific respectively. Those selected for the comparison are the models most commonly used and referenced.

Table 5.1 shows a summary of the calculated longitudinal shrinkage based on the results of each equation with the specific process and dimensional values being substituted in line with the practice of this experiment. The calculated values can be

147

compared to the experimental results which are summarised and presented in Table 5.2. It can be seen that in the case of the experiment conducted in this project larger values of longitudinal distortion are being measured than the published data would predict. The Okerblom model is the most commonly accepted basic model for longitudinal shrinkage but in all cases the model is considerably under predicting compared to the value found in the experiment.

Table 5.2: Measured values for longitudinal distortion

Longitudinal Shrinkage - Experimental Values						
Joint	Bead on Plate			Butt weld		
Weld Speed (mm/min)	700	1000	1300	700	1000	1300
2.0mm	0.83	0.50	0.28	0.97	0.66	0.39
2.5mm	0.71	0.43	0.25	0.82	0.53	0.32
3.0mm	0.66	0.35	0.23	0.61	0.40	0.24

A possible explanation for the under prediction of the models is that in the experiment it is quite difficult to separate the effects of each of the individual distortion factors. Therefore, when the longitudinal shrinkage is measured and calculated this value is being influenced by the bowing distortion that is occurring in the lengthwise direction of the plate. The effect of the bowing will be to make the longitudinal distortion measured appear to be larger than the value of the pure longitudinal shrinkage. If this is considered for a specific example such as the butt weld experiment carried out on the 2.0mm material at 700mm/min weld speed, then it is seen the experimental measured shrinkage is 0.97mm. This compares to the predicted value which ranges between 0.122mm and 0.350mm depending on the formula used. In this case the bowing distortion was measured at 1966mm. This bowing distortion gives rise to an angle of the segment of a circle fitted through the curved plate of 10.214°, based on the nominal 350mm plate length from the experiment. Using this to find the curved length of the plate, this gives a length of 350.46mm. Therefore in that particular case there will be an approximate 0.46mm difference between the measured straight line shrinkage and the curved line shrinkage of the plate. If this difference is taken into consideration with the straight

148

line measured shrinkage then the true longitudinal shrinkage will be found. Therefore the actual longitudinal shrinkage is found to be 0.51mm for that one case. However, this is still an error of around 30% when compared to the highest of the calculated predictions. It is much closer to the predicted values, and therefore demonstrates the influence of bowing distortion. Evaluating the other extreme value, for the 3.0mm thick plates welded at 1300mm/min weld speed, the curvature accounts for a 0.04mm difference. This will reduce the measured value of 0.24mm to 0.20mm as a true measure. However in practical terms these effects do occur together so the full experimental values need to be used to make an easy prediction tool for a designer to accurately predict distortion and incorporate it into a design, rather than simply calculating the individual effect. Therefore a tool or method of predicting the overall shrinkage shape based on the combined effects would be most beneficial to a designer to assist in planning to overcome or accommodate the effects of weld distortion.

5.2.2 Transverse Distortion

This section will consider the comparison of the transverse distortion results to the predicted values. Some of the formulae for transverse distortion have previously been discussed in Chapter 2 and were summarised in Table 2.6. For the purposes of this comparison a number of the commonly accepted formulae will be chosen and the predictions calculated. The formulae used in this section can be summarised as follows:

Guiaux: $\delta_T = 0.18 \cdot b_w$ $\qquad$ (Equation 5.6)

This is a simple empirical based approximation established by Guiaux [1962] that relates to the width of the weld in butt welds, and cited by many authors in review papers such as Berthet, Gerbeaux, Piette and Renault [1988], and Verhaeghe [1998]. It is used here for its simplicity.

Okerblom: $\delta_T = 0.293 \cdot \dfrac{1}{t} \cdot \dfrac{q}{v} \cdot \dfrac{\alpha}{\rho.c}$ $\qquad$ (Equation 5.7)

Okerblom [1958] established his models based on experimentation using varying widths of steel bar. In the form presented here the formula is also only valid for bead on plate or butt welds, for fast moving heat sources, where the penetration is more than 40% of the plate thickness. For very long or slow moving welds he proposes a treatment in line with longitudinal distortion instead.

Malisius: $\delta_T = 1.3 \cdot \left(0.6 \cdot \alpha_{pl} \Delta T \cdot C \cdot \dfrac{A_w'}{t} + \alpha_w \Delta T \cdot b_w \right)$ (Equation 5.8)

Malisius whose work is discussed by Masubuchi [1980] and others, presented his equation which allows for terms that represent the contraction of the base material and also one for the contraction of the weld metal. The value of the constant, C, in the equation is process dependent.

Guyot: $\delta_T = 0.1716 \cdot \dfrac{A_w'}{t} + 0.0121 \cdot b_w$ (Equation 5.9)

Guyot [1947] based his model on the work of Malisius but refined his model to be specific to steel plates and specific welding technique.

Capel: $\delta_T = C \cdot \dfrac{q}{v} \cdot \dfrac{1}{t_w}$ (Equation 5.10)

Capel, as cited in Verhaeghe [1998] developed his equation based on experiments and derived and equation that contains a constant, C, that is this time material rather than process specific.

Blodgett: $\delta_T = 0.10 \cdot \dfrac{A_w}{t}$ (Equation 5.11)

Blodgett [1966] undertook extensive experiments on steel plates of varying thickness and also considered the influence of edge preparation in his study, to derive an equation relating the area of deposited weld and material thickness. This produced a simple equation that provides a relatively easy estimate of transverse distortion.

150

Leggatt: $\delta_T = (1+v) \cdot \eta \cdot \dfrac{\alpha}{\rho.c} \cdot \dfrac{q}{v.t}$ *(Equation 5.12)*

Leggatt [1980] used both theoretical and experimental investigations to derive his equation. He found his equation to be valid for a range of processes and steels, and also found it to be independent of gap or edge preparation of the joint and valid for both butt and bead on plate samples.

In Chapter 2 several other distortion models for transverse shrinkage were discussed. However, for the comparison here they are not included. The models of Watanbe and Satoh [1961] are not considered as they were derived specific to the MMA welding process. Hansen [1973] proposed a model but his work is based on edge prepared butt welds and as the case study company does not use edge preparation then it is not applicable to this investigation. Gilde [1958] put forward a model for steels however this model is similar to that of other authors and it is difficult to determine how some of its parameters are defined therefore it has been excluded from the comparison. Numerous other models exist some of which cover material thicknesses outside the scope of this investigation and those chosen are considered to be a representative selection of the widely accepted published models. Using the values applicable to the experiments conducted in this study then the predicted distortion values for transverse distortion were calculated based on the equations documented above. The results for these calculations can be found in Table 5.3. Whilst not all of the equations are strictly valid for each sample type, they have been included in all cases for comparison, as generally a fully penetrated bead on plate sample should distort in a similar manner to a comparable sized restrained butt weld sample. However a partially penetrated bead on plate weld will show a smaller transverse distortion as the parent metal beneath the fusion zone will act to prevent the transverse shrinkage.

The experimental results for transverse distortion measured in experiment undertaken as part of this study are shown as a summary in Table 5.4. Whilst the values do not show the same high levels of disagreement that was seen in the longitudinal models they still do not tend to follow any one particular model that has been offered. It can be seen that the Guiaux model always provides an upper bound

151

on the maximum value of the distortion, in that it consistently over predicts, when compared to the experiment.

Table 5.3: Calculated transverse distortions

Thickness	2.0mm					
Joint	Bead on Plate			Butt weld		
Speed	700	1000	1300	700	1000	1300
Guiaux	1.062	1.008	0.954	1.440	1.386	1.332
Okerblom	0.169	0.118	0.091	0.169	0.118	0.091
Guyot	0.578	0.548	0.519	0.783	0.754	0.724
Malisius	0.578	0.548	0.519	0.783	0.754	0.724
Capel	0.500	0.350	0.269	0.500	0.350	0.269
Blodgett	0.295	0.280	0.265	0.400	0.385	0.370
Leggatt	0.428	0.247	0.150	0.428	0.247	0.150

Thickness	2.5mm					
Joint	Bead on Plate			Butt weld		
Speed	700	1000	1300	700	1000	1300
Guiaux	1.026	0.972	0.918	1.260	1.206	1.152
Okerblom	0.135	0.095	0.073	0.135	0.095	0.073
Guyot	0.558	0.529	0.499	0.685	0.656	0.627
Malisius	0.558	0.529	0.499	0.685	0.656	0.626
Capel	0.400	0.280	0.215	0.400	0.280	0.215
Blodgett	0.285	0.270	0.255	0.350	0.335	0.320
Leggatt	0.307	0.163	0.085	0.307	0.163	0.085

Thickness	3.0mm					
Joint	Bead on Plate			Butt weld		
Speed	700	1000	1300	700	1000	1300
Guiaux	0.990	0.936	0.882	1.170	1.134	1.098
Okerblom	0.113	0.079	0.061	0.113	0.079	0.061
Guyot	0.538	0.509	0.480	0.636	0.617	0.597
Malisius	0.538	0.509	0.480	0.636	0.617	0.597
Capel	0.333	0.233	0.179	0.333	0.233	0.179
Blodgett	0.275	0.260	0.245	0.325	0.315	0.305
Leggatt	0.227	0.106	0.041	0.227	0.106	0.041

Table 5.4: Measured values for transverse distortion

Transverse Shrinkage - Experimental Values						
Joint	Bead on Plate			Butt weld		
Weld Speed (mm/min)	700	1000	1300	700	1000	1300
2.0mm	1.18	0.75	0.40	1.19	1.01	0.91
2.5mm	0.91	0.70	0.28	1.02	0.92	0.80
3.0mm	0.77	0.53	0.24	0.88	0.77	0.67

Both Okerblom and Leggatt appear to considerably under predict the distortion for the arrangement and conditions studied in this project. The Guyot and Malisius equations can be seen to be equivalent to each other from substituting the values for the experiment, but still don not agree with the experimental results.

One factor which will influence the transverse distortion is the value of any weld gap in a butt weld sample. Most of the models that have been used for the comparison were developed based on no gap condition existing in the weld set-up. However, as the experiment was set up to replicate the industrial practice of the case study company the nominal weld gap was designed into the experiment to be 0.5mm. Due to tolerances there will of course be some variation of this weld gap both between samples and along the length of each weld. The weld gap will certainly lead to increased shrinkage in the transverse direction, as additional material has to be added to fill this gap and therefore increasing the weld bead area and the heat input. However it is not possible to quantify exactly how much this will contribute to the overall transverse distortion from this study. A separate experiment would need to be conducted varying this weld gap in order to quantify this effect in the experimental set-up.

In addition, as was the case with the longitudinal distortion, then the influence of the other distortions will have an additive effect to the distortion that has been measured and recorded as transverse shrinkage. In particular the effect of the angular distortion on the measured value will be significant to the transverse distortion. For example a 4° angular distortion will result in a measured width reduction across 2 nominally

150mm plates of 0.2mm, which would be typical of the butt weld transverse distortion results. For the bead on plate samples the average angular distortion is about 7.5° which would give rise to a typical 0.32mm increase in the measured transverse distortion.

Therefore for bead on plate samples the angular distortion will act to increase the measured value of transverse distortion. Likewise for the butt weld samples the effect of the weld gap and the angular distortion will both act to increase the measured value of the transverse distortion. If as examples of this the experimental values are amended accordingly, then for the 2.5mm thick bead on plate samples produced at 1000mm/min weld speed the true transverse distortion will be reduced from the measured value of 0.75mm down to 0.43mm. This value lies between the predictions from the Malisius and Capel/Blogdett models. Doing likewise for the butt weld sample at 2.5mm thick and 1000mm/min, the measured value of 0.92mm would reduce to 0.72mm due to the removal of the angular distortion effect. This would further reduce by an amount that at this stage cannot be quantified from this experiment but will lie between 0.0 and 0.5mm reduction due to the weld gap effect. Therefore the likely true transverse distortion is in the region of 0.72mm to 0.22mm, which again is more in line with the predicted values from the formulae.

However as previously stated, to be of maximum benefit then a designer would wish to know the combined effect on transverse shrinkage in a joint from all distortions so consideration could be included into the designs based on one simple calculation. Therefore a specific equation relating to the range of interest of the case study company could be developed and applied at the design stages.

5.2.3 Angular Distortion

Some of the models for angular distortion where summarise in Table 2.5 in Chapter 2. Here the most applicable models for predicting angular distortion have been selected and used to present a comparison to the experimental results. The formulae used in this section can be summarised as follows:

154

Okerblom: $\beta_f = C \cdot \eta_m \cdot \dfrac{q}{v.t_c^2}$ (Equation 5.13)

Okerblom [1955] developed his model from his experiments on bead on plate samples, and is valid for parabolic shaped weld profiles, and where p/t < 0.6. An efficiency was used which accounts for the heat fusing the base material, and a constant which is dependent on the joint configuration. Subsequent researchers such as Gray, Spence and North [1975] have found this equation can also be valid for butt welds with the constant adjusted accordingly.

Leggatt: $\beta_f = 0.22 \cdot \dfrac{q}{v} \cdot \dfrac{1}{t_c^2}$ if p< t/2 (Equation 5.14)

Leggatt [1980] showed in experiments on bead on plate samples that the angular distortion for single pass welds peaks to a maximum, which was described as occurring at a penetration which is half the material thickness. After this value the angular distortion decreases with increasing heat input. He suggests it is the effect of the restraint from the unfused material that limits the angular distortion, and if penetration is deeper then the unfused material yields. Based on this the equation was adjusted to provide an empirical relationship for higher penetration welds.

Table 5.5: Calculated angular distortions

Thickness	2.0mm					
Joint	Bead on Plate			Butt weld		
Speed	700	1000	1300	700	1000	1300
Okerblom	8.61	6.03	4.64	11.06	7.74	5.95
Leggatt	18.86	13.20	10.15	24.43	17.10	13.15

Thickness	2.5mm					
Joint	Bead			Butt		
Speed	700	1000	1300	700	1000	1300
Okerblom	5.51	3.86	2.97	7.08	4.95	3.81
Leggatt	12.07	8.45	6.50	12.64	8.85	6.81

Thickness	3.0mm					
Joint	Bead			Butt		
Speed	700	1000	1300	700	1000	1300
Okerblom	3.83	2.68	2.06	4.91	3.44	2.65
Leggatt	8.38	5.87	4.51	7.37	5.16	3.97

Using these equations calculations of the predicted angular distortion for the joints in the experiment can be made. These are recorded in Table 5.5. These can be compared to the experimental values which are summarised in Table 5.6.

Table 5.6: Measured values for angular distortion

Angular Distortion - Experimental Values						
Joint	Bead on Plate			Butt weld		
Weld Speed (mm/min)	700	1000	1300	700	1000	1300
2.0mm	6.45	6.63	6.59	4.46	3.42	2.94
2.5mm	7.67	7.58	7.04	3.93	3.24	2.81
3.0mm	8.65	8.21	6.19	3.62	3.07	2.45

From the calculation in Table 5.5 it is possible to see that there is not a particularly good agreement to the experimental vales that were recorded. In previous discussions in Chapter 4 the method used to calculate the angular distortion was described, along with its shortcomings. The angular distortion measured is taken as an average across each section cut in order to ensure a consistent measurement. This was done by best fitting straight lines through the points on either side of the weld. Therefore this would tend to result in a smaller angular distortion that may actually be occurring. If the length taken either side of the weld used for the best fit was altered then the angular distortion value changed due to the change of the best fit straight line. In order to further evaluate the accuracy of the angular distortion results then an alternative measurement method would need to be developed that measured the angular distortion over a consistent area close to the weld bead. However what could be observed and has been discussed in detail in Chapter 4 is the effect of the penetration on the angular distortion.

5.2.4 Bowing Distortion

In Chapter 2 some of the equations for predicting bowing distortion were described, and these were summarised in Table 2.7. The equations used for this comparison are summarised and discussed as follows:

$$\text{Okerblom:} \quad \frac{1}{R} = 0.335 \cdot \eta \cdot \frac{q}{v} \cdot \frac{\alpha}{\rho \cdot c} \cdot \frac{y}{J} = 235 \cdot \eta \cdot \frac{y}{EI} \cdot \frac{q}{v} \qquad \text{(Equation 5.15)}$$

Okerblom [1955] derives his equation based on the effective force in the longitudinal shrinkage of the weld acting offset to the neutral axis to produce bowing.

$$\text{Horst Pflug:} \quad \frac{1}{R} = 42 \cdot \frac{\sigma_y}{E} \cdot \frac{A_w \cdot y}{J} = 9830 \frac{y}{EI} \cdot A_w \qquad \text{(Equation 5.16)}$$

Horst Pflug [1956] derived his equation based on the work of Okerblom but uses slightly different formulation in his equation.

$$\text{Blodgett:} \quad \frac{1}{R} = 0.04 \cdot \frac{A_w \cdot y}{J} = 8400 \cdot \eta \cdot \frac{y}{EI} \cdot A_w \qquad \text{(Equation 5.17)}$$

Blodgett [1960] derived his equation based upon the flex of a structure. He included in his work validation based on a variety of sections including both T and I sections.

In his review paper Verhaeghe [1998] uses the tendon force concept to compare the terms used in these equations. The rewriting of these formula based upon tendon force is shown as the second part of each equation above.

The values of the sections and parameters used for the experiment were substituted into the above equations to derive predictions of the bowing distortion, expressed as the radius of curvature for ease of reporting. These values can be found in Table 5.7. The experimental results found in this study are summarised in Table 5.8 to allow a comparison to be made.

Table 5.7: Calculated bowing distortions

Thickness	2.0mm					
Joint	Bead on Plate			Butt weld		
Speed	700	1000	1300	700	1000	1300
Okerblom	977	1396	1815	1955	2793	3630
Horst Pflug	1086	1144	1209	1602	1665	1732
Blodgett	1589	1674	1769	2344	2435	2534

Thickness	2.5mm					
Joint	Bead on Plate			Butt weld		
Speed	700	1000	1300	700	1000	1300
Okerblom	1527	2182	2836	3054	4363	5672
Horst Pflug	1405	1484	1571	2289	2391	2503
Blodgett	2056	2170	2298	3348	3498	3662

Thickness	3.0mm					
Joint	Bead on Plate			Butt weld		
Speed	700	1000	1300	700	1000	1300
Okerblom	2199	3142	4084	4398	6283	8168
Horst Pflug	1748	1849	1962	2958	3052	3152
Blodgett	2557	2704	2870	4327	4464	4611

Table 5.8: Measured values for bowing distortion

Bowing Distortion - Experimental Values						
Joint	Bead on Plate			Butt weld		
Weld Speed (mm/min)	700	1000	1300	700	1000	1300
2.0mm	1686	1711	1722	1966	2318	3659
2.5mm	1720	1773	1847	2868	3769	5038
3.0mm	1762	1822	1899	4071	4854	6853

From the results presented above it can be seen that generally the trends and values for bowing distortion for the butt weld sample agree very well with the predictions from the Okerblom model. The higher weld speed experiments in the thickest plate exhibit the highest errors at 22% and 16% respectively, however most other values lie within 10% or better of the value calculated by the Okerblom model. It can also

158

be seen that the experimental values are generally smaller than the prediction therefore the curvature of the section is greater than expected. Given the method used to calculate the curvature based on best fitting a single curve through the experimental scanned points at each section then some error is not to be unexpected. However the general agreement to the model gives a good indication of its applicability. The bowing distortion is probably the distortion that when measured is influenced least by the other distortion effects and therefore it is perhaps not unsurprising that this shows the best correlation to the published works. The bead on plate samples exhibit much greater curvature and hence lower values of radius of curvature, R. In this particular setup and experiment it would appear that the overall Horst Pflug model gives the closest correlation to the bead on plate bowing distortion results. Although at 2.0mm material thickness it is the Blodgett model that appears to correlate more closely to the bead on plate results, with errors less than 6% for this particular thickness. However for bowing distortion on the bead on plate samples no one model can be said to give the levels of general agreement seen with the butt welds to the Okerblom model. Therefore there is value in generating specific equations to suit the case study company's typical range of applications that may give a better approximation for a designer to consider in their design.

5.3 Distortion Prediction

In order to make best use of the data generated from the experiment, then the initial step to utilise this to create some simple equations that characterise the distribution. Such equations can then be used by designers to evaluate joints for the distortions that will occur and decide if they need to compensate for the predicted distortion in the design. This section looks at the generation of such equations and the validity of these. In order to do this the initial experimental data is once again examined to see if any simple relationships exist. It is also used to generate response surfaces for the individual distortion outcomes. Subsequent analysis of the best fit response surface can then generate equations to characterise the response and judge if this makes a suitable equation that could be used by a designer for quick and simple distortion prediction.

159

In order to generate the equations, and for these to be of use, then it needs to be decided upon the design space envelope that these need to cover. From the experiment, two factors were varied to give four primary distortion responses. Therefore, the practical range of the input parameters in relation to the case study company needs to be determined. The first factor varied was material thickness. At the case study company they manufacture products in thicknesses ranging from 1.5mm thick material, although 2.0mm is a more common lower bound, up to 6.35mm thick. However the 6.35mm thicknesses are extremely rare and in practise the upper limit on thickness tends to be between 4.0 and 5.0mm for press forming considerations. Therefore for this study the design space that will be used and the experimental data extrapolated to fit to will be limited to ranging between 1.5mm and 5.0mm thickness of material. The second factor chosen was welding speed. In practice unless there is a very long straight run then the upper speeds of this study are rarely seen in production. The lower speed is often used however, especially when the weld path is a complex shape and form. In order to attempt to fit the response outside the values used in this experiment then the design space values will be chosen to be slightly wider than used in the experiment. Therefore for this exercise the values of weld speed chosen will be to lie in a range from 500 to 1500 mm/min.

Having decided upon the ranges to be considered in the design space the following sections will look in detail at the derivation of equations relating the experimental variables to the distortion outcomes. It should be remembered that that equations derived in this study are specific to the parameters used in the case study company's processes and therefore do not attempt to be a generalised categorisation of all welding processes and parameters. They also represent one material type and grade, which as mentioned earlier, however, accounts for the majority of the case study company's components at this point in time. The subsequent sections look at the two different weld types and geometries separately, first considering the distortions for the bead on plate sample and then for the butt weld joint.

5.3.1 Generating Equations for Bead on Plate Samples

Firstly, the longitudinal distortions from the bead on plate experiment are considered. Looking at the averaged experimental results separately for variation of both material thickness and weld speed, it is clear that distortions do appear to have a relationship. The family of curves generated from this data is shown in Figure 5.1. Figure 5.1(a) demonstrates that the distortions decrease with increasing material thickness, however whilst the curves are relatively evenly spaced there is not a perfectly linear relationship from the experimental data. Figure 5.1(b) shows a similar relationship for longitudinal distortion as the weld speed is changed. The curves are not equally spaced, and unlike the curves in Figure 5.1(a) they do not follow the same shape as closely as the first relationship. Therefore a simple equation is easily identified to cover the range of experimental outcomes, furthermore for it to be able to be expanded to be valid across the desired range for the design space for a prediction tool.

If these results are then looked at as a response surface across the range of the experimental variables an idea is formed about the nature of any equation to be expanded to a larger region. Figure 5.2 shows the experimental results represented as a surface variation plot. From this it again can be seen that the trend is towards a linear relationship for varying both parameters, but clearly they have some interaction with each other due to the form of the surface. The plots for these investigations are shown as sample studies for both this and the transverse distortion. For all subsequent investigations they are recorded in Appendix III, in order to keep the discussion as concise as possible.

Longitudinal distortion
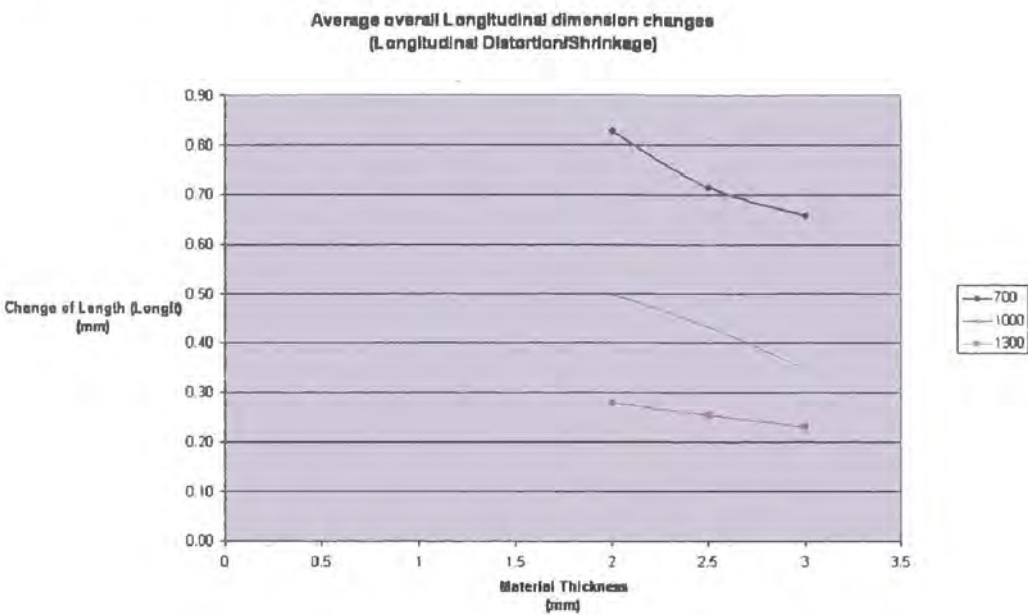
(a) Relationship between material thickness curves
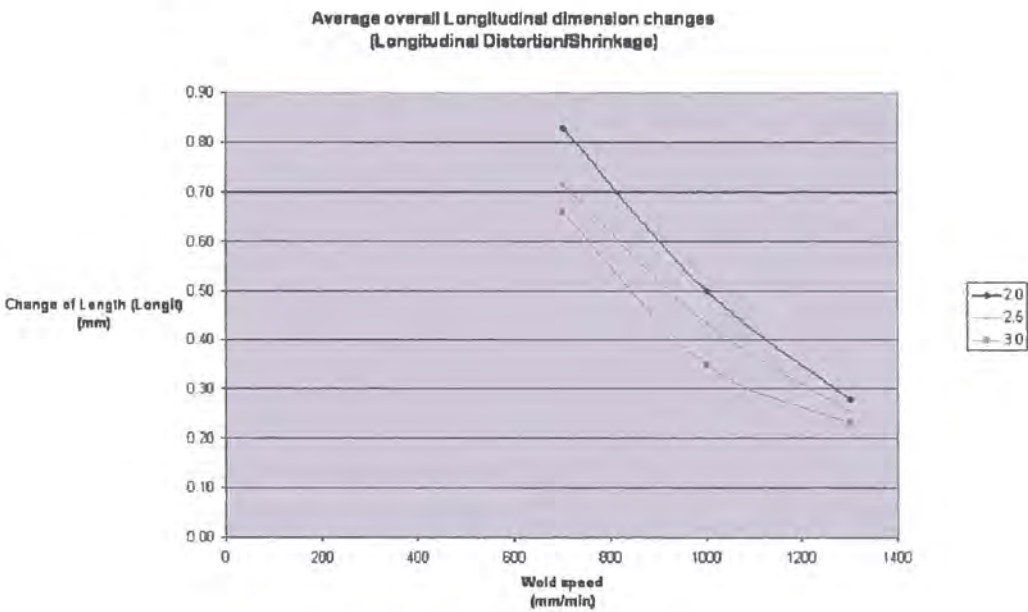
(b) Relationship between welding speed curves

Figure 5.1: Family curves for longitudinal distortion (bead on plate)
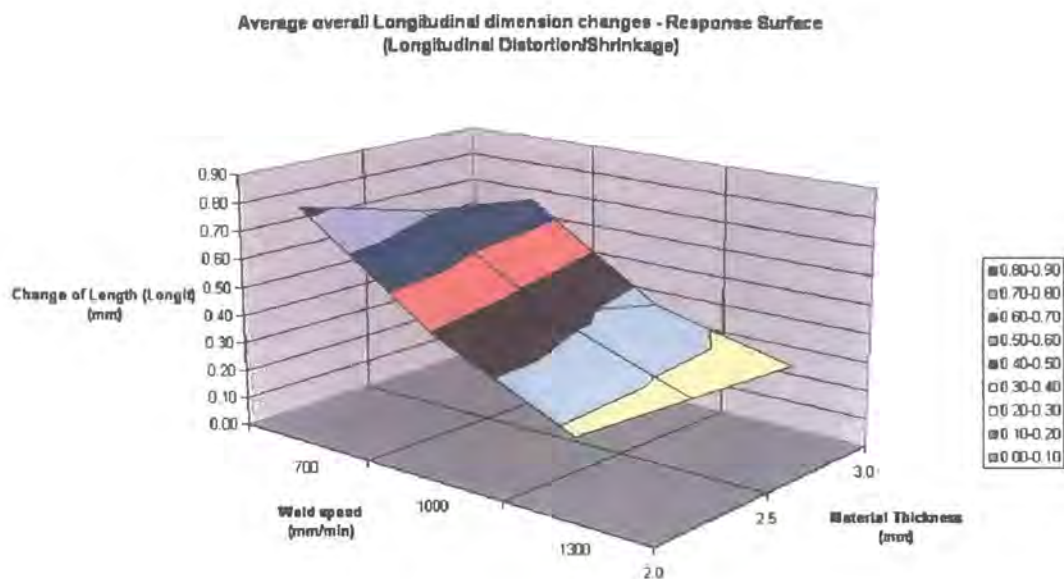
Figure 5.2: Experimental surface for longitudinal distortion (bead on plate)

Therefore, in order to approximate the outcomes across both the experimental space, and subsequently the design space it was necessary to analyse the data using software. In this case the data was fed into a Design of Experiments package to attempt to characterise the response, based on a historical fitting approach. The software chosen was Design Expert by Stat-Ease, as this was software that had previously been used by the case study company and seen to give good results for DoE studies. The averaged experimental data was input as a two factor 3 level experiment, giving rise to 4 responses, each of the distortions, and based on 9 outcomes from varying the factors. This allowed a response surface to be generated and fitted through the historical experimental data. Analysis of the surfaces allowed a best response to be selected and characterised by choosing differing form of the response. Figure 5.3 shows the 3D response surface for the best fit model to the experimental data. In this case the best fit model is a quadratic relationship for each factor. In this and the subsequent plots of response surface the experimental results are shown as 'Design Points', and identified as being either above or below the response surface itself.

163
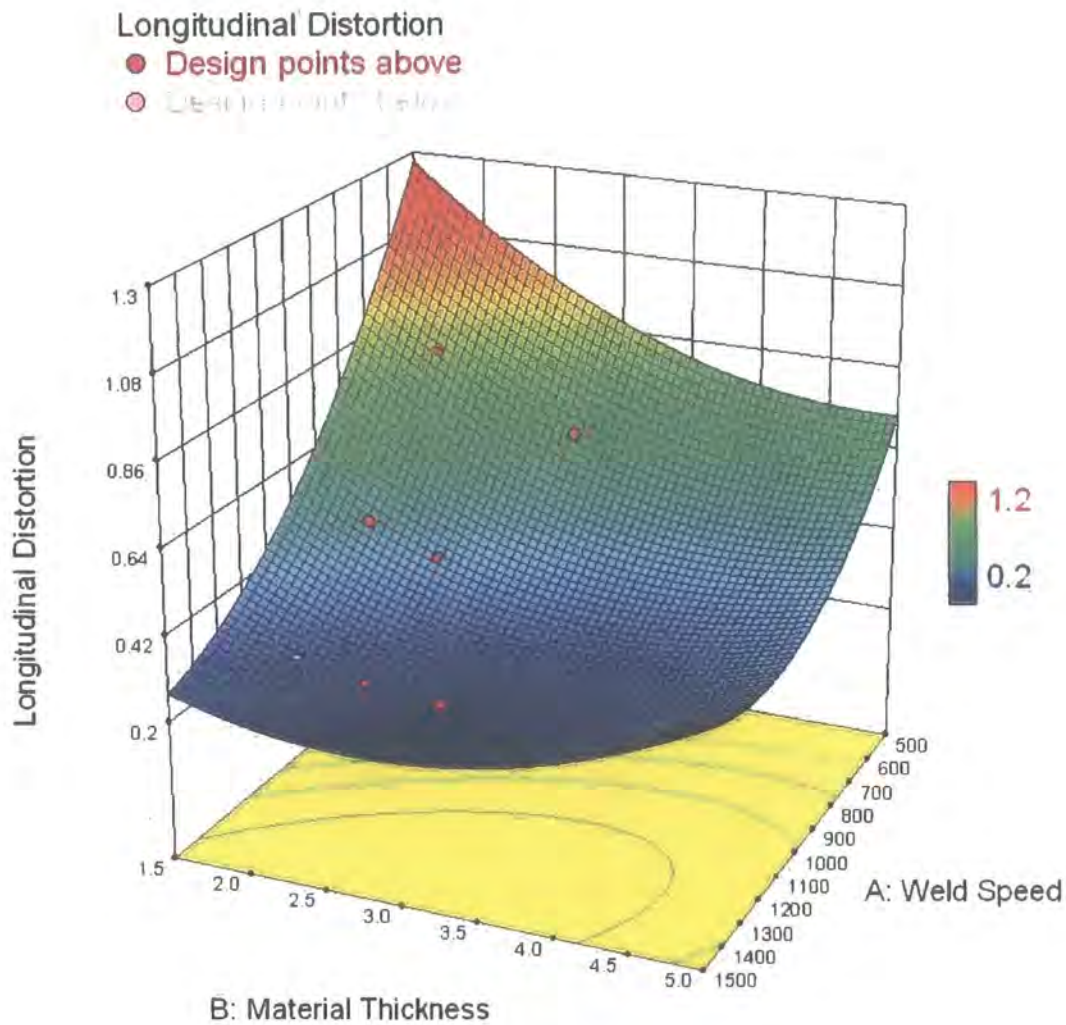
Figure 5.3: Best fit response surface for longitudinal distortion (bead on plate)

From the response surface generated it is possible to extract an equation relating the response to the variable factors. In this case the equation approximating the longitudinal distortion response for the variation of welding speed and material thickness can be found to be expressed as:

$$\delta_L = 3.05963 - 0.00278148.v - 0.55667.t + 0.0002.v.t + 7.40741e\text{-}7.v^2 + 0.046667.t^2$$

(Equation 5.18)

Clearly this is still quite a complex equation, however, it is one that could be quickly evaluated by a designer to make a distortion prediction. It also needs to be remembered that this is a distortion that would appear to be size dependent, therefore the equation would need to be normalised to take into account the weld length to be accurate. The experiments were carried out using a 350mm long plate,

164

but a 10mm start and stop allowance was made to prevent burn through and notching of the plate edges, so the results are effectively from a 330mm long weld. It has been seen previously from the published formula for longitudinal shrinkage that the distortion is proportional to the length of the weld. Therefore to be a correct general prediction for this method and value would need to be divide by 330 to give a distortion per unit length, before being multiplied by the weld length being considered. Therefore the equation should be presented in its generalised form as:

$$\delta_L = \frac{L.(3.05963 - 0.0027815.v - 0.5567.t + 0.0002.v.t + 7.40741e\text{-}7.v^2 + 0.046667.t^2)}{330}$$

(Equation 5.18a)

Alternatively this equation and response curve can be represented in a 2D graphical format with contours and this could be used as a basic look up table for the design space. An example of how this graph could appear is shown in Figure 5.4. Again the result will need to be corrected for the actual weld length, as described above, once the designer has found the approximate longitudinal distortion factor from the graph.

In order to check the validity of the equation then the experimental outcomes were each checked against the equation and the values generated are shown in Table 5.9 which gives an indication as to the fit of the response surface. From this data it can be seen that the equation is a good fit to the experimental data, and based on the methods used to determine this it is suitable to use to navigate the design space with confidence.

Table 5.9: Comparison of longitudinal distortion prediction to experimental data (bead on plate)

Weld Speed *mm/min*	Material Thickness *mm*	Experimental Result *mm*	Predicted Distortion *mm*	Variation Expt -v- pred *mm*	Error *%*
700	2.0	0.83	0.83	0.0011	0.13%
	2.5	0.71	0.73	-0.016	-2.25%
	3.0	0.66	0.65	0.014	2.12%
1000	2.0	0.5	0.49	0.0078	1.56%
	2.5	0.43	0.42	0.011	2.56%
	3.0	0.35	0.37	-0.019	-5.43%
1300	2.0	0.28	0.29	-0.0089	-3.18%
	2.5	0.25	0.25	0.0044	1.76%
	3.0	0.23	0.23	0.0044	1.91%

165
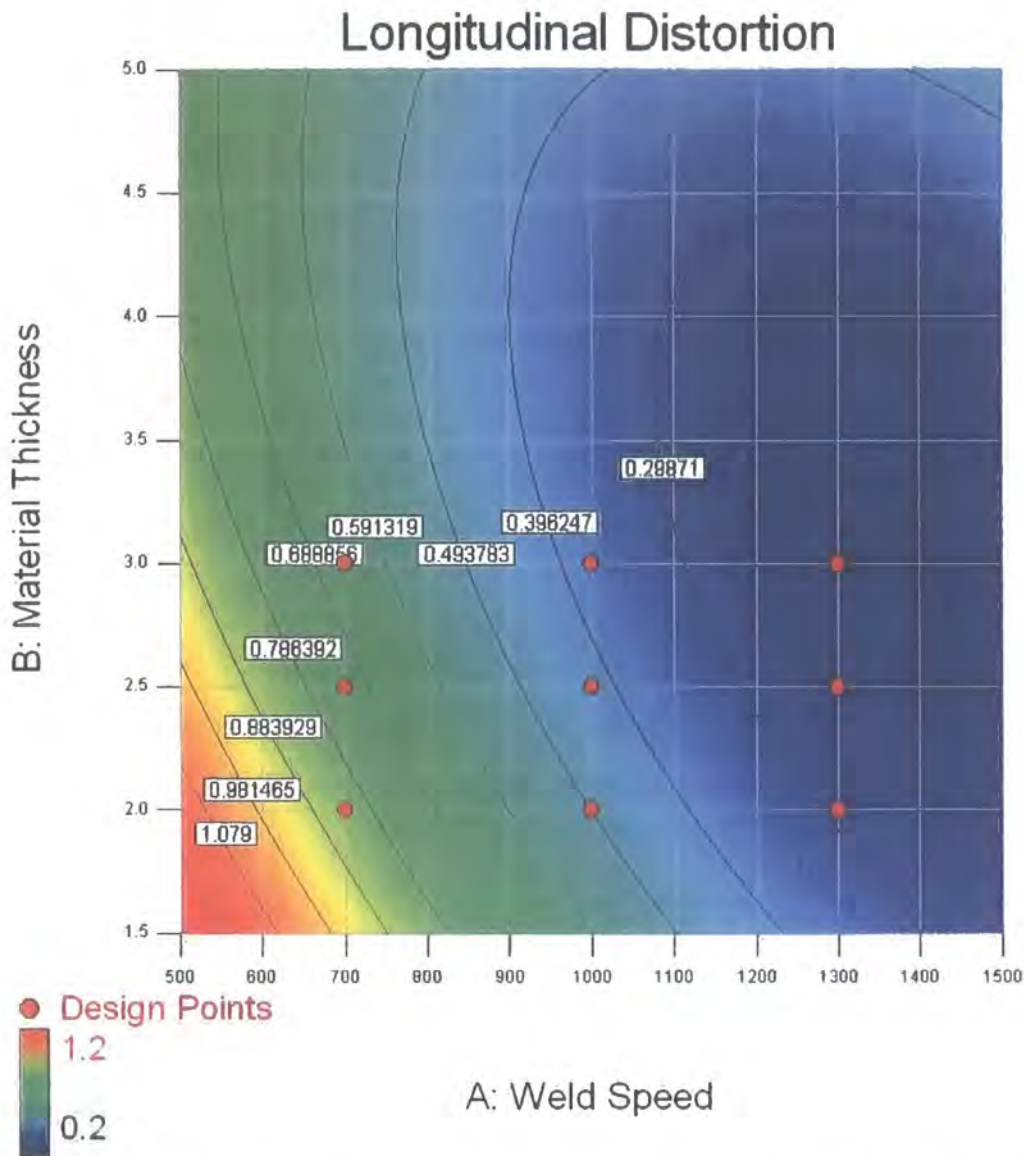
Figure 5.4: 2D representation of longitudinal distortion equation (bead on plate)

Having looked at the longitudinal distortion then a similar approach can be applied to the transverse distortion. Figure 5.5 shows the response to the individual variations, and it can be seen that whilst there is a more even spacing of the response family of curves they again do not follow exactly the same pattern as each other. However looking at these and the experimental response surface in Figure 5.6 then it is possible to suggest that there is more of an underlying linear relationship between the factors. This is due to the very small curvature of the lines fitted through the data which for a simple approximate model could perhaps be ignored.

Transverse distortion
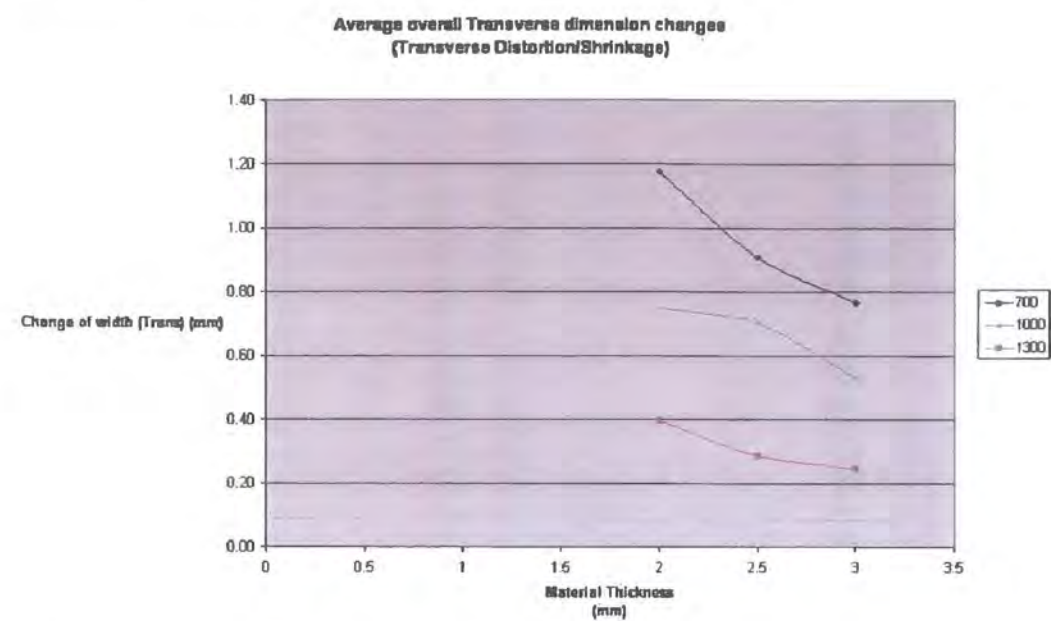
Average overall Transverse dimension changes
(Transverse Distortion/Shrinkage)

(a) Relationship between material thickness curves

Average overall Transverse dimension changes
(Transverse Distortion/Shrinkage)
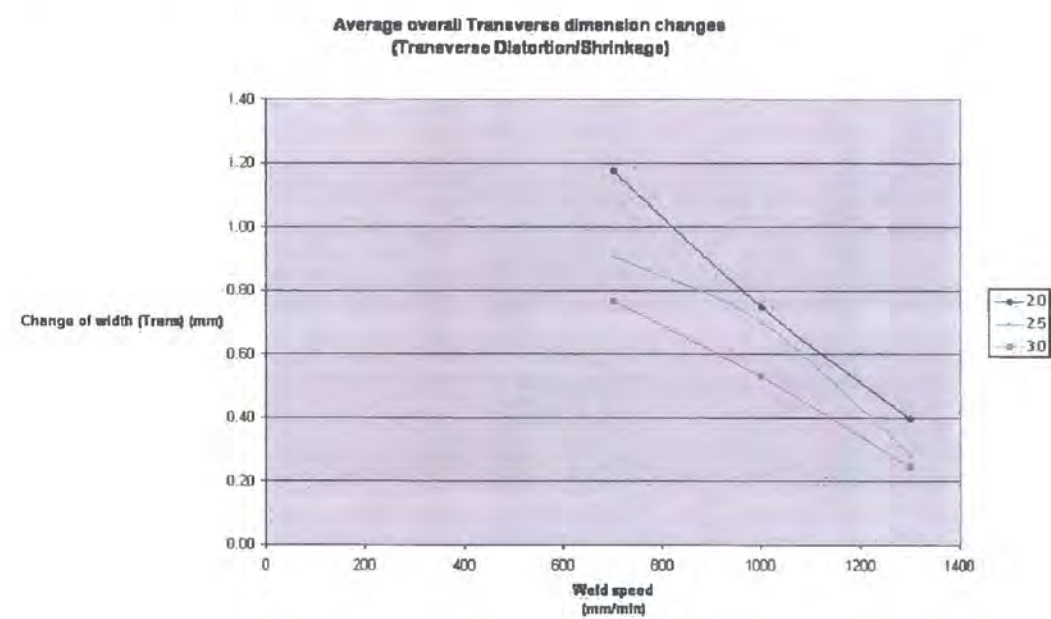
(b) Relationship between welding speed curves

Figure 5.5: Family curves for transverse distortion (bead on plate)

If this is then considered to be the case across the whole experimental space then it is possible to derive some approximate equations which may be valid for the experimental results. Analysis of the experimental results leads to the following equations being derived to approximate the experiment:

167

$\delta_t \approx 1620 / (v.t)$ for $t = 2.0$ and $t = 2.5$ mm   *(Equation 5.19)*

and

$\delta_t \approx 960 / (v.t)$ for $t = 3.0$ mm   *(Equation 5.20)*

where δ_t is transverse distortion (in mm), v is weld speed (in mm/min) and t is material thickness (in mm).

However, these are only valid for the experimental outcomes and as the factor is different depending on the thickness it is not possible to state what the equation would be at other thicknesses outside, or even in between, those considered. Further experiments would therefore be required to establish these other factors so these cannot be considered as generalised equations for the design space to be considered.
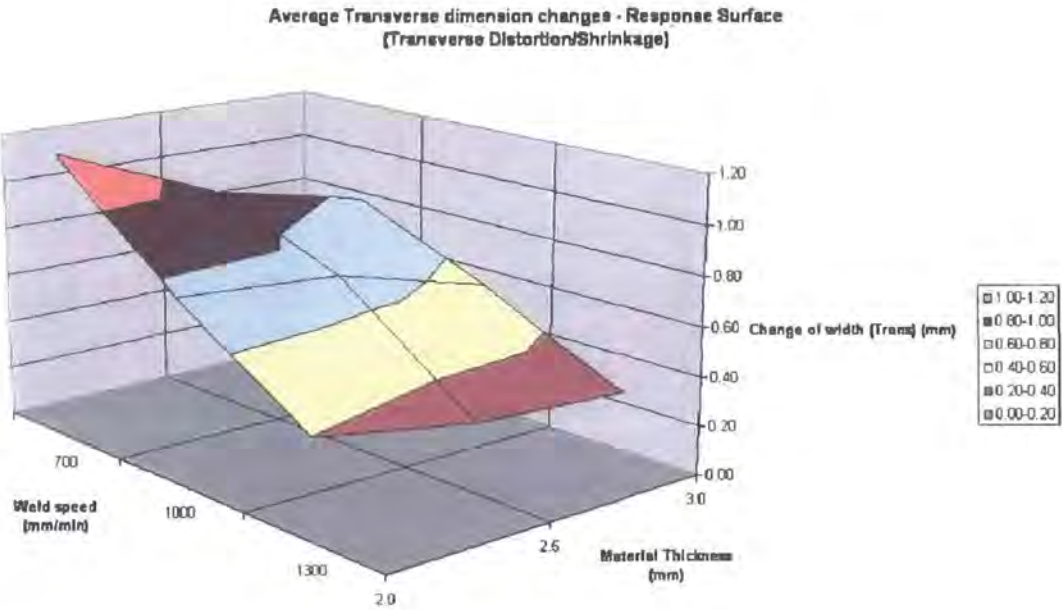
Figure 5.6: Response surface for transverse distortion (bead on plate)

Therefore, in order to establish a generalised equation valid across the design space under consideration that is applicable to the case study company, it is necessary again to utilise the DoE software to assist in best fitting a response to the data and extrapolating this across the full design space. This time the best fit response was based on a linear combination of the factors, and the best fit response surface across the design space can be seen in Figure 5.7.

168
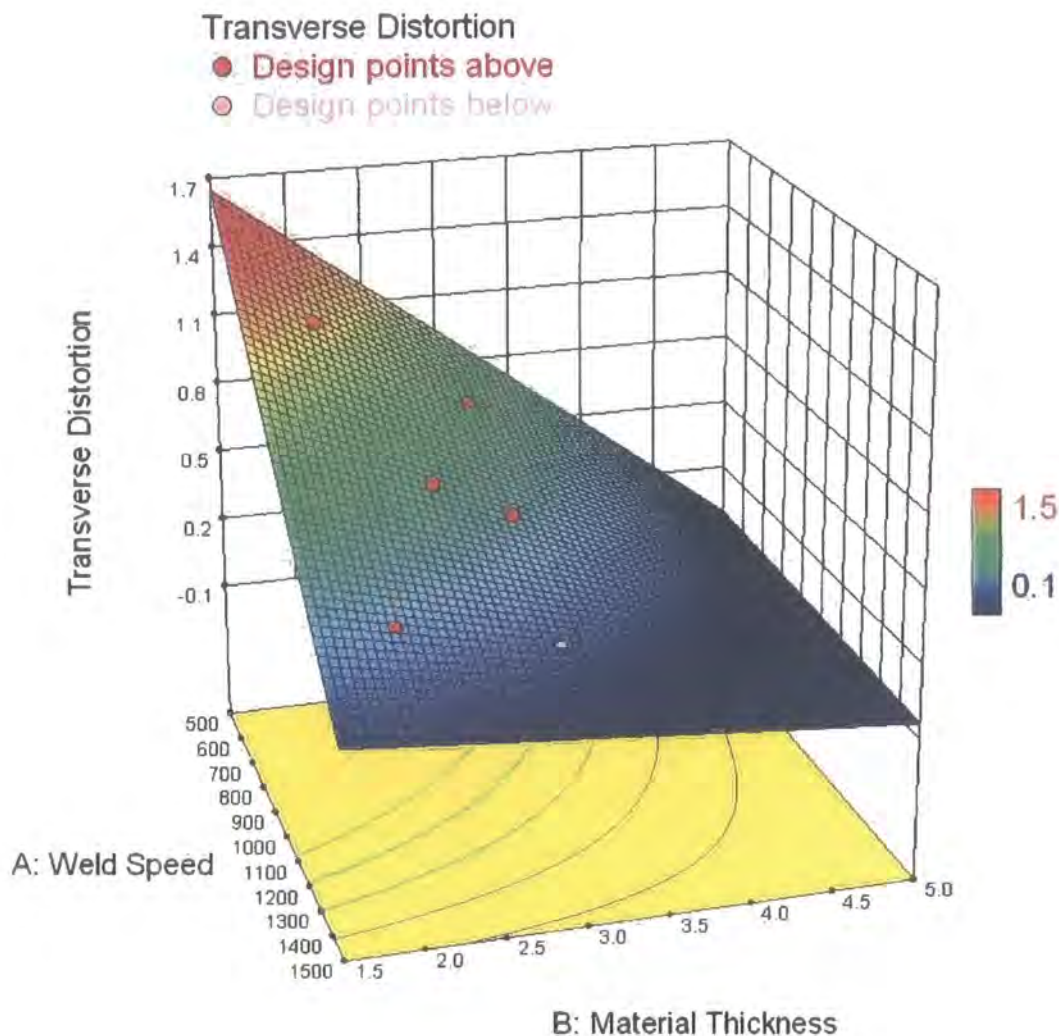
Figure 5.7: Best fit response surface for transverse distortion (bead on plate)

The equation derived by using the software to characterise this response surface for the bead on plate transverse distortion was found to be:

$$\delta_T = 3.41778 - 0.00211944.v - 0.68.t + 0.000416667.v.t \qquad \text{(Equation 5.21)}$$

In order to check the validity of the equation then the experimental points are entered and checked to the predictions. Note that for ease of use, in this and subsequent derived equations the speed is in mm/min rather than mm/s. The results of the comparison are presented in Table 5.10. The fit for the derived equation is not as good as for the longitudinal distortion equation to its data, with some errors being as high as 13%, but generally the equation is a reasonable fit through the data with the errors typically about 5%. However the equation is considerably less complex

169

than the longitudinal equation and the balance needs to be struck between the complexity of the equation for ease of use and the fit of the data.

Table 5.10: Comparison of transverse distortion prediction to experimental data (bead on plate)

Weld Speed mm/min	Material Thickness mm	Experimental Result mm	Predicted Distortion mm	Variation Expt -v- pred mm	Error %
700	2.0	1.18	1.16	0.023	1.95%
	2.5	0.91	0.96	-0.053	-5.82%
	3.0	0.77	0.77	0.0008	0.11%
1000	2.0	0.75	0.77	0.022	2.93%
	2.5	0.7	0.64	0.06	8.57%
	3.0	0.53	0.51	0.022	4.15%
1300	2.0	0.4	0.39	0.014	3.50%
	2.5	0.28	0.32	-0.037	-13.21%
	3.0	0.24	0.25	0.0075	3.13%
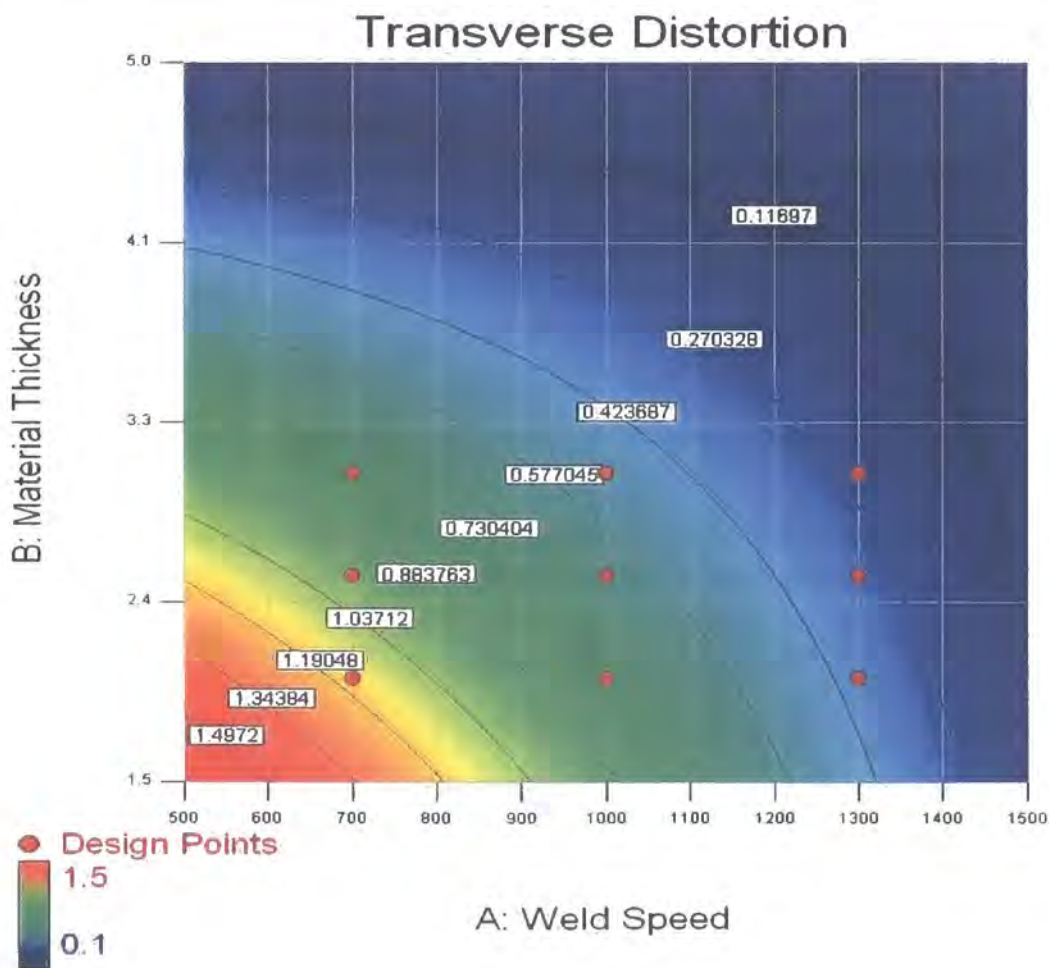
Figure 5.8: 2D representation of the transverse distortion equation (bead on plate)

170

The transverse shrinkage occurs in the weld and region immediate to it, the HAZ, subject to metallurgical change. Therefore this does not really have to be factored to account for plate width dimension. Therefore, the equation derived can therefore be used and applied over the design space directly. Alternatively it can also be represented on a 2D chart and used as a look up tool. An example of how such a chart could look for the transverse distortion is shown in Figure 5.8.
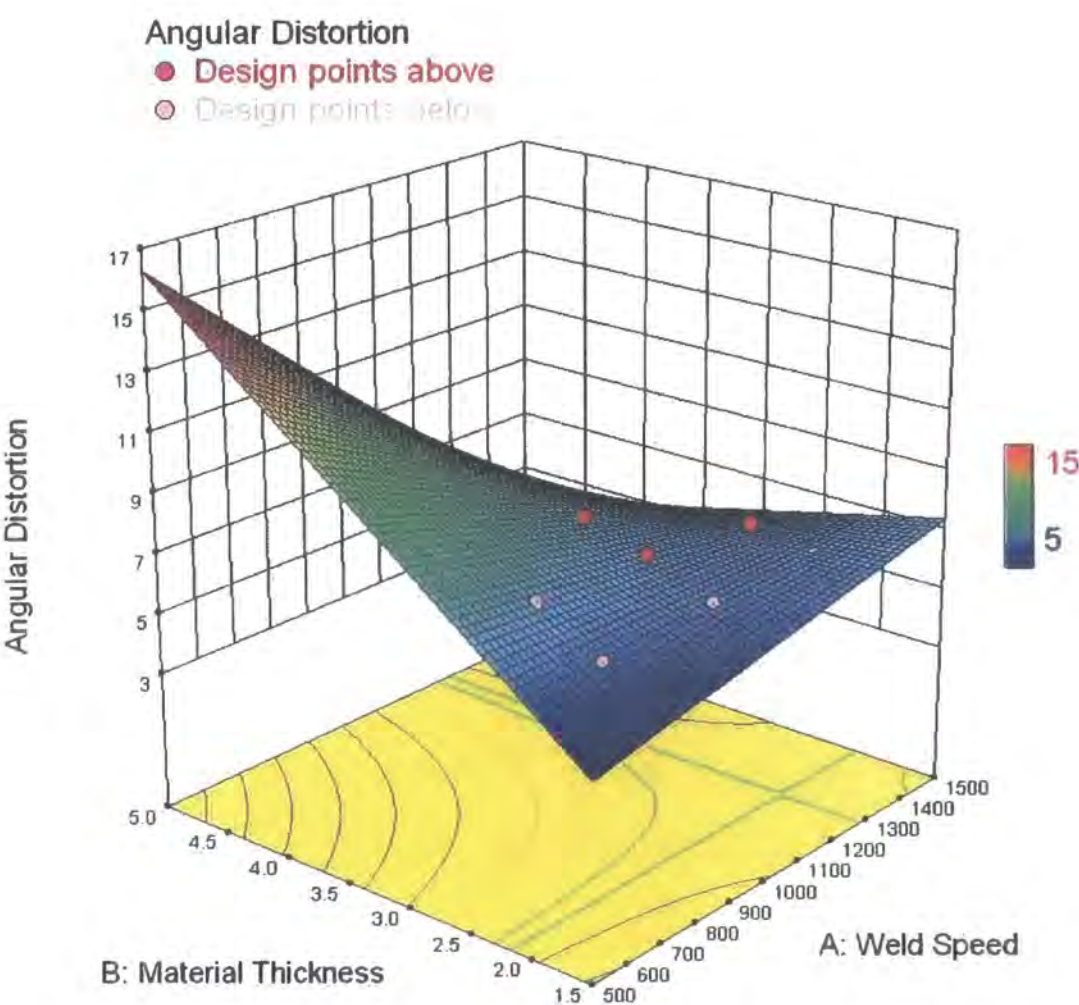
Figure 5.9: Best fit response surface for angular distortion (bead on plate)

The next distortion to consider is the angular distortion. The figures for these factors from the experiments are to be found in Appendix III. The variation of the two factors shows that there is no easily distinguishable relationship between the family of curves for both factors. The results shown as a summary on an experimental response surface again highlights the complex form which makes it difficult to

171

deduce a simple relationship to define the relationship. Utilising the DoE software to map the results and extrapolate over the whole design space then it is possible to form a basic equation that can define the angular distortion. The response surface generated over the design space for the angular distortion is shown in Figure 5.9. It is found that the response surface can be characterised by the following equation:

$$\beta_f = -4.78778 + 0.00919444.v + 5.46.t - 0.004333.v.t \qquad \text{(Equation 5.22)}$$
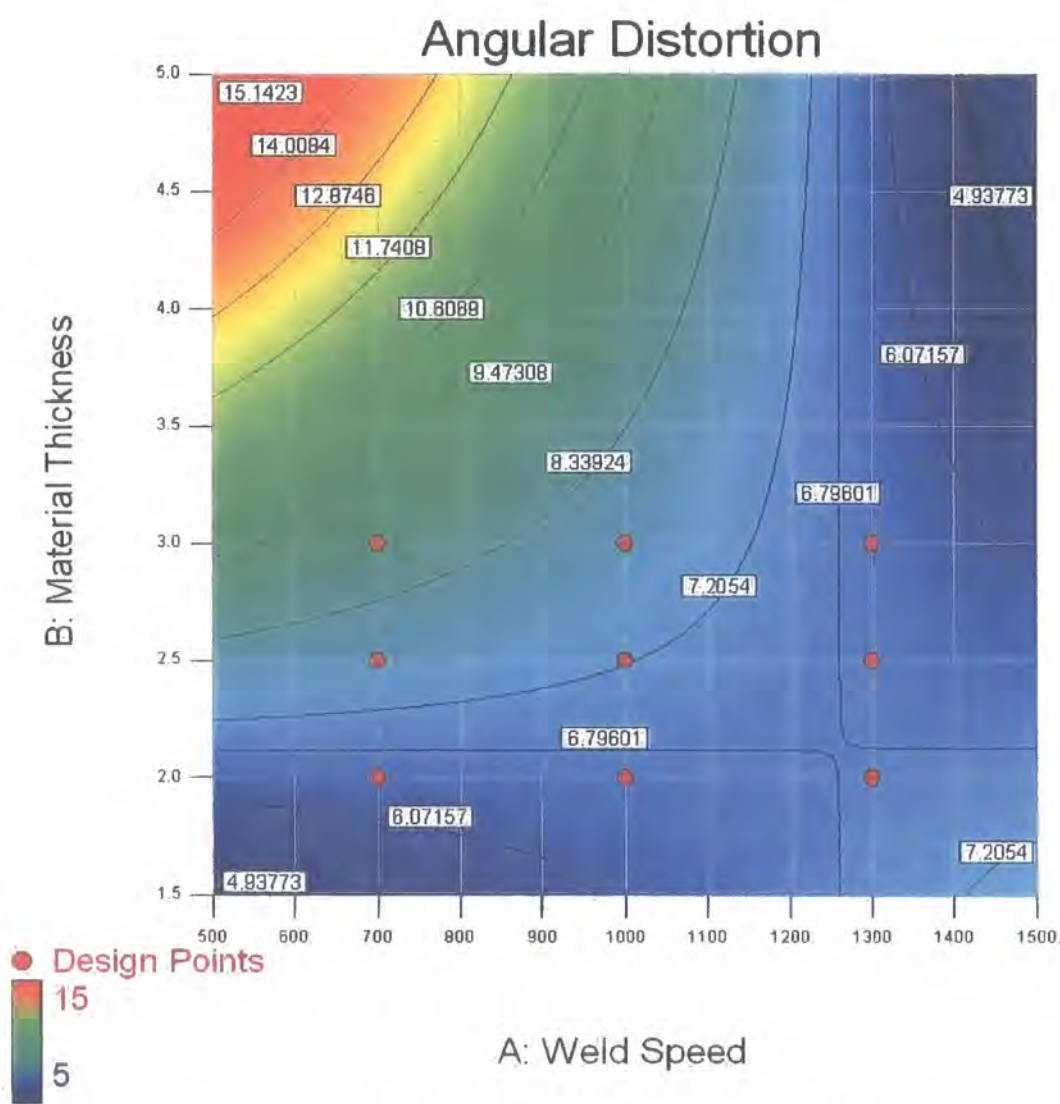
Figure 5.10: 2D representation of the angular distortion equation (bead on plate)

In order to check the validity of the equation then the experimental points are entered and checked to the predictions. The results of which are presented in Table 5.11.

Table 5.11: Comparison of angular distortion prediction to experimental data (bead on plate)

Weld Speed mm/min	Material Thickness mm	Experimental Result Degrees	Predicted Distortion Degrees	Variation Expt -v- pred Degrees	Error %
700	2.0	6.45	6.50	-0.052	-0.81%
	2.5	7.67	7.72	-0.045	-0.59%
	3.0	8.65	8.93	-0.28	-3.24%
1000	2.0	6.63	6.66	-0.03	-0.45%
	2.5	7.58	7.22	0.36	4.75%
	3.0	8.21	7.79	0.42	5.12%
1300	2.0	6.59	6.82	-0.23	-3.49%
	2.5	7.04	6.73	0.31	4.40%
	3.0	6.19	6.65	-0.46	-7.43%

From the comparison of results it can be seen that whilst this equation does fit the data, some the errors however are larger than the longitudinal equation generated. The maximum error between the experimental and predicted results is in the region of 7.5%. Also in considering the complex form of the experimental response surface and as has previously been discussed that the angular distortion is not purely an effect of thickness and speed, then the equation needs to be used with caution, especially when the combination of factors lies outside of the experimental space. Figure 5.10 shows a 2D representation of the equation as a series of iso-curves to represent the response surface, which is another way the equation could be used by a designer as a quick reference tool.

The final distortion to be considered for the bead on plate samples is the bowing distortion. Again the variation of the individual factors is considered, for which the figures can be found in appendix III. The relationship has been seen to be quite evenly spaced which would tend towards a linear relationship, however this is not directly obvious from the simple investigation. Therefore applying the DoE software to generate a response surface through the data and extrapolating across the design space, then the output can be seen as the response surface in Figure 5.11
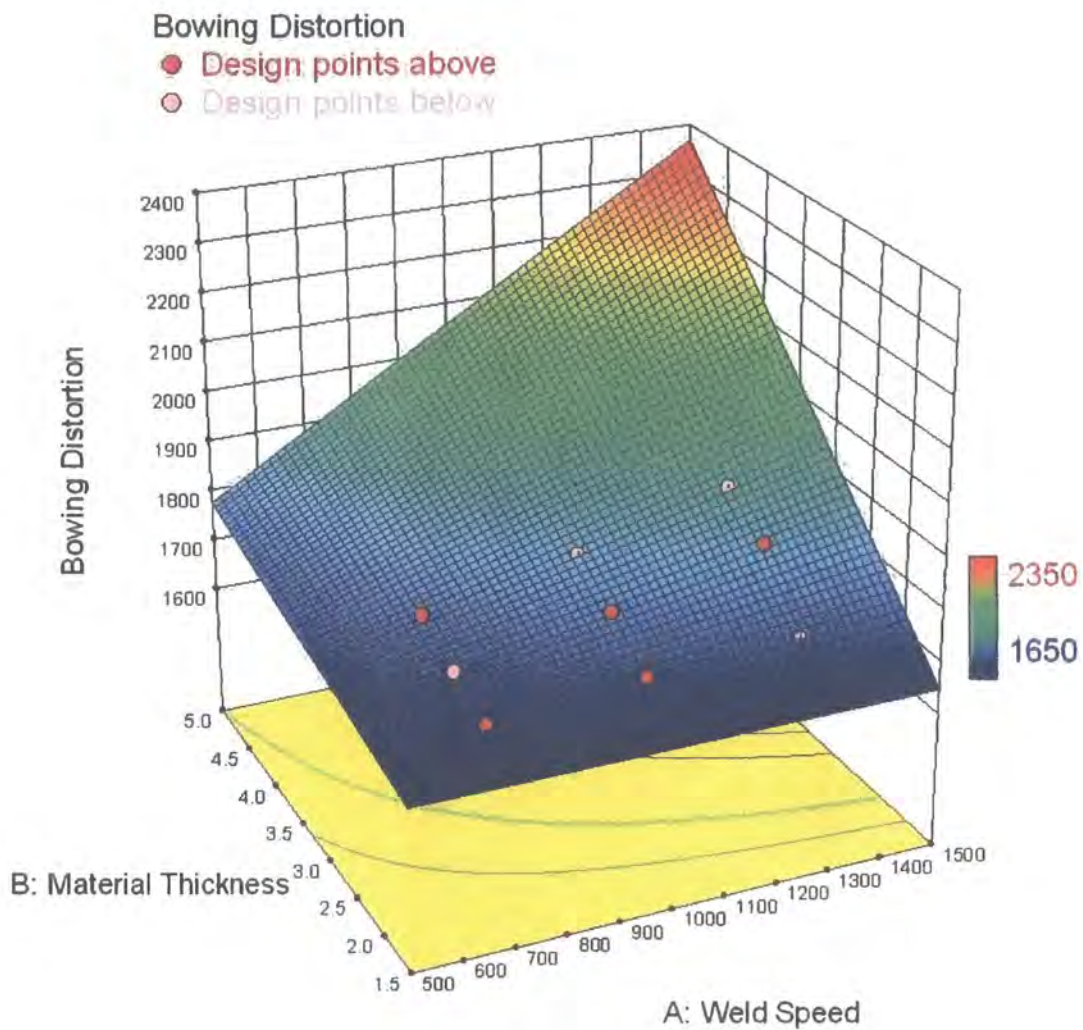
Figure 5.11: Best fit response surface for bowing distortion (bead on plate)

From the response surface then the equation characterising this is found to be:

R = 1722.16667 - 0.25417.v – 47.t + 0.16833.v.t   *(Equation 5.23)*

If the results from this equation are compared to the averaged experimental results then it is possible to determine if the equation is a good fit. Table 5.12 documents the results of this comparison. Generally from these results it can be seen that the equation gives a very good fit at these points with the maximum error being less than 1.5%, although generally the results can be seen to be in even better correlation with errors much lower than this.

Table 5.12: Comparison bowing distortion prediction to experimental data (bead on plate)

Weld Speed mm/min	Material Thickness mm	Experimental Result mm	Predicted Distortion mm	Variation Expt -v- pred mm	Error %
700	2.0	1686	1685.92	0.083	0.00%
	2.5	1720	1721.33	1.33	0.08%
	3.0	1762	1756.75	5.25	0.30%
1000	2.0	1711	1710.67	0.33	0.02%
	2.5	1773	1771.33	1.67	0.09%
	3.0	1822	1832.00	-10.00	-0.55%
1300	2.0	1722	1735.42	-13.42	-0.78%
	2.5	1847	1821.33	25.67	1.39%
	3.0	1899	1907.25	-8.25	-0.43%

Another way to represent the equation and response surface is as the 2D graph as shown in Figure 5.12 which provides a quick and easy way for a designer to predict the distortion given the material thickness and weld speed combination.

Using the approaches described equations have been derived for each of the distortions for the bead on plate samples. These equations are valid for the material and parameters of the case study company based on the experimental outcomes, and have been extrapolated to cover the companies typical design space. Therefore in the case study company for the chosen material, with thickness ranges from 1.5mm to 5.0mm and weld speeds ranging from 500 to 1500 mm/min then the following equations may be applied to predict distortion at the design stage for a bead on plate weld configuration:

Longitudinal distortion:

$$\delta_L = \frac{L.(3.05963 - 0.0027815.v - 0.5567.t + 0.0002.v.t + 7.40741e\text{-}7.v^2 + 0.046667.t^2)}{330}$$

(Equation 5.18a)

Transverse distortion:

$$\delta_T = 3.41778 - 0.00211944.v - 0.68.t + 0.000416667.v.t \qquad (Equation\ 5.21)$$

Angular distortion:

$$\beta_f = -4.78778 + 0.00919444.v + 5.46.t - 0.004333.v.t \qquad (Equation\ 5.22)$$

Bowing distortion:

$$R = 1722.16667 - 0.25417.v - 47.t + 0.16833.v.t \qquad (Equation\ 5.23)$$

175
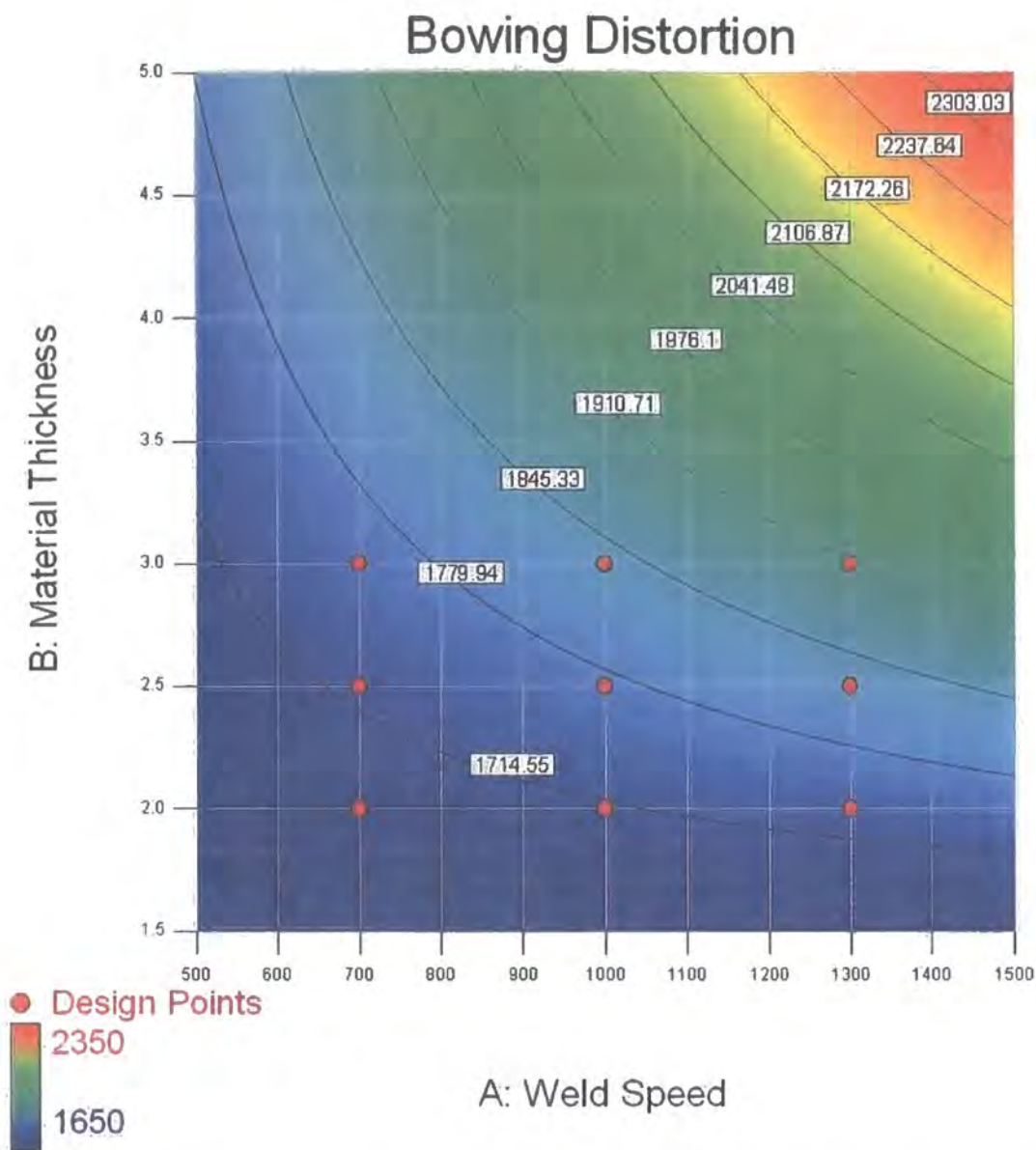
Bowing Distortion

Figure 5.12: 2D representation of the equation for bowing distortion (bead on plate)

5.3.2 Generating Equations for Butt Weld Samples

Following the same approach used for the bead on plate samples, the investigation to find equations for the butt weld design was carried out. The family of response curves were generated for each type of distortion for both varying material thickness and weld speed independently. The experimental space response surface was created for each set of results. However, the distortion responses did not have expressions that simply allowed the results to be expanded to fit the design space of the case

176

study company. The graphs from these investigations are presented in Appendix III for completeness, and excluded here for brevity.

Following the historical data fitting using the DoE analysis software then response surfaces were generated for each response and experimental outcome. The response surface generated for the longitudinal distortion extended to the design space of the case study company is shown in Figure 5.13.
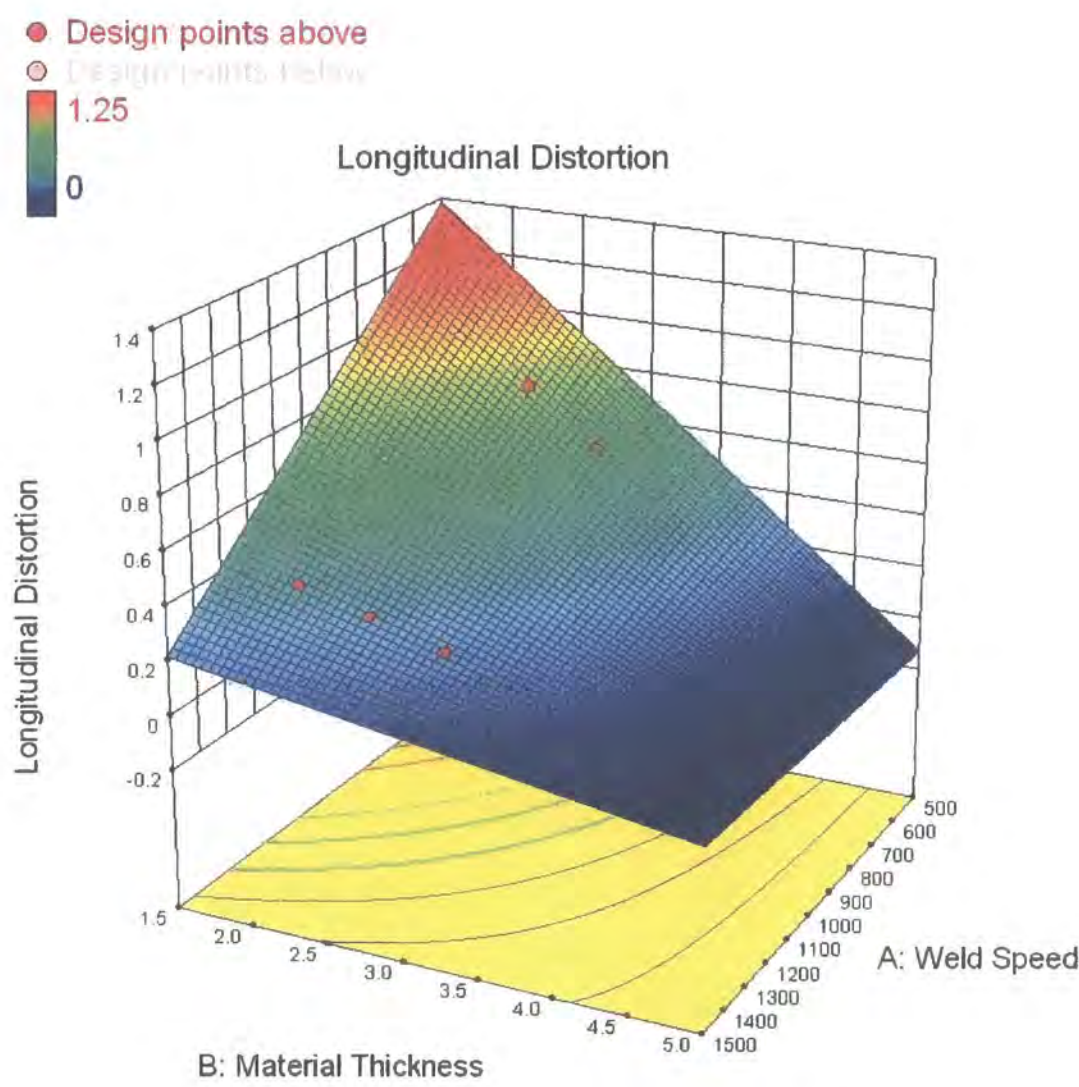
Figure 5.13: Best fit response surface for longitudinal distortion (butt weld)

From this response surface an expression was derived relating the longitudinal distortion to the material thickness and weld speed. This was then normalised to

allow for the effect of weld length and the following generalised equation developed:

$$\delta_L = \frac{L. \ (\ 2.87111 - 0.00168056.v - 0.60667.t + 0.00035.v.t\ )}{330}$$

<div align="right">(Equation 5.24)</div>

The values of the experimental data points were substituted into this equation in order to check its validity and fit to the data. The results for this comparison are presented in Table 5.13.

Table 5.13: Comparison of longitudinal distortion prediction to experimental data (butt weld)

Weld Speed mm/min	Material Thickness mm	Experimental Result mm	Predicted Distortion mm	Variation Expt -v- pred mm	Error %
	2.0	0.97	0.97	-0.0014	-0.14%
700	2.5	0.82	0.79	0.029	3.54%
	3.0	0.61	0.61	0.00028	0.05%
	2.0	0.66	0.68	-0.017	-2.58%
1000	2.5	0.53	0.55	-0.019	-3.58%
	3.0	0.4	0.42	-0.021	-5.25%
	2.0	0.39	0.38	0.0069	1.77%
1300	2.5	0.32	0.31	0.013	4.06%
	3.0	0.24	0.23	0.0086	3.58%

It can be seen that the expression is a good fit to the experimental data, with the maximum error being in the region of 5%. Several of the experimental points lie almost exactly on the response surface best fitted through the data. The equation generated takes a linear form with an expression for the combined effect of thickness and speed also. The response of this expression to the input factors is not dominated by any one particular term, with the values of the term for thickness effect, speed effect, and combined effect each having a similar influence on the resultant distortion value.

The equation can also be represented in a 2D graphical form with iso-contours as previously demonstrated with the other equations. It needs to be remembered in using the graphical format for longitudinal distortion as a quick reference tool, that

the value found from the graph needs to be normalised to account for the weld length, as described previously and included in the general form of the equation.
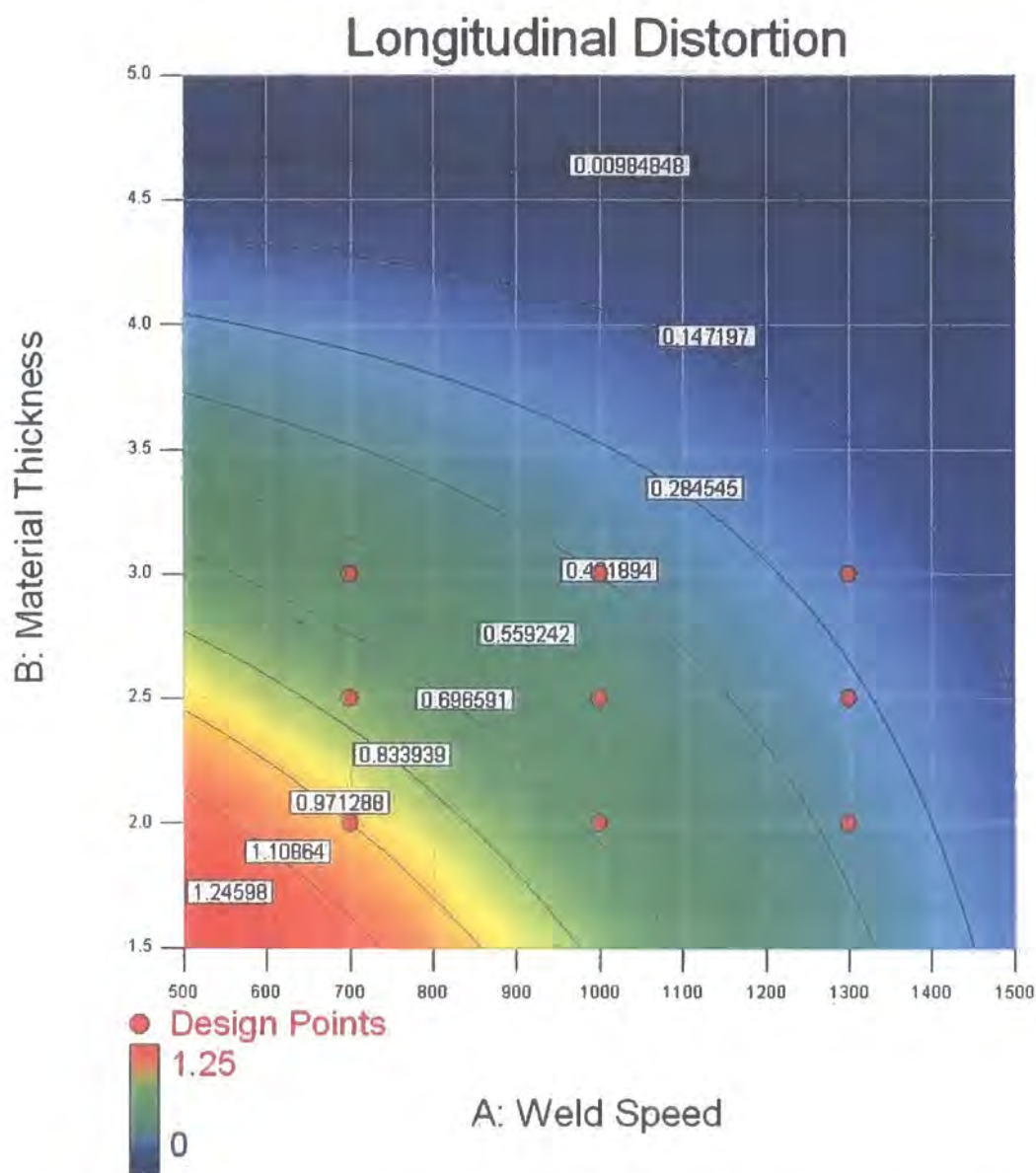
Figure 5.14: 2D representation of the equation for longitudinal distortion (butt weld)

The approach was then applied to the transverse distortion to generate the response surface based on the butt weld results shown in Figure 5.15. From the form of the response surface it can be seen that the resultant expression to characterise this will be a linear response based on each factor. The equation characterising this response surface was found to be:

$$\delta_T = 1.96056 - 0.0003944.v - 0.2633.t \qquad \text{(Equation 5.25)}$$
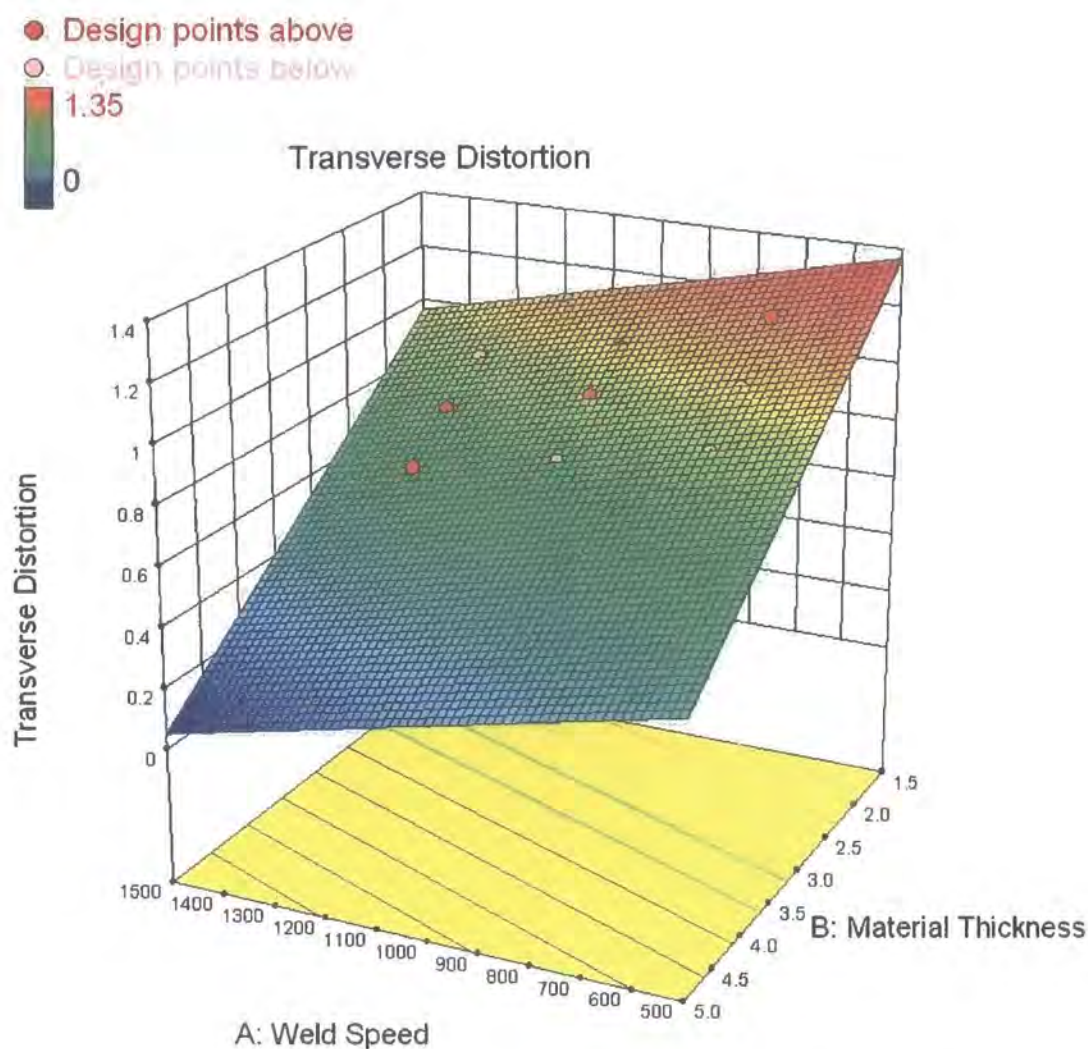
Figure 5.15: Best fit response surface for transverse distortion (butt weld)

Table 5.14: Comparison of transverse distortion prediction to experimental data (butt weld)

Weld Speed	Material Thickness	Experimental Result	Predicted Distortion	Variation Expt -v- pred	Error
mm/min	*mm*	*mm*	*mm*	*mm*	%
	2.0	1.19	1.16	0.032	2.69%
700	2.5	1.02	1.03	-0.0061	-0.60%
	3.0	0.88	0.89	-0.014	-1.59%
	2.0	1.01	1.04	-0.029	-2.87%
1000	2.5	0.92	0.91	0.012	1.30%
	3.0	0.77	0.78	-0.0061	-0.79%
	2.0	0.91	0.92	-0.011	-1.21%
1300	2.5	0.8	0.79	0.011	1.38%
	3.0	0.67	0.66	0.012	1.79%

180

The experimental values were once more substituted into this expression to assess the fit to the data. The results from this comparison are found in Table 5.14. This shows that the fit of the equation to the experimental results is very good. The maximum error is under 3%, although generally the results are even better than this. Also from studying the equation it can be seen that it is the term relating to thickness that has a more significant response on the overall distortion result.

The equation is again presented in its 2D graphical format for use by a designer as a quick reference guide, in Figure 5.16
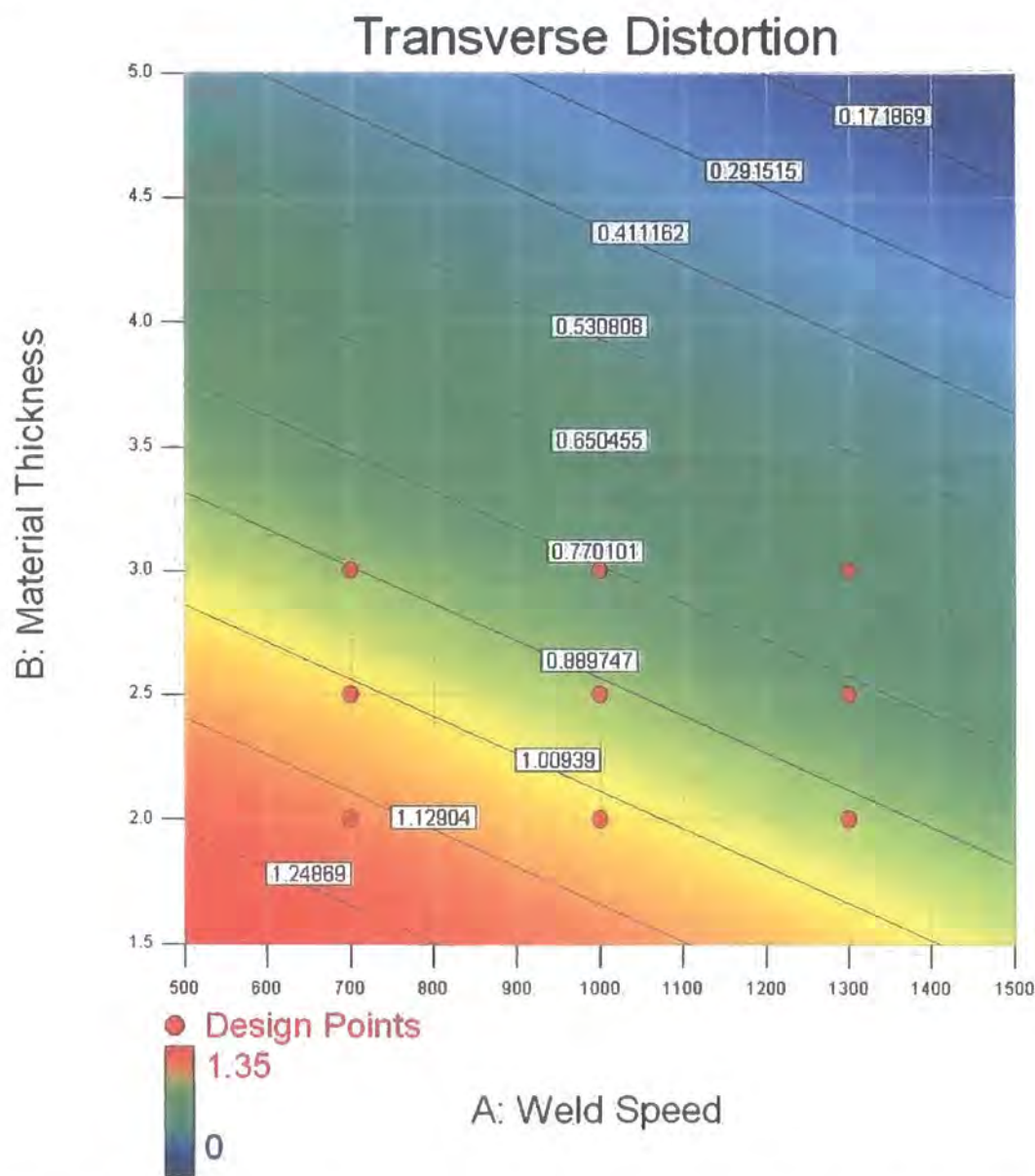
Figure 5.16: 2D representation of the equation for transverse distortion (butt weld)

The angular distortion was modelled in the same way based on the experimental results. However, in fitting the response surface to this data there was not a particularly good fit that gave the same level of correlation and significance as was found with the other expressions. The initial fit to the angular distortion resulted in the response surface shown in Figure 5.17.
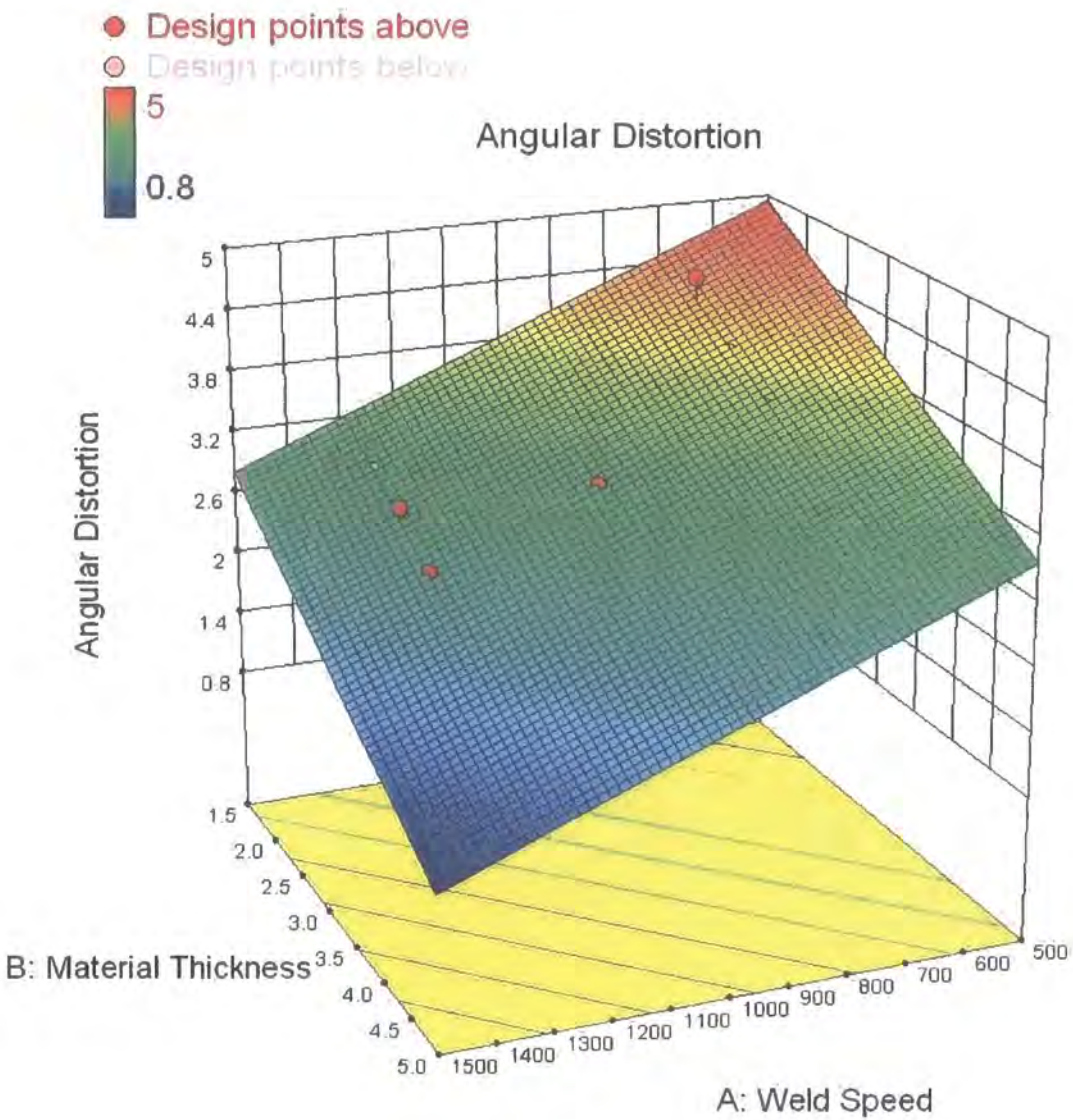
Figure 5.17: Best fit response surface for angular distortion (butt weld)

This generated a response surface based on a linear relationship of the two factors to the angular distortion. In order to attempt to find a better fit to the experimental data for the response surface then the outcome was subject to several mathematical transformations in order to see if this significantly effected the correlation of the

response surface to the experimental data. It was found from this exercise that the fit could be improved by applying a reciprocal transformation to the data, and then the best fit to this reciprocal of angular distortion was a linear expression. The resultant response surface relating the angular distortion, as a reciprocal, to the input factors of weld speed and material thickness is shown in Figure 5.18. The equation representing this response surface was found to be:

$$1 / \beta_f = 0.05113.t + 0.00019033.v - 0.012319 \qquad \textit{(Equation 5.26)}$$

This equation can be rewritten to give a direct expression for angular distortion as follows:

$$\beta_f = 1 / (0.05113.t + 0.00019033.v - 0.012319) \qquad \textit{(Equation 5.26a)}$$
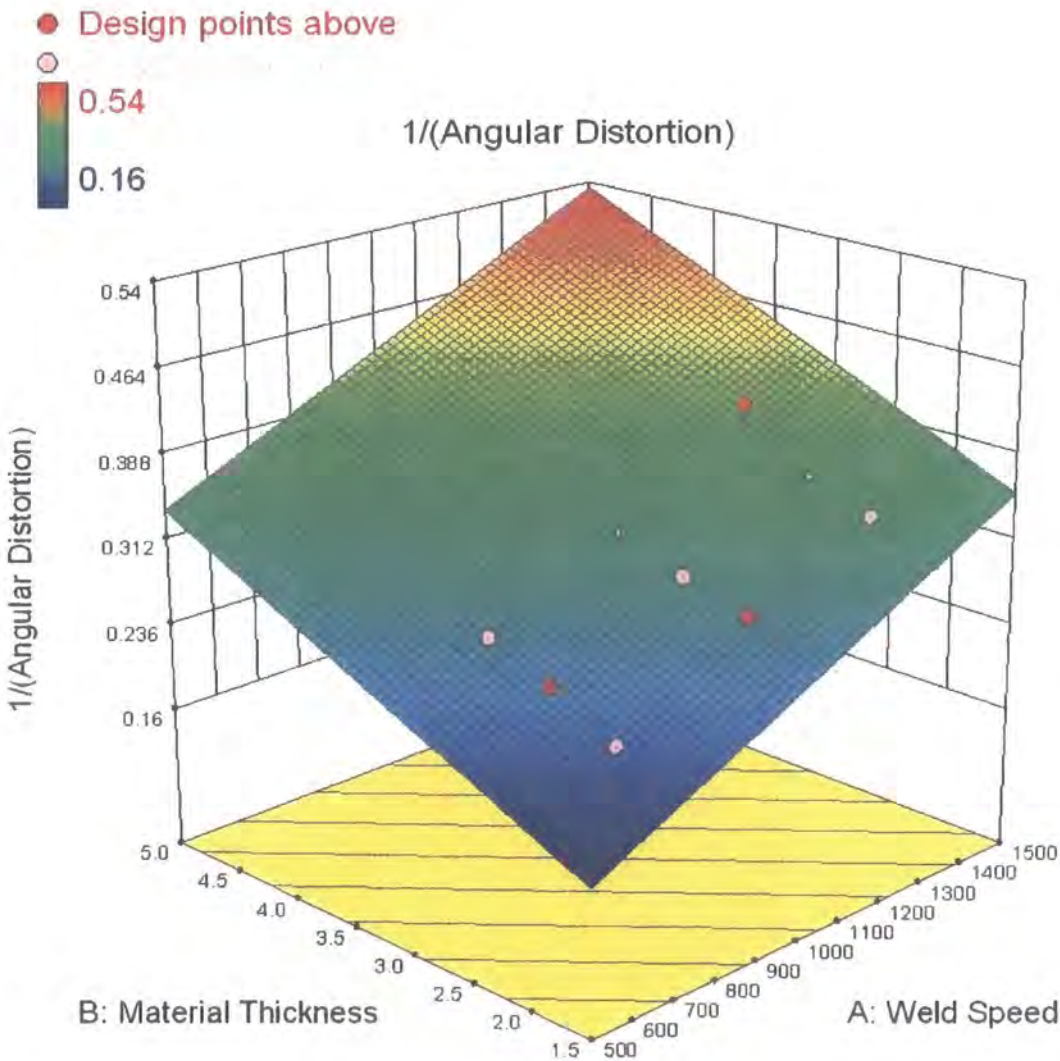
Figure 5.18: Best fit response surface for 1/angular distortion (butt weld)

183

Using the equation for the reciprocal of angular distortion, as shown in equation 5.26, then a comparison can be made for the fit of the experimental data to the prediction. The results for the comparison are shown in Table 5.15. It can be seen that the equation provides a good fit to the experimental data, with a maximum error of less than 4%, although generally the errors are much smaller than this maximum.

1/(Angular Distortion)
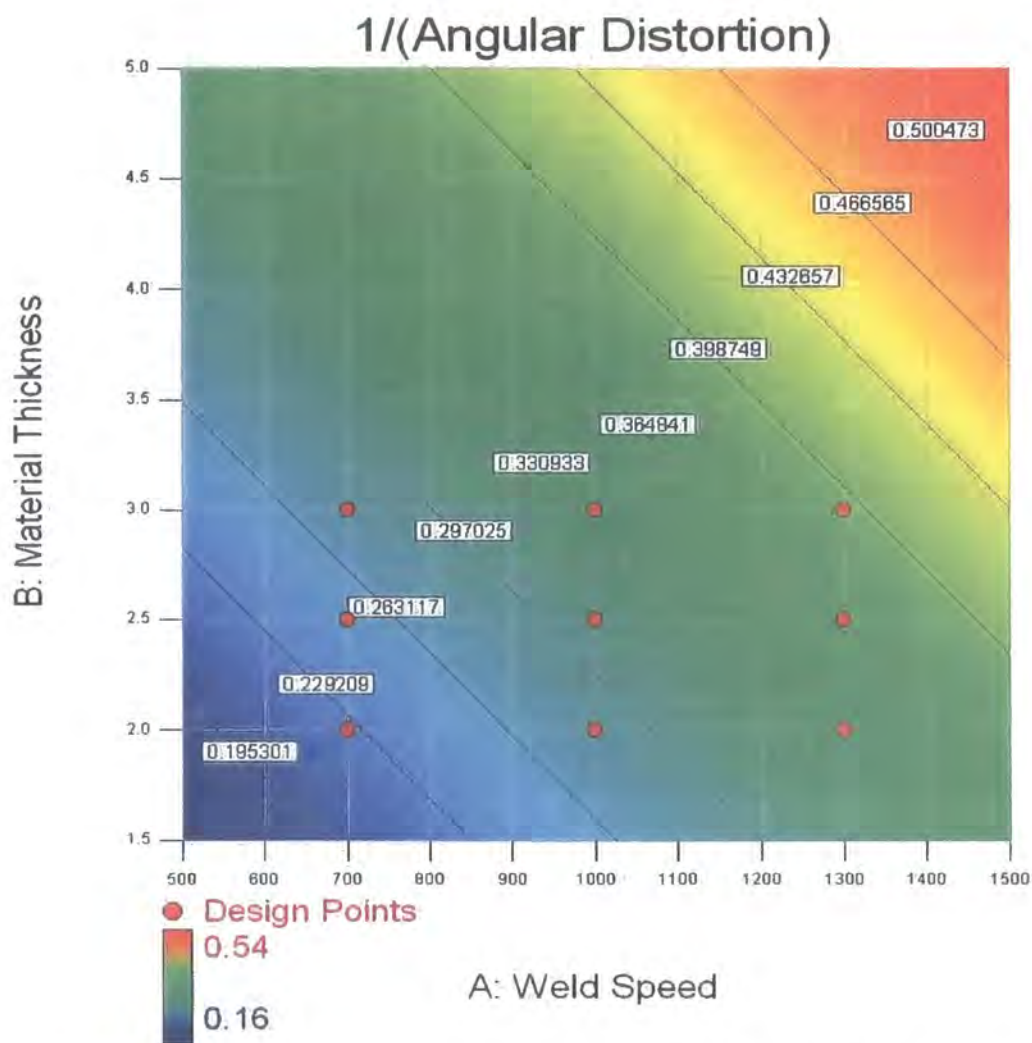
Figure 5.19: 2D representation of the equation for 1/angular distortion (butt weld)

Neither of the two factors dominates the expression more than the other in this form of the equation. This is more evident when the 2D graphical representation of the equation is looked at, as shown in Figure 5.19, where the iso-contours can be seen to run at almost 45 degrees. This form for representing the equation can be used as a quick reference tool for a designer to generate an approximate value for the

response, remembering that the answer is the reciprocal of the angular distortion, therefore needs to be transformed back.

Table 5.15: Comparison of angular prediction to experimental data (butt weld)

Weld Speed mm/min	Material Thickness mm	Transformed Experimental Result Degrees	Predicted Result Degrees	Variation Expt -v- pred Degrees	Error %
700	2.0	0.22	0.23	-0.0015	-0.68%
	2.5	0.25	0.25	0.0031	1.24%
	3.0	0.28	0.28	-0.00065	-0.23%
1000	2.0	0.29	0.28	0.0084	2.90%
	2.5	0.31	0.31	-0.0009	-0.29%
	3.0	0.33	0.34	-0.0094	-2.85%
1300	2.0	0.34	0.34	-0.002	-0.59%
	2.5	0.36	0.37	-0.012	-3.33%
	3.0	0.41	0.39	0.015	3.66%

The final distortion response to be analysed is the bowing distortion for the butt weld samples. It was found that a good fit to the experimental data could be obtained by using a quadratic form for the equation of the response surface. However this results in a complex expression, as was seen for the bead on plate longitudinal response, with equation 5.18. The graph for the response surface for the bowing distortion based on the quadratic fit is shown in Figure 5.20. In order to attempt to simply the expression then the use of mathematical transforms was considered. In this particular case the transforms produced a comparable level of fit to the data if the square root of the bowing distortion value was considered. The benefit this had was that it enabled the equation to be expressed in a far simpler form than the quadratic expression. The response surface based on the transformed response, using square root, is shown in Figure 5.21. The equation characterising this response surface can be shown to be:

$$\sqrt{R} = 21.09434.t + 0.02196.v - 20.24817 \qquad \textit{(Equation 5.27)}$$

This can be rewritten as follows to show the calculate the bowing distortion:

$$R = (21.09434.t + 0.02196.v - 20.24817)^2 \qquad \textit{(Equation 5.27a)}$$

185
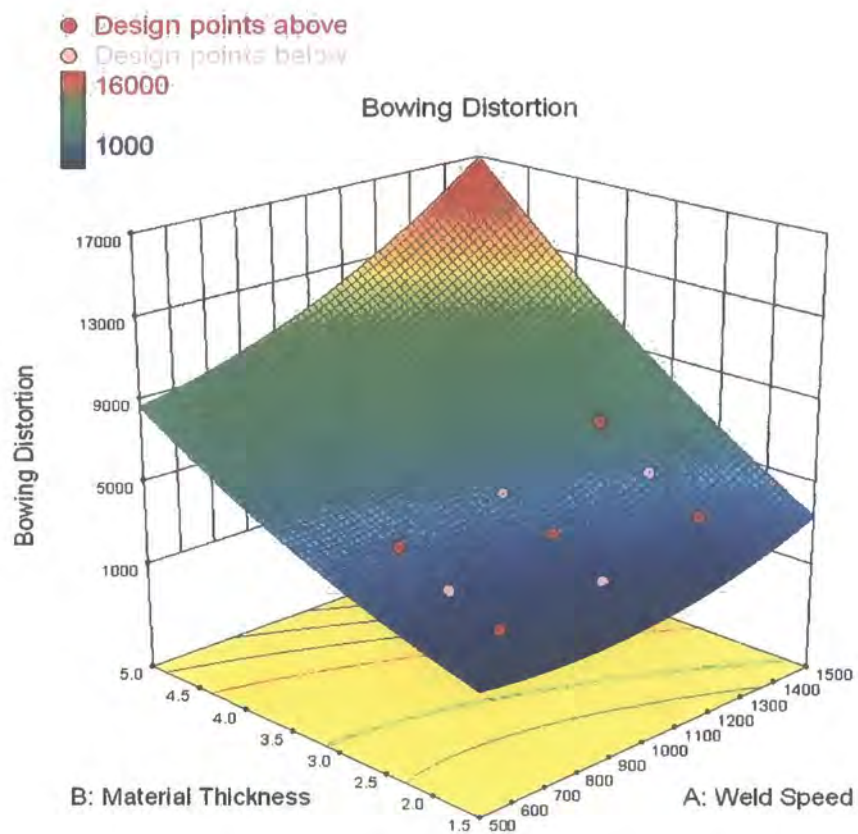
Figure 5.20: Best fit response surface for bowing distortion (butt weld)
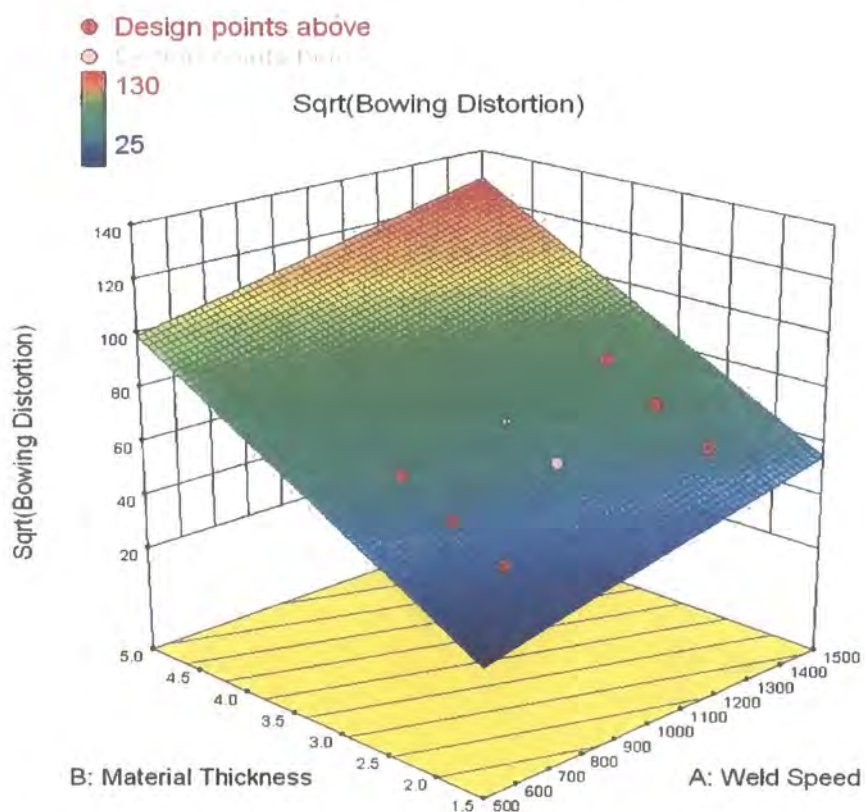
Figure 5.21: Best fit response surface - square root of bowing distortion (butt weld)

186

The values of the factors for the experimental results were substituted into the equation to generate predictions and allow a comparison to the actual experimental results to be made. The summary of this comparison is shown in Table 5.16. It can be seen that generally there is a very good fit of the equation to the experimental data, with 5 of the points being in the region of 1% error or less. The maximum error is seen to be just over 6%. From examining the equation then it is seen that the response is more sensitive to the factor of material thickness.

Table 5.16: Comparison of bowing distortion prediction to experimental data (butt weld)

Weld Speed mm/min	Material Thickness mm	Transformed Experimental Result Mm	Predicted Result mm	Variation Expt -v- pred mm	Error %
	2.0	44.34	42.38	1.96	4.42%
700	2.5	53.55	52.93	0.63	1.18%
	3.0	63.8	63.47	0.33	0.52%
	2.0	48.15	51.14	-2.99	-6.21%
1000	2.5	61.39	61.68	-0.29	-0.47%
	3.0	69.67	72.23	-2.56	-3.67%
	2.0	60.49	59.9	0.59	0.98%
1300	2.5	70.98	70.44	0.54	0.76%
	3.0	82.78	80.99	1.79	2.16%

The equation can again be represented in the 2D graphical form, for easy of use as a quick reference tool by a designer, however the transformation of the result must be remembered to be undertaken. This graph can be seen in Figure 5.22.

Having now considered all of the responses it can be seen that it is possible to generate equations that characterise the distortion responses over the case study company's design space based on the experimental results. Whilst these equations are best fit approximations, it has been shown that the errors arising from these equations all generally lie within acceptable limits for a prediction tool. The maximum error from the prediction equations to the butt weld results is just over 6%. Therefore in the case study company for the chosen material, with thickness ranges from 1.5mm to 5.0mm and weld speeds ranging from 500 to 1500 mm/min

then the following equations may be applied to predict distortion at the design stage for a butt weld configuration:

Longitudinal distortion:

$$\delta_L = \frac{L.\ (\ 2.87111 - 0.00168056.v - 0.60667.t + 0.00035.v.t\ )}{330}$$

(Equation 5.24)

Transverse distortion:

$$\delta_T = 1.96056 - 0.0003944.v - 0.2633.t$$

(Equation 5.25)

Angular distortion:

$$\beta_f = 1\ /\ (0.05113.t + 0.00019033.v - 0.012319)$$

(Equation 5.26a)

Bowing distortion:

$$R = (21.09434.t + 0.02196.v - 20.24817)^2$$

(Equation 5.27a)
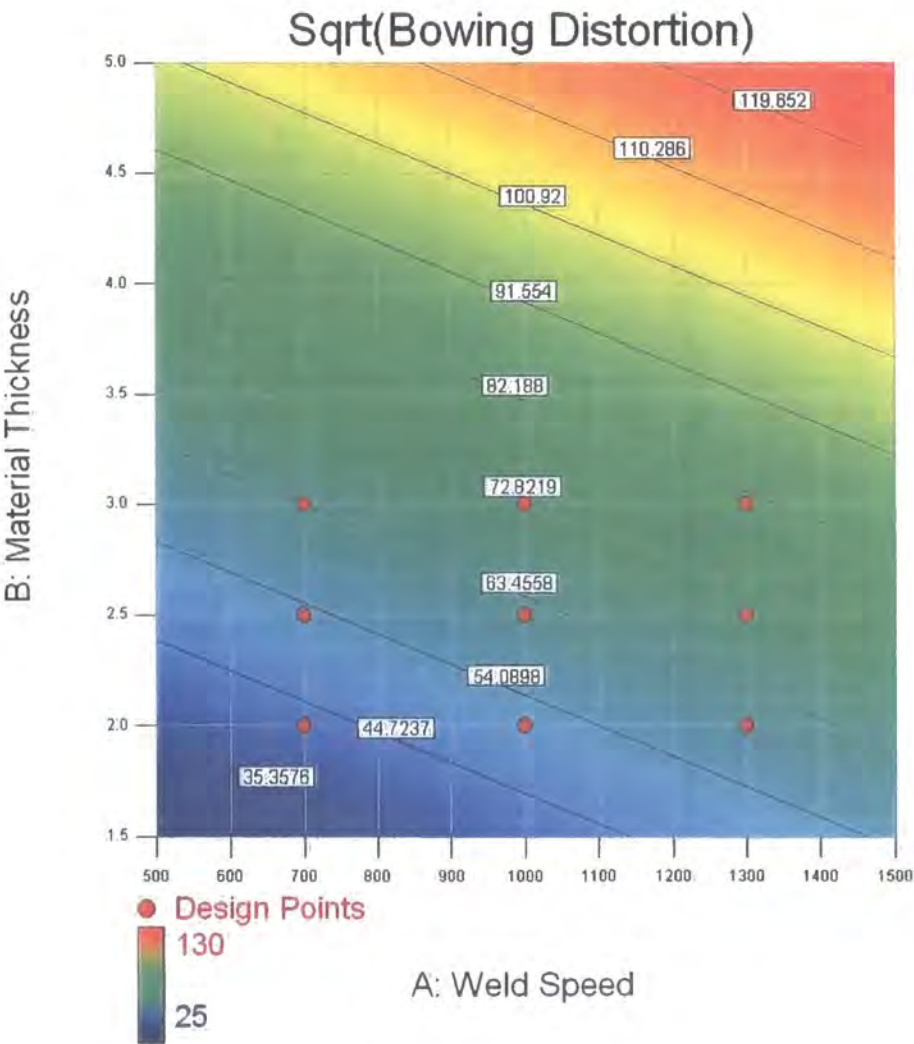
Figure 5.22: 2D representation of the bowing distortion equation (butt weld)

188

5.3.3 Example of Applying the Distortion Prediction to Design

Having generated equations to enable the prediction of weld distortion and discussed how to apply these then an example is presented to illustrate clearly the possible approach.

For the purpose of the example a butt weld joint design will be considered. This is a simple butt weld to be in keeping with the findings to date. Indicative values are chosen to lie within the design space of the case study company. Therefore in the example two plates are welded together, each plate having the dimension of 600mm long and 200mm wide, and being manufactured from 2.8mm thick XF350 material. It is also assumed that the plates will be welded together at 1200mm/min weld speed. The values chosen are specifically different for the experimental dimensions to illustrate how the equations can be applied to any combination of factors within the case study company's design space. The typical arrangement and layout for such a design can be seen in Figure 5.23 (a).

The designer will design the parts based on the nominal dimensions required for the finished product. This is the usual current design practice of the case study company. If these plates are then welded together using a butt weld the finished product will contain distortions. The typical shape that this welded product will finish up after processing can be seen in Figure 5.23(b). Here it can be seen that the product will exhibit all of the major distortion discussed in this project, and will be away from the nominal dimensions. If these distortions are too big and take the product out of tolerance then the process engineers will have to come up with methods of correcting the distortion. This could be by additional operations such as straightening or presetting of the parts. However, at this stage the process will have already had costs established and quoted to the customer for the automotive environment in which the case study company does business. Therefore the cost of additional operations will have to be carried by the manufacturer and not passed on to the customer. This will directly reduce any profit on this part. The bowing and angular distortions may be possible to correct by such simple methods, however if the length and width dimensions are critical then these will need to be corrected also.

It may be possible that sequencing the weld by breaking it into a series of smaller weld runs and spreading these out may reduce the overall distortion, but this will increase the cycle time, and therefore once more increase the manufacturing cost base. In addition this requires additional development after a facility is available and this has limitations on how much any process can be varied. This may therefore require additional capital investment to achieve the desired results. Capital investment will have to be recovered through being apportioned to the piece price. Again as this is already set by this stage then the increased investment will result in reduced profit.

If processing changes cannot control the longitudinal and transverse dimensions of the part to a low enough level to maintain the finished product within tolerance then the only other option is to modify the parts going into the process to compensate. As the case study company works in the high volume automotive sector, product volumes can be in hundreds of thousands of units, therefore all child components will be manufactured of tooling for cycle time considerations and repeatability. Therefore to modify the components to compensate for distortion by increasing their length or width in order to maintain or achieve end product tolerance will require tooling modifications. This has several effects: Firstly the tooling modifications will have to be paid for, which will have to be funded by the manufacturer. The tooling modifications will have a lead-time, which introduces the risk of delays. If these delays cause the supplier to fail to achieve a customer milestone then not only does this lead to customer dissatisfaction, but opens the possibility of penalty costs. In order to maintain production or even pre volume supply and ramp up, whilst the tools are modified, the supplier will have to manufacture additional panels from a prototype route to the new intended dimensions. As this is not the production route then this is again more costly, reducing project margins, but also it could jeopardise and affect maturation of the production processes and product, delaying customer sign off and acceptance, and therefore delaying final tooling payments. This is because it is common practice in the automotive business for the customer who may be paying for the tooling to hold back a significant value of the tooling order to only be release on produce sign of based on dimension and process performance.

(a) As designed

(b) Distorted shape if made as designed

(c) Design modified from predictions

(d) Final welded product on nominal
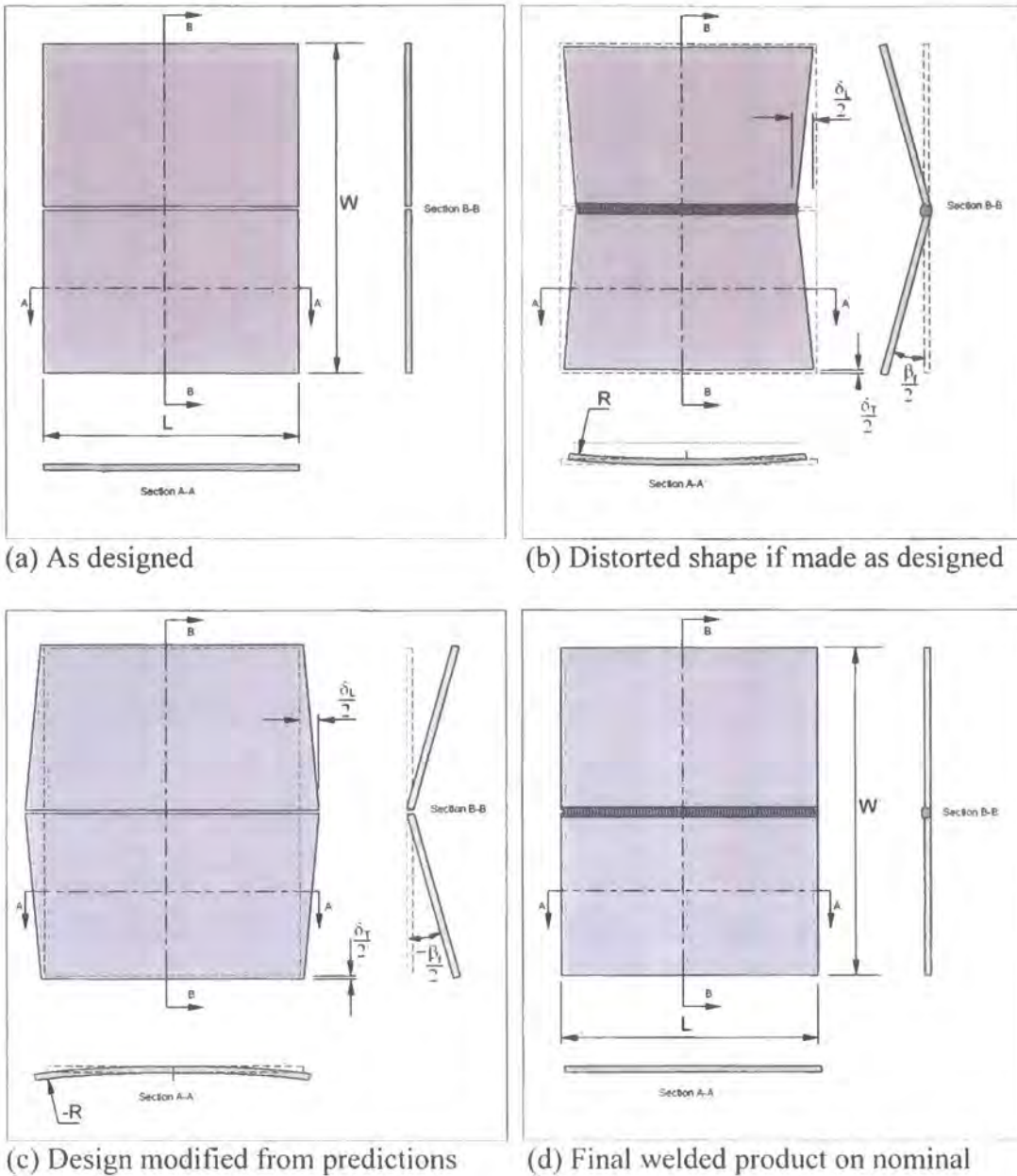
Figure 5.23: Distortion prediction applied to a butt weld design

Therefore, even in such a simple component, the possible impact from not considering distortion effects is high. Failing to do so presents the real prospect of increased costs, rework, and modifications all of which reduce the profitability of the product.

Having seen the possible implications of not making allowances and modifications at the design stage it illustrates the importance of the predicting distortion effects from the welding process in the design. This is because it happens before any

191

tooling or processes exist, and before costs have been quoted. Based on the dimensions of the plates to be welded, a designer can take these values and substitute these into the previously generated equations. Putting these values into equations 5.24, 5.25, 5.26a and 5.27a respectively then the following values can be calculated as follows:

$$\delta_L = \frac{600.\ (\ 2.87111 - 0.00168056.1200 - 0.60667.(2.8) + 0.00035.1200.(2.8)\ )}{330}$$

$$= 0.6032mm$$

$$\delta_T = 1.96056 - 0.0003944.1200 - 0.2633.(2.8)$$

$$= 0.75mm$$

$$\beta_f = 1\ /\ (0.05113.(2.8) + 0.00019033.1200 - 0.012319)$$

$$= 2.784°$$

$$R = (21.09434.(2.8) + 0.02196.1200 - 20.24817)^2$$

$$= 4247mm$$

Using the knowledge gained and discussed previously in this report, then these values can be used to adjust the dimensions and form of the component parts to allow for distortion. The longitudinal dimension of the plate needs to be increased by the 0.6mm calculated, and this should be applied as an increase in length at the edge that will be welded, the other edge dimension should remain at its initial length and the allowance applied equally to each end of the plate, i.e. half of the longitudinal shrinkage allowance applied to each end of the weld edge. For the transverse dimension then both plates should be increased in width by a value that is half of the 0.75mm transverse shrinkage allowance that has been calculated. The angular distortion may be allowed for by presetting the plates from the nominal position by half of the calculated angular distortion change, either side of the weld. This should be on the opposite side to the weld, and it would be possible to introduce this by designing the fixture to have this allowance. Finally the bowing distortion needs to be compensated for. This would have to be done by introducing the bowed form into the component plate. In order to do this an additional press tool would be needed, but as the costs have not been quoted this can be built into the overall product costs, if this is considered when the part is still in design. The bow

will be in the opposite direction to the side the weld is applied to the component. An illustration of the form these modifications would take to the pre welded components can be seen in Figure 5.23(c).

Having made these modifications the product can then be developed and produced with reduced risk to the profitability of such a component. In making a pre allowance for the distortion that is occurring from the welding process and using the specific derived equations to calculate the appropriate values of distortion, the product should deliver a manufactured result that will lie within tolerance and be in line with the nominal dimensions desired by the designer in the original design. This is illustrated as an example in Figure 5.23(d).

5.4 Improvements Based on Sources of Error and Variation

In the previous discussions in this chapter and Chapter 4, some of the potential sources of error and variation have been mentioned and investigated. However, in order to cover some further aspects that would offer scope for improvement to increase the experimental accuracy and speed of results processing then this section is included.

Previously, the problems associated with the initial scanning method, using a laser track ball have been discussed. This meant that the pre and post weld samples were measured using different methodologies. Clearly having welded the samples it is not possible to repeat the measurement of the pre weld scanning using the revised non-contact method. The initial measurement approach required significant fitting and manipulation of the sparse scan data, all of which is prone to error and approximations. This therefore means that the actual measured and calculated dimensions for the pre weld plates will not be as accurate as the post weld scans. Ideally both the pre and post weld plates should be measured using the same methodology, and by choice this would now be the non contact method for any future experiments of this nature. In the scanning process it is important to ensure the scan captures the edges of the plates fully and not just the top surface. Whilst

193

this was attempted in the post weld scans, some sections still did not capture the edge as clearly as may have been desired. Capturing the edge and top surface avoids any minor measurement errors if a point does not lie exactly on the edge of a plate.

An additional benefit that using non-contact scanning to generate point clouds for both the pre and post weld samples is that they can then be manipulated and analysed in the same post processing package. This would allow direct comparison of pre and post scans, which could be aligned to each other in the post processing software. To do this the areas of the scans around the datum tooling holes in the plates could be selected on both scans and aligned using a best fit alignment to orientate the scans together to each other. This would allow sections to be cut through both point clouds simultaneously and the distortion results then measured directly on the two clouds. This guarantees that the measurements taken are the actual difference, and not taken at two sections that may be slightly different position on each point cloud. Whilst this error is likely to be small the benefit it gives in speeding up post processing would be considerable, and provides a much more visual assessment of the results as they are generated.

In considering some aspects of the experiment then several other areas have been identified which would offer scope for improvement. When processing the pre-weld samples then there was significant variation seen in the dimensions between individual plates. In some individual plates the dimensions of length or width showed variation of approaching 0.5mm arising from the manual manufacturing processes used to produce the plates. This also showed itself as a variation over the family of plates used in the experiment to produce a range of plate dimensions that varied by over 2mm in overall distribution. This variation was again in part due to the manual preparation method of the sample plates and also the fact that the plates had to be produced in batches therefore slight variations in set up may have occurred during their manufacture. In order to reduce this variation then it would be prudent for future samples for any further experiments to be produced by using a blanking tool to press out the plates. An additional benefit is this would exactly represent the case study company's production process. Based on data from the case study company, the likely spread of dimensions would be greatly reduced to a very tight

and consistent distribution and individual plate dimension variation virtually eliminated. If a more consistent and accurate pre-weld plate could be produced then it may even be possible to eliminate the pre-weld measurement step, if the manufacturing process for the plates can be demonstrated to be repeatable, stable and capable.

The pre weld plates all had datum edges identified, and offset datum holes incorporated to provide fixture and orientation location, however there is still scope for manual error in loading the samples. The plates could still be loaded in 2 orientations if the edge orientation was not observed by the operator loading the fixture. Therefore a third tooling hole should be introduced to totally avoid any manual effect of incorrect orientation. It would be simple to introduce this into the welding fixture and plate samples.

A further improvement that could be made concerns the weld gap. The fixture was designed based on the case study company's practice of welding a gap of nominally 0.5mm dimension. This gap size is determined from the maximum gap size the weld wire and process will tolerate. It has been shown in the comparison to the published data that, especially for transverse shrinkage, the influence of the gap size contributes to the overall distortion result. Due to the tolerances from the manufacturing process for the plates and fixture, then the weld gap size used in the experiment may have varied. There was a clearance between the tooling location pins and the plate tooling holes to allow for these manufacturing tolerances; however this will have allowed some variation in weld gap size. Whilst tolerances can be improved by the use of more robust manufacturing processes for the sample plate production, some minor variation can never be eliminated. Therefore it would be useful to establish the exact weld gap for each sample joint welded to determine if this is influencing the result. To do this it is recommended that the gap size be gauged, probably using feeler gauges, at either end of the weld joint prior to the plates being welded.

The improvements to the overall set up would act not only to improve the measurement accuracy but to speed up the data processing. Due to the volume of

data generated, post processing was an extremely time consuming to process, requiring multiple steps, cross referencing, and calculation, all of which in themselves induces further scope for human error. Whilst the results have been thorough checked and reviewed, minimising the number of steps in this process, reduces the possibility of errors occurring in the first instance.

5.5 Conclusions and Summary

In this chapter the experimental results were reviewed in comparison to the published work. It was seen that generally at first sight the experimental results did not appear to agree with the published data and equations presented by other authors. This required further investigation and explanation, to gain a better understanding of the effects occurring in the experiments. It was seen that some of the difference between experimental and theoretical results could be accounted for due to the effect of the combination of the various distortions occurring together. These acted in a way to give measured results higher than would be predicted.

The longitudinal distortions were seen to be influenced by the value of bowing distortion which acted to increase the measured distortion. This effect was quantified and it was shown that it had a significant effect on the individual result. The transverse distortion was influenced by the angular distortion acting in combination with it. Again the values were calculated and the effect on the measured results was demonstrated. For the transverse distortion, it was still found that even having accounted the effects of angular change there was still discrepancy to the published equations. It was discussed that due to the welding set up of the case study company an additional influence on this mode of distortion was the weld gap size. The experiment was set up based on a nominal gap size, but the exact influence of this on the distortion outcomes could not be determined from the experiment as it was not set up as a process variable with the intention of doing so. However it could be stated that due to the differences to the published models, which are based on no weld gap assumptions, then the influence of a weld gap is to increase the transverse distortion. The angular distortions, which were found to be influenced by material

196

thickness, welding speed and penetration, gave generally poor agreement to the published equations. Finally the bowing distortion results showed there was good agreement on the butt weld samples to the published models from Okerbloms equation. However the agreement for bead on plate samples was not as specific to one particular model, although the trend seemed in line with the model of Horst Pflug at the thicker gauges and Blodgett at the thinnest material.

As there was a general discrepancy to the published data, in the main due to the combination effect of the distortions not being included in the published expressions, then it was necessary to attempt to develop some new models specific to the materials and process variables of the case study company. These models were developed with the design end user in mind to show overall factors to be included as design compensations. The final approach used to assess the overall experimental results in order to generate a response that could be characterised in an equation form was based on using DoE, and the Design Expert software tool by Stat-Ease was employed. Using this approach response surfaces for the experimental results were obtained which could then be varied in form to obtain a good fit to the data. Following this, from the best fit response, specific equations relating to the design space of the case study company were developed for each distortion type and for both bead on plate and butt weld joints. These equations were evaluated to check the validity across the range of the experiment and generally it was found that they could be used to approximate a distortion value that would be accurate within 6% or less based on the investigations undertaken in this project. The equations were also presented in a graphical form that a designer could quickly used to evaluate the effect, which would allow easy and rapid consideration without need to carry out detailed calculation. These could be assessed by a designer with very basic knowledge about a design and not requiring specific process information except an estimation of weld speed to be used. The equations for each joint type, specific to the case study company, are considered to be valid over a range of material thicknesses (t) based on XF350 material from 1.5mm to 5.0mm thick and weld speeds (v) from 500mm/min to 1500mm/min. These can be found as equations 5.18a, 5.21, 5.22 and 5.23 for the bead on plate weld, for longitudinal, transverse,

angular and bowing distortions respectively. Likewise equations 5.24, 5.25, 5.26a and 5.27a were correspondingly developed for the butt weld case.

Using the equations generated an example was given of how a simple butt weld design could be refined using knowledge of distortion effects at the design stages. This included discussion of the consequences for not taking such steps to illustrate the power and importance that such an approach can have. The combined effects of the distortions were evaluated by using the four equations for the weld and it was then discussed how to apply these in practice to the design. It was shown that if this is carried out then a designer can adjust the design of a component to allow for the effects of these distortions by incorporating an allowance for these into the design. The example showed how in doing this a post welded component could be designed at the outset to produce a product to nominal dimensions.

Finally a brief discussion summarised some of the findings from undertaking the experiment and analysis of the results that could be used in order to refine the process of carrying out similar experiments in future. This centred on consistent measurement methods and refinements to the manufacturing methods used in the plate preparation, with some changes to the experimental procedure.

Chapter 6: Conclusions and Future Work

.

6.1 Introduction

This chapter presents the main conclusions arising from the work undertaken in this project. The overall conclusions are discussed briefly and related to the intended aims of the project. The project, in summary, consisted of several major aspects including a review of published work relating to distortion prediction, the development and carrying out of an experiment to evaluate distortion specific to the typical process properties and arrangements of the case study company, the evaluation of the experimental outcomes against the existing published equations, before finally suggesting a method to predict distortion based on these results. Finally this chapter is concluded with a short discussion about areas of further work relating to this work.

6.2 Conclusions from the Investigation

This project was set up to investigate predicting weld distortions in the design phase of automotive components, and utilised experimental methods to establish these for some basic weld geometries and types. The experiment was carried out based on the variation of two factors, material thickness and weld speed. It was demonstrated that increasing either or both factors acted generally to reduce the overall distortion outcome.

The longitudinal distortion was shown to occur at a maximum at the weld centreline and this decreased as the transverse distance from the weld increased towards the edges of the plate. Transverse distortion was found to occur as a uniform shrinkage in the main body of the weld away from the start and stop effects, and it was also found to increase to this constant value quite quickly at the start of a weld and vice versa at the end. Therefore it is considered that careful programming of the weld speed to give a variable speed profile at the start and end of the weld, coming to the constant required speed in the body of the weld would likely result in a uniform transverse distortion along the whole weld length. The angular distortion was found be able to be approximated across the width of the component and varied little over

200

the length of the weld. Therefore a method to compensate for the angular distortion would be to introduce a preset angle opposite in direction, of the value of the angular change. The angular distortion was seen not only to be influenced by the weld speed and material thickness but also the level of penetration. The bowing distortion occurred consistently across plate and could therefore be accounted for by inducing a negative pre bend in the plate of the value the welding process induced in the flat plate.

In comparing the distortions to the predicted values based on published equations it was found the equations generally were under predicting when compared to the measured results from the experiment. However further study indicated that when the combination effect of the distortions was accounted for then the values measured were more in line with the published models. The distortion effects do not occur in isolation and therefore in order for a designer to understand the real effect on a component and adjust correctly for this it is the combined distortion value that should be calculated. Particularly good agreement was seen to the model of Okerblom for bowing distortion in the bead on plate samples manufactured in the experiment.

In studying the results it was possible to see that there was a relationship between the variables of the experiment and the distortion values, however it was not one that could simply be extracted and used as valid across a full range of inputs without careful consideration. By limiting the range of application to the design space of the case study company for the variables, some relationships between the experimental variables and distortions were drawn by using the DoE tool Design Expert. Equations have been generated relating the combined distortion effect values to give results for longitudinal, transverse, angular and bowing distortion. These are based on the parameters of material thickness and weld speed, and separate equations for both bead on plate and butt joint welds generated. Using these equations a designer can determine the overall distortion and decide if the design needs to be changed accordingly to compensate. An alternative format for these equations was presented based on a 2D graphical format with iso-contours that could be used to quickly

determine an approximate distortion value rather than having to calculate the results from an equation.

It has therefore been shown that it is possible to make simple reliable predictions of distortion outcomes, before a product ever exists, to evaluate these effects in the design phase. However further work will be needed to broaden and generalise the approach and allow it to be used in complex real geometries based on multiple weld joints.

6.3 Recommendations for Future Work

Having demonstrated that the approach could derive equations for simple joint types then recommendations for further work to build upon these foundations can be made.

In conducting the experimental part of this project only bead on plate and butt welds sample had to be considered due to the volume of data generated. However clearly there are many more joint types in practical terms than those considered in this initial investigation. Having established the validity of the approach then it would be useful to extend the study to investigate other basic joint types. Indeed the basic set up and work has already been carried out to examine the same effects on tee joint samples. Additional joint types that could be investigated include overlap joints and tee joints that have a flanged edge which is welded. These are both commonly used in the case study company.

Having established the results for basic joints based on the plate sizes used in this experiment then it would be useful to validate if there is a size effect by increasing and decreasing both the length and the width of the plates used for the experiment. In addition, as already highlighted previously in the discussion of the results then it would be interesting to evaluate and quantify the effect of the weld gap.

Extensive experimentation is both time consuming and expensive. In addition the combination of multiple joints has not yet been considered. Therefore, having established a thorough knowledge base of distortion results then it would be beneficial to utilise computer aided simulation approaches to maximise the benefit of the studies. A next step would be to develop a CAE model that replicates the basic experiment and develop this to generate correlation to the experimental results. When a model has been generated to correlate the experimental results it can then be used with higher degree of confidence to predict the distortions occurring in other simple joint arrangements. Combining CAE with DoE provides a powerful tool to examine large design problems and build up a wider range of results than would be possible by experimentation alone. Once a comprehensive database of distortion results is available, these can be used with there corresponding equations to produce simple models and simulations. This data could then be used with an approach based on finite elements to code expressions to specific weld joints. If this can be done then more complex geometrical assemblies can be studied, and these can be validated to produce confidence in the method. If this provides good correlation then it would form the basis of a general and quick method for evaluating the influence of distortion at the design stage. Also if it is quick to use then the effects of changes made to overcome distortion problems can be evaluated also. This would not be dissimilar to approaches being used by other researchers such as volume shrinkage methods; however it would be based on developing specific elements coded to the equations of distortion for the case study company.

A more long term direction if the above approach could be validated would be to combine the distortion prediction tool with optimisation software to look at the sequential build up of the weld distortion and to attempt through weld sequence optimisation to reduce the distortion to a minimum.

References and Bibliography

References and Bibliography

AWS A5.18/A5.18M:2005, Specification for Carbon Steel Electrodes and Rods for Gas Shielded Arc Welding.

Bachorski A, Painter M J, Smailes A.J, and Wahab M.A, 1999, "Finite-element prediction of distortion during gas metal arc welding using the shrinkage volume approach", Journal of Materials Processing Technology 92-93 (1999) 405-409.

Berthet P, Gerbeaux H, Piette M and Renault J-P, 1988, "Deformations et contraintes en soudage", Institut de Soudure, Paris.

Blodgett O.W, 1966, "Design of welded structures". Cleveland, OH, USA: James F. Lincoln Arc Welding Foundation.

Brickstad B, and Josefson B.L, 1998, "A parametric study of residual stresses in multi-pass butt-welded stainless steel pipes", International Journal of pressure Vessels and Piping 75 (1998) 11-25.

BS EN 10002-1:2001 Metallic Materials - Tensile Testing - Part 1: Method of Test at Ambient Temperature.

BS EN 288-3: 2001, Now Withdrawn, Specification and Approval of Welding Procedures for Metallic Materials Part 3: Welding Procedure Tests for the Arc Welding of Steels-CORR 10026; June 1998; Supersedes BS 4870: Part 1: 1981; Superseded by BS EN ISO 15614-1:2004.

BS EN 439:1994 Welding Consumables - Shielding Gases for Arc Welding and Cutting (F).

Deo M.V, and Michaleris P, 2002, "Experimental Verification of Distortion Analysis of Welded Stiffeners" Journal of ship Production, 18(4):215-225.

Fujita Y, Nomoto T, and Matsui S, 1978, "Prevention of Welding Deformation in Thin-Skin Welded Structures.2, Criteria for Preventing Service Failure in Welded Structures; Tokyo; Japan; 26-28 Sept. 1978. pp. 355-360.

Gatovskii K.M, 1973, "Determination of welding stresses and strain with allowance for structural transformations of the metal", Welding Production (English translation of Svarochnoe Proizvodstvo), v 20, N 11.

Gatovskii K.M, and Karkhin V.A, 1980, "Theory of welding stresses and deformations", Leningrad Shipbuilding Institute, Russian (translated).

Gilde J, 1958, "Transverse weld shrinkage", The Welding Journal, Welding research supplement, pp48s Feb 1958.

Goldak J, Bibby M, Moore J, House R, and Patel B, 1986, "Computer modelling of heat flow in welds", Metall Trans 17B (1986) 587-600.

Goldak J, Chakravarti A, and Bibby M, 1984, "A new finite element model for welding heat sources", Metall Trans 15B (1984) 299-305.

Gourd, L.M, 1995, "Principles of welding technology" 3rd edition, London: Edward Arnold, 1995, pbk. ISBN 0340613998.

Gray T.G.F, Spence J, and North T.H, 1975, "Prediction and control of distortion", Rational Welding Design, London Butterworth, ISBN 0-408-70584-1, pp 45-70.

Guan Q, Leggatt R.H, and Brown K.W, 1988, "Low stress non-distortion (LSND) TIG welding of thin-walled structural elements", Industrial Members Report No. 374 - July 1988; The Welding Institute.

Guiaux, 1962, Revue de la Soudure nr 1, Universite de Liege.

Gunnert R, 1955, "Residual welding stress", Almqvist & Wiksell, Stockholm.

Guyot F, 1947, "A Note on the Shrinkage and Distortion of Welded Joints" The Welding Journal, 26 (9), pp 519s-529s.

Hansen B, 1973, "Formulas for residual welding stresses and distortions", Svejsecentralen, Copenhagen.

Hibbitt H, and Marcal P, 1973, "A numerical thermo-mechanical model for the welding and subsequent loading of a fabricated structure", Computers and Structures, 3(5): 1145–1174.

Hicks J.G., Welded joint design. 3rd edition. Abington; Abington Publishing, 1999. ISBN 1 85573 386 2.

Horst Pflug, 1956, "Welding distortions, especially by deep penetration electrodes". Schweisen und Schneiden, (8), heft 4, pp15-122.

Houldcroft P, and John R, 1988, "Welding and Cutting", 1988, Woodhead-Faulkner Ltd.

Iwamura Y, 1974, "Reduction of transverse shrinkage in aluminium butt welds", M.Sc. Thesis, M.I.T., May 1974

Kihara H, and Masubuchi K, 1956, "Studies on the shrinkage and residual welding stress of constrained fundamental joint.", Report No. 24, Transportation Technical Research Institute, No. 7.

Lancaster J, 1992, Handbook of structural welding. Processes, materials and methods used in the welding of major structures, pipelines and process plant. Abington; Abington Publishing, 1992. ISBN 1 85573 029 4.

Leggatt R.H, 1980, "Distortion in welded steel plates", Ph.D. Thesis, Magdalene College, Cambridge UK, July 1980.

Mamlin G.A, 1976, "Preparation for construction of steel bridges", Moscow,1976. Mashgiz, Moscow, Dept of Scientific and Industrial Research, London Translation from Russian.

Masubuchi K, 1980, "Analysis of welded structures. Residual stresses, distortion and their consequences", Oxford: Pergamon Press, ISBN 0 08 022714 7.

Michaleris P, and DeBiccari A, 1997, " Prediction of Welding Distortion.", Welding Journal, 76(4):172–180.

MIG/MAG Welding Guide, 1997, The Aluminium Association, November 1997.

Mishler, H.W, 1989, "Analysis of distortion in gas tungsten arc welds", Edison Welding Institute Research Brief series b8904.

Naka T, 1950, "Shrinkage and Cracking in Welds", Tokyo: Komine Publishing Co.

Narayan K, Shangari S, and Chadda S.K, 1983, "distortion control and tilt correction during welding of nozzles on calandria: a large cylindrical shell of austentic stainless steel", Proceeding of National Welding Seminar, Indian Institute odf Welding, New Delhi, India, paper 3, Nov. 10-12 1983.

Okerblom N.O,1955, "The calculations of deformation of welded metal structures",

Rocchini C, Cignoni P, Montani C, Pingi P, & Scopigno R, 2001, "A low cost 3D scanner based on structured light", Computer Graphics Forum 20 (3), 299-308.

Sasayama T, Masubuchi K, and Moriguchi S, "Longitudinal deformation of a long beam due to fillet welding", Welding Journal, 34-12 (1955), 581s-582s.

Smailes A.J, Wahab M.A, and Painter M.J, 1995, "Finite element prediction of the thermal response of v-joint gas metal arc welds", in: A J Beasley, C G Foster, E S Melerski (Eds), Proc 14th Australasi Conf on the Mechanics of Structures and

Materials, Vol 1, University of Tasmania, Hobart, 11-13 December 1995, pp 319-324.

Taylor G.A, Hughes M, Strusevich N, and Pericleous K, 2002, "Finite volume methods applied to the computational modelling of welding phenomena", Applied Mathematical Modelling 26 (2002) 309-320.

Tsai C.L, Park S.C, and Cheng W.T, 1999, "Welding Distortion of a Thin-Plate Panel Structure", A.W.S. Welding Journal, Research Supplement, 78:156s–165s, 1999.

Tsirkas S.A, Papanikos P, and Kermanidis T, 2003, Numerical simulation of the laser welding process in butt-joint specimens, Journal of Materials Processing Technology 134 (2003) 59-69.

Vergeest J.S.M, and Horváth I, 2000, Delft University of Technology, "3D Object Scanning to Support Computer-Aided Conceptual Design", MicroCad, 2000.

Verhaeghe G, 1998, "Predictive formulae for weld distortion - a critical review" Industrial Members Report No. 641 - June 1998; The Welding Institute.

Vinokurov V.A, 1977, "Welding stresses and distortion", Wetherby: British Library, (Original: Svarochnie deformatsii i napryazjeniya: metodi ikh ustraneniya. Moscow: Mashinostroenie 1968)

Watanabe M, and Satoh K, 1961, "Effect of welding conditions on the shrinkage and distortion in welded structures", Welding Journal 40(8): 377-s to 384-s.

Welding handbook. - Vol. 2 : "Welding processes - arc and gas welding and cutting, brazing and soldering", Miami ; London : American Welding Society.

Welding Technology Fundamentals, American Welding Society 1994, also American Welding Society Website at www.aws.com.

Wells A.A, 1952, "Heat Flow in Welding", Welding Journal, 31, pp263s-267s.

White J.D, Leggatt R.H, and Dwight J.B, 1980, "Weld Shrinkage Prediction", Welding and Metal Fabrication, pp 587-596.

Zhu X.K, and Chao Y.J, 2002, "Effects of temperature-dependent material properties on welding simulation", Computers and Structures, Vol 80 No 11 (2002) pp 967-976.

Appendices

Appendix I – Weld Macro Study

Weld dimensional study

Position along weld (in mm)	50	100	150	200	250	300	Reference diagrams (see also Figure 3.1 - weld section nomenclature):
Bead on plate (ref plate samples 2.0mm plates 41 @ 700mm/min)							
W	6.4	5.9	5.9	6.2	5.9	5.5	
H	1.7	1.5	1.5	2	1.7	2.1	
P	0.9	1	0.7	0.7	1.1	2.1	
XSA	5.4	4.8	4.5	5.6	6.2	7.2	
Butt weld (ref plate samples 2.5mm plates 1/1A @ 700mm/min)							
W	7.2	7.1	6.8	7	7.2	6.3	
H	2.3	2.4	2.2	2.3	2.3	2.9	
P	2.6	2.6	2.6	2.6	2.6	2.6	
Gap	0	0	0	0	0	0	
XSA	10.6	10.7	10	9.8	11.8	15.3	
Tee weld (ref plate samples 2.5mm plates 15/15A @ 1000mm/min)							
Throat	3.3	3.2	3	3	2.9	2.5	
Leg A	3.8	3.7	3.3	3.4	3.1	2.9	
Leg B	4.2	4	4.2	4.3	4.7	5.3*	
Pen A	0.5	0.4	0.6	0.4	0.2	0.2	
Pen B	0.7	0.8	0.5	0.7	0.9	0.8	
Gap	0	0	0	0	0	0	
XSA	7.5	7.3	7.2	7.4	7.1	7	

* undercut 0.14mm

Hardness survey

Method = Vickers micro-hardness, 300g load
Readings taken at 0.5mm intervals

Study undertaken at mid position of weld runs: @150mm section cut

Bead on plate			
2.0mm plates 41 @ 700mm/min			Micrograph for hardness indent positions
Positon	Description	Micro Hardnesss	
1	Weld	235	
2	Weld	219	
3	Weld	216	
4	Weld	212	
5	Haz	176	
6	Parent	162	
7	Parent	171	
8	Parent	157	
9	Parent	162	
10	Parent	158	
11	Parent	161	
12	Parent	156	

Butt			
2.5mm plates 1/1A @ 700mm/min			Micrograph for hardness indent positions
Positon	Description	Micro Hardnesss	
1	Weld	222	
2	Weld	224	
3	FL	121	
4	Haz	189	
5	Haz	181	
6	Haz	173	
7	Haz	170	
8	Parent	164	
9	Parent	161	
10	Parent	169	
11	Parent	173	
12	Parent	174	
13	Parent	168	
14	Parent	169	

Tee Fillet weld			
2.5mm plates 15/15A @ 1000mm/min			Micrograph for hardness indent positions
Positon	Description	Micro Hardnesss	
1	Weld	254	
2	Weld	270	
3	Weld	256	
4	Haz	188	
5	Haz	178	
6	Parent	170	
7	Parent	178	
8	Parent	172	
9	Parent	177	

Weld Macro Graphs - Bead on Plate

Bead on plate (Ref plate sample 2.0mm plate 41 @ 700mm/min)

50mm along weld

100mm along weld

Predicting Weld Distortion in the Design of Automotive Components
Roger O'Brien, MSc Thesis, March2007
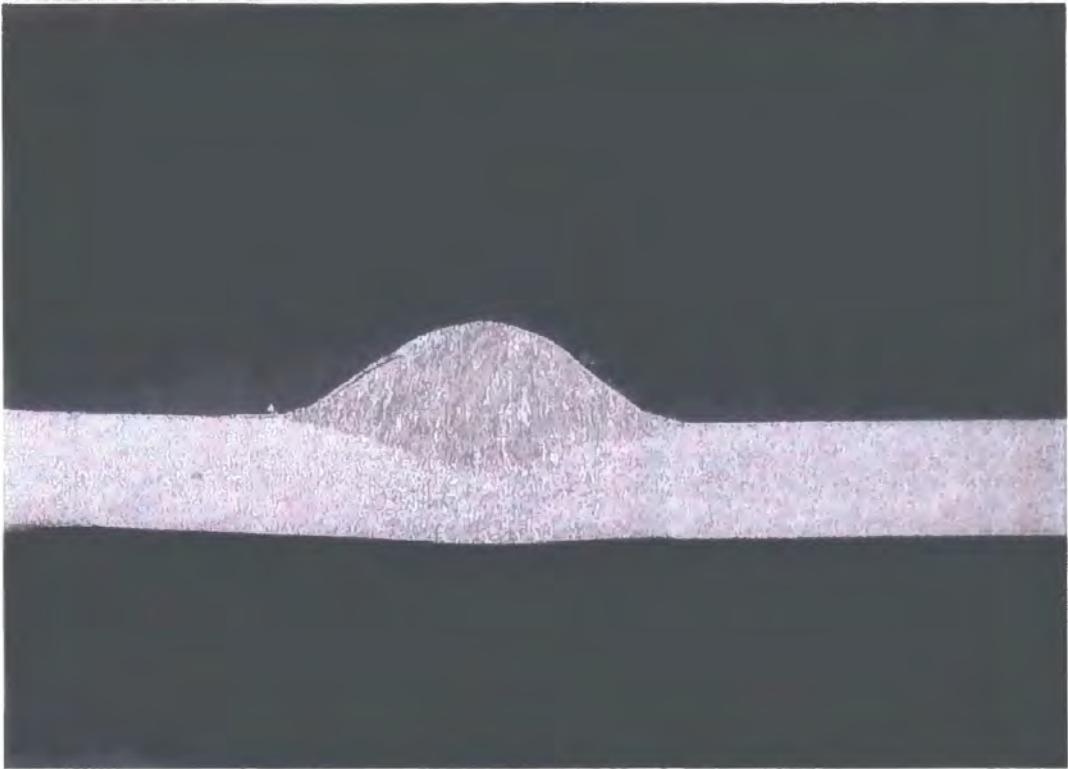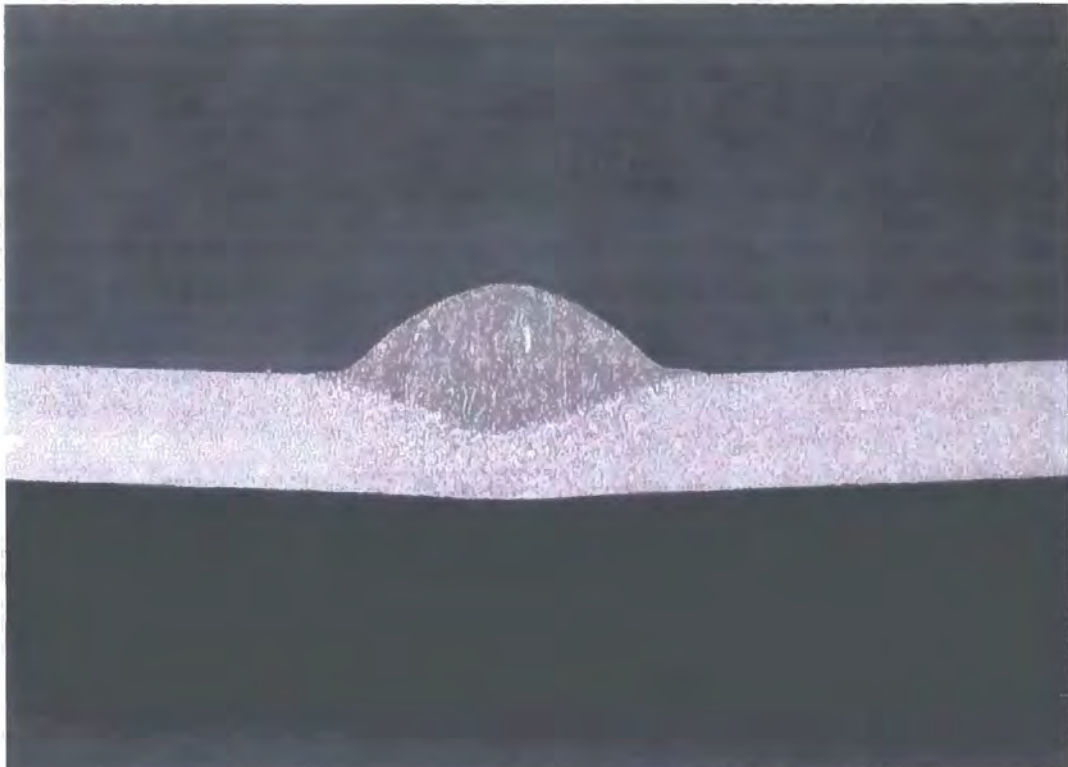
Bead on plate (Ref plate sample 2.0mm plate 41 @ 700mm/min)

150mm along weld

200mm along weld

Predicting Weld Distortion in the Design of Automotive Components
Roger O'Brien, MSc Thesis, March2007
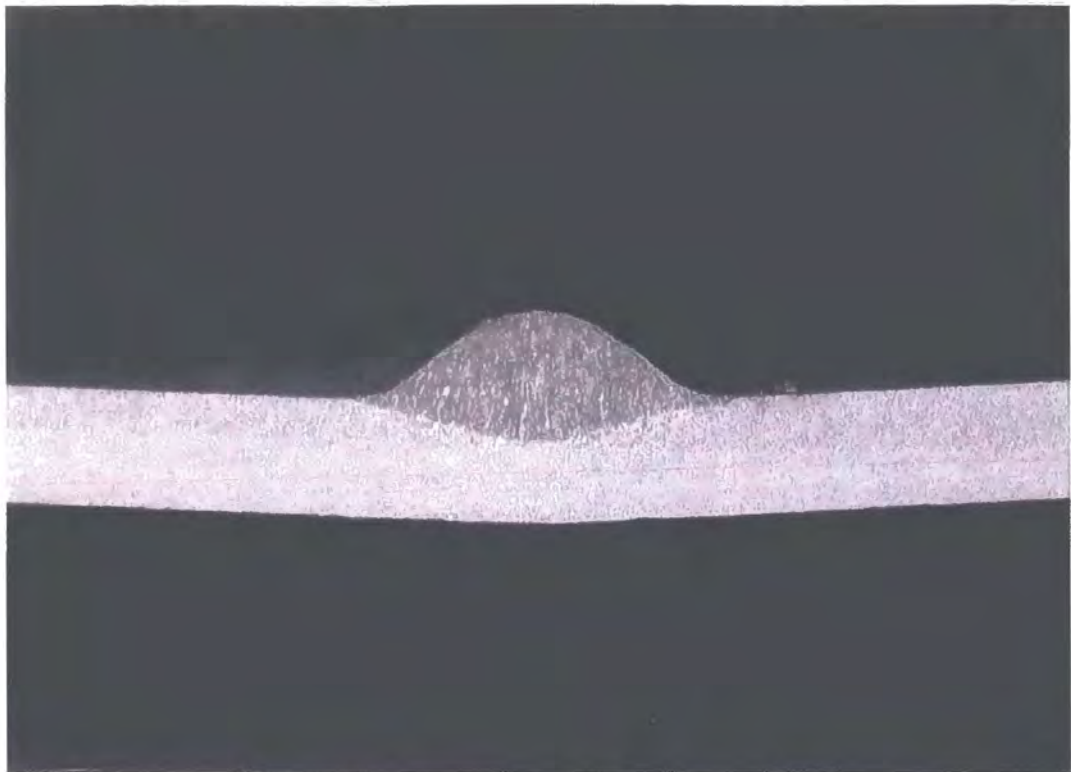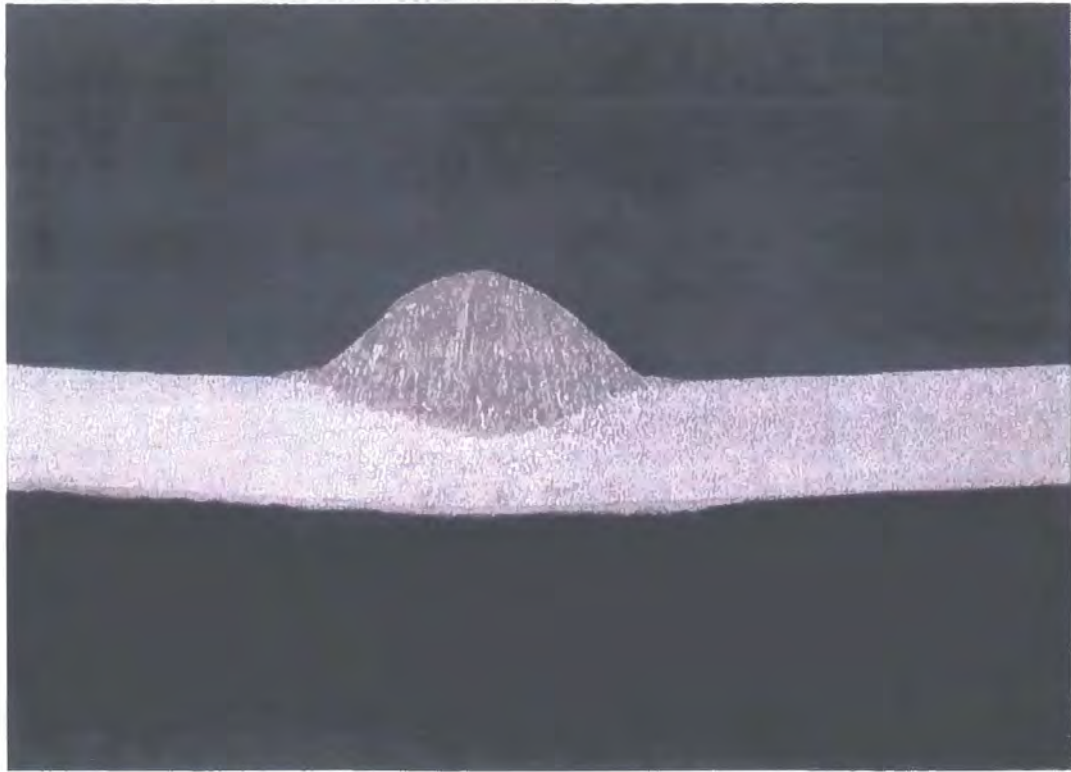
Bead on plate (Ref plate sample 2.0mm plate 41 @ 700mm/min)

250mm along weld

300mm along weld

Predicting Weld Distortion in the Design of Automotive Components
Roger O'Brien, MSc Thesis, March2007
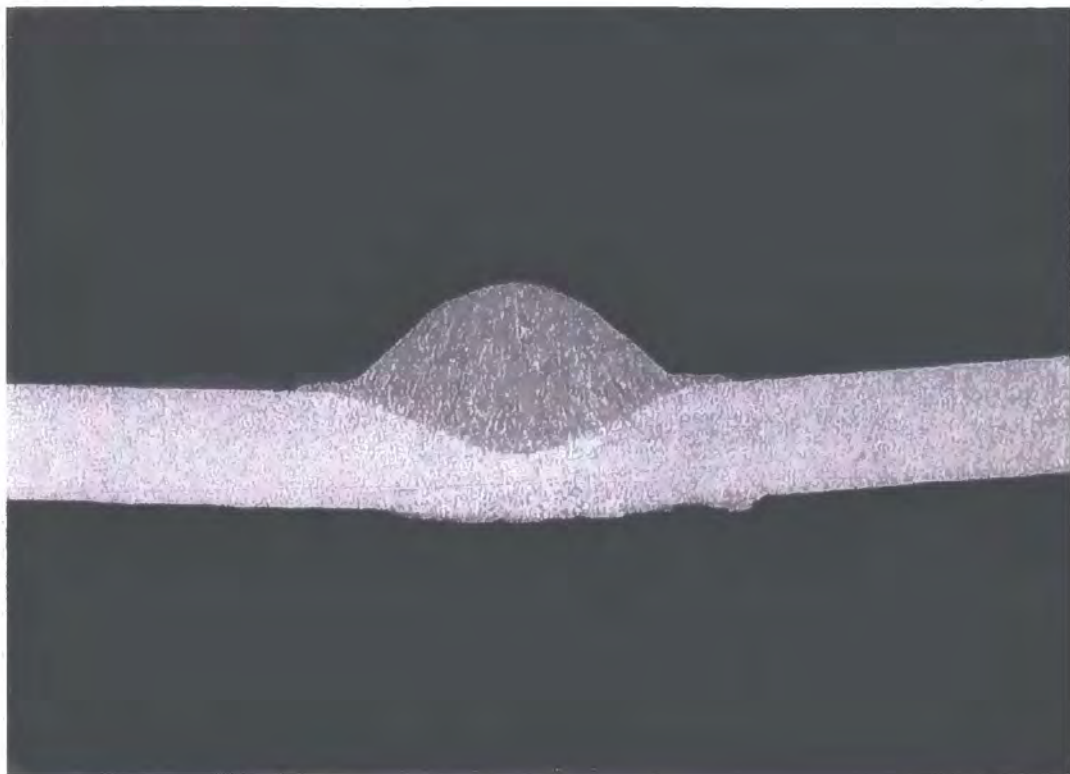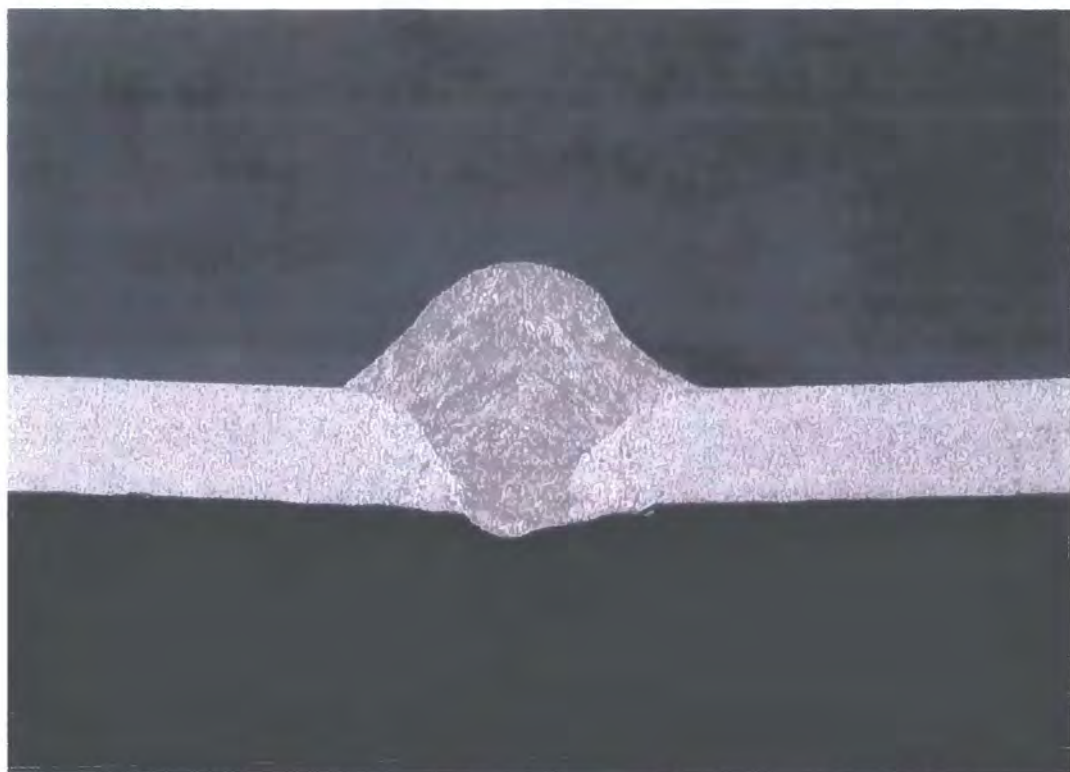
Bead on plate (Ref plate sample 2.0mm plate 41 @ 700mm/min)

Micro Hardness Test on section @ 150mm : showing indent positions

Fine Polished sample for section at 150mm

Bead on plate (Ref plate sample 2.0mm plate 41 @ 700mm/min)
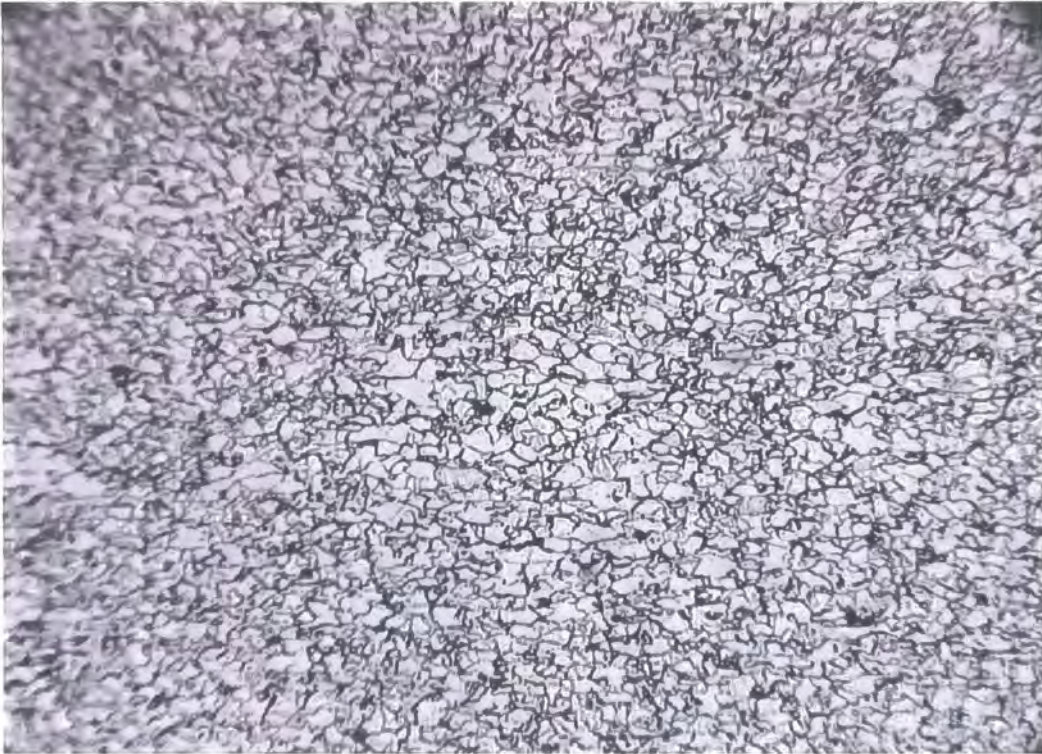
Micro-structure : Weld metal (magnification x 200)

Micro-structure : Inner Heat Affected Zone (magnification x 200)

Bead on plate (Ref plate sample 2.0mm plate 41 @ 700mm/min)

Micro-structure : Mid Heat Affected Zone (magnification x 200)

*Micro-structure : Outer Heat Affected Zone (magnification x 200)*
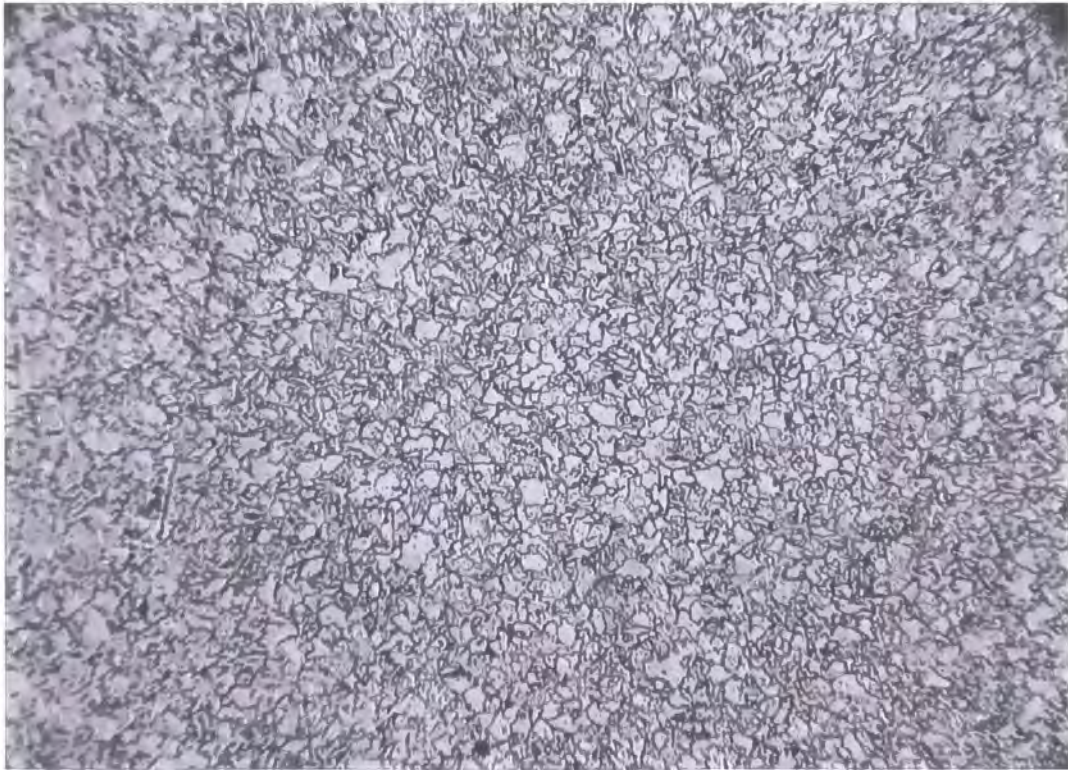
Bead on plate (Ref plate sample 2.0mm plate 41 @ 700mm/min)

Micro-structure : Parent Metal (magnification x 200)
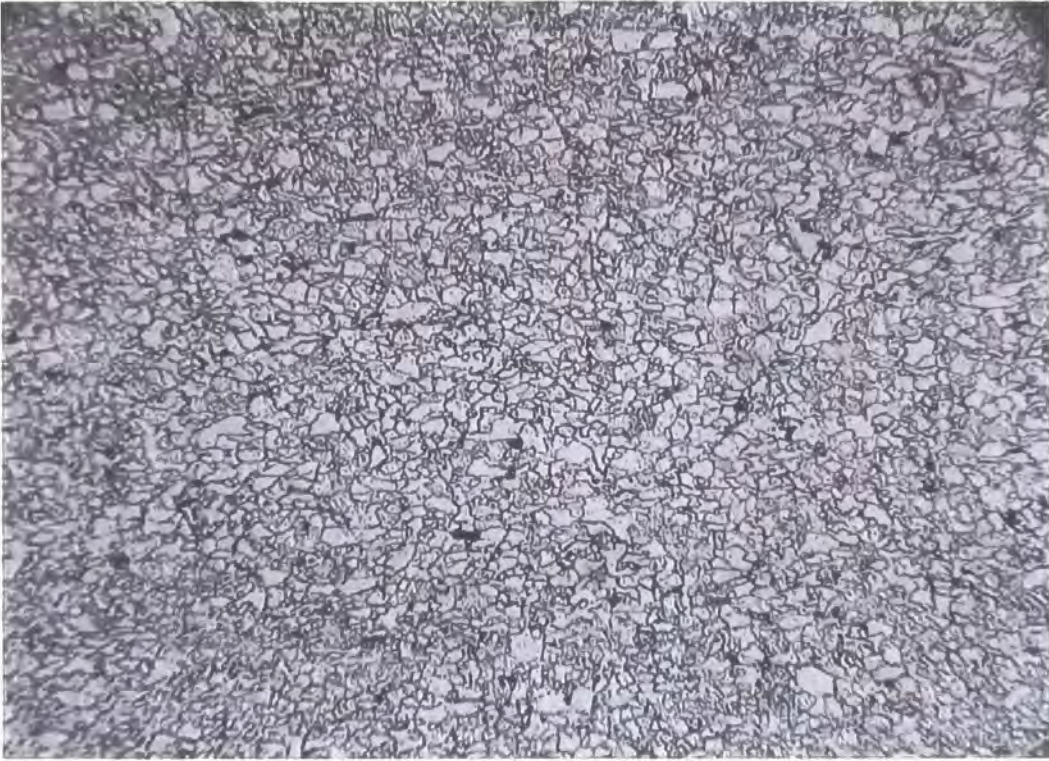
Weld Macro Graphs - Butt Welds

Butt Weld (Ref plate samples 2.5mm plates 1/1A @ 700mm/min)

50mm along weld

100mm along weld

Predicting Weld Distortion in the Design of Automotive Components
Roger O'Brien, MSc Thesis, March2007
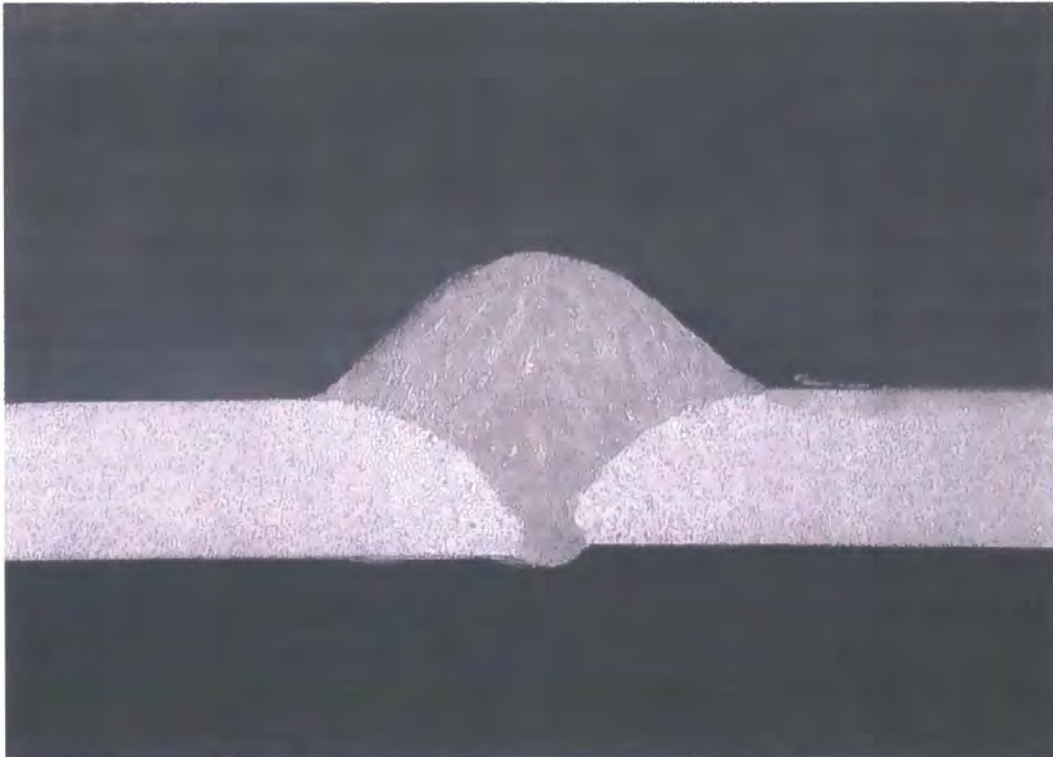
Butt Weld (Ref plate samples 2.5mm plates 1/1A @ 700mm/min)

150mm along weld

200mm along weld

Predicting Weld Distortion in the Design of Automotive Components
Roger O'Brien, MSc Thesis, March2007
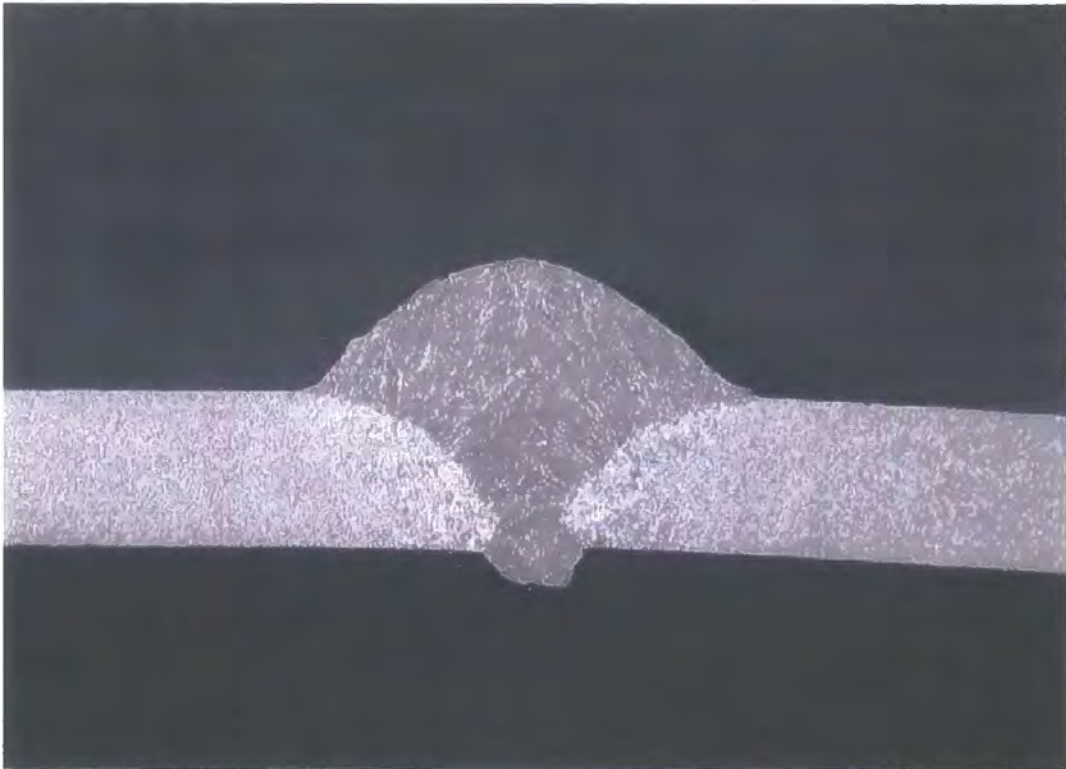
Butt Weld (Ref plate samples 2.5mm plates 1/1A @ 700mm/min)

250mm along weld
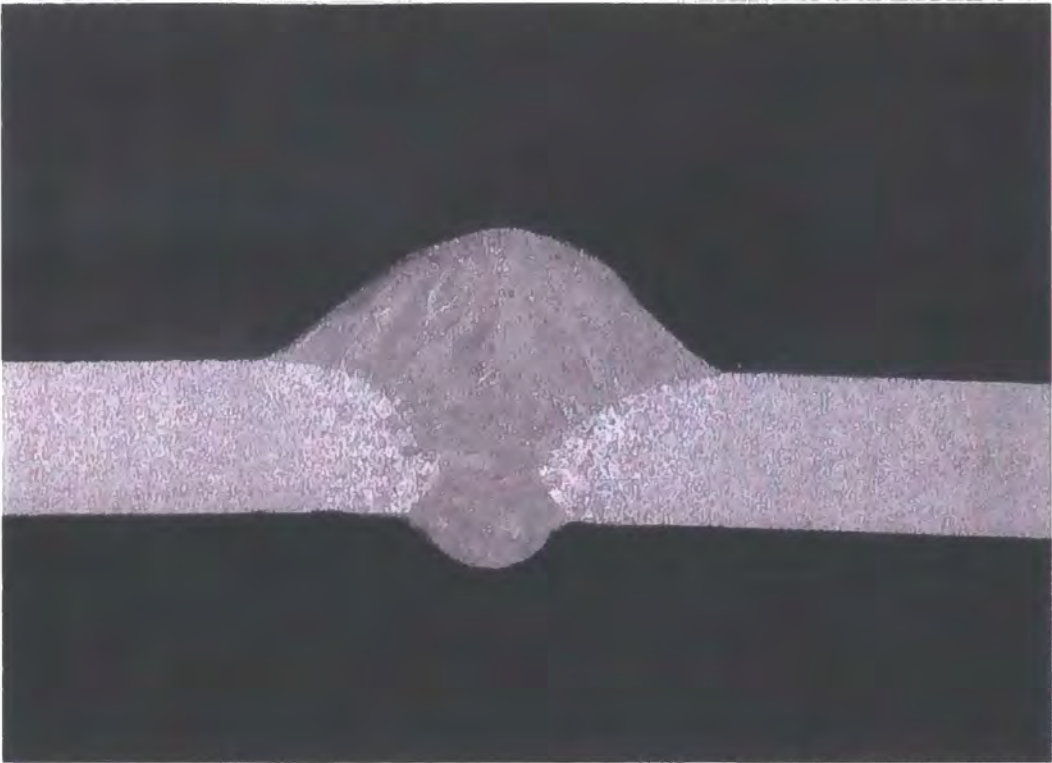
300mm along weld
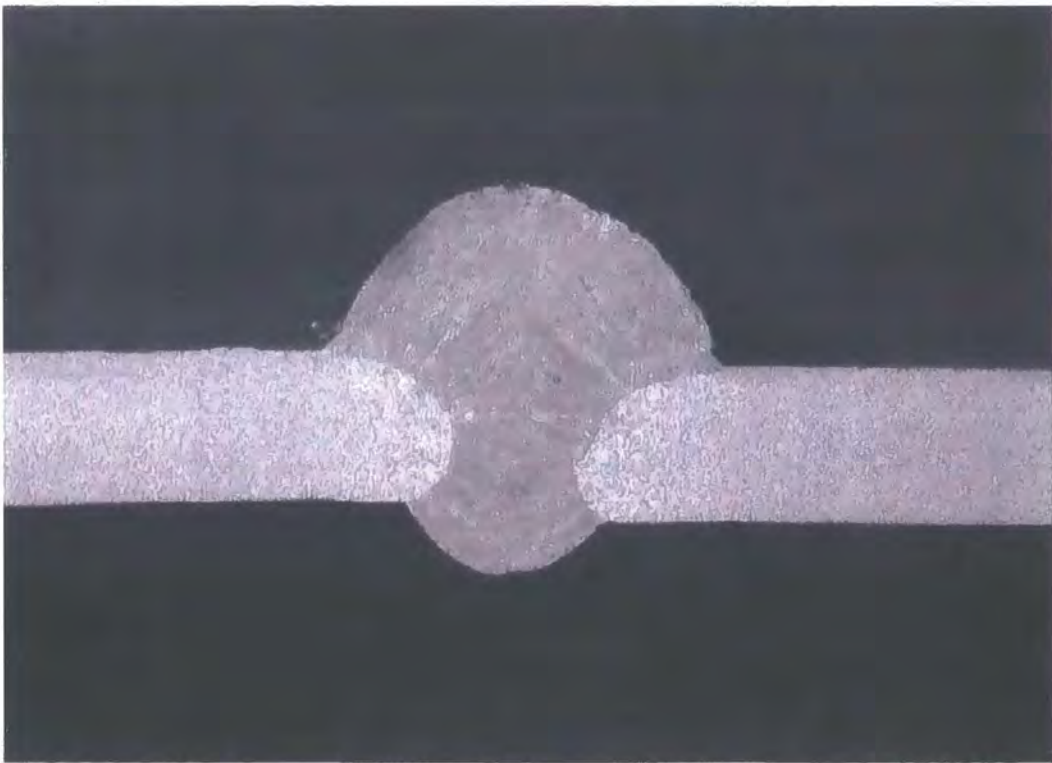
Butt Weld (Ref plate samples 2.5mm plates 1/1A @ 700mm/min)

Micro Hardness Test on section @ 150mm : showing indent positions

Fine Polished sample for section at 150mm

Butt Weld (Ref plate samples 2.5mm plates 1/1A @ 700mm/min)

Micro-structure : Weld metal (magnification x 200)

Micro-structure : Inner Heat Affected Zone (magnification x 200)

Butt Weld (Ref plate samples 2.5mm plates 1/1A @ 700mm/min)

Micro-structure : Mid Heat Affected Zone (magnification x 200)
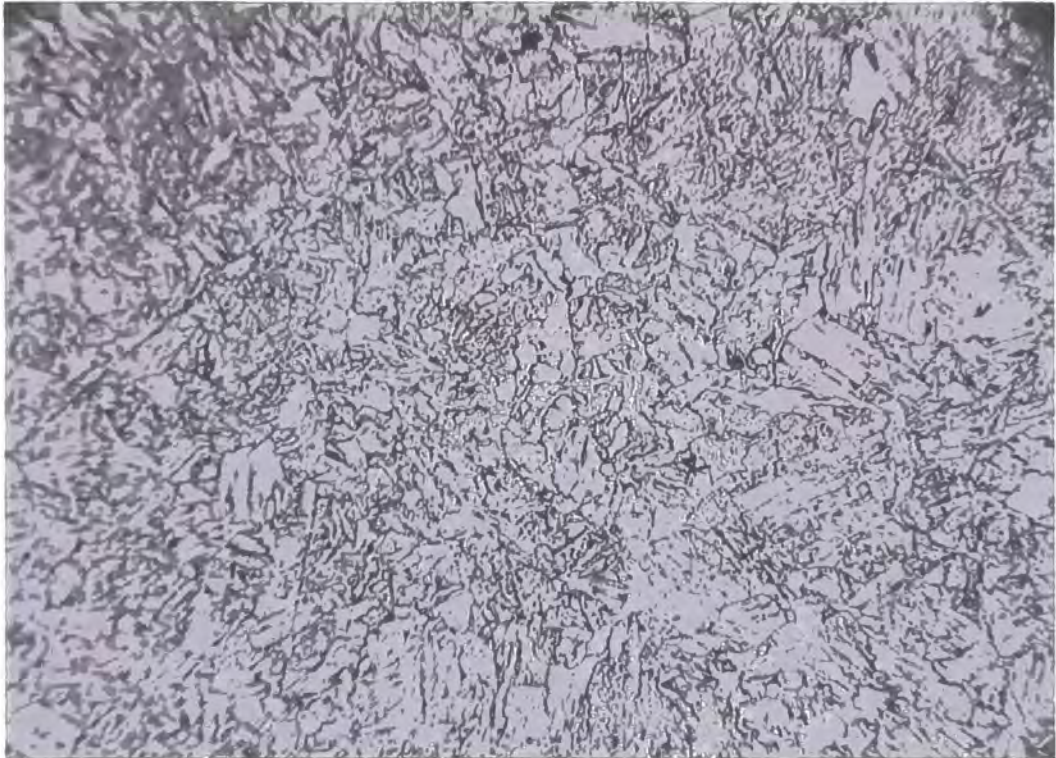
Micro-structure : Outer Heat Affected Zone (magnification x 200)
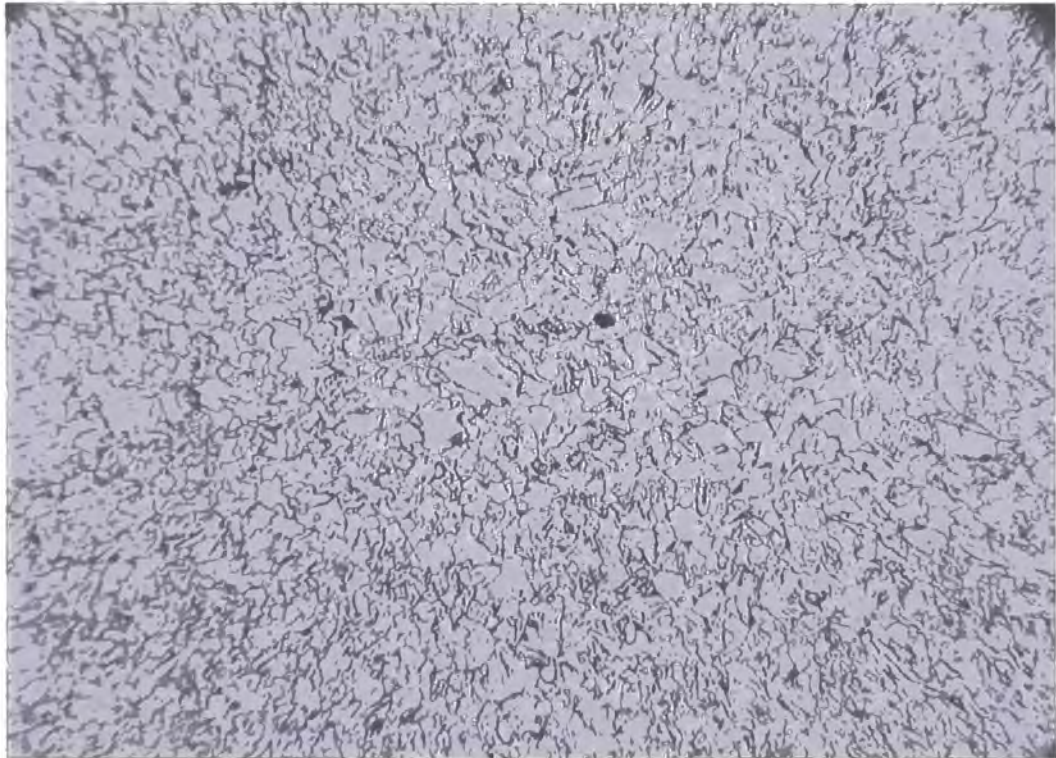
Butt Weld (Ref plate samples 2.5mm plates 1/1A @ 700mm/min)

Micro-structure : Parent Metal (magnification x 200)
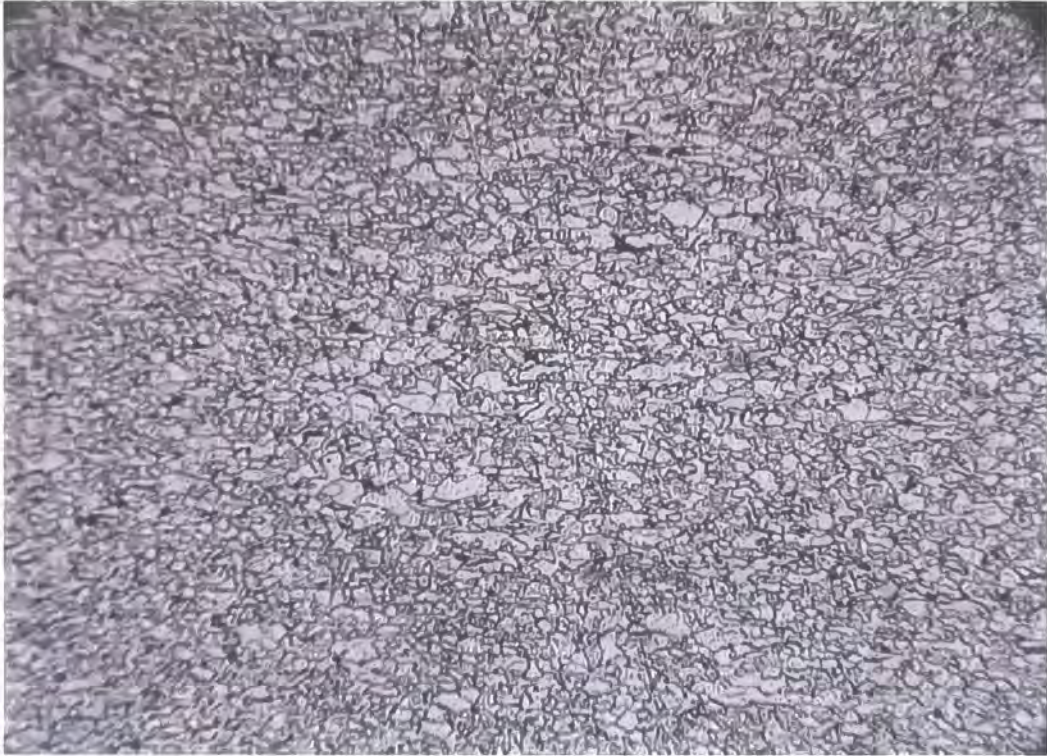
Weld Macro Graphs - Tee Welds

Tee Weld (Ref plate samples 2.5mm plates 15/15A @ 1000mm/min)

50mm along weld
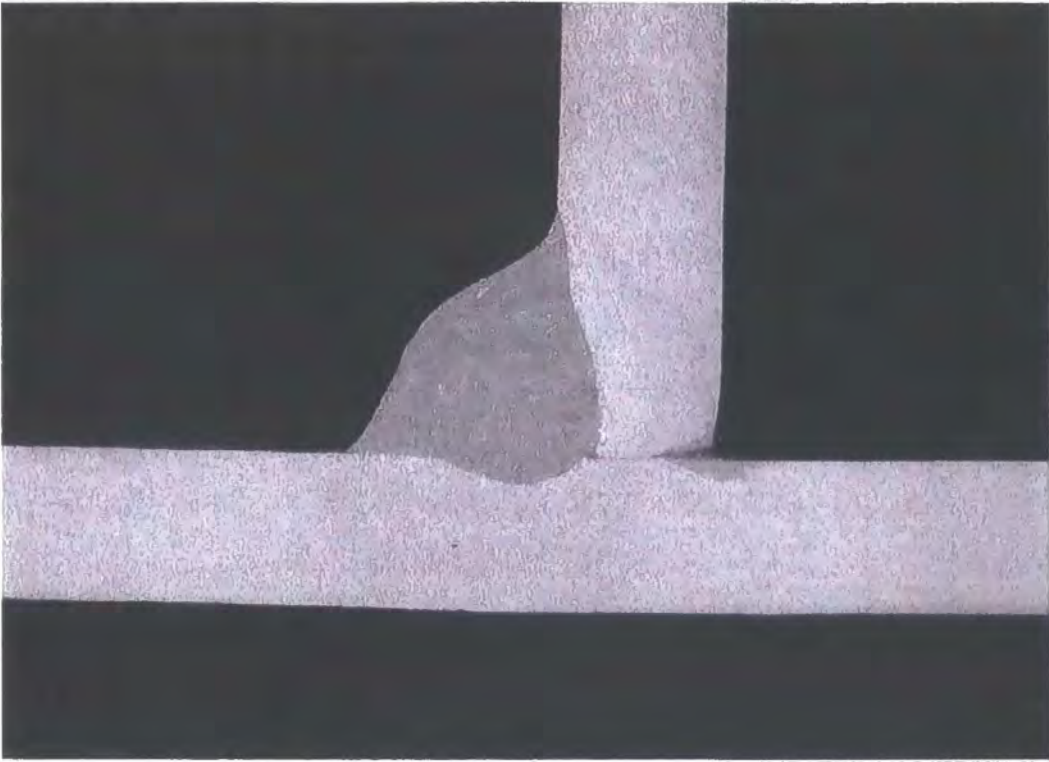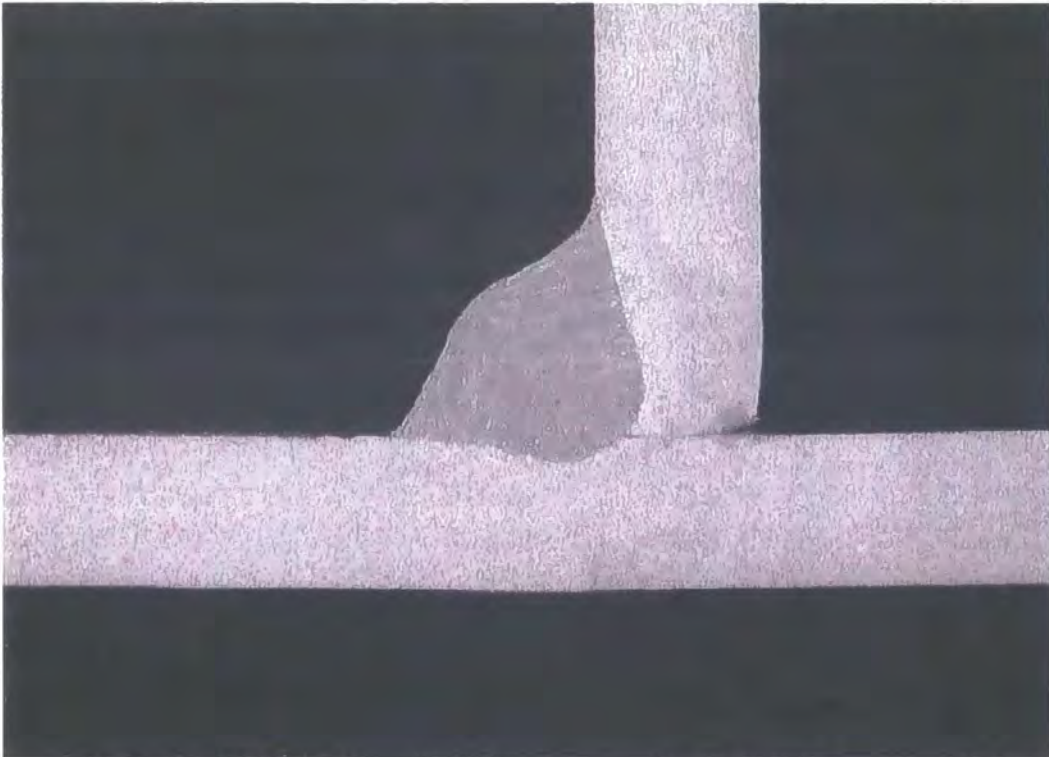
100mm along weld

Tee Weld (Ref plate samples 2.5mm plates 15/15A @ 1000mm/min)

150mm along weld

200mm along weld

Predicting Weld Distortion in the Design of Automotive Components
Roger O'Brien, MSc Thesis, March 2007
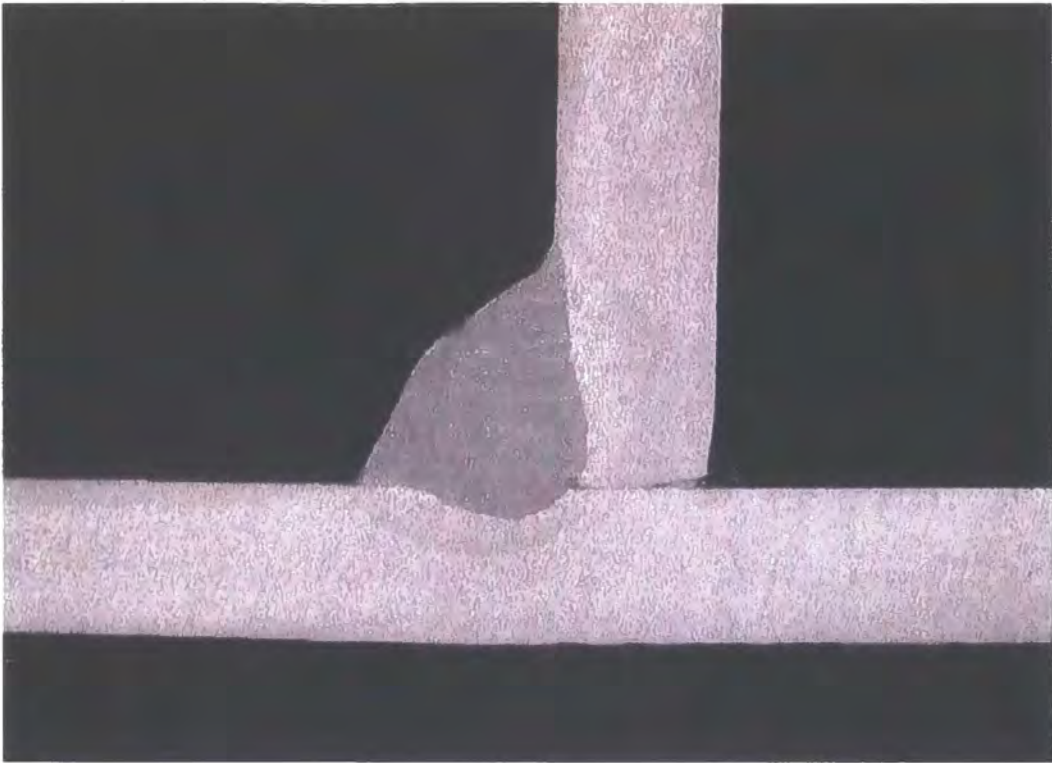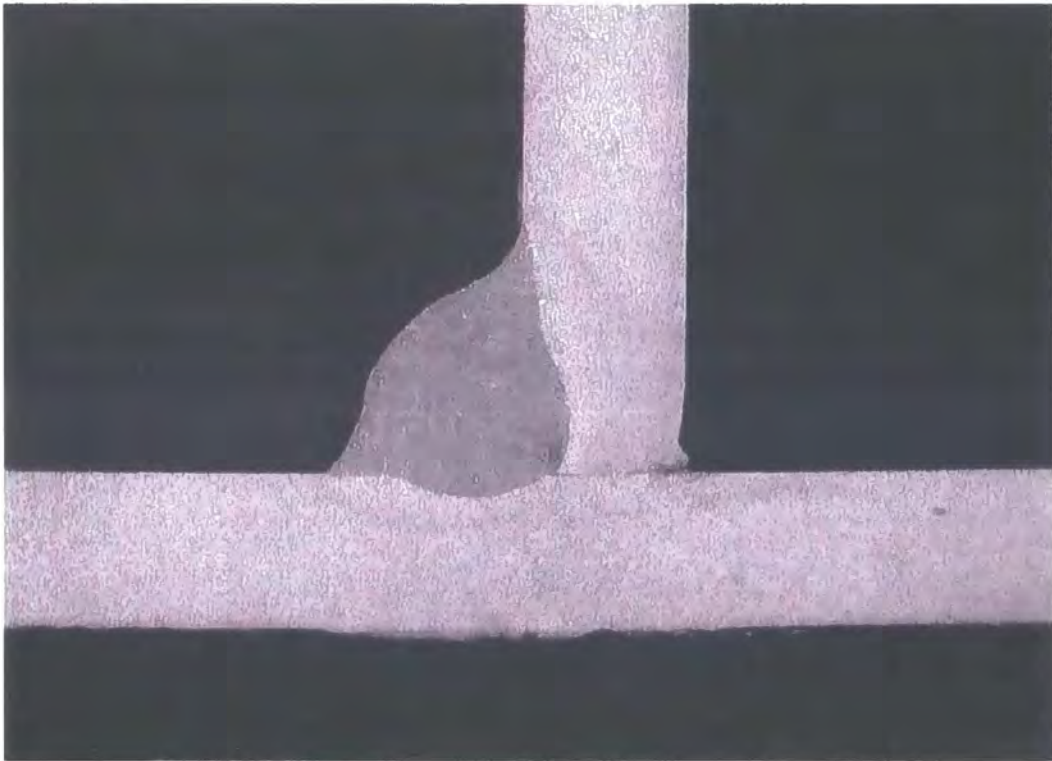
Tee Weld (Ref plate samples 2.5mm plates 15/15A @ 1000mm/min)

250mm along weld
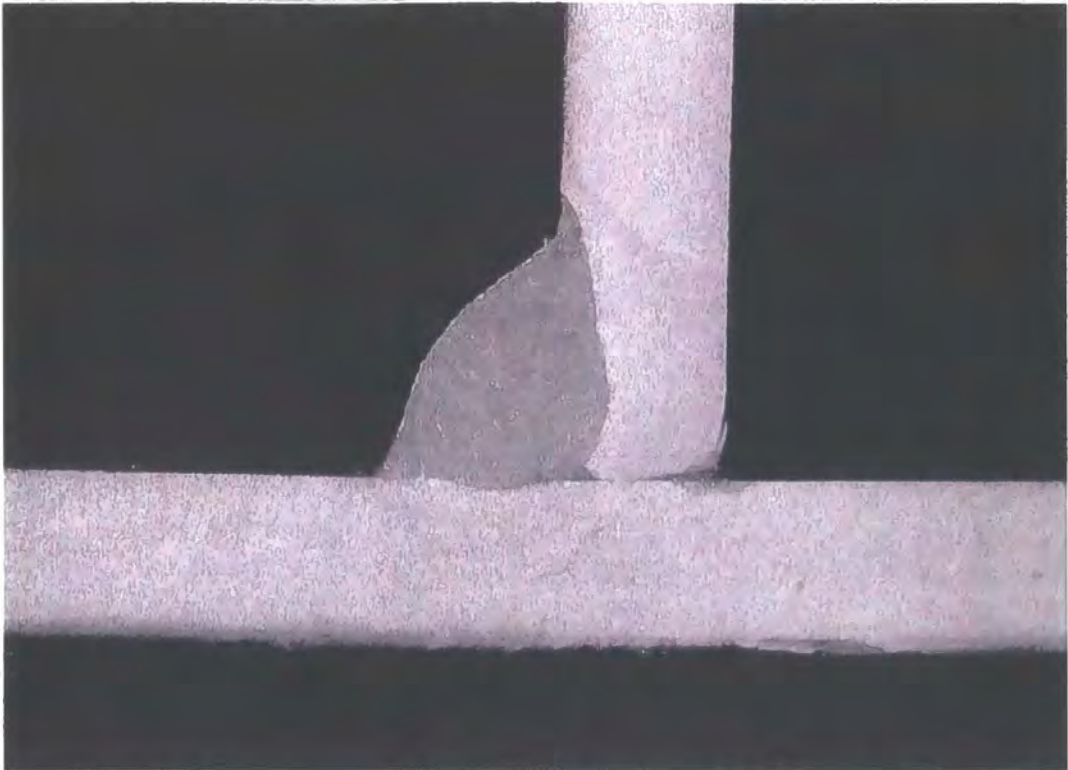
300mm along weld
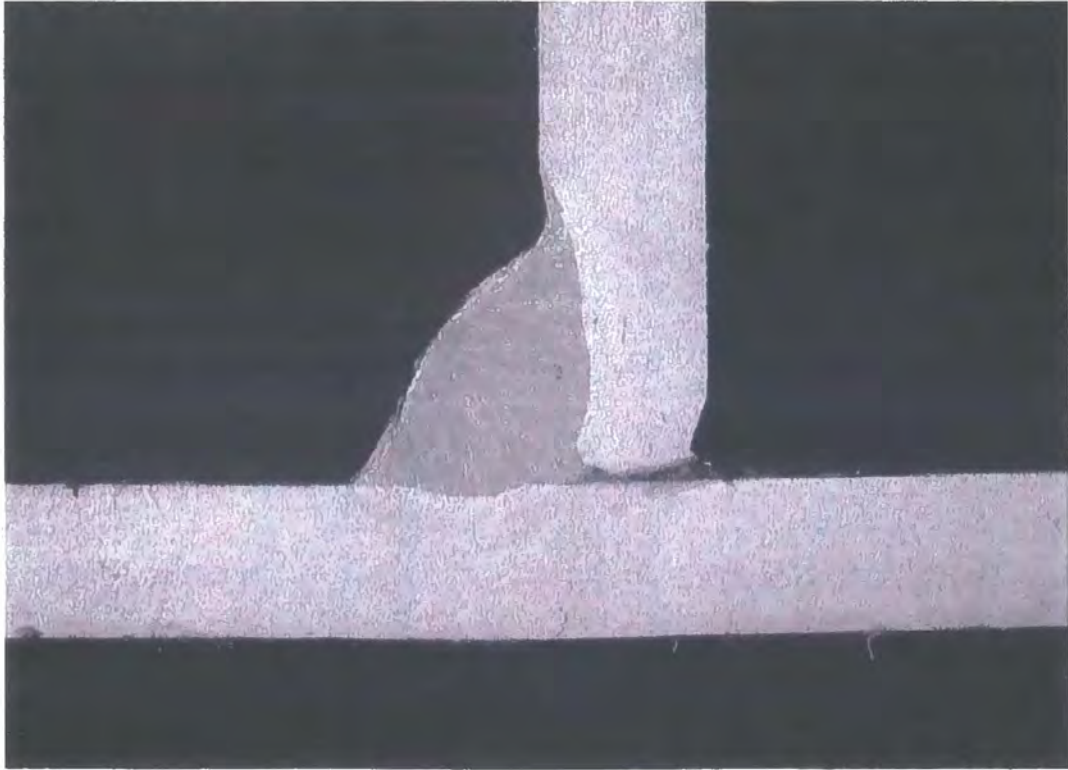
Tee Weld (Ref plate samples 2.5mm plates 15/15A @ 1000mm/min)

Micro Hardness Test on section @ 150mm : showing indent positions

Fine Polished sample for section at 150mm
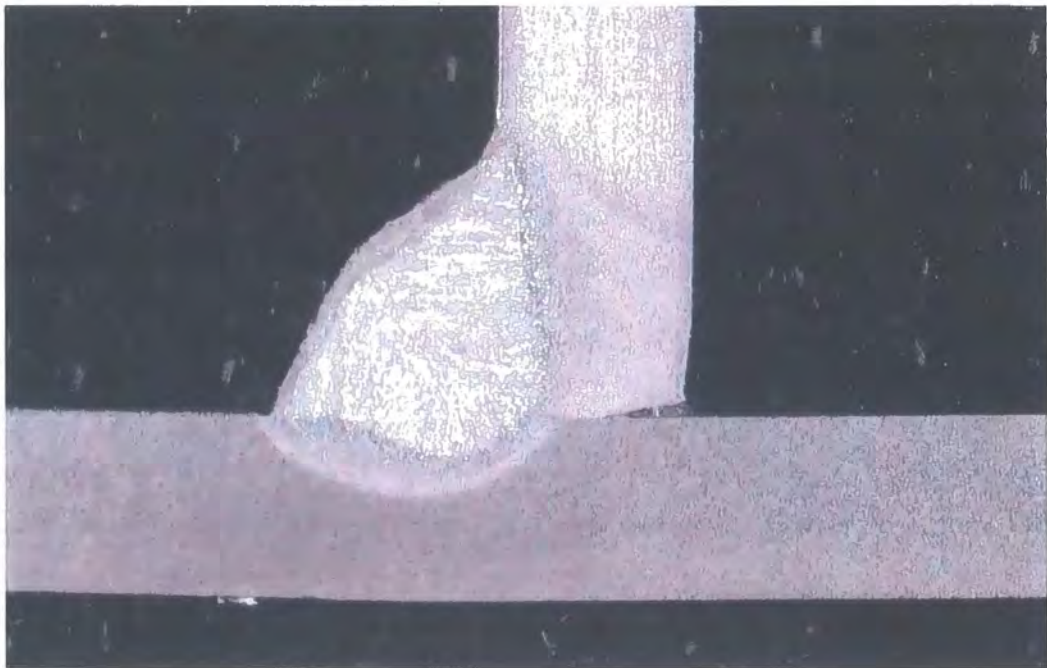
Tee Weld (Ref plate samples 2.5mm plates 15/15A @ 1000mm/min)

Micro-structure : Weld metal (magnification x 200)

Micro-structure : Inner Heat Affected Zone (magnification x 200)

Tee Weld (Ref plate samples 2.5mm plates 15/15A @ 1000mm/min)

Micro-structure : Mid Heat Affected Zone (magnification x 200)

Micro-structure : Outer Heat Affected Zone (magnification x 200)

233

Tee Weld (Ref plate samples 2.5mm plates 15/15A @ 1000mm/min)

Micro-structure : Parent Metal (magnification x 200)

Micro-structure : Heat Affected Zone (magnification x 50)
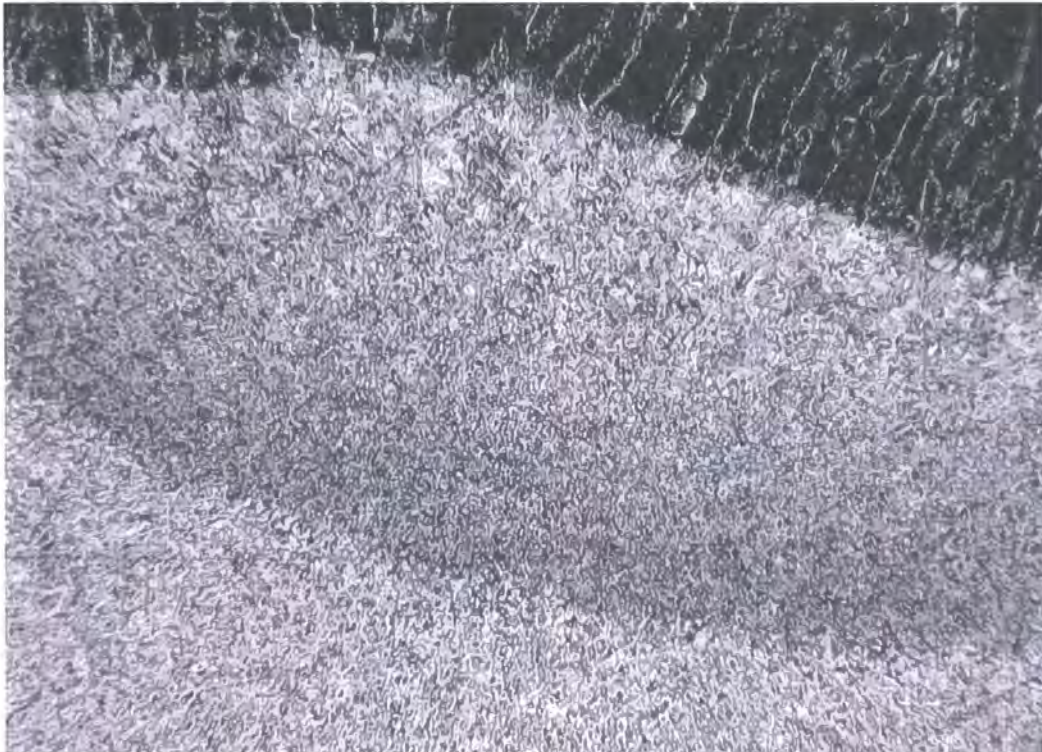
Appendix II – Sample Results Inspection Analysis Reports

Appendix II(i) – Sample report: 2.0mm bead on plate welded at 700mm/min

Preweld Analysis of 2.0mm thick plates

Plate Ref No.	41					
	x=50	x=100	x=150	x=200	x=250	x=300
Calc X Dim	151.01	151.03	151.04	151.06	151.07	151.09
Calc Y Dim	350.15	350.13	350.12	350.10	350.09	350.07
	y=50	y=25	y=9	y=9	y=25	y=50

Plate Ref No.	41	
	dim 0	dim 2	Delta
X dim	151.06	151.18	0.10
Y dim	350.05	350.07	0.12

Plate Ref No.		
	dim 0	dim 2	Delta
X dim	0.00	0.00	0.00
Y dim	0.00	0.00	0.00

All points on Plate lie with 0.08 flatness tolerance - therefore curvature of initial plate can be neglected (Rmax(y) =191406mm, Rmax(x)=35156)

Specimen and plate numbers	Plate thickness (mm)	Weld joint type	Weld speed (mm/min)	weld type	gas flow (l/min)	target weld length (mm)	actual weld length (mm)	wire stick out (mm)
41	2.0	Bead on Pl	700	mig	26	330		20

section results	x = 50			x = 100			x = 150			x = 200			x = 250			x = 300			section results
	Welded	Pre welded	Delta	Welded	Pre welded	Delta	Welded	Pre welded	Delta	Welded	Pre welded	Delta	Welded	Pre welded	Delta	Welded	Pre welded	Delta	
width W (mm)	149.85	151.01	1.16	149.82	151.03	1.21	149.85	151.04	1.20	149.84	151.06	1.22	149.93	151.07	1.14	149.95	151.09	1.13	width W (mm)
angle (weld side) (deg)	173.3	180.0	6.7	173.1	180.0	6.9	173.1	180.0	6.9	173.6	180.0	6.4	173.8	180.0	6.2	174.5	180.0	5.6	angle 1 (weld side) (deg)
approx. Radius of curvature (mm)	568	flat within .6		650	flat within .6		640	flat within .6		576	flat within .6		651	flat within .6		620	flat within .6		approx. Radius of curvature (mm)

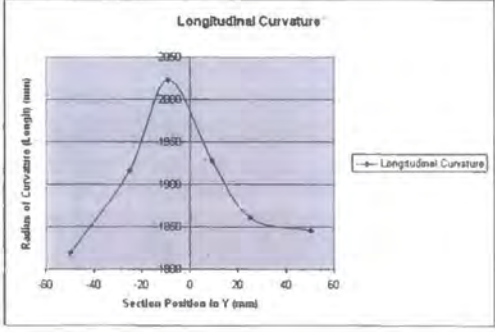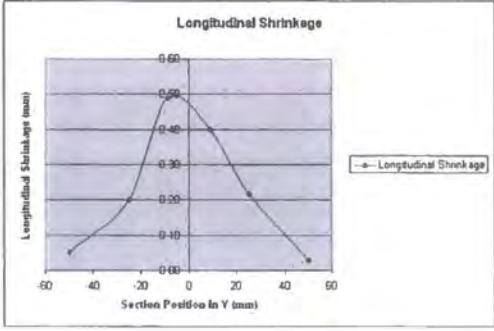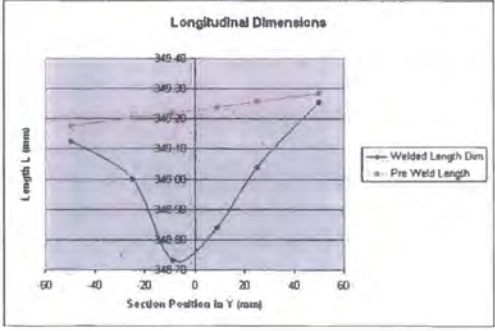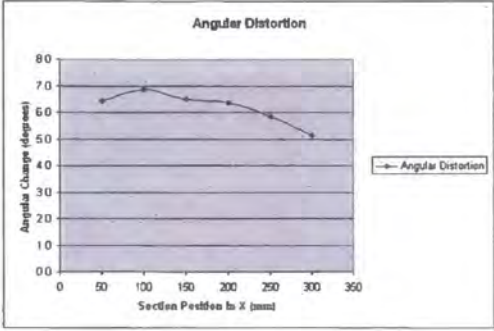| section results	y = -50			y = -25			y = -9			y = 9			y = 25			y = 50			section results
	Welded	Pre welded	Delta	Welded	Pre welded	Delta	Welded	Pre welded	Delta	Welded	Pre welded	Delta	Welded	Pre welded	Delta	Welded	Pre welded	Delta	
length L (mm)	349.75	350.07	0.32	349.33	350.09	0.76	348.85	350.10	1.25	348.96	350.12	1.16	349.18	350.13	0.95	349.63	350.15	0.53	length L (mm)
approx. Radius of curvature (mm)	1642	flat within .6		1692	flat within .6		1737	flat within .6		1754.5	flat within .6		1677	flat within .6		1615	flat within .6		approx. Radius of curvature (mm)

Origin at end of plates and co-incident with weld line

Transverse Dimensions

Transverse Shrinkage

Transverse Curvature

Angular Distortion

Longitudinal Dimensions

Longitudinal Shrinkage
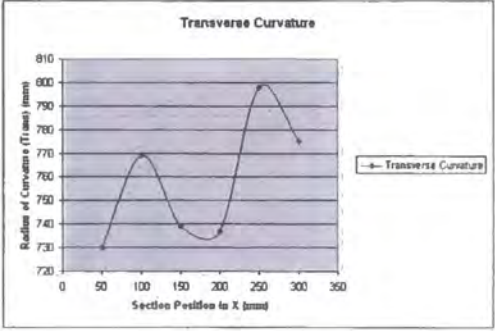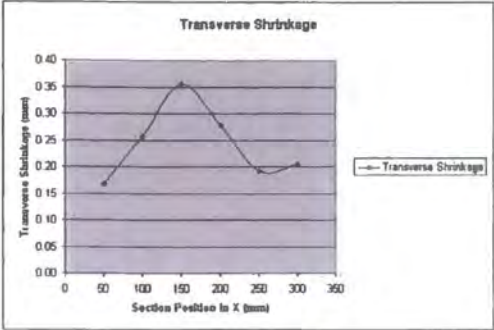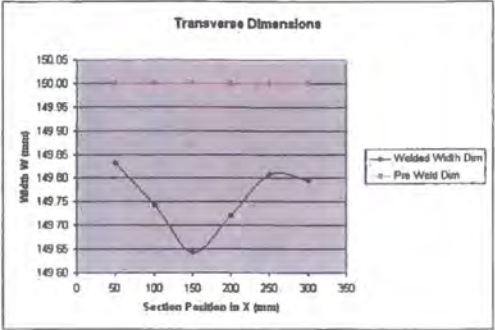

Longitudinal Curvature

237

Specimen and plate numbers	Plate thickness (mm)	Weld joint type	Weld speed (mm/min)	weld type	gas flow (l/min)	target weld length (mm)	actual weld length (mm)	wire stick out (mm)
45	2.5	Bead on Pl	1000	mig	26	330		20

section results	x = 50			x = 100			x = 150			x = 200			x = 250			x = 300			section results
	Welded	Pre welded	Delta	Welded	Pre welded	Delta	Welded	Pre welded	Delta	Welded	Pre welded	Delta	Welded	Pre welded	Delta	Welded	Pre welded	Delta	
width W (mm)	149.65	150.15	0.50	149.35	150.15	0.80	149.38	150.15	0.77	149.37	150.15	0.78	149.46	150.15	0.69	149.48	150.15	0.67	width W (mm)
angle (weld side) (deg)	172.4	180.0	7.6	171.7	180.0	8.3	171.8	180.0	8.2	172.0	180.0	8.0	172.7	180.0	7.3	174.1	180.0	5.9	angle 1 (weld side) (deg)
approx Radius of curvature (mm)	580	flat within .6		566	flat within .6		470	flat within .6		539	flat within .6		471	flat within .6		542	flat within .6		approx Radius of curvature (mm)

section results	y = -50			y = -25			y = -9			y = 9			y = 25			y = 50			section results
	Welded	Pre welded	Delta	Welded	Pre welded	Delta	Welded	Pre welded	Delta	Welded	Pre welded	Delta	Welded	Pre welded	Delta	Welded	Pre welded	Delta	
length L (mm)	349.84	349.97	0.13	349.56	349.98	0.42	349.42	349.99	0.57	349.28	349.99	0.71	349.41	350.00	0.59	349.84	350.01	0.17	length L (mm)
approx Radius of curvature (mm)	1743	flat within .6		1780	flat within .6		1817	flat within .6		1801	flat within .6		1765	flat within .6		1731	flat within .6		approx Radius of curvature (mm)

Transverse Dimensions

Transverse Shrinkage

Transverse Curvature

Angular Distortion

Longitudinal Dimensions

Longitudinal Shrinkage

Longitudinal Curvature

239

Specimen and plate numbers	Plate thickness (mm)	Weld joint type	Weld speed (mm/min)	weld type	gas flow (l/min)	target weld length (mm)	actual weld length (mm)	wire stick out (mm)
58	3.0	Bead on Pl	1300	mig	26	330		20

section results	x = 50 Welded	Pre welded	Delta	x = 100 Welded	Pre welded	Delta	x = 150 Welded	Pre welded	Delta	x = 200 Welded	Pre welded	Delta	x = 250 Welded	Pre welded	Delta	x = 300 Welded	Pre welded	Delta	section results
width W (mm)	149.83	150.00	0.17	149.74	150.00	0.26	149.64	150.00	0.36	149.72	150.00	0.28	149.81	150.00	0.19	149.80	150.00	0.21	width W (mm)
angle (weld side) (deg)	173.6	180.0	6.4	173.1	180.0	6.9	173.5	180.0	6.5	173.6	180.0	6.4	174.2	180.0	5.8	174.9	180.0	5.1	angle 1 (weld side) (deg)
approx. Radius of curvature (mm)	730	flat within .6		769	flat within .6		739	flat within .6		737	flat within .6		798	flat within .6		775	flat within .6		approx. Radius of curvature (mm)

section results	y = -50 Welded	Pre welded	Delta	y = -25 Welded	Pre welded	Delta	y = -9 Welded	Pre welded	Delta	y = 9 Welded	Pre welded	Delta	y = 25 Welded	Pre welded	Delta	y = 50 Welded	Pre welded	Delta	section results
length L (mm)	349.13	349.18	0.05	349.00	349.20	0.20	348.73	349.22	0.49	348.84	349.24	0.40	349.04	349.26	0.22	349.26	349.28	0.03	length L (mm)
approx. Radius of curvature (mm)	1819	flat within .6		1916	flat within .6		2023	flat within .6		1928	flat within .6		1861	flat within .6		1845	flat within .6		approx. Radius of curvature (mm)

Origin at end of plates and co-incident with weld line

Transverse Dimensions

Transverse Shrinkage

Transverse Curvature

Angular Distortion

Longitudinal Dimensions

Longitudinal Shrinkage

Longitudinal Curvature

241

Preweld Analysis of 2.0mm thick plates

Plate Ref No.	2				x=50	x=100	x=150	x=200	x=250	x=300
	dim 1	dim 2	Delta							
X dim	150.70	150.64	-0.07	Calc X Dim	150.59	150.60	150.67	150.67	150.66	150.66
Y dim	349.63	349.51	-0.12	Calc Y Dim	349.55	349.59	349.62			
					y=100	y=50	y=9			

Plate Ref No.	2A				x=50	x=100	x=150	x=200	x=250	x=300
	dim 1	dim 2	Delta							
X dim	150.59	150.64	0.05	Calc X Dim	150.60	150.60	150.61	150.62	150.63	150.63
Y dim	351.66	351.54	-0.12	Calc Y Dim	351.58	351.62	351.66			
					y=100	y=50	y=9			

All points on Plate lie with 0.08 flatness tolerance - therefore curvature of initial plate can be neglected (Rmax(y) =191406mm, Rmax(x)=35156)

Plate Ref No.	2-2A					
	x=50	x=100	x=150	x=200	x=250	x=300
Calc X Dim	301.29	301.29	301.29	301.28	301.28	301.28
Calc Y Dim	351.58	351.62	351.65	349.62	349.59	349.55
	y=100	y=50	y=9	y=-9	y=-50	y=-100

Specimen and plate numbers	Plate thickness (mm)	Weld joint type	Weld speed (mm/min)	weld type	gas flow (l/min)	target weld length (mm)	actual weld length (mm)	wire stick out (mm)
2-2A	2.0	Butt	700	mig	26	330		20

section results	x = 50			x = 100			x = 150			x = 200			x = 250			x = 300			section results
	Welded	Pre welded	Delta	Welded	Pre welded	Delta	Welded	Pre welded	Delta	Welded	Pre welded	Delta	Welded	Pre welded	Delta	Welded	Pre welded	Delta	
width W (mm)	300.21	301.29	1.08	300.12	301.29	1.17	299.98	301.29	1.31	300.03	301.28	1.25	300.08	301.28	1.20	300.14	301.28	1.14	width W (mm)
angle (weld side) (deg)	175.3	180.0	4.7	175.3	180.0	4.7	175.7	180.0	4.3	175.6	180.0	4.4	175.7	180.0	4.3	175.7	180.0	4.3	angle 1 (weld side) (deg)
approx Radius of curvature (mm)	1882	flat within .6		2032	flat within .6		2125	flat within .6		1898	flat within .6		2032	flat within .6		2157	flat within .6		approx Radius of curvature (mm)

section results	y = -100			y = -50			y = -9			y = 9			y = 50			y = 100			section results
	Welded	Pre welded	Delta	Welded	Pre welded	Delta	Welded	Pre welded	Delta	Welded	Pre welded	Delta	Welded	Pre welded	Delta	Welded	Pre welded	Delta	
length L (mm)	349.02	349.55	0.53	348.53	349.59	1.06	348.14	349.62	1.49	350.30	351.65	1.35	350.70	351.62	0.92	351.09	351.58	0.49	length L (mm)
approx Radius of curvature (mm)	2076	flat within .6		2059	flat within .6		2041	flat within .6		2045	flat within .6		1811	flat within .6		1765	flat within .6		approx Radius of curvature (mm)

Origin at end of plates and co-incident with weld line

Transverse Dimensions

Transverse Shrinkage

Transverse Curvature

Angular Distortion

Longitudinal Dimensions

Longitudinal Shrinkage

Longitudinal Curvature

244

Specimen and plate numbers	Plate thickness (mm)	Weld joint type	Weld speed (mm/min)	weld type	gas flow (l/min)	target weld length (mm)	actual weld length (mm)	wire stick out (mm)
5-5A	2.5	Butt	1000	mig	26	330		20

section results	x = 50			x = 100			x = 150			x = 200			x = 250			x = 300			section results
	Welded	Pre welded	Delta	Welded	Pre welded	Delta	Welded	Pre welded	Delta	Welded	Pre welded	Delta	Welded	Pre welded	Delta	Welded	Pre welded	Delta	
width W (mm)	300.05	300.80	0.75	299.89	300.85	0.96	299.89	300.91	1.02	299.88	300.97	1.09	300.00	301.03	1.03	300.54	301.08	0.54	width W (mm)
angle (weld side) (deg)	176.5	180.0	3.5	176.6	180.0	3.4	176.7	180.0	3.3	176.8	180.0	3.3	176.9	180.0	3.1	177.0	180.0	3.1	angle 1 (weld side) (deg)
approx. Radius of curvature (mm)	2172	flat within .6		2125	flat within .6		2282	flat within .6		2221	flat within .6		2458	flat within .6		2508	flat within .6		approx. Radius of curvature (mm)

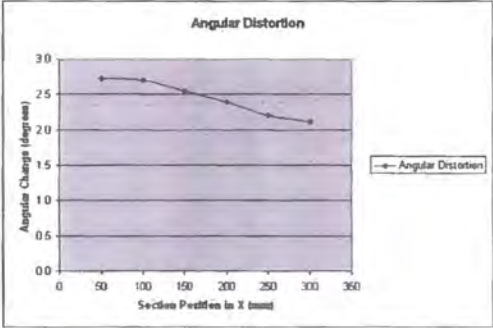| section results	y = -100			y = -50			y = -9			y = 9			y = 50			y = 100			section results
	Welded	Pre welded	Delta	Welded	Pre welded	Delta	Welded	Pre welded	Delta	Welded	Pre welded	Delta	Welded	Pre welded	Delta	Welded	Pre welded	Delta	
length L (mm)	350.61	350.85	0.25	350.30	350.73	0.43	349.89	350.62	0.73	349.85	350.72	0.87	350.26	350.83	0.57	350.71	350.97	0.26	length L (mm)
approx. Radius of curvature (mm)	4508	flat within .6		4268	flat within .6		4499	flat within .6		3825	flat within .6		3290	flat within .6		3194	flat within .6		approx. Radius of curvature (mm)

Origin at end of plates and co-incident with weld line

Transverse Dimensions

Transverse Shrinkage

Transverse Curvature

Angular Distortion

Longitudinal Dimensions

Longitudinal Shrinkage
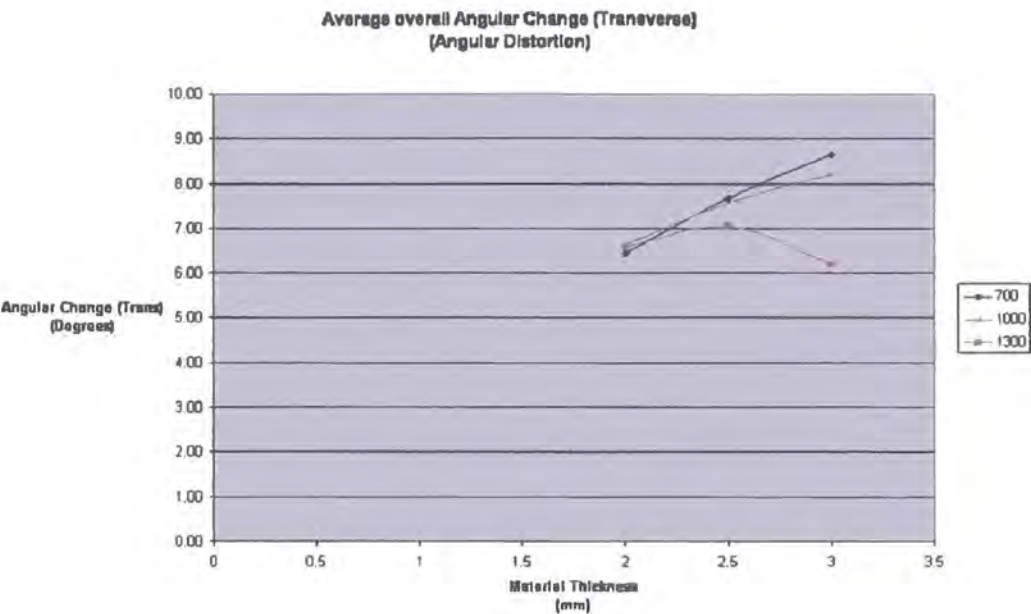

Longitudinal Curvature

246

Specimen and plate numbers	Plate thickness (mm)	Weld joint type	Weld speed (mm/min)	weld type	gas flow (l/min)	target weld length (mm)	actual weld length (mm)	wire stick out (mm)
7-7A	3.0	Butt	1300	mig	26	330		20

section results	x = 50			x = 100			x = 150			x = 200			x = 250			x = 300			section results
	Welded	Pre welded	Delta	Welded	Pre welded	Delta	Welded	Pre welded	Delta	Welded	Pre welded	Delta	Welded	Pre welded	Delta	Welded	Pre welded	Delta	
width W (mm)	300.57	301.10	0.54	300.44	301.08	0.65	300.29	301.06	0.77	300.23	301.05	0.82	300.29	301.03	0.74	300.48	301.01	0.53	width W (mm)
angle (weld side) (deg)	177.3	180.0	2.7	177.3	180.0	2.7	177.5	180.0	2.8	177.6	180.0	2.4	177.8	180.0	2.2	177.9	180.0	2.1	angle 1 (weld side) (deg)
approx Radius of curvature (mm)	3180	flat within .6		3203	flat within .6		3551	flat within .6		3679	flat within .6		3878	flat within .6		3800	flat within .6		approx Radius of curvature (mm)

section results	y = -100			y = -50			y = -9			y = 9			y = 50			y = 100			section results
	Welded	Pre welded	Delta	Welded	Pre welded	Delta	Welded	Pre welded	Delta	Welded	Pre welded	Delta	Welded	Pre welded	Delta	Welded	Pre welded	Delta	
length L (mm)	349.95	350.05	0.10	349.83	350.08	0.25	349.76	350.10	0.34	350.11	350.49	0.38	350.21	350.48	0.28	350.35	350.44	0.09	length L (mm)
approx Radius of curvature (mm)	8962	flat within .6		8405	flat within .6		7115	flat within .6		5677	flat within .6		5445	flat within .6		5513	flat within .6		approx Radius of curvature (mm)

Origin at end of plates and co-incident with weld line

Transverse Dimensions

Transverse Shrinkage

Transverse Curvature

Angular Distortion

Longitudinal Dimensions

Longitudinal Shrinkage

Longitudinal Curvature

248
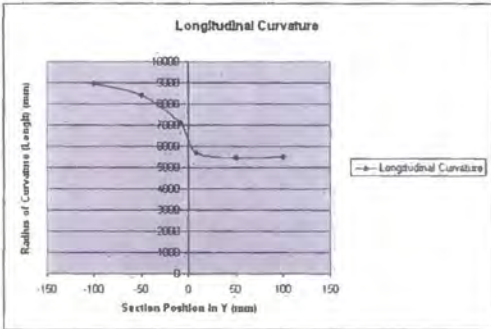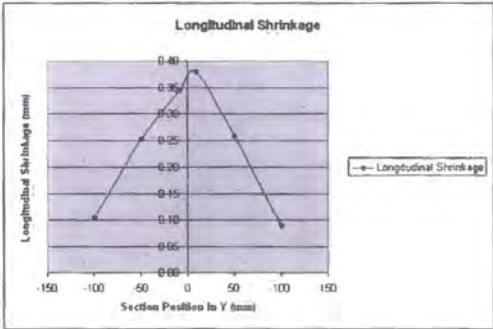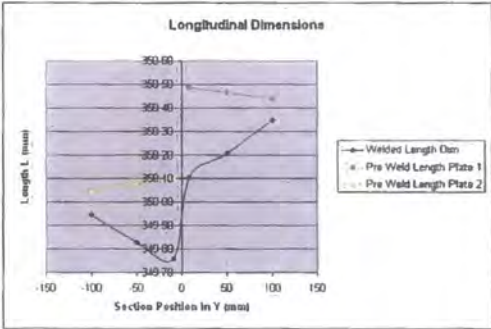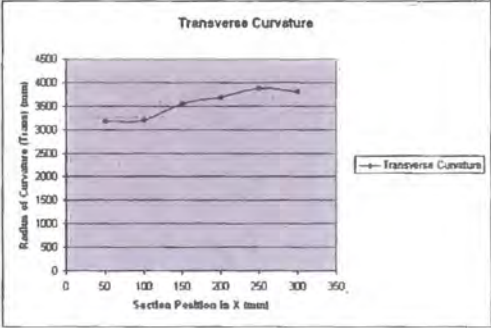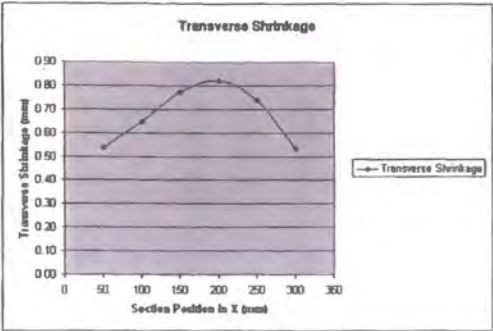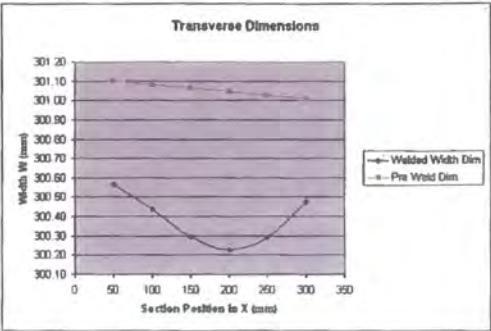
Appendix III – Additional Experimental Response Graphs

Bead on plate – Angular distortion
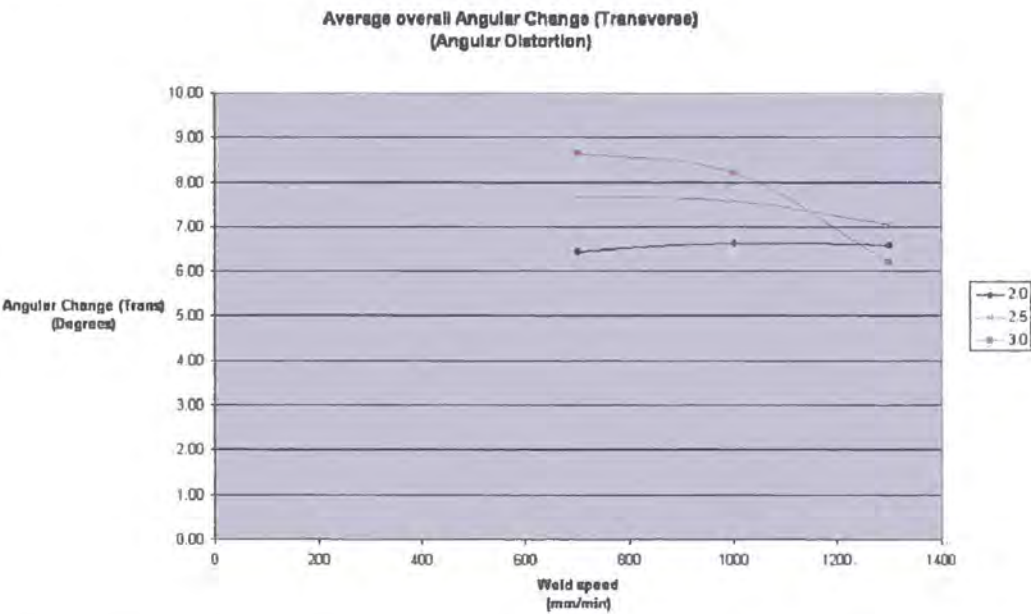
Average overall Angular Change (Transverse)
(Angular Distortion)

(a) Relationship between material thickness curves

Average overall Angular Change (Transverse)
(Angular Distortion)

(b) Relationship between welding speed curves

Family curves for angular distortion in bead on plate weld samples

249
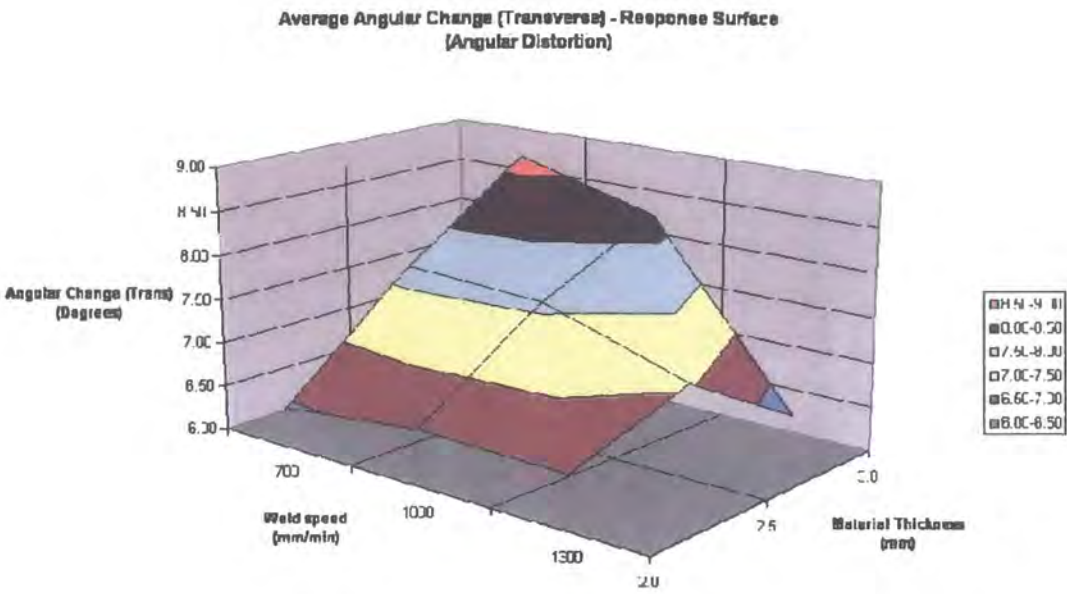
Experimental response surface for angular distortion in bead on plate weld samples

Bead on plate – Bowing distortion
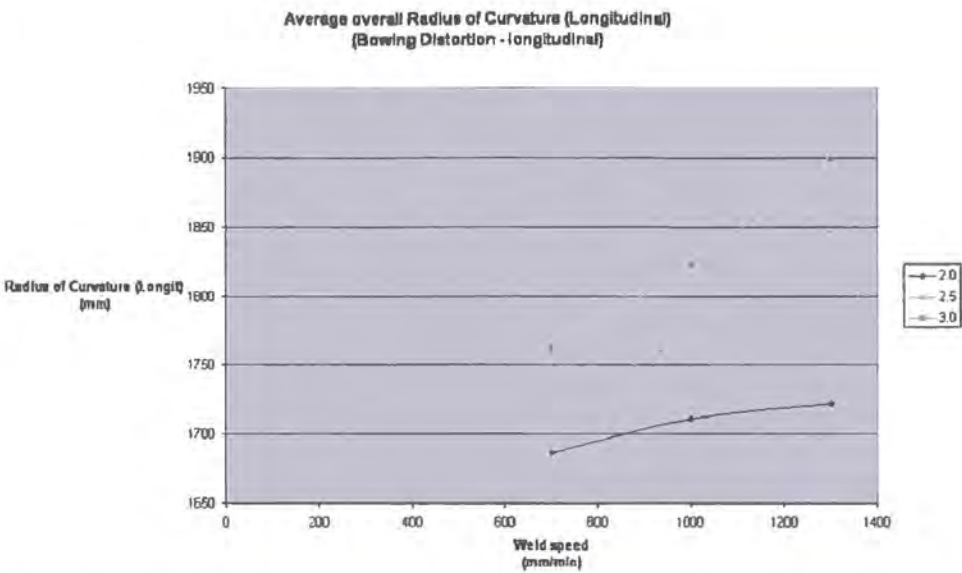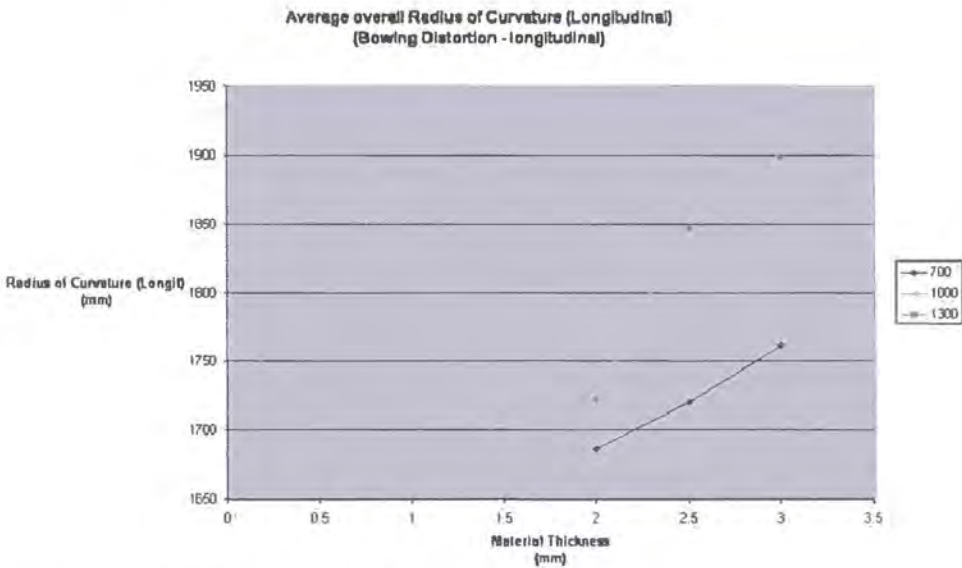
Average overall Radius of Curvature (Longitudinal)
(Bowing Distortion - longitudinal)

(a) Relationship between material thickness curves

Average overall Radius of Curvature (Longitudinal)
(Bowing Distortion - longitudinal)

(b) Relationship between welding speed curves

Family curves for bowing distortion in bead on plate weld samples

251
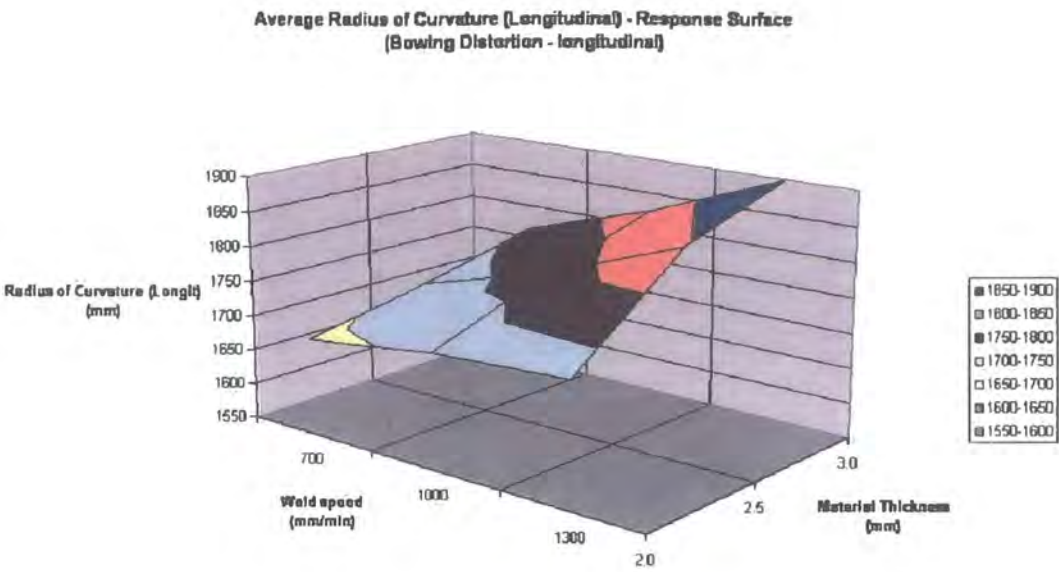
Experimental response surface for bowing distortion in bead on plate weld samples

Butt Weld - Longitudinal distortion

**Average Longitudinal dimension changes
(Longitudinal Distortion/Shrinkage)**

(a) Relationship between material thickness curves

**Average Longitudinal dimension changes
(Longitudinal Distortion/Shrinkage)**

(b) Relationship between welding speed curves

Family curves for longitudinal distortion in butt weld samples

Response surface for longitudinal distortion in butt weld samples

<u>Butt Weld - Transverse distortion</u>
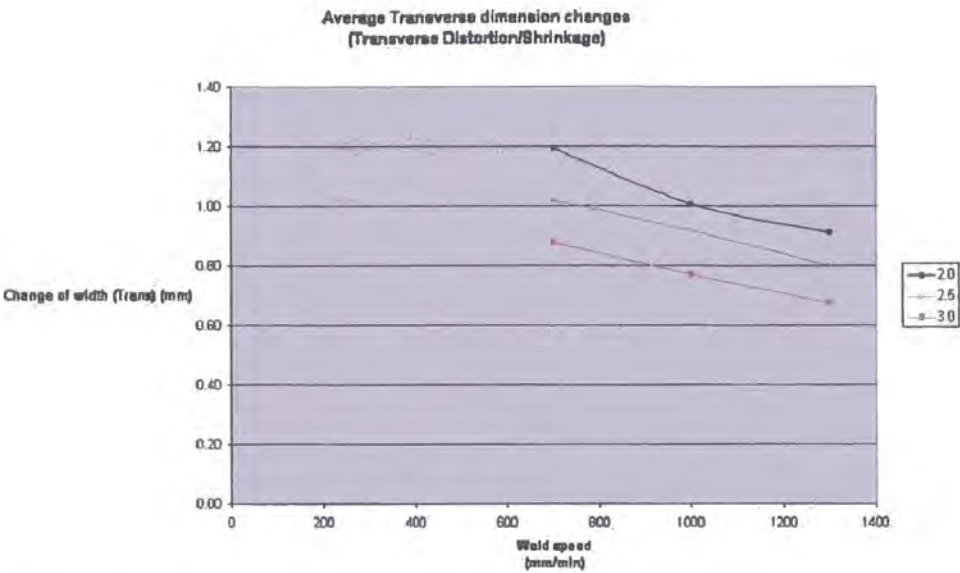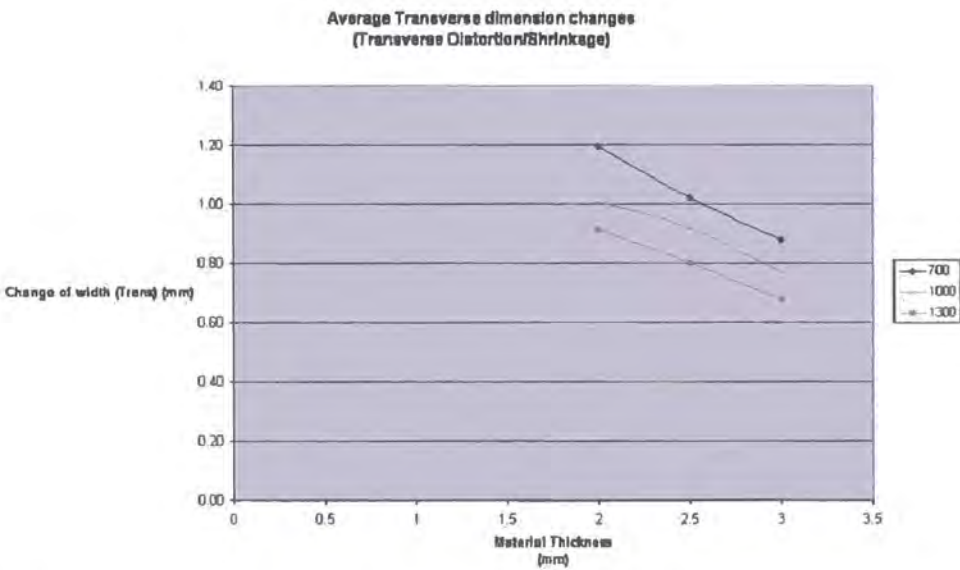
**Average Transverse dimension changes
(Transverse Distortion/Shrinkage)**

(a) Relationship between material thickness curves

**Average Transverse dimension changes
(Transverse Distortion/Shrinkage)**

(b) Relationship between welding speed curves

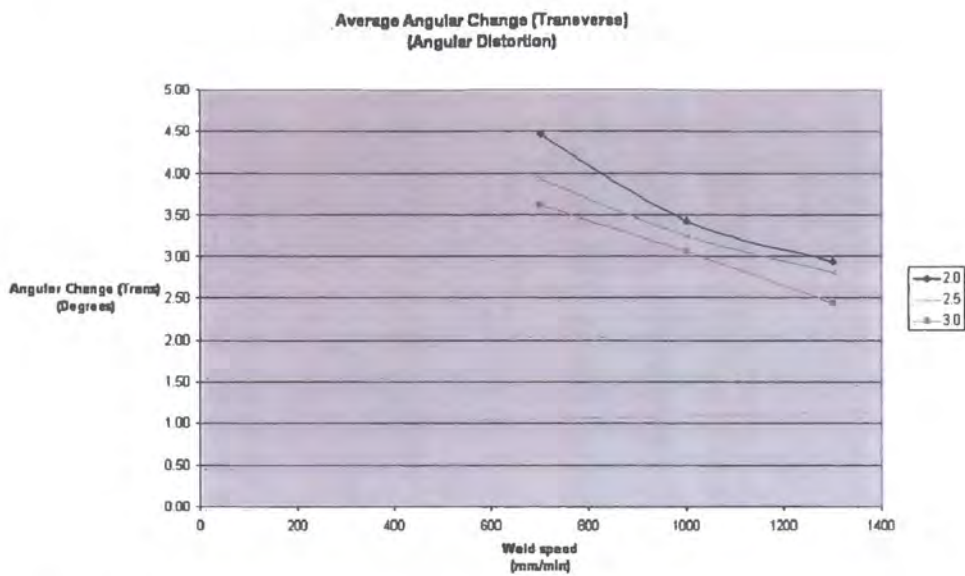Family curves for transverse distortion in butt weld samples

Average Transverse dimension changes - Response Surface
(Transverse Distortion/Shrinkage)
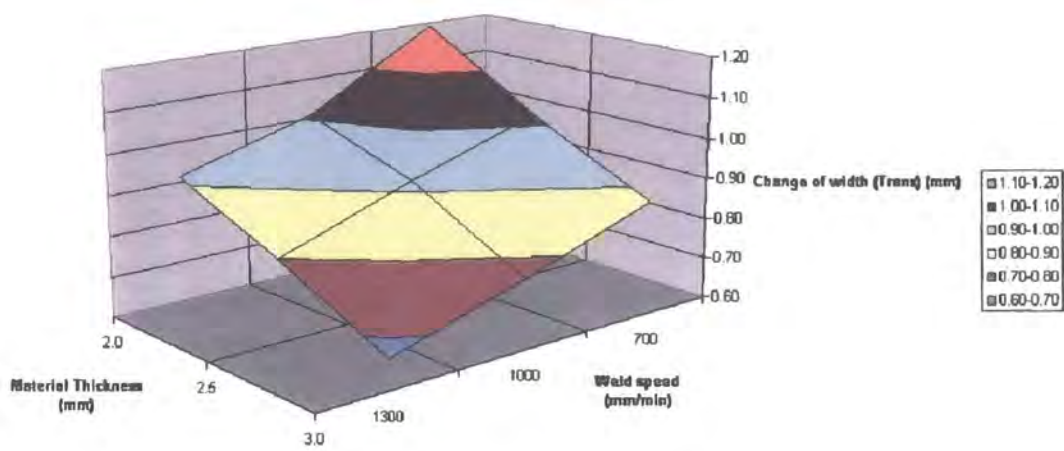
Response surface for transverse distortion in butt weld
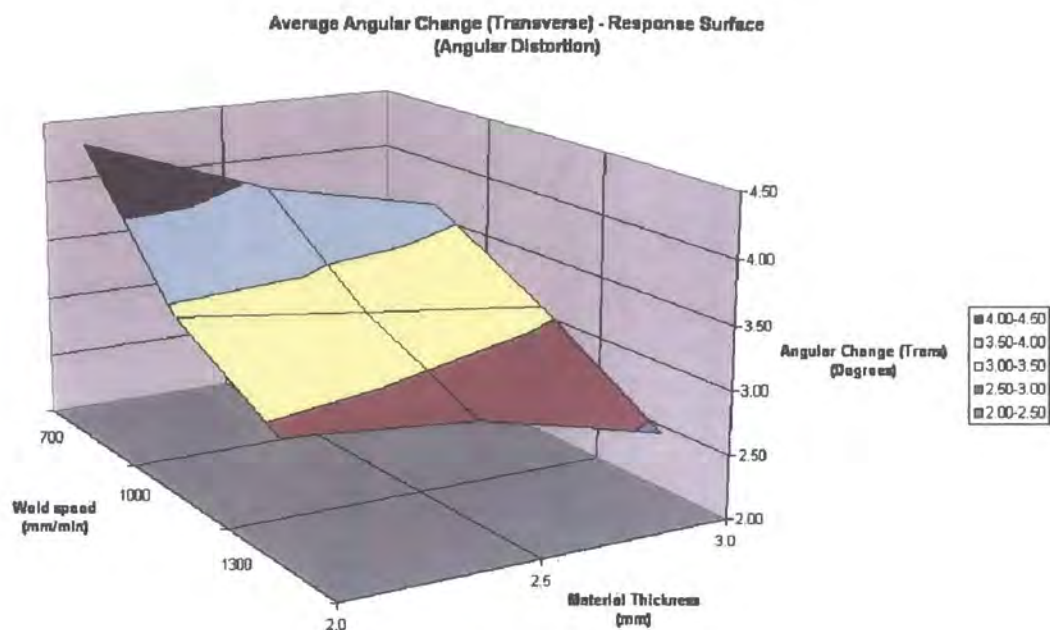
Butt weld - Angular distortion
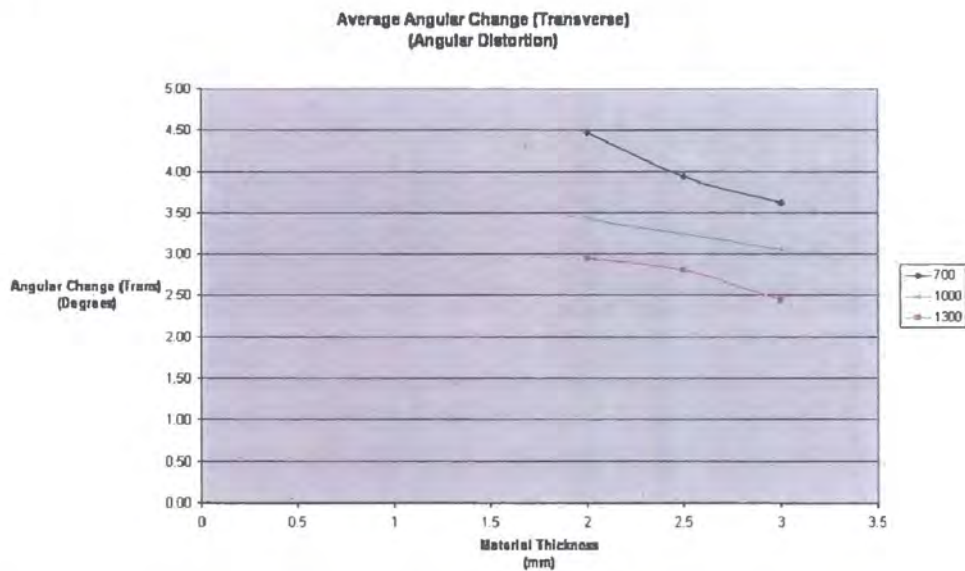
Average Angular Change (Transverse)
(Angular Distortion)

(a) Relationship between material thickness curves

Average Angular Change (Transverse)
(Angular Distortion)

(b) Relationship between welding speed curves

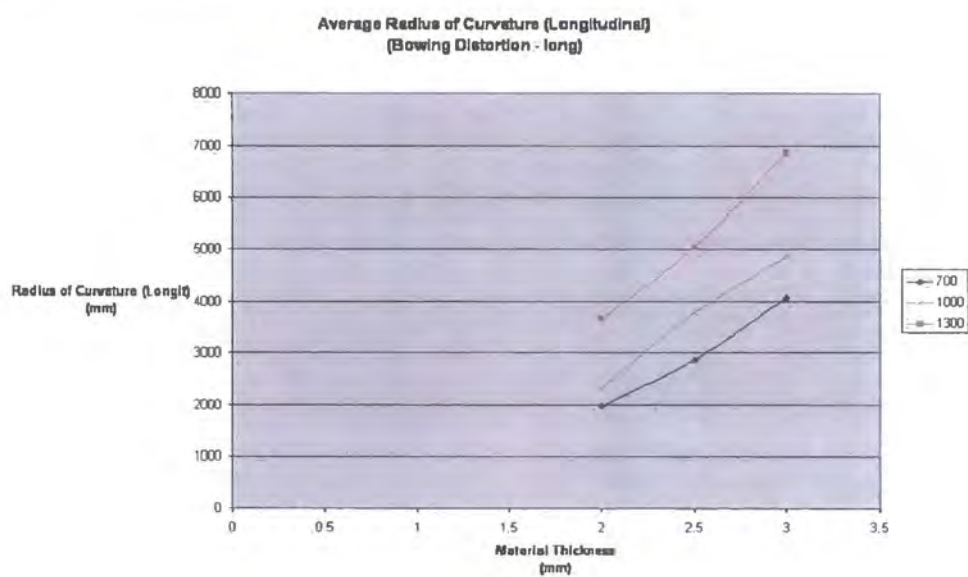Family curves for angular distortion in butt weld samples

Response surface for angular distortion in butt weld samples
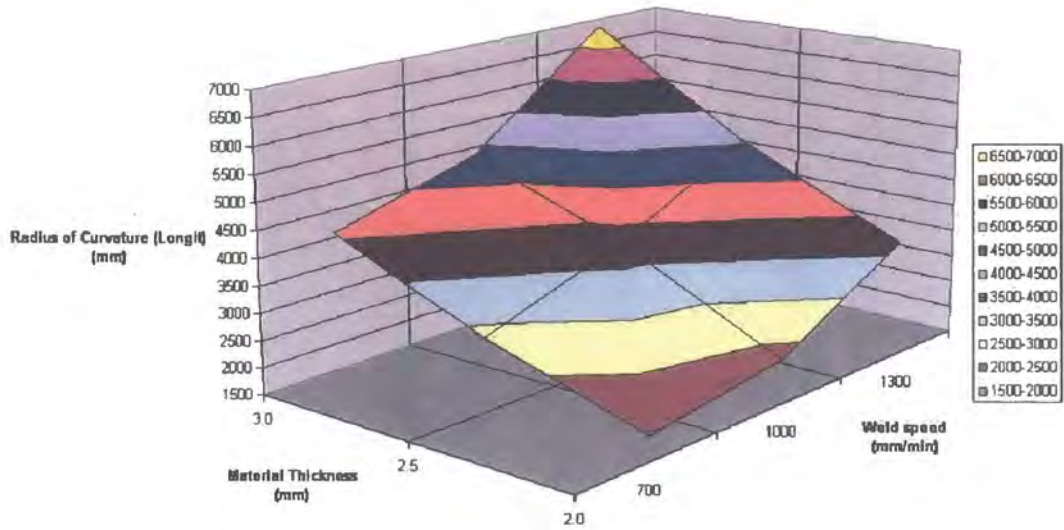
Butt Weld - Bowing distortion
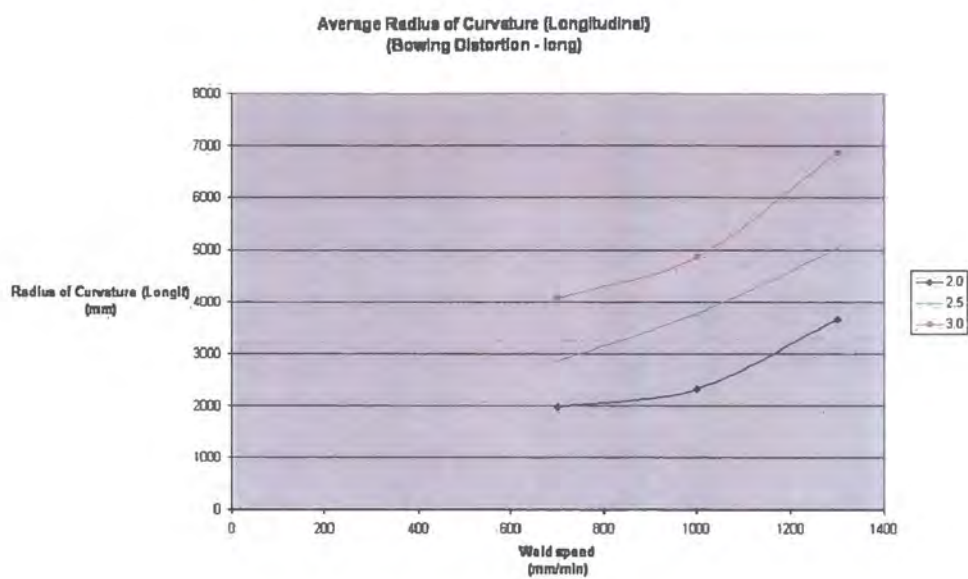
(a) Relationship between material thickness curves

(b) Relationship between welding speed curves

Family curves for bowing distortion in butt weld samples

Average Radius of Curvature (Longitudinal) - Response Surface
(Bowing Distortion - long)

Response surface for bowing distortion in butt weld